SPACECRAFT DESIGN PROJECT

HIGH LATITUDE COMMUNICATIONS SATELLITE

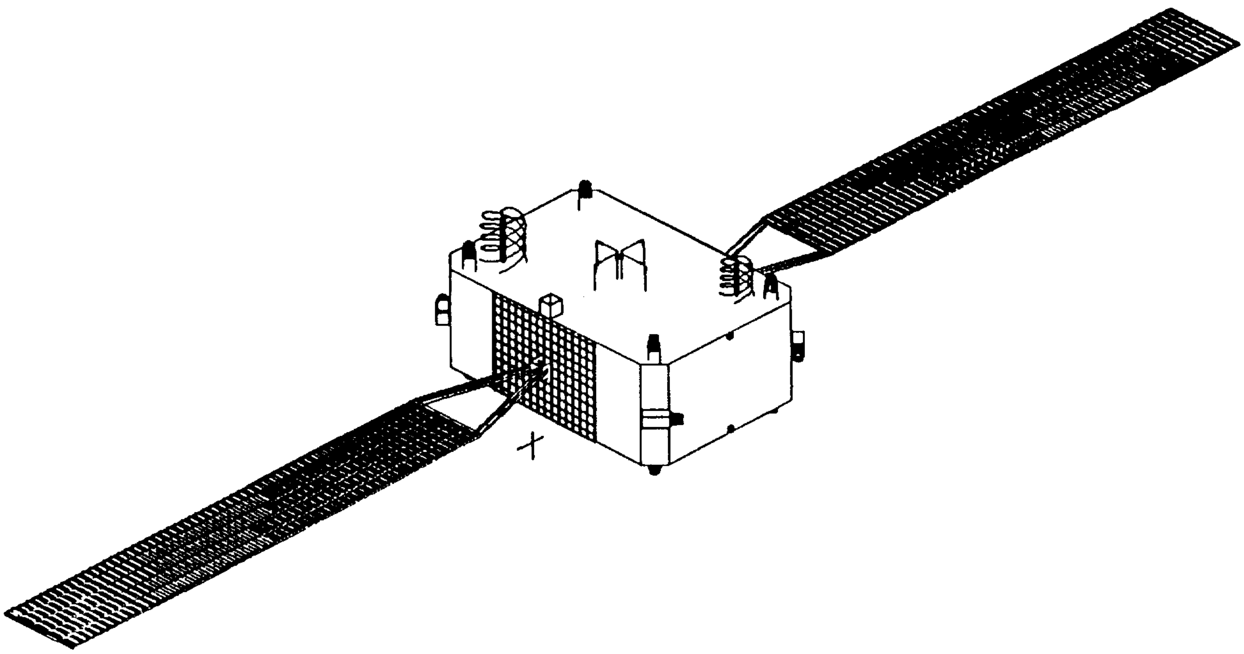

December 1989

NAVAL POSTGRADUATE SCHOOL

MONTEREY, CALIFORNIA

(NASA-CR-[illegible]) SPACECRAFT DESIGN PROJECT: HIGH LATITUDE COMMUNICATIONS SATELLITE Final Report (Naval Postgraduate School) [illegible] CSCL 22B

N91-11[illegible]

Unclas

G3/18 [illegible]

SPACECRAFT DESIGN PROJECT TEAM

Carl Josefson

Jack Myers

Mike Cloutier

Steve Paluszek

Gerry Michael

Dan Hunter

Dan Sakoda

Wes Walters

Dennis Johnson

Terry Bauer

Charlie Racoosin

Butch Lugtu

COURSE
AE-4871
Advanced Spacecraft Design
Fall 1989
Course Instructor
Prof. B. Agrawal

This project was sponsored by the NASA/Universities Space Research Association
Advanced Design Program

ACKNOWLEDGEMENTS

The project team would like to thank Prof. B. Agrawal for his guidance and support throughout this effort. We also want to thank Profs. R. Kolar, R. W. Adler, G. A. Myers, and A. Kraus, of the Naval Postgraduate School for their assistance. The following personnel from the Naval Research Laboratory also contributed to the success of the project: Mike Brown, Shannon Coffey, Chris Garner, Marv Levinson, and Tom Kawecki. Finally, we would like to thank Mr. J. D. Burke, our NASA center representative, and Dr. J. H. Kwok from the Jet Propulsion Laboratory for their assistance.

TABLE OF CONTENTS

LIST OF TABLES

LIST OF FIGURES

I. INTRODUCTION

The spacecraft design project was part of AE-4871, Advanced Spacecraft Design. The project was intended to provide experience in the design of all major components of a satellite. Each member of the class was given primary responsibility for a subsystem or design support function. Support was requested from the Naval Reasearch Laboratory to augment the Naval Postgraduate School faculty. Analysis and design of each subsystem was done to the extent possible within the constraints of an eleven week quarter and the design facilities (hardware and software) available.

The project team chose to evaluate the design of a high latitude communications satellite as representative of the design issues and tradeoffs necessary for a wide range of satelites.

A. SPACECRAFT DESCRIPTION

The High-Latitude Communications Satellite (HILACS) will provide a continuous UHF communications link between stations located north of the region covered by geosynchronous communications satellites, ie, the area above approximately 60° N latitude. HILACS will also provide a communcations link to stations below 60° N via a relay net control station (NCS), which is located with access to both the HILACS and geosynchronous communications satellites. The communications payload will operate only for that portion of the orbit necessary to provide specified coverage.

The satellite orbit is elliptic with perigee at 1204 km in the southern hemisphere and apogee at 14930 km. The orbit inclination is 63.4° to eliminate rotation of the line of apsides. The orbit period is 4.8 hours, during which each spacecraft will be operating approximately 1.6 hours. The complete constellation will consist of three spacecraft equally spaced in mean anomaly.

The reaction control (RCS) and the stationkeeping propulsion subsystem is a monopropellant hydrazine sytem. There are four 38-N thrusters for the initial apogee adjustment and twelve 2-N thrusters for the RCS and stationkeeping. The propellant is contained in four tanks with internal pressurant bladders.

The satellite is three-axis stabilized by four reaction wheels with thrusters providing redundancy and reaction wheel desaturation. The spacecraft is nadir pointing with antenna pointing accuracy of $\pm 0.5°$. The satellite rotates about its yaw axis so as to maintain the solar panel axis (roll axis) normal to the sun line, providing maximum solar power efficiency. The attitude control subsystem (ACS) will utilize four sun sensors, two earth sensors, and a three-axis rate-sensing gyroscope. The orientation of the four reaction wheels provides redundant operation.

The electric power subsystem (EPS) is a single bus, fully regulated system with bus voltage of 28 volts. The EPS consists of two solar array panels, a 16-cell, 12 amp-hour nickel-hydrogen battery, power control circuitry, and a shunt resistor bank. The EPS provides 343 watts at end-of-life (EOL) at aphelion with a 10% margin. The solar arrray is comprised of GaAs solar cells, selected for their superior radiation tolerance.

The telemetry, tracking, and control (TT&C) subsystem design provides for both autonomous operations and direct control by a mid-latitude ground control station. The NCS will also be able to perform some TT&C functions.

The thermal control subsystem is primarily a passive system, with radiators on the satellite faces mounting the solar array panels, which will always be oriented parallel with the sun line. The other surfaces of the spacecraft will be insulated to maintain internal temperatures within acceptable limits. The passive system is augmented by heaters for equipment/locations requiring unique treatment.

The primary spacecraft structural support is the central tube, which provides the load bearing structure for the equipment panels and fuel tanks. The central tube is also designed to provide for the design loads resulting from stacking of three satellites for launch.

B. LAUNCH AND ORBIT INJECTION SEQUENCE

All three satellites will be launched simultaneously on a single Delta/STAR 48 launch vehicle. The launch will take place from the Kennedy Space Center, and will place the three satellites initially into a 15729 KM x 1204 KM orbit at the desired inclination. The relative sizes of the launch and mission orbits are shown in Fig. I-1. The launch vehicle final stage will provide spin stabilization for the three stacked spacecraft during transfer to the initial orbit and upon achieving this orbit, the spacecraft will be mechanically separated from the launch vehicle bus such to ensure adequate separation for the individual final orbit insertion burns (Fig. I-2, 1). As each satellite is separated from the final stage it will be spinning about a stable axis, eliminating the need for additional stabilization during the sun/earth acquisition phase. The satellites remaining on the final stage will be stabilized by this stage until they too are detached following a short time period to ensure adequate spacecraft separation (Fig.I-2, 2). In this initial orbit, the spacecraft will acquire the sun and then the earth to assume their earth pointing, three-axis stabilized configuration; then will deploy their solar arrays (Fig. I-2, 3 and 4). This will allow the spacecraft to achieve electrical and thermal stability prior to insertion into the mission orbit. Following the array deployment and spacecraft orientation, the trailing satellite in the launch orbit will be reoriented and at perigee will be slowed by a 1.73

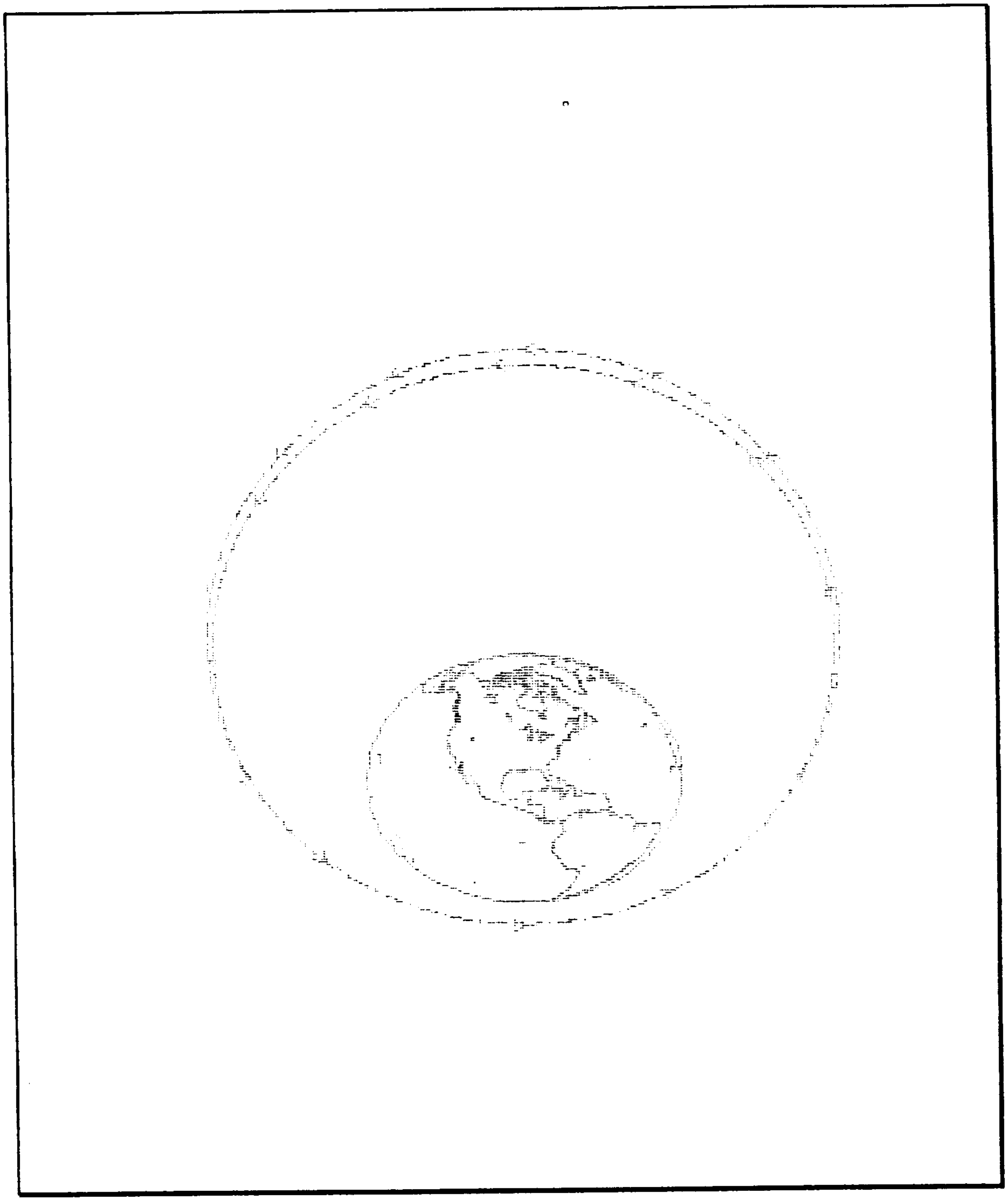

Figure I-1. Launch and Mission Orbits

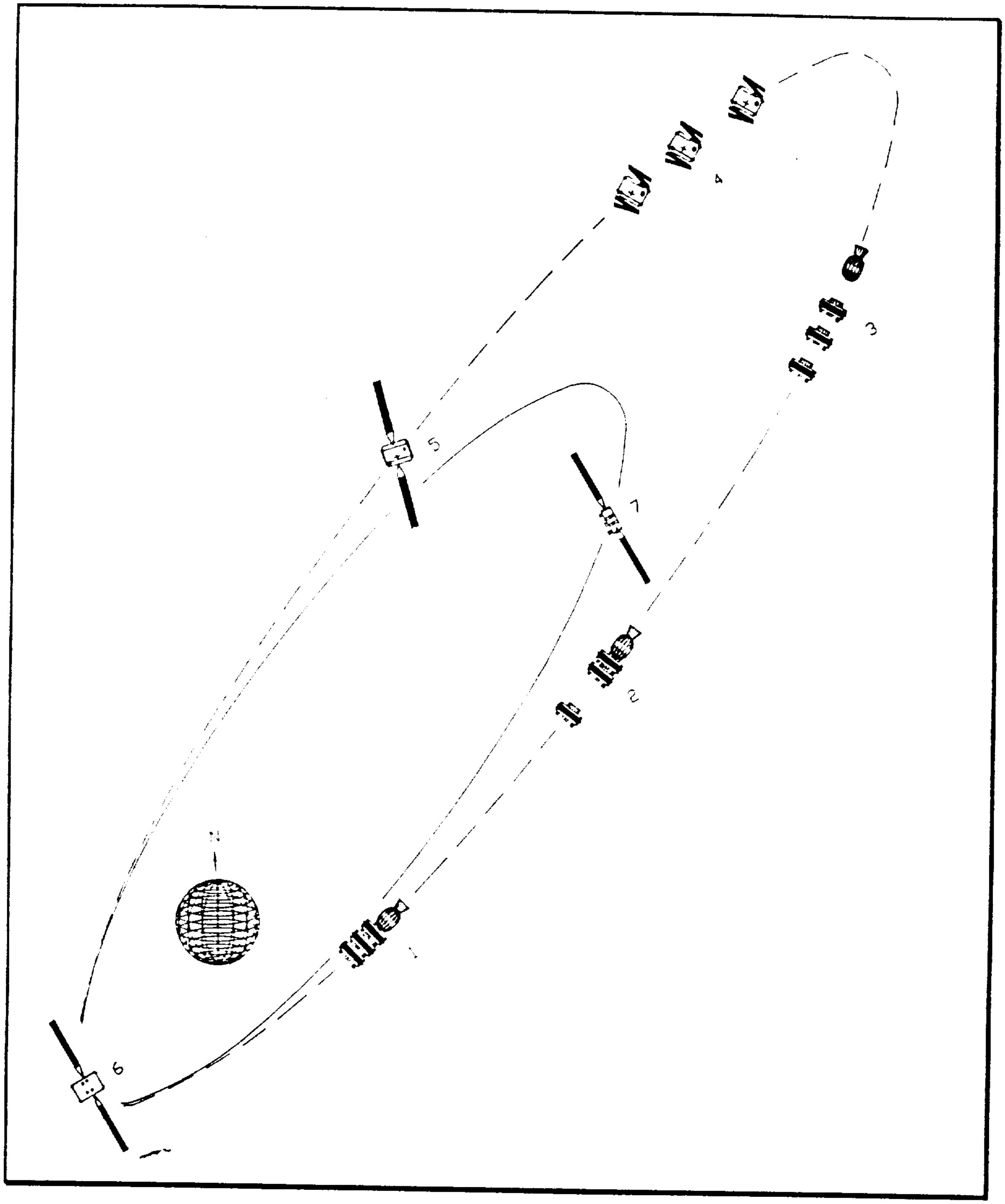

Figure I-2. Launch Sequence/Orbit Insertion

minute burn of the four 38-N thrusters (Fig. I-2, 5). This burn will provide the -42.2 m/s ΔV needed to place this satellite into the 14933 KM x 1204 KM mission orbit (Fig. I-2, 6). Since the mission orbit has a 4.8 hour period compared to the 5.0 hour period of the launch orbit, the second spacecraft will be aligned for insertion 8 orbits later, with the final spacecraft aligned following an additional 8 orbits. This sequence will put the entire plane of satellites in position 80 hours after the initial spacecraft is inserted into the mission orbit. This relatively long period between the insertion of each satellite also provides for the accurate determination of orbital parameters of the preceding spacecraft and adjustment on subsequent insertions as needed.

II. ORBITAL DYNAMICS

A. SELECTION OF ORBIT

The mission orbit was initially chosen to meet the preliminary specifications. These requirements dictated the perigee altitude of 1204 km (650 NM), the orbital period of 4.8 hours and that the orbit be at the critical inclination to minimize the precession of the argument of perigee. From these specifications, the other orbital data were determined and are summarized in Table II-1.

TABLE II-1. ORBITAL DYNAMICS SUMMARY

Mission Orbit:	
Apogee	14933 KM (8063 NM)
Perigee	1204 KM (650 NM)
Period	4.8 HR
Inclination	63.435 deg (critical inclination)
Argument of perigee	270 deg
Ascending node	TBD
Eccentricity	0.47517
Constellation:	3 Satellites spaced evenly in mean anomoly (1.6 HR)
Launch:	
Vehicle	Delta/Star 48
Apogee	15729 KM (8493 NM)
Perigee	1204 KM (650 NM)
Period	5.0 HR
Inclination	63.435°
Insertion Burn:	
Δ V at perigee	-42.2 m/s (-138.5 ft/s)
Isp	225 s
Efficiency	.99
Initial Mass	412 Kg (908.3 lbm)
Propellant Mass	8.04 Kg (17.73 lbm)
Burn time (four motor)	1.73min
Perigee Motor:	4 x RRC MR-50F

Thrust (each, steady state)	38.7 N (8.7 lbf)
Mass flow (each)	0.0174 Kg/s (.03828 lbm/s)
Array Hinge Moment at Insertion:	
Array Mass	6.2 Kg (13.6 lbm)
Array Arm	2.64 m (8.7 ft)
Acceleration	0.376 m/s^2 (1.23 ft/s^2)
Hinge Moment	6.15 N-m (4.14 lbf-ft)
Station Keeping:	
ΔV (monthly) ($d\omega/dt$ = .12 deg/month)	11.14 m/s (36.5 ft/s)
ΔV (total, 4 yrs)	534.84 m/s (1754.3 ft/s)
Isp	225 s
Efficiency	.99
Initial Mass	412 Kg (908.3 lbm)
Propellant Mass (total)	89.5 Kg (197.4 lbm)
Eclipse:	
Maximum duration	37.5 min
Approximate number during 3 yr lifetime	900
Orbit Perturbations:	
Ascending node	-0.425 deg/day
Line of apsides:	
Critical inclination	0.03 deg/month
.1 deg inclination error	0.12 deg/month
Inclination (maximum)	< 0.1175 deg/yr

It was determined that this orbit provides the desired 24 hour coverage for the entire region north of 60 degrees North latitude through the use of three satellites spaced evenly in mean anomaly (1.6 Hr), with active payloads during the portion of the orbit when each satellite's ground track is above 50 degrees North latitude. This coverage will require a transmitted beam width (assuming a zero degree elevation angle at the receiver) of 40 degrees at 50 degrees North and 35 degrees at apogee. Figure II-1 shows an "off earth" view of the mission orbit, with Figure II-2 detailing the ground track of a single orbit with the accompanying ground swath for a 40 degree beam width. In this configuration, each satellite will remain above 50 degrees North for one hour and 54 minutes of each orbit, providing 18 minutes of overlap during which two spacecraft are in sight of any ground station above this latitude for coordination of the switching of the active satellite. The relatively low altitude of this mission orbit and the reduced spacecraft mass resulting from the elimination of the need for a separate perigee kick motor allow for the simultaneous launch of three satellites on a single launch vehicle, and consequently simplify the on orbit positioning of the entire constellation. Additionally, due to the small maneuver required to insert each spacecraft into the mission orbit from the launch orbit, the satellites can be oriented into their earth pointing, three axis attitude immediately upon separation from the launch bus. This will allow each spacecraft to achieve thermal and electrical power stability prior to being inserted into the mission orbit.

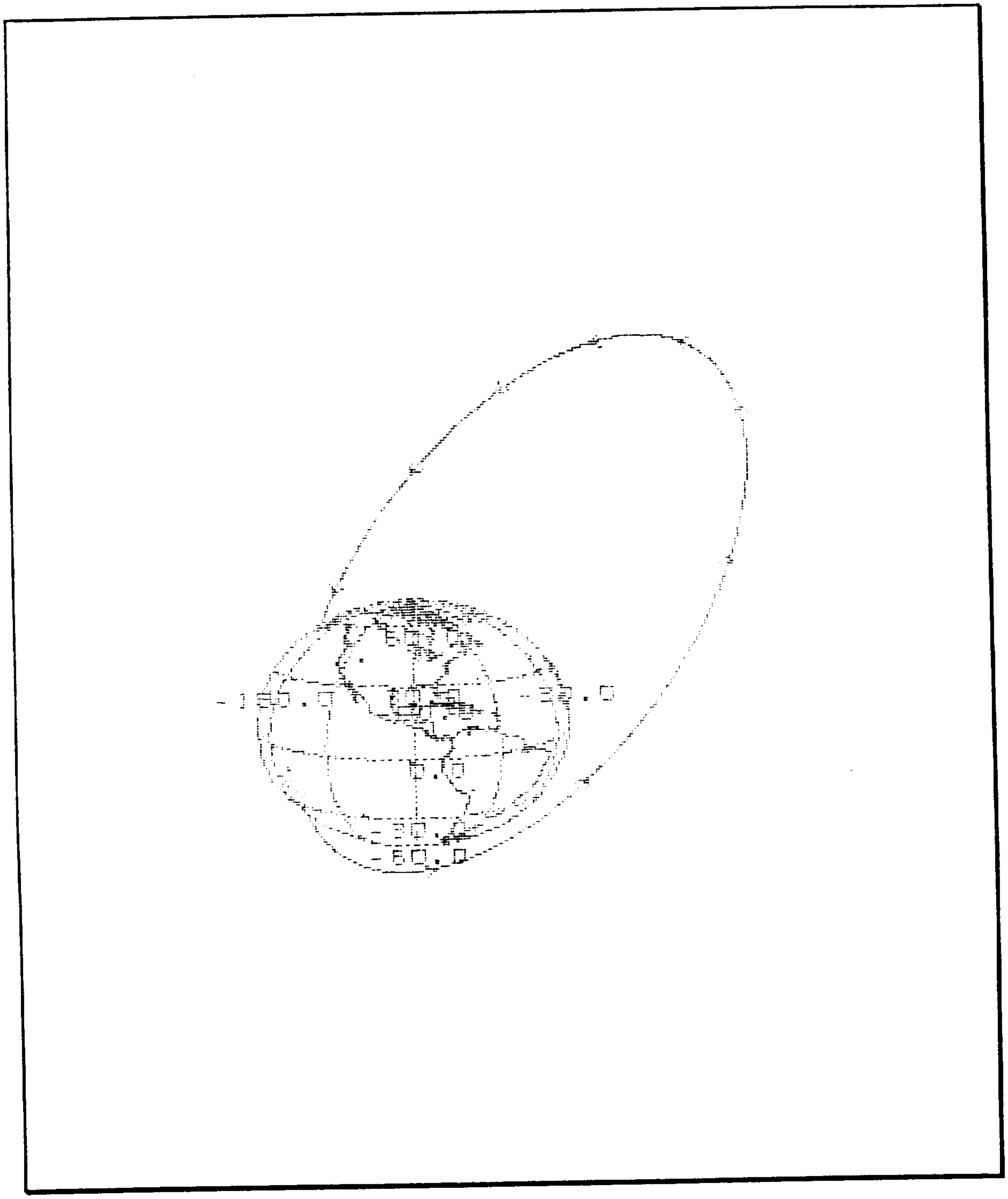

Figure II-1. Mission Orbit

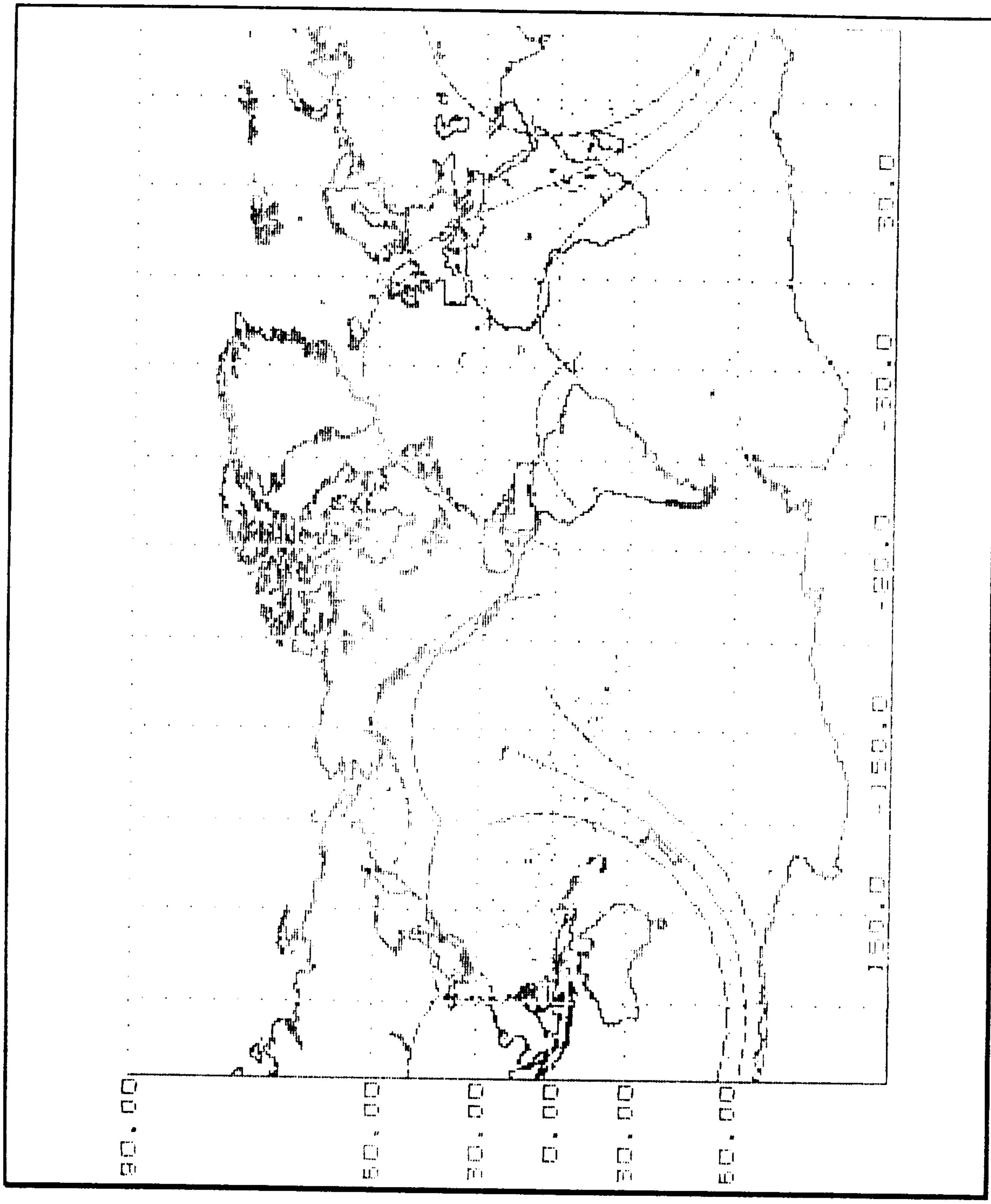

Figure II-2. Single Orbit Ground Track and Swath

Alternate orbits were also considered for this mission. These additional orbits all had the same perigee, inclination and argument of perigee, but had periods of up to 12 hours and a resulting higher apogee of up to 39261 km

(21199 NM). These orbits were also suitable for the defined mission, and would have satisfied the 24 hour coverage requirement through the use of only two spacecraft, again equally spaced in mean anomaly. These orbits were abandoned for this project primarily to simplify the final design through the elimination of a separate perigee motor and the accompanying complexities associated with the need for an orbit transfer to achieve final orbit. For the 12 hour orbit, transfer to the mission orbit from a 1204 km (650 NM) circular parking orbit would have required an estimated 731.4 kg of fuel for a solid perigee kick motor - approximately 1.9 times the satellite beginning of life (BOL) mass. Additionally, considerations such as electrical power, thermal control and attitude control would have to have been addressed, and would have complicated the final design beyond that required. Data for a 10 hour and a 12 hour orbit, as well as that for the selected 4.8 hour mission and associated 5.0 hour launch orbit, are given in Table II-2.

TABLE II-2. ALTERNATE ORBITS

Parameter	10 Hour	12 Hour	4.8 Hour	5.0 Hour
Perigee Altitude (KM)	1204	1204	1204	1204
Apogee Altitude (KM)	33169	39261	14933	15729
Perigee Radius(KM)	7582	7582	7582	7582
Apogee Radius(KM)	39548	45639	21311	22107
Semi-major Axis (KM)	23565	26610	14446	14846
Period (HR)	10.0	12.0	4.8	5.0
Vperigee (KM/S)	9.3932	9.4956	8.8063	8.8489
Vcircle 650NM (KM/S)	7.2508	7.2508		

ΔV (KM/S)	2.1424	2.2448		-.0422
Mp (KG)	679.5	731.4		7.21

B. STATION KEEPING / ORBIT PERTURBATIONS

1. Inclination

The time rate of change of inclination due to the gravitational effects of the moon and the sun were computed and are summarized in Table II-3 and Figure II-3. In both cases, the rate is periodic in the right ascension of the orbit ascending node which is decreasing at the daily rate of -0.425 degrees. This causes the inclination rate to cycle completely in 847 days, with a maximum value of 0.1175 deg/yr throughout the 3 year lifetime of the satellite. Since this represents the worst case alignment of the sun and the moon during the mission, the actual values should be computed for these bodies based on their true positions for a given launch date - recognizing that the resulting perturbation would actually be no larger than 0.1175 deg/yr. The error in inclination which would accumulate would only be that which represents the satellite life beyond one of the 847 day cycles. With this small change in inclination there is no need to budget propellant for station keeping for inclination drift.

TABLE II-3. INCLINATION PERTURBATIONS

	DEG	RAD
ORBIT INCL	63.435	1.107
SUN INCL	23.450	0.409
MOON INCL	18.300	0.319
	28.600	0.499

ORBIT RIGHT ASCENSION (DEG)	(RAD)	SUN DI/DT (DEG/YR)	MOON DI/DT (DEG/YR) i=18.3	MOON DI/DT (DEG/YR) i=28.6	TOTAL DI/DT (DEG/YR) i=18.3	TOTAL DI/DT (DEG/YR) i=28.6
0.00	0.000	0.000	0.000	0.000	0.000	0.000
15.00	0.262	0.013	0.021	0.037	0.034	0.050
30.00	0.524	0.024	0.038	0.067	0.062	0.091
45.00	0.785	0.031	0.051	0.086	0.082	0.117
60.00	1.047	0.034	0.056	0.092	0.090	0.126
75.00	1.309	0.032	0.055	0.085	0.088	0.118
90.00	1.571	0.027	0.049	0.069	0.076	0.096
105.00	1.833	0.021	0.039	0.048	0.060	0.068
120.00	2.094	0.013	0.028	0.027	0.042	0.041
135.00	2.356	0.008	0.018	0.011	0.026	0.019
150.00	2.618	0.003	0.010	0.002	0.014	0.005
165.00	2.880	0.001	0.005	-0.001	0.006	0.000
180.00	3.142	0.000	0.000	0.000	0.000	0.000
195.00	3.403	-0.001	-0.005	0.001	-0.006	0.000
210.00	3.665	-0.003	-0.010	-0.002	-0.014	-0.005
225.00	3.927	-0.008	-0.018	-0.011	-0.026	-0.019
240.00	4.189	-0.013	-0.028	-0.027	-0.042	-0.041
270.00	4.712	-0.027	-0.049	-0.069	-0.076	-0.096
285.00	4.974	-0.032	-0.055	-0.085	-0.088	-0.118
300.00	5.236	-0.034	-0.056	-0.092	-0.090	-0.126
315.00	5.498	-0.031	-0.051	-0.086	-0.082	-0.117
330.00	5.760	-0.024	-0.038	-0.067	-0.062	-0.091
345.00	6.021	-0.013	-0.021	-0.037	-0.034	-0.050
0.00	0.000	0.000	0.000	0.000	0.000	0.000

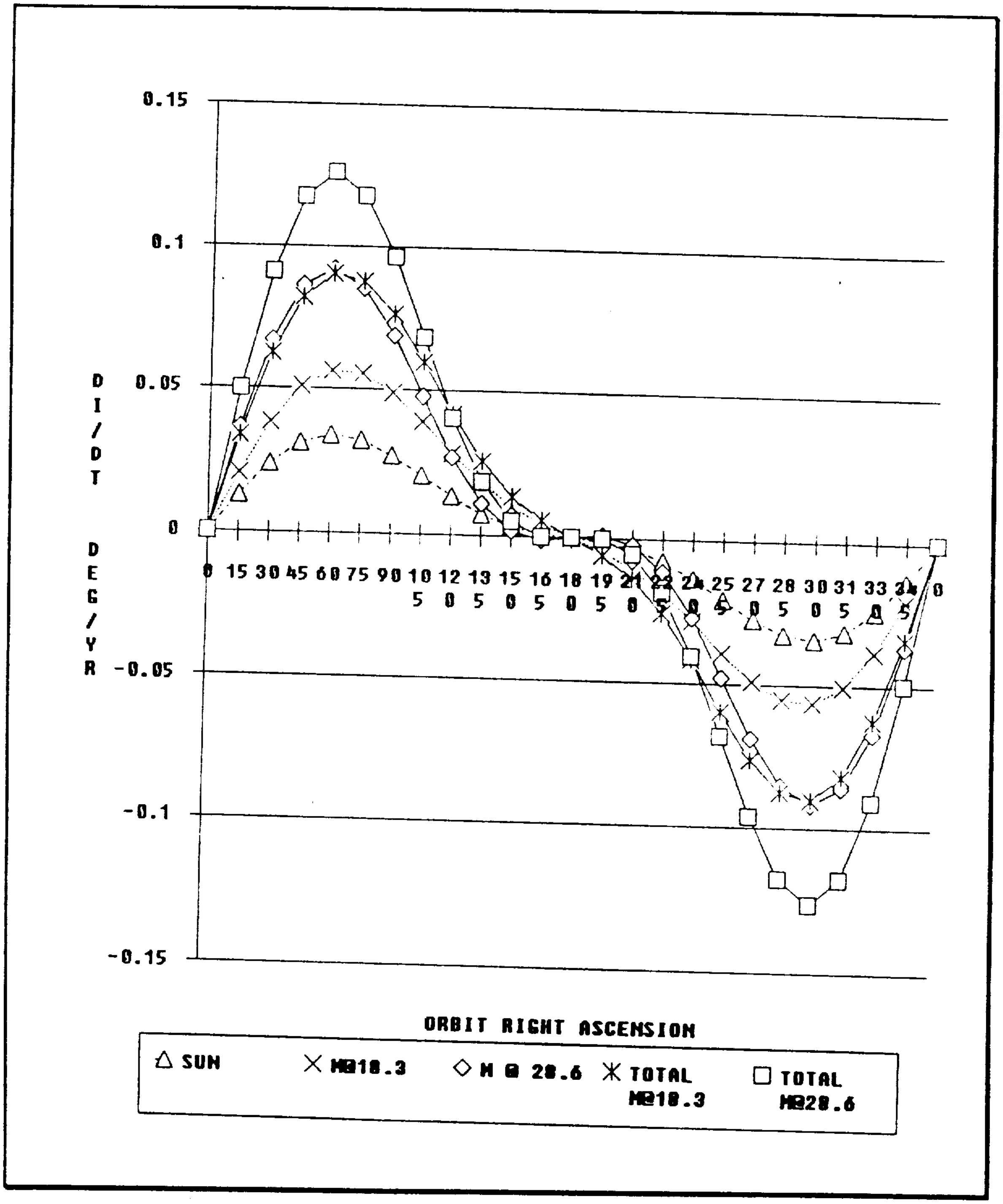

Figure II-3. Inclination Perturbations

2. Argument of Perigee

Even though the satellites will be placed at the critical inclination, there will be drift of the argument of perigee due to higher order effects. The long period dynamic equations (the system was normalized to remove those short period terms dependent only on mean anomaly) of the mission orbit were numerically integrated using a Runge-Kutta 4th order fixed step integrator. The analysis included perturbations to a Keplerian orbit due to the J_2, J_3, J_4, J_5 zonal harmonics. From this analysis, the mission orbit proved to be very stable in argument of perigee. The argument of perigee will drift through 360 degrees with a period of 1100 years. This represents a yearly rate of 0.33 degrees. However, the orbit is very sensitive to errors in inclination. A 0.1 degree error in inclination reduces the period of the circulation of the argument to 250 years - a rate of 1.44 degree/year. For a fixed spacecraft lifetime of 3 years, there is no need to budget propellant to correct for this small amount of drift. The ground coverage of the communications package includes sufficient margin to absorb up to approximately 5 degrees of error in positioning of the perigee. However, since the solar array (the limiting factor for spacecraft life) has the capacity to provide power for a substantial period beyond the planned 3 year satellite life, propellant has been budgeted to correct drift of the argument of perigee through four years. This station keeping will require a change in direction of the spacecraft velocity vector of 1.44 degrees each year. Done at the midpoint of the orbit, between the perigee and apogee, this represents a change in velocity of 133.7 m/s directed along the outward normal to the orbit. Using the attitude control thrusters, this will require a total of 81.8 kg (180 lbm) of propellant over four years. The current satellite design provides adequate capacity for this requirement as well as approximately 50 kg of additional propellant as margin.

C. ATTITUDE CONTROL / SOLAR ARRAY POINTING

Since the mission payload requires that the spacecraft be earth pointing, the satellite will have to continually pitch as it travels through the orbit. Additionally, the spacecraft will have to continually yaw to facilitate solar array pointing. This yaw, coupled with the rotation of the solar arrays about their longitudinal axes will allow the arrays to maintain their orientation normal to the sun. The amount of yaw required each orbit is a function of the angle β between the solar orbit plane and the satellite orbit plane. This relationship is given in the following equation: [Ref. 1]

$$\beta = A\,(B \sin\gamma \cos\Omega - \cos\gamma \sin\Omega) - C \sin\gamma$$

β = orbit plane illumination angle

$A = \sin(i)$ $\quad$ i = orbit inclination = 63.435 deg

$B = \cos(\varepsilon)$ $\quad$ ε = solar orbit inclination = 23.44 deg

$C = \cos(i)\sin(\varepsilon)$

γ = sun central angle (measured ccw from vernal equinox to current position of sun relative to earth)

Ω = right ascension of the satellite orbit ascending node

This angle will be at a minimum of 0 degrees and will reach maximum value of 87 degrees, and will change at a relatively slow rate as the satellite right ascension decreases at the daily rate of -0.425 deg and the solar central angle increases at the rate of 0.98565 deg/day. During each orbit, the satellite yaw will total $4 \times (90 - |\beta|)$ degrees to maintain array pointing. This yaw will be in the form of a "nodding" motion of the spacecraft as it will be in a cycle from zero to $+(90 - |\beta|)$ and back, then to $-(90 - |\beta|)$ and back, one entire cycle each orbit. Figure II-4 details the periodic nature of β as γ and Ω change daily, and Figures

II-5 and II-6 show the commanded yaw angle as a function of beta for 360 degrees of sun rotation angle.

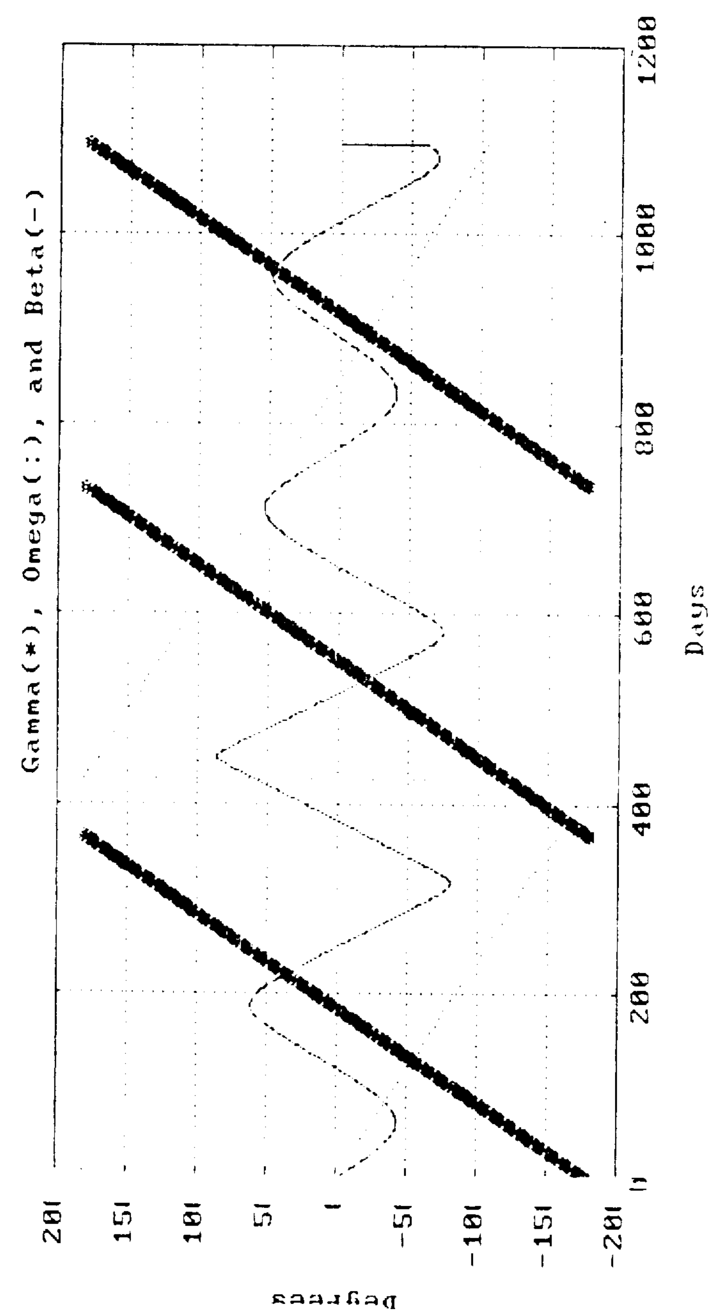

Figure II-4. Orbit Plane Illumination Angle

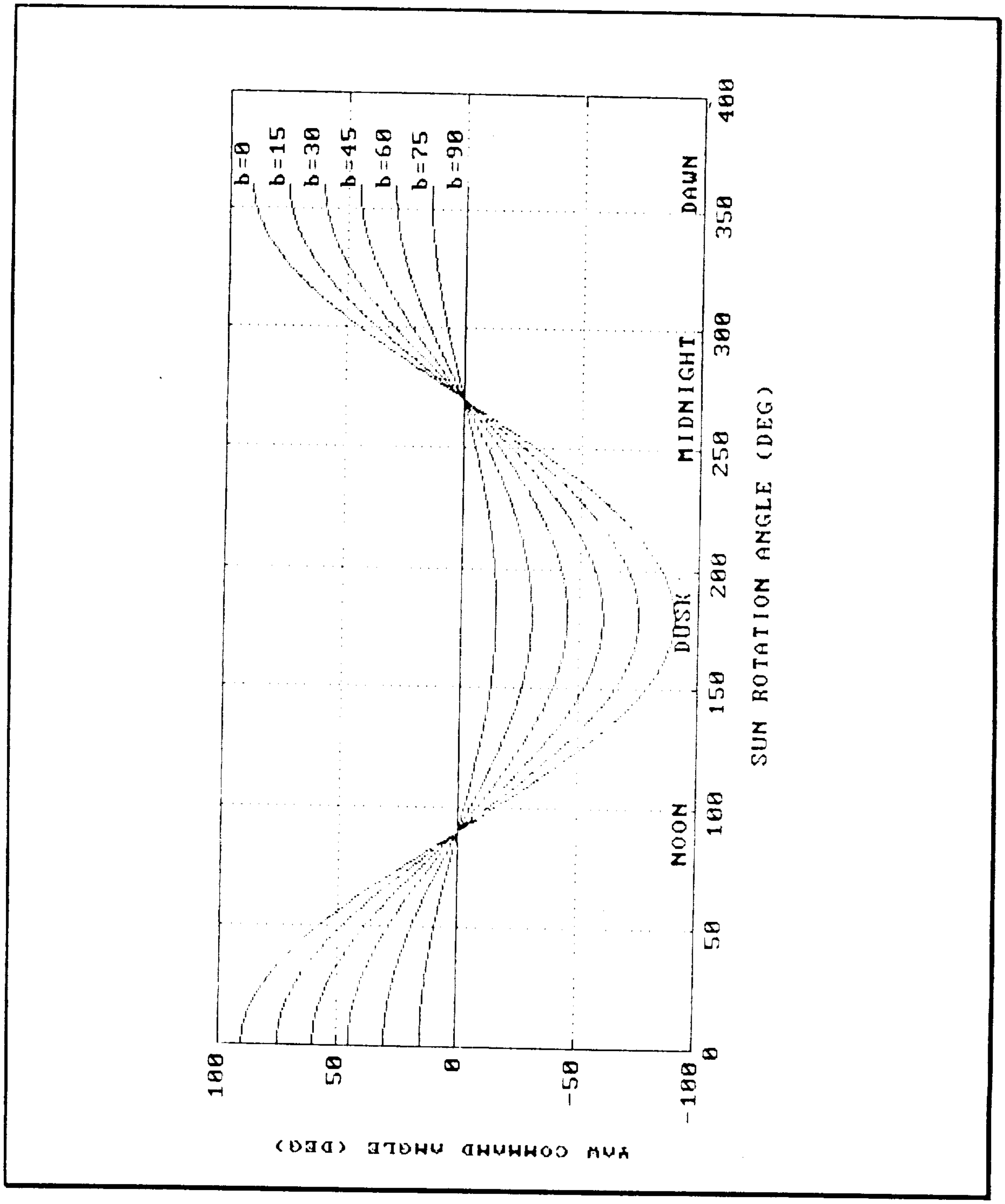

Figure II-5. Commanded Yaw Angle (+β)

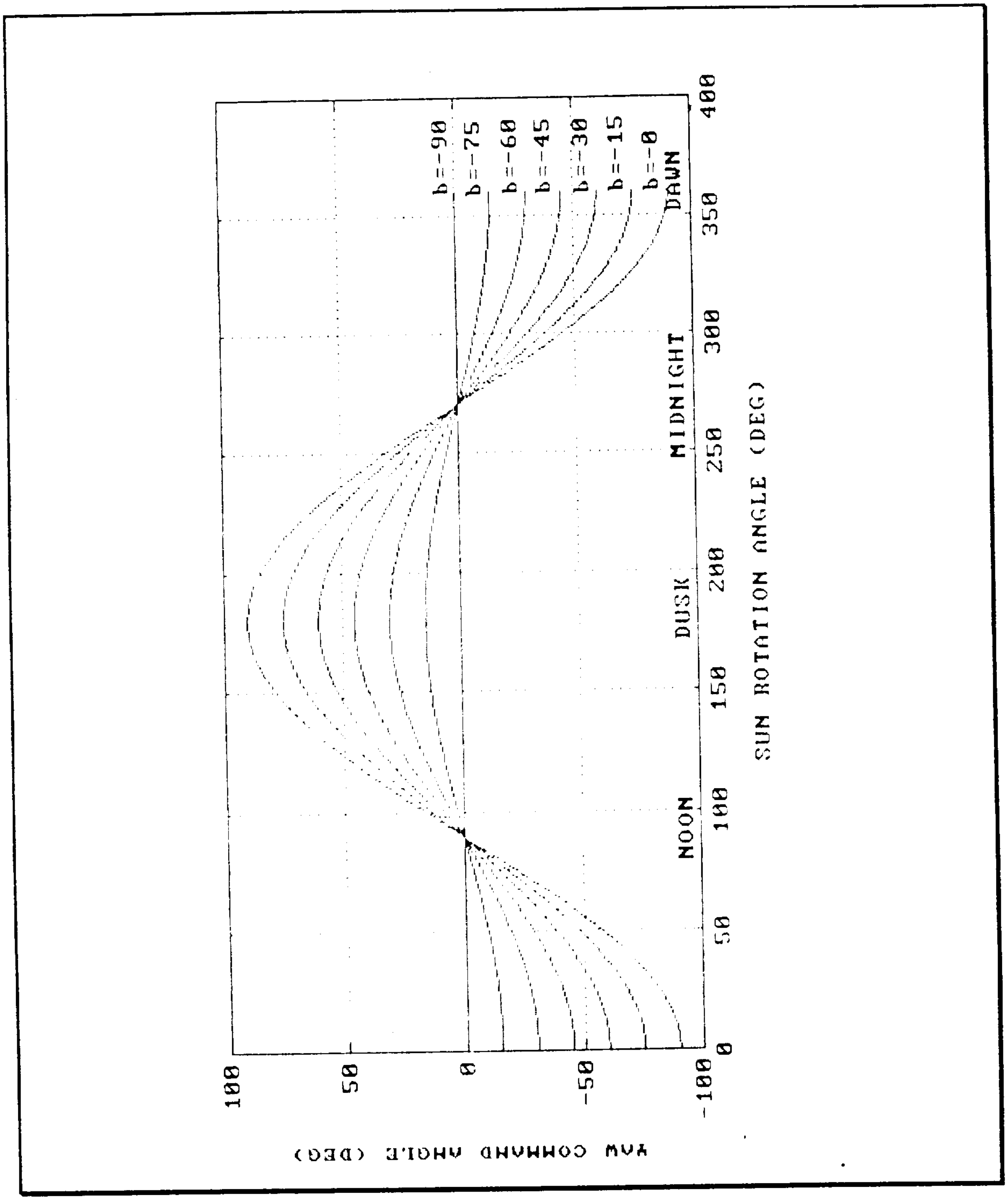

Figure II-6. Commanded Yaw Angle (-β)

The angle between the solar array normal and the incident sunlight is given by the following equation: [Ref. 2]

$$\cos \Theta = (\cos \alpha \cos \rho \sin \beta + \sin \alpha \cos \tau \cos \beta - \cos \alpha \sin \rho \sin \tau \cos \beta)$$

$\cos \Theta$ = angle between array normal and incident sunlight

α = array articulation angle between the array normal axis and the local horizontal, measured positive away from the earth

ρ = spacecraft yaw angle measured ccw from inertial north

β = orbit plane illumination angle (see above)

τ = angle from solar noon, measured in the direction of the satellite orbit from the point on the orbit closest to the sun (local noon)

Figures II-7 and II-8 are representative plots of this sun angle through a single orbit for two different sun/orbit orientations. They detail the periodic nature of both the array articulation angle (α) and the satellite yaw angle (ρ) with the resulting normal incidence of the array (Θ) and the incoming sunlight maintained.

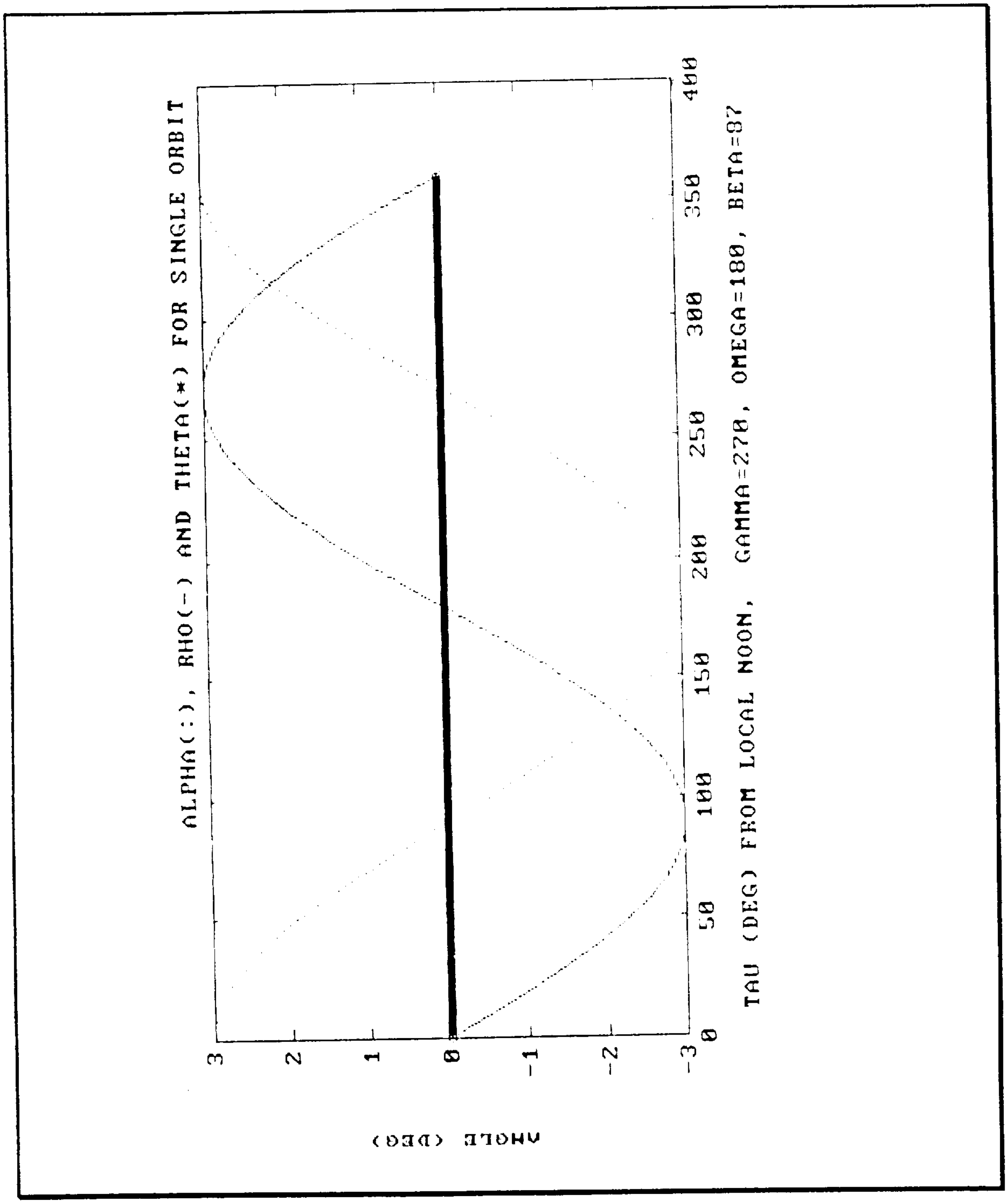

Figure II-7. Solar Array Pointing

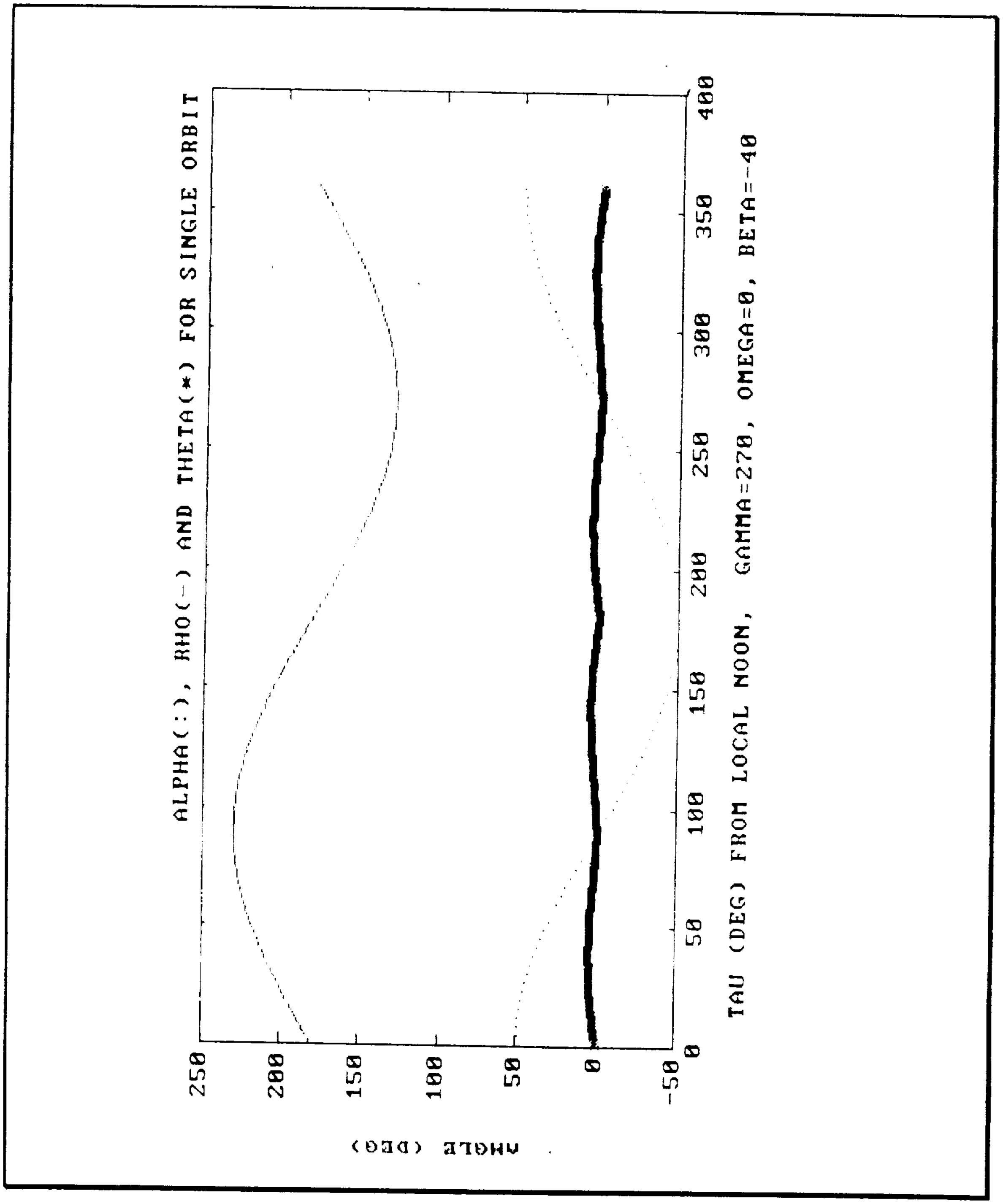

Figure II-8. Solar Array Pointing

D. SOLAR ECLIPSE PERIODS

Since the orbital plane is precessing, there will be times when the spacecraft will be illuminated during its entire orbit. During these orbits, electrical power will be supplied to the satellite entirely by the solar arrays. Batteries will be needed however to provide power during the times that the spacecraft orbit and the sun position are such that the spacecraft receives no solar illumination during some portion of its orbit. With a perigee of 1204 KM, this will only occur for orbit plane illumination angles of less than 57.3 degrees (arcsin(Re/(Re+650))). Starting at zero for the orbit right ascension (Ω), and 180 degrees for the sun central angle (γ), Figure II-4 shows how these two angles and the resulting illumination angle propagate. For this starting orientation, there will be 901 days out of the 1095 day planned lifetime during which the spacecraft will experience an eclipse of some duration. Since apogee is at the orbits northernmost point, this eclipse period will be at a maximum when the sun is at winter solstice, its southernmost point, and the angle between the orbital plane and the solar plane is zero. With this sun-earth orientation, altitudes out to 9649 KM are eclipsed, with a resulting period of 37.5 minutes during which the solar arrays are not illuminated. At five orbits per day, this specifies the need for batteries which can provide spacecraft bus power for up to 37.5 minutes through 4500 or more cycles.

III. SPACECRAFT CONFIGURATION

A. EQUIPMENT LAYOUT

The primary considerations involved in developing the HILACS configuration were: a) to size the satellite for the Delta launch vehicle; b) to shape the satellite and distribute the mass to achieve the proper moment of inertia ratio for stability during a transfer orbit phase if required; c) to use the east and west faces as equipment panels for thermal considerations since these faces will always be oriented parallel to the vector to the sun; and d) to maintain as much modularity in the equipment layout as possible.

To achieve redundancy and to distribute the fuel mass it was decided to use four fuel tanks. The basic shape of the satellite (1.9 m x 1.3 m x 0.7 m) was driven by the geometry of placing the four fuel tanks around the center tube within the Delta payload envelope (Fig. III-1). A fuel tank is mounted in each corner along the center line in height.

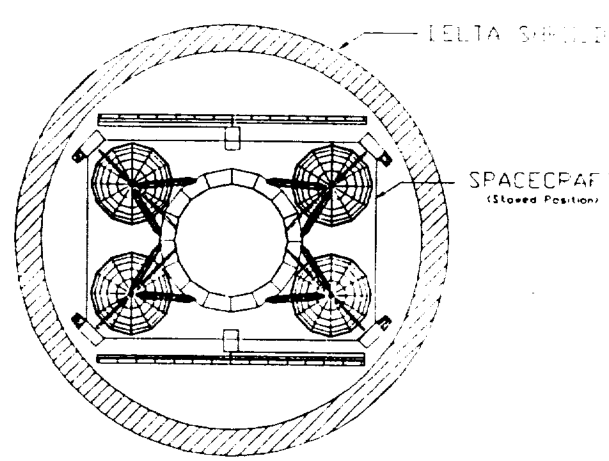

Figure III-1. Delta Payload Envelope.

The center tube consists of a 0.37 m long center cylinder of radius 0.375 m with conical sections on each end. The radii of the conical sections are 0.4776 m to accomodate the PAM-D interface ring and the stacking rings (Fig. III-2).

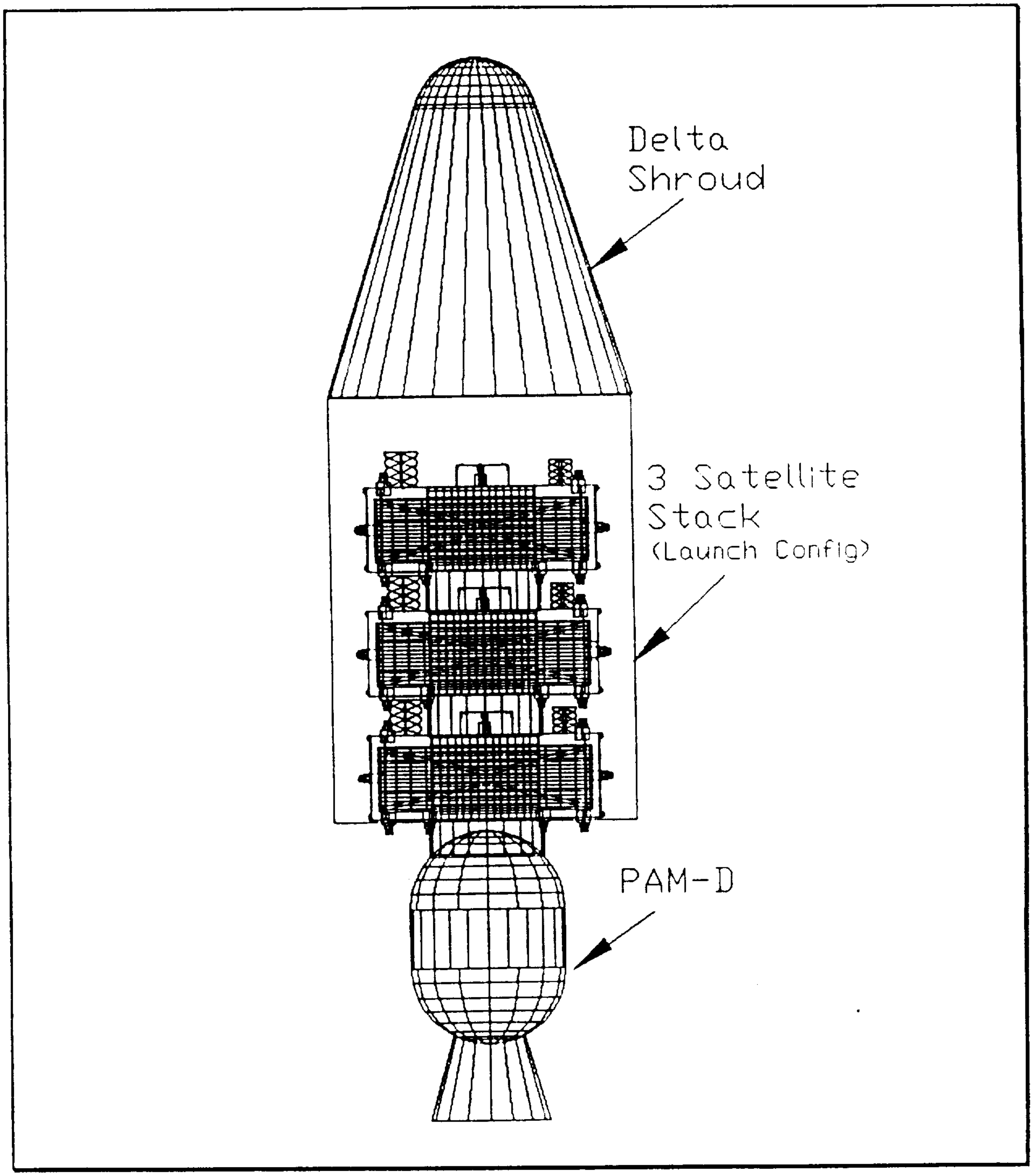

Figure III-2. Launch Configuration.

From the top view, each corner of the satellite is cut off on a 45° angle 13 cm in from the corner giving the satellite an octagonal shape (Fig. III-3). A 2.2 N thruster is mounted at mid-height on each of these four sheared off corners to provide control about the yaw-axis. The yaw-axis and roll-axis reaction wheels are attached to the center tube at mid-height along the north-south center line. The pitch-axis reaction wheel is mounted on the south face of the satellite. The fourth reaction wheel, for redundancy, is oriented at a 45° angle to all three principle axes. It is mounted on the north face between the fuel tanks near the anti-earth face.

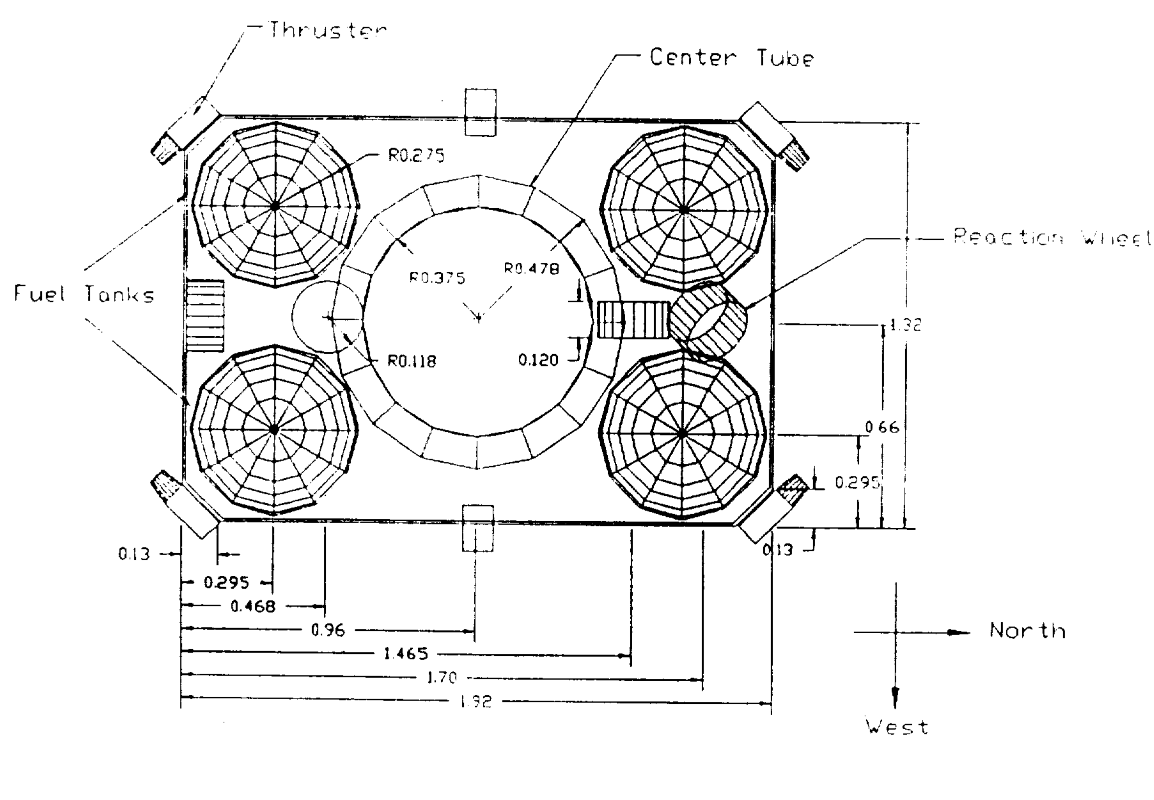

Figure III-3. Top View, Mid-Height

1. Earth Face (Fig. III-4).

The nadir pointing requirement dictated that the three antennas be mounted on the earth facing side along the yaw-axis. The cross pole antenna is mounted in the center of the earth face. The two helical antennas are mounted one in the southwest corner and one in the northeast corner centered above the fuel tanks. Four 2.2-N thrusters are mounted one in each corner 14.5 cm from each edge. The earth sensor is mounted centered along the west edge of the earth face.

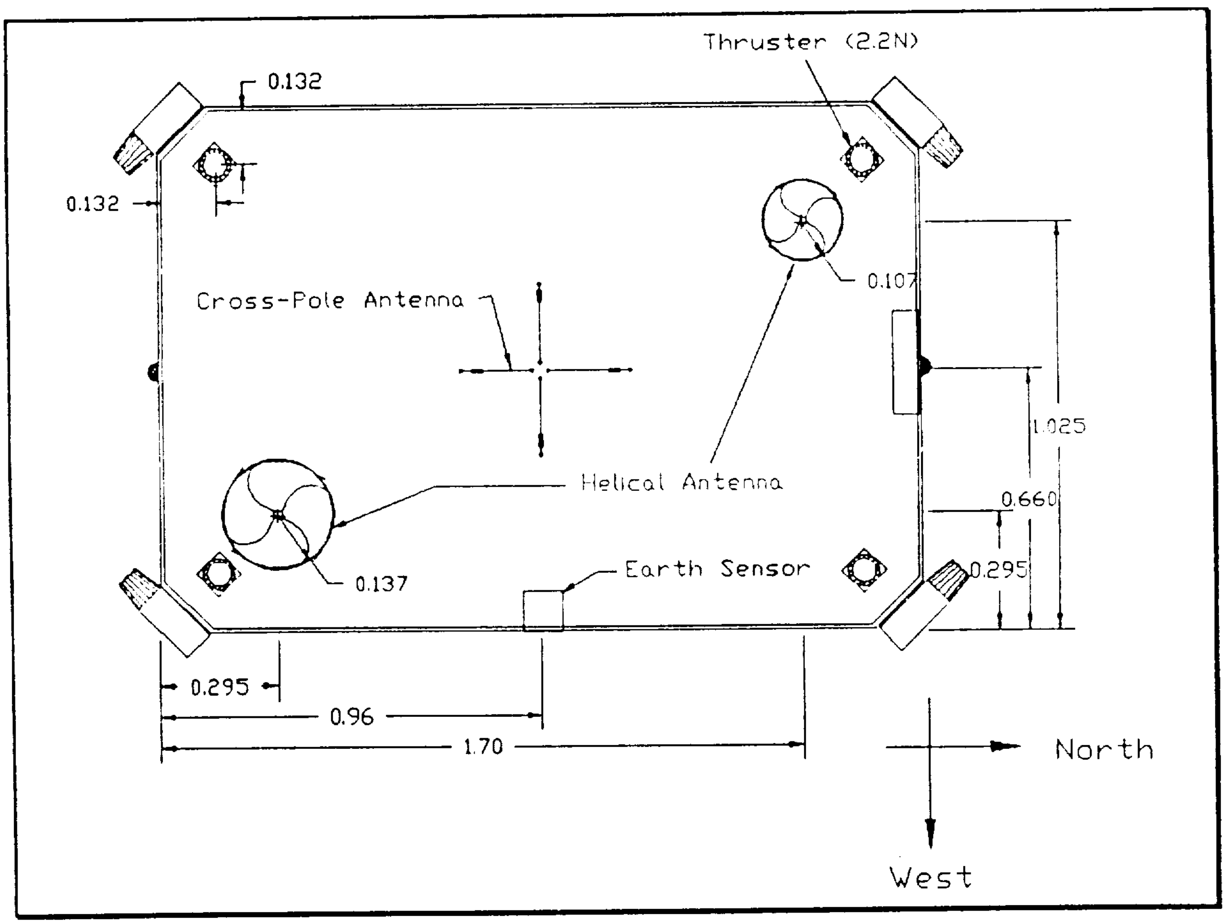

Figure III-4. Earth Face.

2. Anti-earth Face (Fig. III-5).

A 2.2-N thruster is mounted in each corner 14.5 cm in from each edge. There are also four 38-N thrusters used for orbit injection mounted around the outer edge of the center tube.

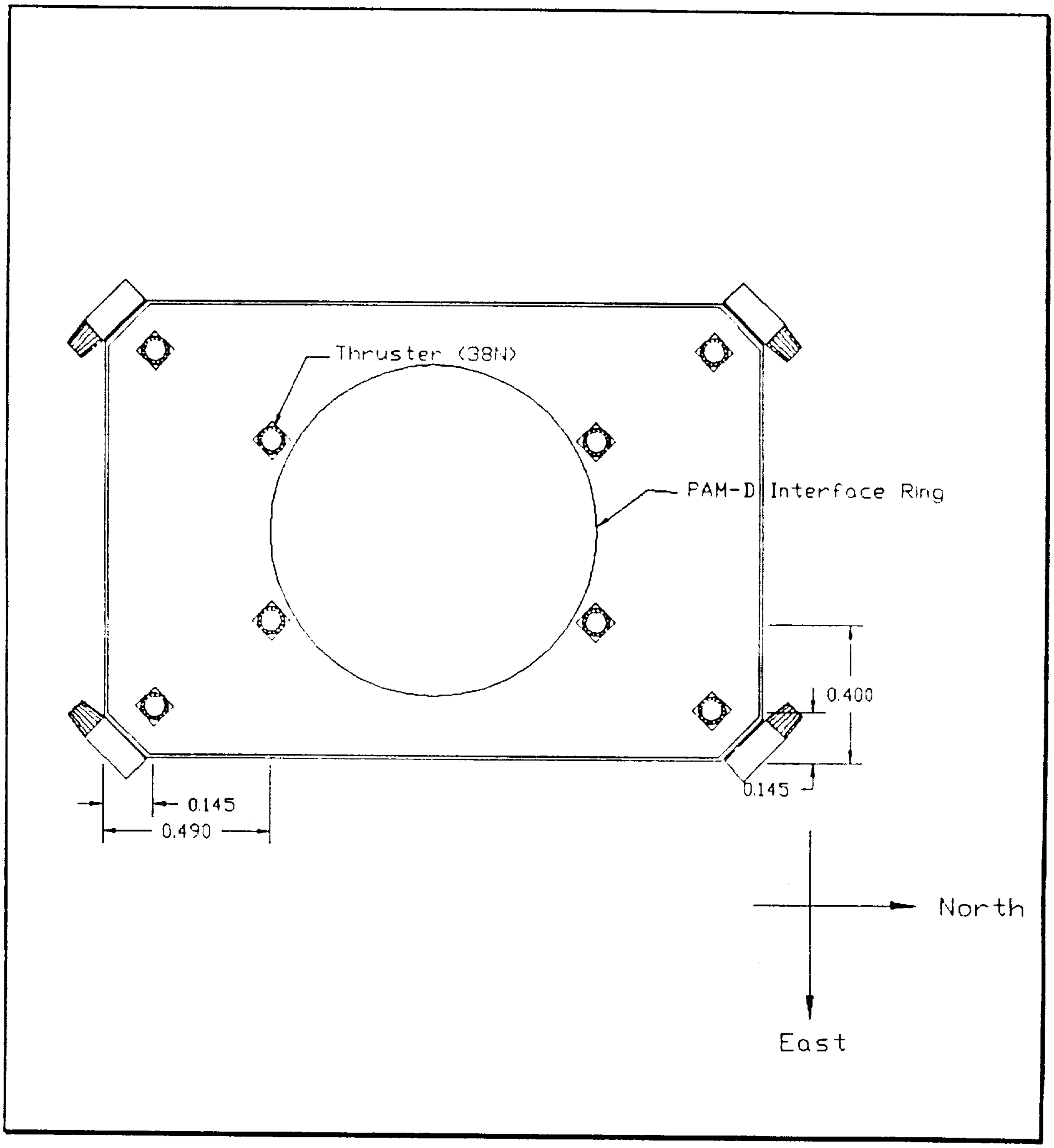

Figure III-5. Anti-Earth Face.

3. West Face (Fig. III-6).

The west face was used to house the payload subsystem. All of the payload components are mounted on the west face between the fuel tanks. One of the two thermal radiators (0.7 m x 0.9 m) is centered on the outside of the face. The solar array extends from the center of the face. The solar array is 0.533 m wide, 3.576 m in length and has a 0.85 m extension to prevent shadowing and facilitate folding the array.

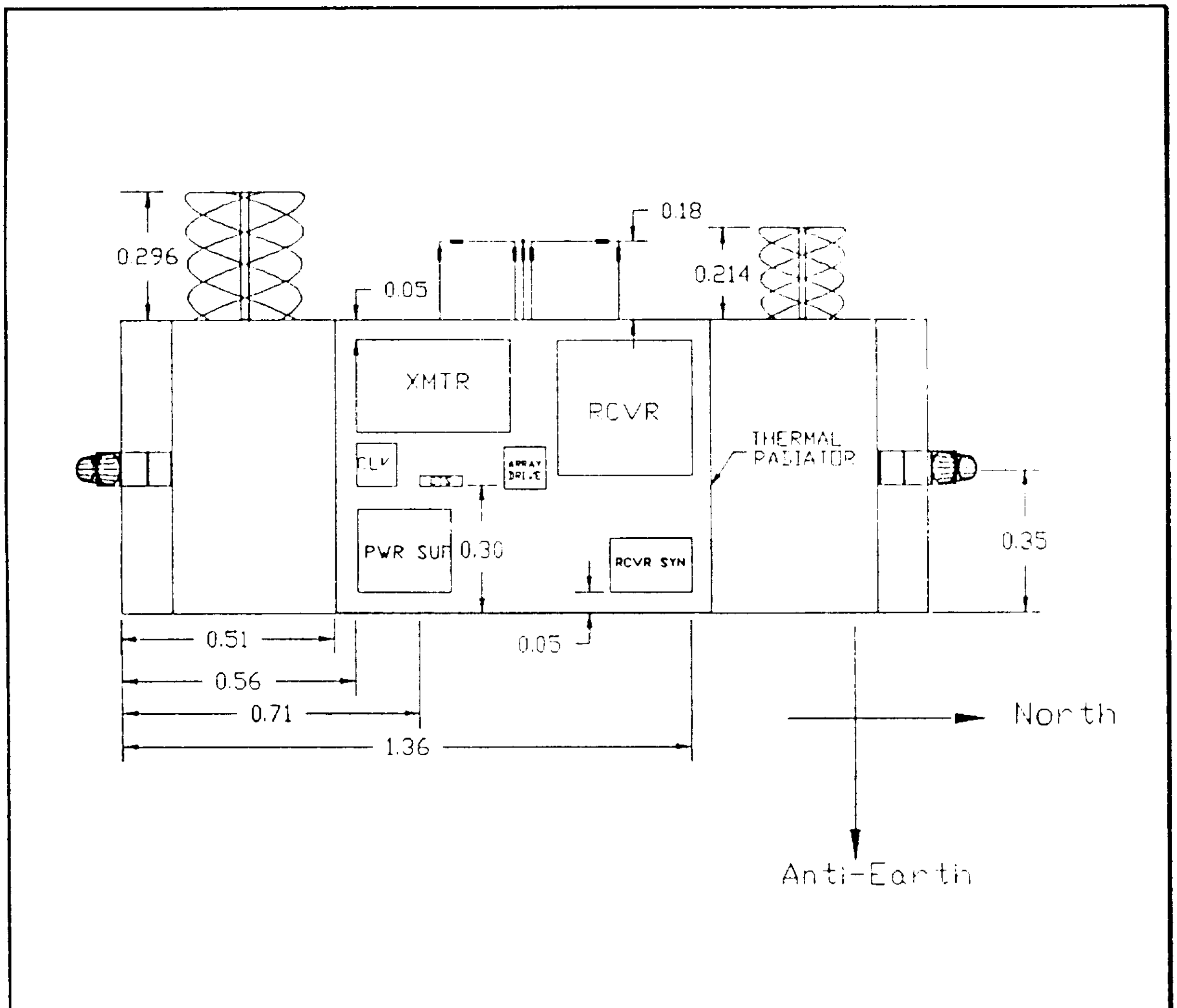

Figure III-6. West Face.

4. East Face (Fig. III-7).

The telemetry subsystem and the electrical power subsystem are mounted on the east face. The second thermal radiator is centered on this face. Extending from the center of the face is a solar array assembly identical to the one on the west face.

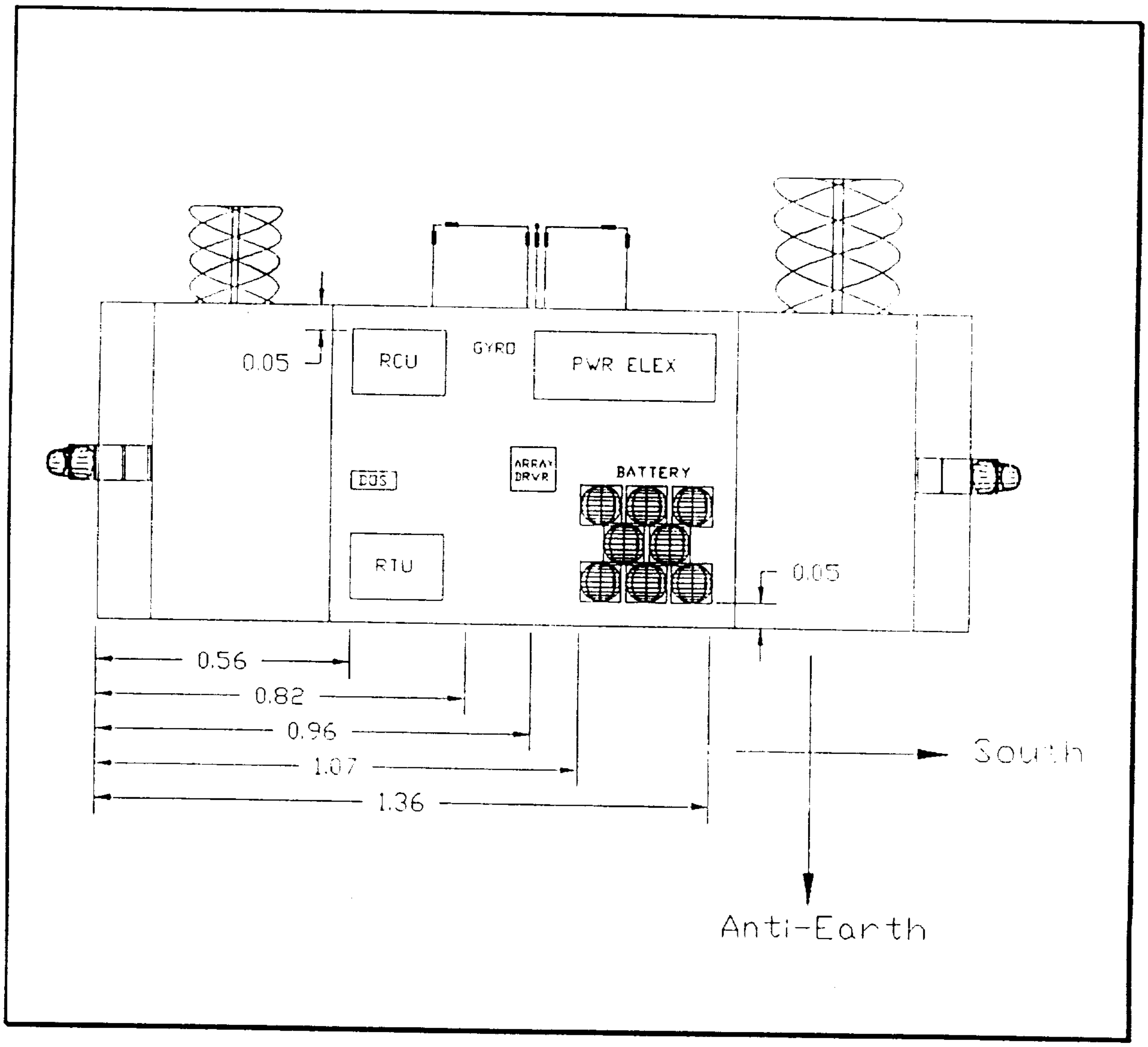

Figure III-7. East Face.

5. North Face (Fig. III-8).

The attitude control computer and electronics assembly is mounted on the north face. Two sun sensors are mounted centered along the earth and anti-earth edges.

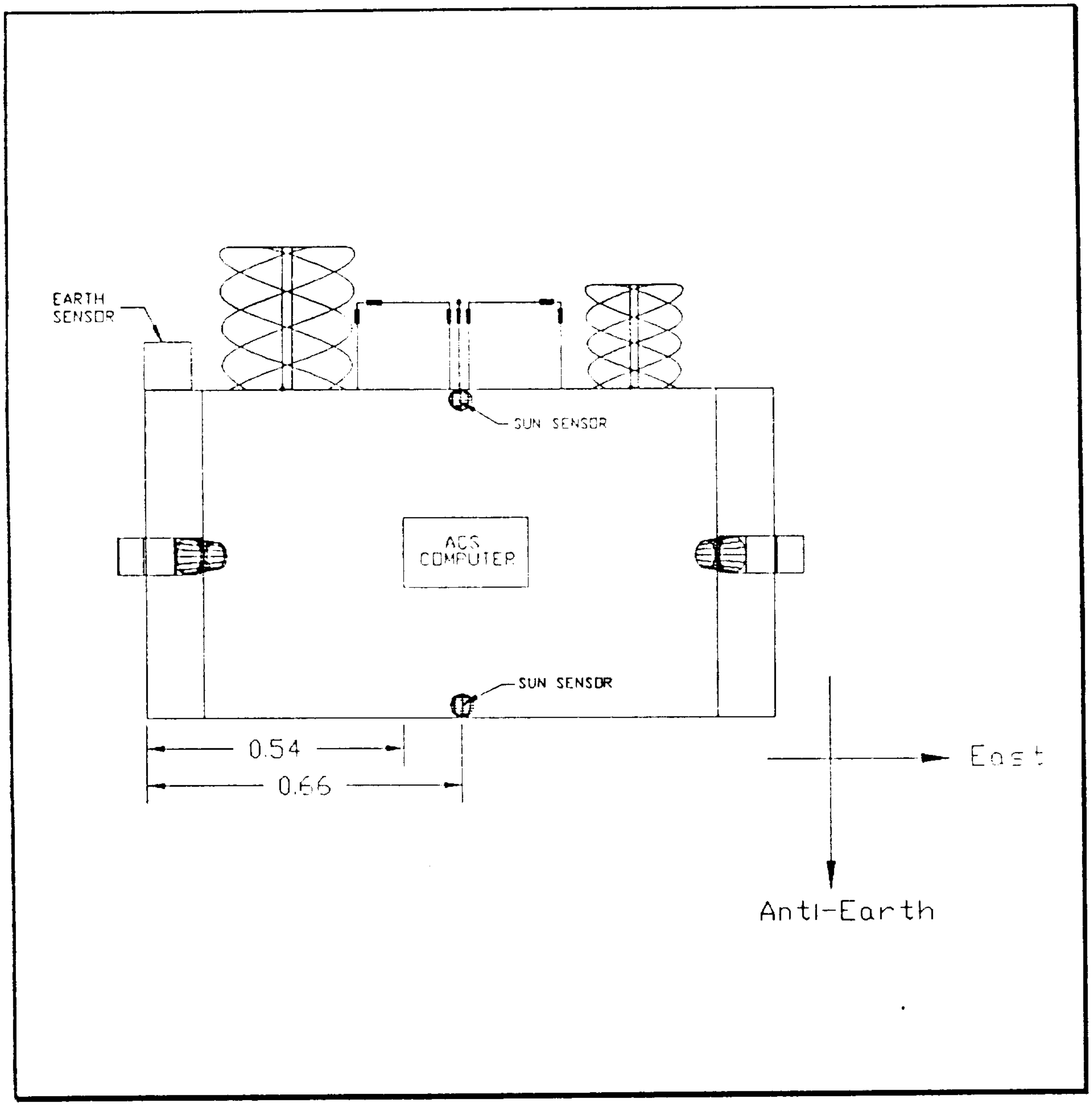

Figure III-8. North Face.

6. South Face (Fig. III-9).

The pitch-axis reaction wheel is mounted on the south face. Two more sun sensors are mounted in the same configuration as on the north face.

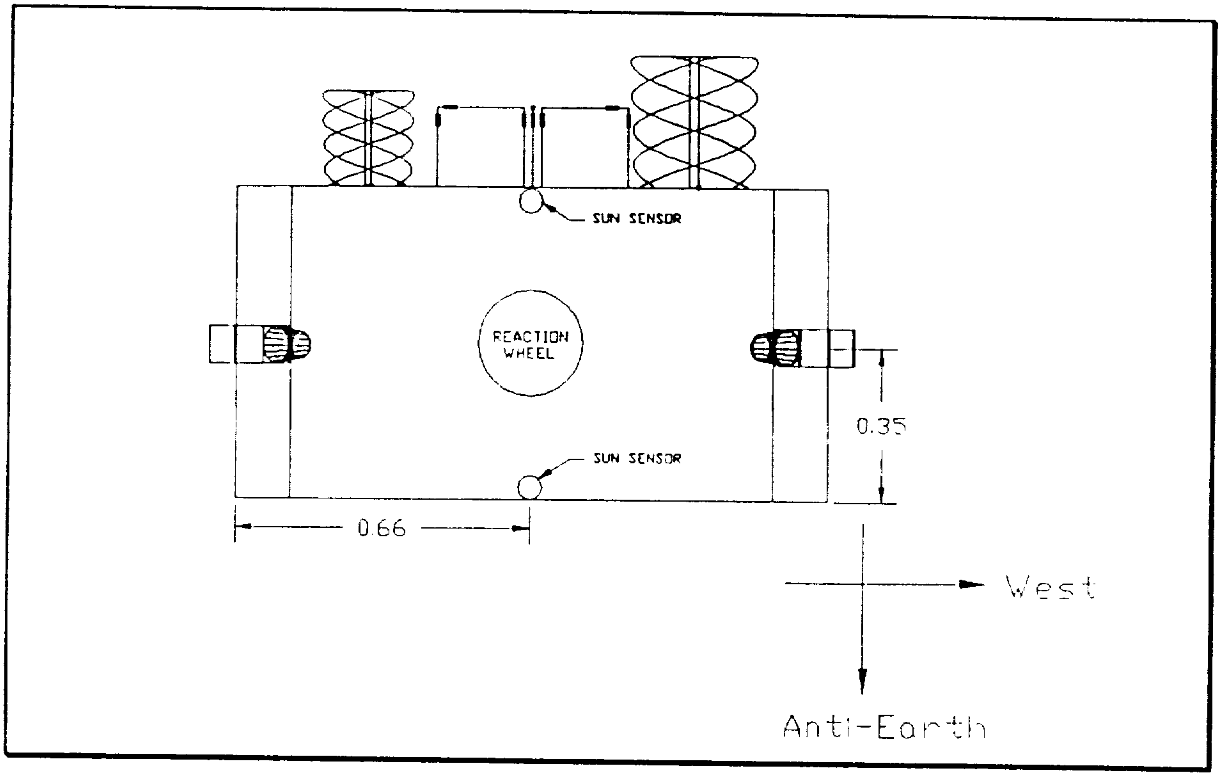

Figure III-9. South Face.

B. STRUCTURE SUBSYSTEM

The structure subsystem design began with initial sizing of the cylindrical support, frustum interface shell, and equipment panels. Aluminum 6061-T6 was chosen for reasons of ease of machining and its strength-to-weight ratio. The structural configuration was designed to accommodate a Delta II launch with three satellites in a stacked configuration.

1. Functional Description

The functional requirements of the spacecraft structure are to support the weight of three spacecraft under design loads for a Delta II. A design tradeoff for the spacecraft was to employ identical designs for all three spacecraft. This forces an overdesigned structure for two of the three spacecraft. The spacecraft is designed to support loads through the central support assembly. This assembly consists of a frustum cone shell attached to the Delta II 3712B interface, a central cylindrical shell, and a similar frustum cone shell at the top of the spacecraft which attaches to the interface between each spacecraft.

A majority of the equipment mass is located on the East and West panels which are designed to withstand 30 g's and have a fundamental frequency above 25 Hz. The panels were designed to support 92.2 kg each of equipment mass. Load paths are provided to the central support assembly by means of panels attached to the North and South ends of the equipment panels. These support panels are also used to secure the four propellant tanks for axial loads. Lateral load support for the propellant tanks is provided by struts attached to the top and bottom of the tanks and to the central support assembly.

2. Subsystem Design

Table III-1. Design Constraints for Delta II Launch.

Natural Frequencies	Lateral	Axial
Spacecraft	15 Hz	35 Hz
Equipment Panel	25 Hz	35 Hz
Solar Panel	35 Hz	-
Limit Loads		
Max. Lateral Condition	3.0 g	2.2 g
Max. Axial	-	6.0 g
Lateral Dynamic Loads	30 g	-
Factor of Safety = 1.5		
Margin of Safety = 10%		

a. Central Support Assembly

Table III-1 gives the design constraints of a Delta II launch. The central support assembly is shown in Fig. III-10. This assembly provides the load path for the equipment panels, propellant tanks, and two other satellites. The central support assembly is an aluminum monocoque structure using aluminum 6061-T6.

The fundamental frequency for the stacked configuration in lateral bending was found to be well below the required 15 Hz for the Delta II launch. Because of this, the thickness values for the central support assembly were increased to raise the fundamental frequency for lateral bending. The values used are shown in Fig. III-10.

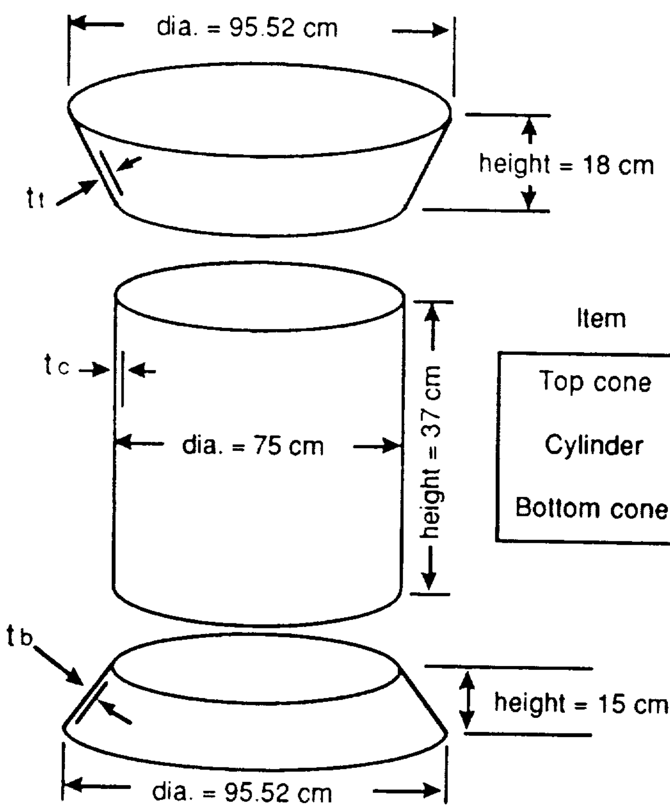

Item	Thickness for static loading	Thickness used in finite element
Top cone	1.826 mm	3.50 mm
Cylinder	1.369 mm	3.50 mm
Bottom cone	3.424 mm	7.00 mm

Figure. III-10. Central Support Assembly.

b. Equipment Panels

The equipment panels, located on the East and West faces of the satellite, are made of aluminum 6061-T6 honeycomb sandwich material. These panels were designed to support 92.2 kg of component mass under 30 g's dynamic loading and to have a fundamental frequency above 25 Hz. Fig. III-11 shows the equipment panel thickness values. The honeycomb material used for the equipment panels was used throughout the spacecraft for the North, South, Earth-facing, anti-Earth facing, attachment panels, and propellant support panels.

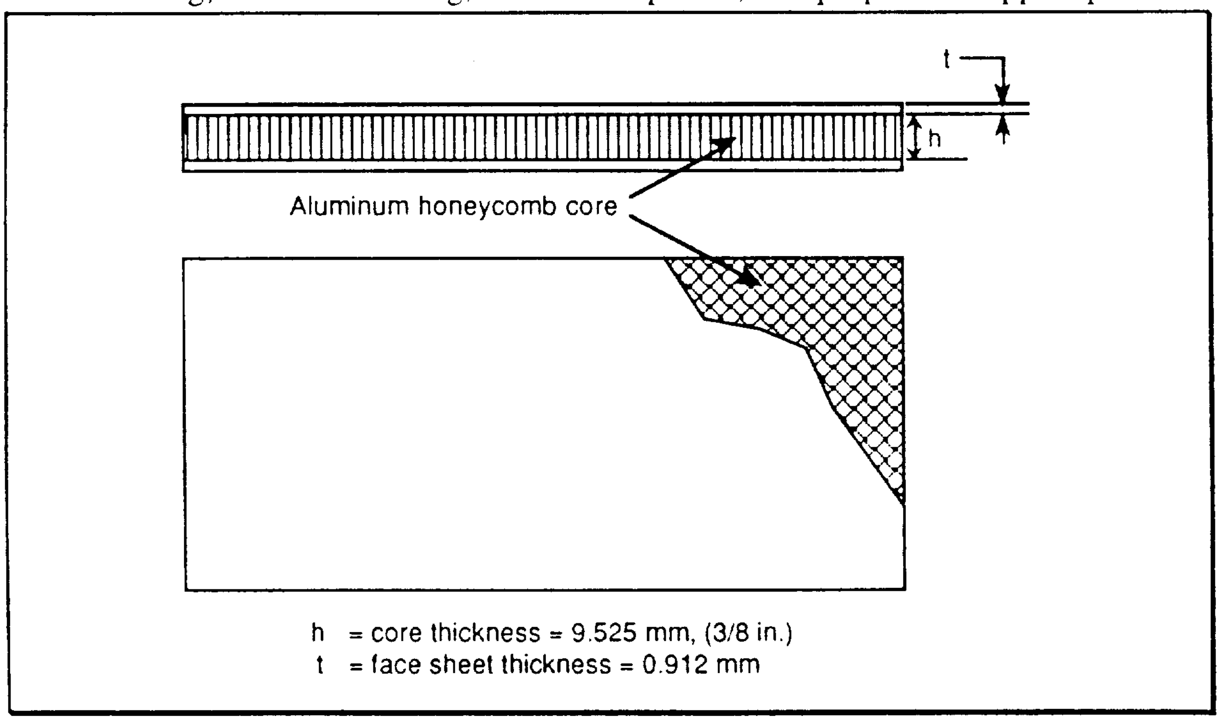

Figure. III-11. Aluminum Honeycomb Panel.

Figure III-12 shows the configuration for the propellant tank support panels. The propellant tank supports use the same honeycomb sandwich material used for the equipment panels for axial support of the propellant tanks. Lateral support is provided by four hollow cylindrical struts attached at the top and bottom of the propellant tanks and to the central support assembly. The hollow cylindrical struts are 5.08 cm (2 in.) outer diameter, and have thickness of 1.5 mm.

c. Propellant Tank Supports

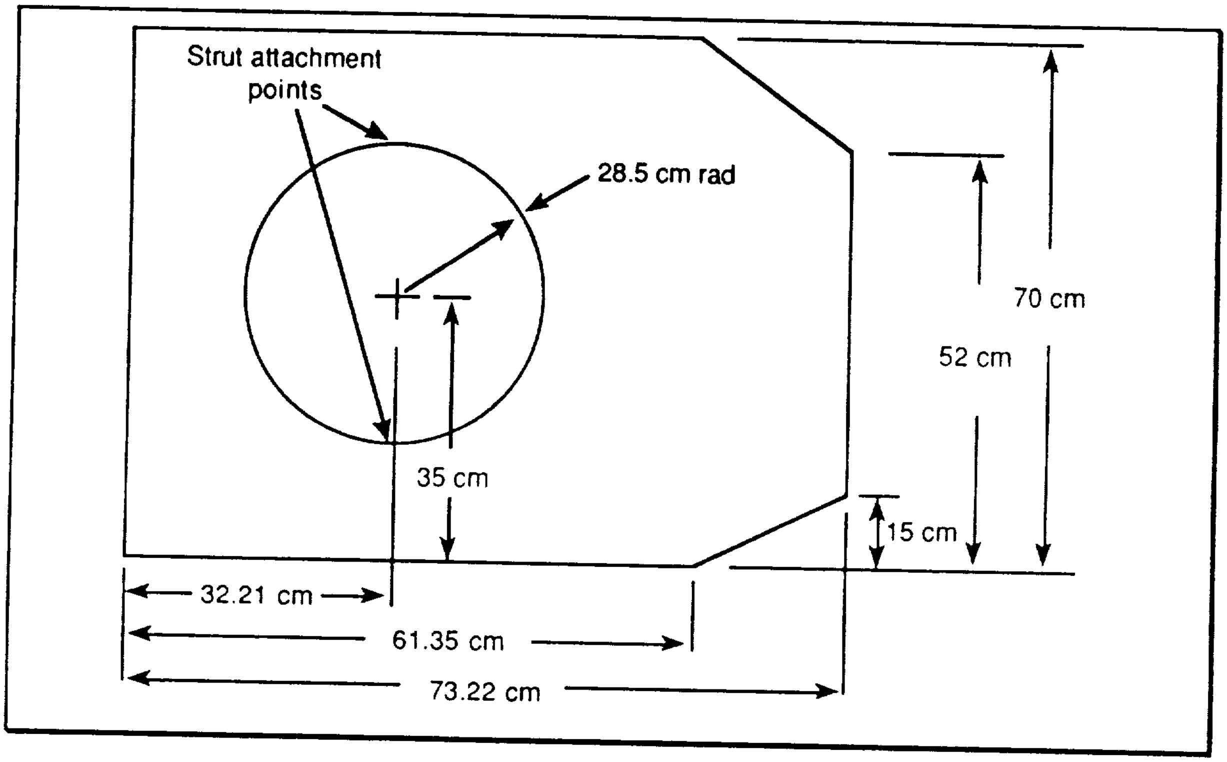

Figure. III-12. Propellant Tank Support Panel.

d. Solar Array Panels

The solar array panels are also aluminum honeycomb sandwich material but have dimensions of 1.65 m by 0.51 m, and mass of 6 kg. The fundamental frequency of the solar array panels in the stowed configuration (folded in half) is 497.6 Hz. The solar array design was driven by the need to shield the back of the solar cells from radiation rather than any structural requirements. The solar array honeycomb material has core thickness, $h = 16$ mm, and face thickness, $t = 0.13$ mm. The frequencies for the deployed solar cell arrays were not considered.

e. Modal Frequencies

The modal frequencies and eigenvalues of the spacecraft are given in Table III-2. The first six modes are modes of the equipment panels (East and West panels). Lateral bending of the spacecraft is not evident until the seventh mode which has a frequency of 104.0 Hz. The fundamental frequency for lateral bending of the stacked configuration was estimated by calculating an effective stiffness of the spacecraft and modeling the three stacked satellites as a uniform cantilever beam. The fundamental frequency for the stacked configuration was estimated at 6.22 Hz. Due to the limitation on time, the frequency issue could not be resolved.

Table III-2. Modal Frequencies and Eigenvalues for Spacecraft.

Mode	Frequency (cps)	Eigenvalue
1	42.71	7.2004D+04
2	42.99	7.2946D+04
3	68.02	1.8264D+05
4	68.12	1.8318D+05
5	80.69	2.5706D+05
6	81.47	2.6201D+05
7	103.99	4.2690D+05
8	119.52	5.6391D+05
9	129.11	6.5813D+05
10	129.39	6.6095D+05

The frequency given for this spacecraft configuration is still below the design constraint of a payload for the proposed Delta II launch. Remedial options may be to: (i.) secure the stacked spacecraft payload at a number of points along the axis, (ii.) increase the moment of inertia of the support cylinder and frustum shells, (iii.) choose a material for the support cylinder and frustum shells that has higher stiffness such as beryllium, (iv.) use a combination of the options, or, (v.) perform additional analysis considering the dynamic coupling between the payload and the launch vehicle to determine if the low fundamental frequency for the stacked configuration is indeed an unsatisfactory condition.

f. Structure Mass Summary

Table III-3 is a summary of the structural elements and associated masses. Estimates of the peripheral support elements such as the brackets/fasteners and support rings are values taken from the Intelsat V satellite. An additional 4.54 kg (10 lbs) was added as an estimate of the required attachment fittings for the assembly of the main support structure which involves mating the support cylinder with the two frustum shells and the attached panels (Earth facing and Anti-Earth facing panels).

Table III-3. Structural Mass Summary.

Structural Element	Mass (kg)
West Face Equipment Panel	0.918
East Face Equipment Panel	0.918
Lower Frustum of Cone	9.082
Cylindrical Support	8.192
Upper Frustum of Cone	5.221
(4) Propellant Support Panel	0.162
(8) Short Hollow Circular Strut	0.271
(8) Long Hollow Circular Strut	0.383
(4) Attachment Panel	0.086
North Face	0.624
South Face	0.624
Earth Facing Panel	1.670
Anti-Earth Facing Panel (with hole)	1.179
Structural Fasteners/Brackets	1.840
(2) Conical Support Ring	0.274
(2) Cylinder Support Ring	0.163
(4) Tank Ring	1.180
Support Structure Assembly Fittings	4.536
Total	**46.622 kg**

3. Subsystem Performance

The structure subsystem has arrived at a design with considerable margin for the prescribed loads of a Delta II launch. The lower frustum shell which interfaces with the 3712B attachment fitting of the Delta II has a margin of safety, M.S. = 359 %. This is due to the increase in thickness to 7.00 mm of the bottom frustum shell in trying to accommodate the stacked configuration frequency problem. The cylinder of the central support assembly has M.S. = 836.4 % as a result of the increase in thickness to 3.50 mm. The top frustum shell with a thickness of 3.50 mm has M.S. = 304 %.

The spacecraft shows a fundamental frequency of 42.71 Hz for the finite element model. This mode is the two equipment panels oscillating in phase. An increase of 184.7 % in the frequency of the equipment panels from the required 15 Hz is evident. This is due mainly to a decrease in the required mass the equipment plates support from the initial design. The problem of a low lateral frequency for the stacked configuration remains unresolved, however.

The propellant tank supports have been designed to support the loads for the propellant tanks. However, the hollow cylindrical struts used for lateral support of the propellant tanks have not been optimized. This may be a task for follow-on work. Additional work in the structures area may include: (i.) analysis of the solar arrays in the deployed configuration, (ii.) design of a mechanism for the deployment of the solar arrays, (iii.) resolving the lateral bending frequency problem of the stacked launch configuration, and (iv.) optimizing the design for structure weight.

The structure mass of 46.6 kg shows 11.4 % of the total spacecraft weight. Although the mass fraction is high, this is due mainly to the stacked configuration for launch.

C. MASS SUMMARY

Table III-4. Mass Budget

SUBSYSTEM	MASS (KG)
TT&C	13.712
PAYLOAD	21.871
ATTITUDE CONTROL SYSTEM	17.130
ELECTRICAL POWER SYSTEM	48.550
REACTION CONTROL SYSTEM	34.666
THERMAL CONTROL SYSTEM	42.634
STRUCTURE	46.622
DRY MASS	225.185
PROPELLANT	145.212
WET MASS	370.397
MARGIN	41.520
TOTAL MASS	411.917

Table III-5. Propulsion Mass Breakdown.

Propellant (stationkeeping)	136.77 kg
Propellant (delta V change)*	7.21 kg
Propellant (desaturation)**	1.00 kg
Twelve 2-N Thrusters (12x0.319 kg)	3.83 kg
Four 38-N Thrusters (4x0.735kg)	2.94kg
Tanks (4x5.897kg)	23.59kg
Tubings, Valves and Fittings	4.31 kg
Nitrogen Pressurant	0.23 kg
Total	**179.88 kg**

* See Appendix A for computation.

** See Appendix F for computation.

D. POWER SUMMARY

Table III-6. Satellite Power Summary

Power Requirements	Power (watts)
Payload	101.05
TT & C	11.22
EPS	20
ACS/RCS	70
Thermal Control	50
Wire Losses	7.05
Total Loads	259.32
Battery Charge Power	52.5
Total Sunlight Load	311.82
Ten Percent Margin	31.18
Total Design Power	343.00

Table III-7. Eclipse loads

Eclipse Power Requirements	Power (watts)
EPS	20
ACS/RCS	70
Thermal	50
Total Eclipse Loads	140

IV. PAYLOAD

A. FUNCTIONAL DESCRIPTION

1. Requirements

a. Mission

The mission of this satellite dictates a highly elliptic orbit at a 63.4° inclination. The ground stations are assumed to be located anywhere above 60° North latitude. To link these stations with a geosynchronous satellite, a central station, acting as a hub, must be located within the footprint of a geosynchronous satellite and HILACS. The location of this net control station (NCS), must be approximately 60° North latitude. A fourth site must be considered as well. This site is the source for data transmitted to the geosynchronous satellite and, it will be assumed, is the location for ground control for its net of satellites including HILACS. It will be assumed that this station is located at approximately 40° North (a location which maximizes the number of possible locations on the earth) and it will be designated the mid-latitude ground station (MLG).

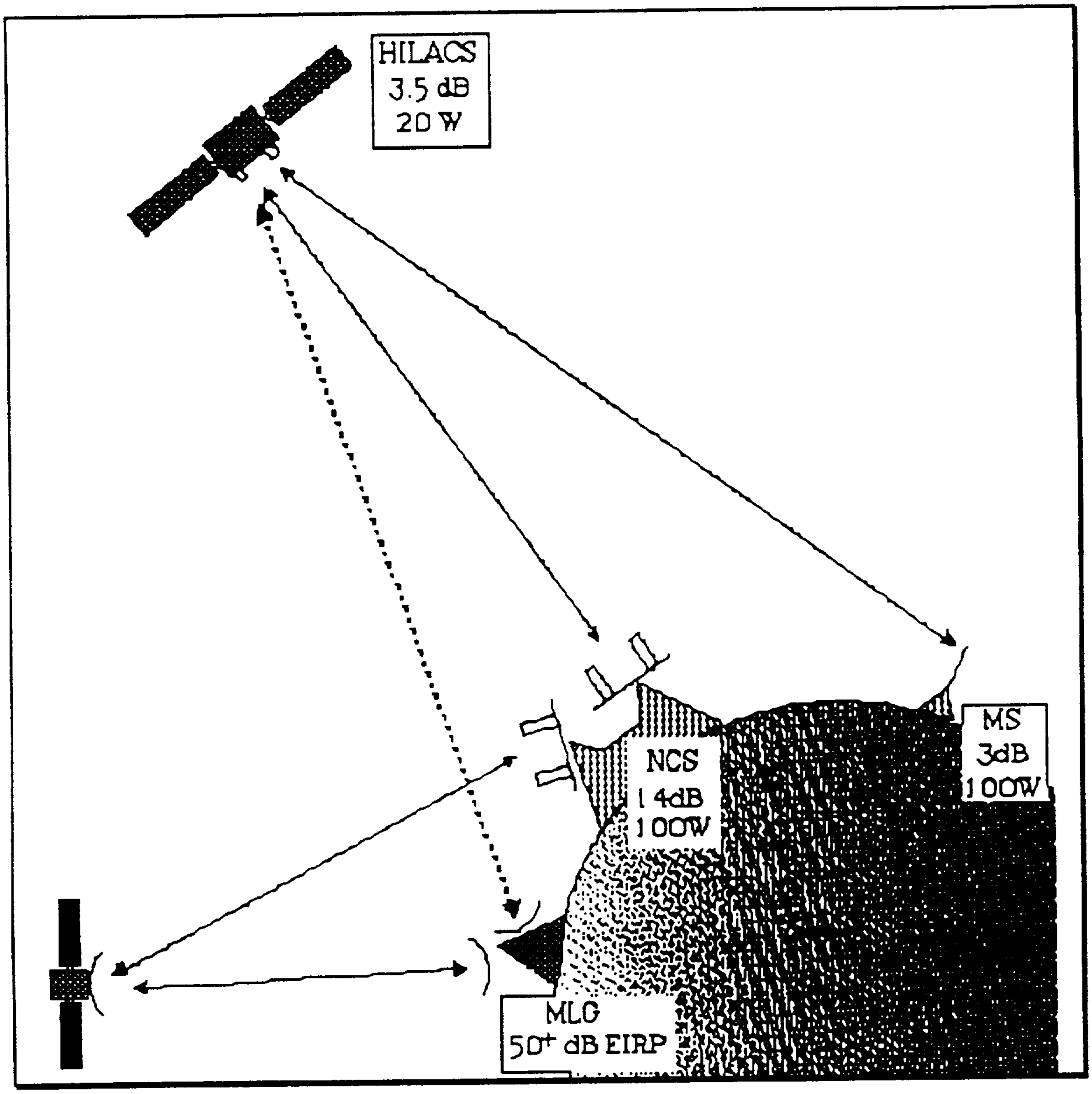

Figure IV-1

b. Frequency and Data Rate

The communication system operates at UHF with an uplink frequency of 350 MHz and a downlink frequency of 253 MHz. The link will operate at a data rate of 4800 bps using coherent BPSK modulation. For this link, as will be explained later, a linear block error correction coding scheme is used resulting in a coded bit rate of 9600 bps.

2. Summary of Subsystem Operation

a. Operating Scheme

The net operates in a hub-polling scheme in which the NCS controls access to the net in accordance with the needs of the users. This style of operation permits a variable number of users and maximizes the channel's data rate for this simplex link. The NCS polls each station prior to transmit to ensure it is ready to receive data and if they have any data to transmit. The NCS then relays data from the MLG (via a geosynchronous satellite) and from other stations on the net to the specific station. It then receives data from the station and readdresses these messages for further relay. It then repeats the process for each station on the link.

b. NCS Functions

The NCS monitors satellite positions and ephemeris and predicts the position of the next ascending satellite. It establishes link with the ascending satellite and performs a systems check prior to its activation. The NCS then determines the optimal altitude to introduce this satellite into the net and to release the descending satellite. It is conceivable that the NCS could operate two satellites simultaneously to ensure the most reliable communications throughout the region above 60° North latitude. The NCS also monitors the satellite health transmitted via the link.

c. MS Operations

The mobile ground stations, with their wide beamwidth, low gain antennas, need only turn on their receivers to the default position and wait to be polled. Once polled, they establish link and move to an allocated slot for the remainder of their time on the link.

B. SUBSYSTEM DESIGN AND HARDWARE DESCRIPTION

1. Link Parameters

Since this link is operated in a simplex mode only, its bandwidth is not limited as in a typical multiple access system. For this link a bit-duration bandwidth product of 2.0, resulting in a bandwidth of 19.2 kHz, is used as a compromise between minimizing the noise bandwidth and the intersymbol interference.

2. Equipment Parameters

a. MLG

It is assumed that the MLG is an established site with high gain antennas, high power transmitters and low noise receivers. Since the telemetry system operates in UHF, a high gain helical antenna array with 25 dB of gain is used. The transmitter will have a capability of up to 1000 W (30 dBW), so it will be optimally adjusted to maintain an EIRP (P_tG_t) just below saturation for the satellite system. The receiver system will have an effective temperature (T_e) of 150°K.

b. NCS

The NCS has two sets of helical arrays with 14 dB of gain. This value of gain is based on a requirement for a greater beamwidth at this site. The greater beamwidth will allow for a less accurate pointing system to compensate for the satellite movement during their operational periods. The station will require two of these antennas to provide a link with the active, descending satellite and with the ascending satellite in preparation for its activation. The effective noise temperature (T_e) at the receiver front end is computed to be 290°K for a noise figure of 3 dB relative to 290°K. It will be assumed that this station can transmit with a power of 100 Watts (20 dBW).

c. MS

The ground stations are assumed to be mobile limiting their antenna to a crossed dipole design with a gain of 3 dB. The receivers' noise figure is 6 dB causing them to have T_e's of 865°K. The station's transmit power is also assumed to be 100 Watts (20 dBW).

d. Satellite

The satellite antennas have gains of 3.5 dB with a transmit power of 20 Watts (13 dBW). The receiver's noise figure is assumed to be 2 dB.

e. Component System Temperatures

Before the link budget calculations can be performed the system temperature of each component must be calculated and the losses expected in the link must be determined. The system temperature is calculated after the antenna cable and at the receiver front end. The receiver noise figures relative to 290°K were listed earlier, the coaxial cable temperature is also assumed to be 290°K for each system. The antenna temperature (T_a) is dependent upon the gain of the antenna and the direction it is pointing. The MLG, with its relatively high gain antenna, which is pointing away from the earth has an assumed temperature of 150°K. Because the NCS and the mobile stations have low gain antennas with a correspondingly wider field of view, their T_a is assumed to be approximately the temperature of the earth or 290°K. Since the satellite's antenna is pointing at the earth its T_a is also equal to 290°K.

3. Losses

a. Link Losses

The losses associated with a communications link are typically atmospheric loss and free space propagation loss. At UHF atmospheric loss is small and can be neglected [Ref. 7; pg 235]. Free space loss (L_s) is approximately 190 dB for the ranges in this link.

b. Interference Effects

The other interference affects in this link are due to intersymbol interference (ISI) which is due to bandlimiting the signal, the propagation effects from multi-path interferences and reception of other signals (and their harmonics) within the system bandwidth.

i. ISI

Since this link is operated at a relatively low channel capacity a relatively large bandwidth of twice the bit rate, or $2R_b$ is used. The large bandwidth minimizes the effect of ISI [Ref. 8; pg 444].

ii. Fading

Multi-path, or fading is caused by several factors including: transmitter to receiver geometry, terrain features, antenna gain and elevation angle. This link will be exercising the extremes in all of these factors and so it is estimated that fading will have a much more severe affect for this link than ISI. Because the geometry will be changing due to the relative motion of the satellite and ground stations the effect of fading will be time varying. Terrain effects can be minimized by optimizing the location of the ground station. To decrease the effect of the fading which will appear in the form of a "burst error," a linear block code is used in the signal. This block code with a code rate of twice the data rate is effective when fades last for short periods of time. If long term effects plague the ground station, modifications may be necessary such as elevating the ground plane, to limit multipath, adding an second antenna to create spatial diversity, installing a directional, tracking antenna or moving the ground station to a site less susceptible to the effects of multi-path.

iii. Interference

The military UHF operating band established for this transponder is separated in frequency from the strong VHF signals such as TV and the heavily populated commercial systems in use throughout the world It is also below the SHF bands that are typically used by communication satellites. The interference effects will be due to harmonics of military UHF voice communications. These effects will be more transient than the fading effects, so the block coding should effectively minimize this interference effect.

4. Antenna Design

a. Requirements

i. Design Criteria

For the system operation the required minimum beamwidth is 28°. Such a beamwidth would correspond to an antenna gain of approximately 15 dB and a structure too large and too massive for this spacecraft. Since high directivity is not a constraint the minimum gain required for the link was computed be performing serval iterations of link calculations. The results indicated that a satellite antenna gain of 2-3 db will not significantly degrade performance of the link. With the gain requirement relaxed other constraints could be included in the antenna design. For ideal stacking of the satellites on the launch vehicle a maximum separation of .3 m was required. An antenna was chosen which would fit in this area and also provide the required operational characteristics.

ii. Operating Bandwidth

With the tight constraint on the antenna dimensions the antenna designs chosen had to be resonant and therefore have an operating bandwidth of approximately 4% [Ref. 9]. Therefore, a separate antenna was required for the uplink and downlink. Additionally, a third antenna designed to operate on both frequencies was used for the telemetry.

b. Description

i. Resonant Quadrifilar Helix

This antenna was chosen since it is compact, has a wide beamwidth (approximately 110°), it is simple in design and has circular polarization. The antenna was sized using the following equation [Ref. 10].

$$L_{ax} = N\sqrt{\frac{1}{N^2}(L_{ele} - Ar_0)^2 - 4\pi^2 r_0^2} \tag{4-1}$$

where L_{ax} is the axial length of the antenna, L_{ele} is the length of one element and r_0 is the radius of the antenna. To determine the size of the uplink and downlink antennas several combinations of values of r_0, L_{ele} and N were used in equation (4-1). This analysis resulted in determining that a quarter-turn, half-wavelength antennas with dimensions of approximately one-quarter wavelength for L_{ax} and $2r_0$ are optimal.

ii. Crossed Dipole

This antenna was used as a backup for the quad-helixes and as the transmit and receive antenna for the TT&C system. It is composed of two orthogonal, center fed, half-wavelength antennas [Ref. 11]. The antenna is sized for the downlink frequency of 253 MHz, for a length of .593 m. It has a resonating circuit, (a trap) which electrically shortens the antenna for the higher uplink frequency of 350 MHz or .429 m. The antenna is placed at .15 m above the ground plane to create the required radiation pattern [Ref. 12].

TABLE IV-1. MASS/POWER SUMMARY

Subsystem	Mass(kg)	Avg Power (W)
Receiver	6.73	7.02
Freq Synthesizer	1.73	5.25
Power Supply	1.82	2.06
Transmitter	6.18	35.00
Clock	0.45	1.20
Uplink Antenna	1.5	
Downlink Antenna	1.68	
TT&C Antenna	0.45	
Ground Plane	0.42	
Coaxial Cable	.91	

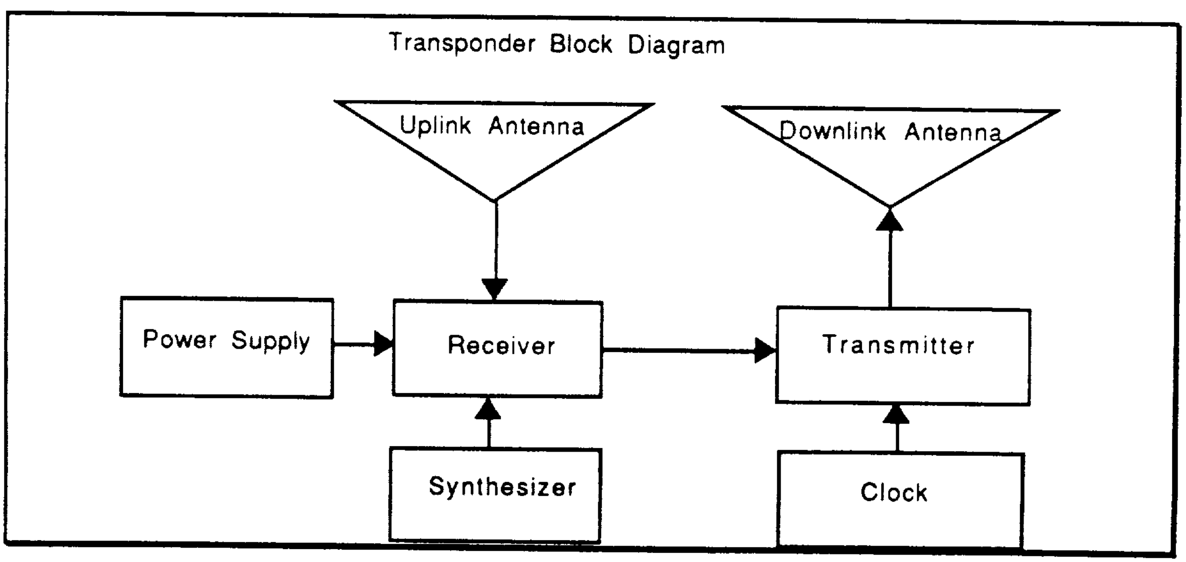

Figure IV-2

C. Subsystem Performance

1. Link Budget Calculations

a. Requirement

The link budget calculations were performed for each worst case two-way communication path. Worst case was considered as the point in which the satellite was at apogee and the two stations were at a maximum slant range based on an elevation angle of 5°.

b. Description

The total link carrier to noise ratio was computed by individually computing the the uplink and downlink carrier to noise ratios with the following formulas [Ref 8; pp 131,133]:

$$\left(\frac{C}{N}\right)_u = \frac{EIRP}{L_a L_T}\left(\frac{c}{4\pi f_u d_u}\right)^2\left(\frac{G_u}{T_u}\right)\frac{1}{kB} \tag{4-2}$$

and

$$\left(\frac{C}{N}\right)_d = \frac{EIRP}{L'_a L'_T}\left(\frac{c}{4\pi f_d d_d}\right)^2\left(\frac{G}{T}\right)\frac{1}{kB} \tag{4-3}$$

With these values calculated the carrier to noise ratio for the link was calculated using [Ref. 8; pg 134]:

$$\frac{C}{N} = \left[\left(\frac{C}{N}\right)_d^{-1} + \left(\frac{C}{N}\right)_u^{-1}\right]^{-1} \tag{4-4}$$

2. Margin

The values for the carrier to noise ratios for the communication paths between the NCS to the MS, the MS to the NCS and the MLG to HILACS for

TT&C. The values were then converted to energy per bit to noise spectral density ratio (assuming only additive white gaussian noise in the link) and a margin, in dB was determined. To calculate the margin, it was assumed that the probability of bit error Pb(E) was assumed to be small ($<10^{-6}$) which permitted an approximation for the complementary error function to be used. The following equation was used:

$$P_b(E) = \frac{1}{\sqrt{2\pi}} \sqrt{\frac{N_o}{E_b}}\, e^{-\left\{\frac{\left(\frac{E_b}{N_o}\right)^2}{2}\right\}} \qquad (4\text{-}5)$$

b. Results

The link budgets are listed in table D-1 thru D-3. The following results were obtained:

TABLE IV-2. LINK MARGIN

Link	Margin(dB)
NCS-MS	30.48
MS-NCS	41.48
MLG-HILACS	63.65

V. ELECTRIC POWER SYSTEM DESIGN

A. FUNCTIONAL REQUIREMENTS

The electrical power system (EPS) performs the functions of electrical power generation, storage, conditioning and distribution for the on-orbit operation of the satellite. The majority of the generated power is consumed by the communications payload, with the balance used for the general operation of the spacecraft bus; attitude control; thermal control; telemetry, tracking and control (TT&C); and the electric power system itself. The communications payload system will operate only when the satellite ground track is above 50° N latitude. The TT&C system will operate only during sunlight periods of the cycle. The remaining systems will require power throughout the orbit.

The general system configuration consists of two flat panel arrays for sunlight period power and storage batteries for eclipse periods. The cell type used for the array is 6 mil thick GaAs cells manufactured by Spectrolab. These cells are made from an 11 mil substrate and milled to a 6 mil thickness to reduce mass. The batteries are 12 amp-hour nickel-hydrogen batteries manufactured by Eagle Picher. The spacecraft is earth pointing, three-axis stabilized with the satellite/array combination providing two degrees of freedom to maintain the array's normal incidence to the sun.

1. Requirements and Overview

The spacecraft bus will operate off of a single 28 volt bus.. Tables V-1 and V-2 provide summaries of the end of life (EOL) maximum and eclipse load power requirements of the satellite. For design purposes, the satellite is assumed to be launched at apehelion and thus the three year period will end at apehelion.

TABLE V-1. SATELLITE POWER REQUIREMENTS

Power Requirements	Power (watts)
Payload	101.05
TT & C	11.22
EPS	20
ACS/RCS	70
Thermal Control	50
Wire Losses	7.05
Total Loads	259.32
Battery Charge Power	52.5
Total Sunlight Load	311.82
Ten Percent Margin	31.18
Total Design Power	343.00

TABLE V-2. ECLIPSE LOADS

Eclipse Power Requirements	Power (watts)
EPS	20
ACS/RCS	70
Thermal	50
Total Eclipse Loads	140

2. Summary of Subsystem Operation

The subsystem will be arranged as shown in figure V-1. The shunt regulator will maintain the bus voltage at 28 volts during sunlight periods and the battery charge/discharge unit is responsible for maintaining eclipse loads and charging the battery. The arrays are switchable to allow for single array operation during periods when the required power is less than one array can supply. Auxiliary voltage levels of 32 and 42 volts for use by the propulsion and attitude control subsystems will be generated from the 28 volt bus using dc-dc converters.

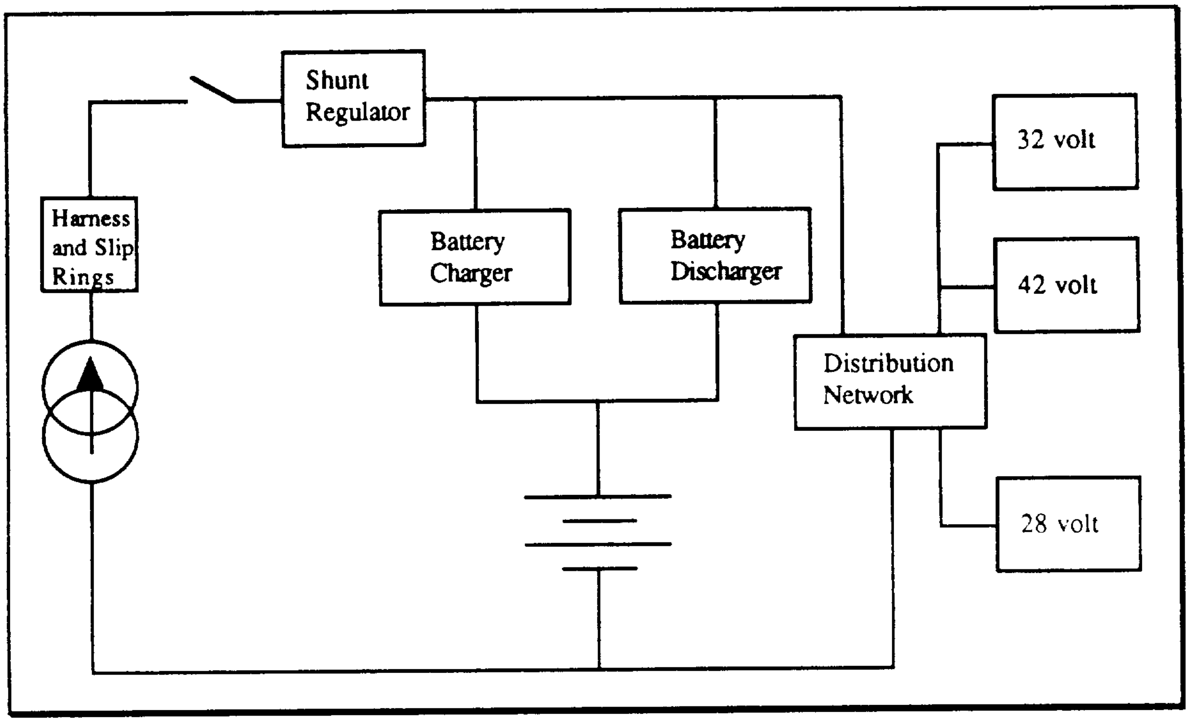

Figure V-1. Functional Block Diagram of EPS System

B. EPS DESIGN AND HARDWARE DESCRIPTION

1. Solar Array Design

The solar arrays are designed to perform as flat panel arrays maintaining a normal incidence to the sun. This orientation is accomplished by having two degrees of freedom in the system: 1) satellite rotation about the yaw axis, and 2) solar array rotation about the array longitudinal axis. The arrays will be split into two independent, switchable systems to allow for their individual operation in order to minimize the requirement for power dissipation during satellite beginning of life (BOL). One array will be switched off line until bus voltage requirements dictate it be activated.

The selected GaAs solar cells have an effective area of 7.97 cm^2 in a 2 cm by 4 cm rectangular cell and an areal mass of 0.086 g/cm^2. Prior to milling, the 11 mil cells have an areal mass of 0.154 g/cm^2. The milling process saves 55% on the mass of the cells. The cells used in the array have the following capabilities under AM0 conditions:

- I_{sc} = 232.0 mA
- V_{oc} = 1014.0 mV
- I_{mp} = 219.5 mA
- V_{mp} = 876.0 mV
- P_{mp} = 192.3 mW
- Efficiency = 17.83%

a. Radiation Effects and Shielding Requirements

The orbit apogee of 8063 nm places the satellite in the lower portion of the Van Allen radiation belts. The resulting radiation effects on the solar cells are extreme and represent the primary limiting factor of the satellite lifetime. To determine the radiation received by the cells, the orbit is divided into altitude bands and the fraction of time the satellite is in each band is calculated. A yearly radiation flux is computed from tabulated data using these prorated altitudes, and the total radiation is the sum of the amounts received from the panel front and back over the three year period.

The array will be mounted on a substrate of 16 mm thick aluminum honeycomb core with a 0.13 mm aluminum facesheet. The array substrate thicknesses and shielding effectiveness are listed in table V-3. [Ref. 14, vol. 1:p. 12.2-1]

TABLE V-3. ARRAY SUBSTRATE RADIATION EFFECTS

Structure	Thickness (cm)	Shield Effectiveness (mm)
Thermal Paint	0.0043	0.03
Al Facesheet	0.013	0.16
Core Adhesive	0.007	0.06
Al Core	1.6	0.19
Core Adhesive	0.007	0.06
Al Facesheet	0.013	0.16
Epoxy/Glass	0.01	0.08
RTV-118	0.007	0.03
Total Thickness	1.6613	0.77
Back Shield Thickness	(in mils)	30.315

The primary goal of the solar array design is to provide required EOL power while minimizing the mass of the arrays. Toward this end, a comparison was made of array mass using both 30 mil and 20 mil coverslips. Although 20 mil coverslips experience more radiation degradation and result in larger arrays, they still satisfy EOL power requirements with less mass than the 30 mil coverslips, and were therefore chosen for the design. All calculations from this point are for the 20 mil cover slips.

Table V-4 lists the satellite altitudes, the time spent between each altitude for each orbit, and the front and back shield radiation effects for one MeV electrons in one year. Table V-5 lists similar data for proton effects on voltage and current. [Ref 13:pp. 3-141–3-152, 6-37–6-39]

TABLE V-4. ORBIT ALTITUDE VS. ELECTRON RADIATION EFFECTS

Altitude (nm)	Time In Range (min)	Front Shield Electrons	Back Shield Electrons
650-800	6.95	4.67E+10	3.32E+10
1000	3.89	5.30E+10	3.67E+10
1250	3.72	9.68E+10	6.68E+10
1500	3.22	1.16E+11	7.91E+10
1750	2.98	1.22E+11	8.15E+10
2000	2.84	1.19E+11	7.70E+10
2250	2.77	1.13E+11	7.09E+10
2500	2.73	1.10E+11	6.81E+10
2750	2.72	1.07E+11	6.67E+10
3000	2.73	1.08E+11	6.85E+10
3500	5.56	2.37E+11	1.63E+11
4000	5.78	2.83E+11	2.03E+11
4500	6.11	3.59E+11	2.61E+11
5000	6.54	4.59E+11	3.38E+11
5500	7.11	6.12E+11	4.58E+11
6000	7.88	8.37E+11	6.35E+11
7000	19.59	3.06E+12	2.37E+12
8000	38.41	7.15E+12	5.55E+12
8063	12.41	2.78E+12	2.15E+12

TABLE V-5. ORBIT ALTITUDE VS. PROTON RADIATION EFFECTS

Altitude	Front Protons (I_{sc})	Front Protons (V_{oc} and P_{max})	Back Protons (I_{sc})	Back Protons (V_{oc} and P_{max})
650-800	3.57E+12	4.80E+12	2.97E+12	3.72E+12
1000	5.08E+12	7.11E+12	4.08E+12	5.30E+12
1250	1.12E+13	1.69E+13	8.44E+12	1.16E+13
1500	1.95E+13	3.16E+13	1.35E+13	1.98E+13
1750	3.08E+13	5.29E+13	1.98E+13	3.08E+13
2000	4.01E+13	7.18E+13	2.41E+13	3.89E+13
2250	4.53E+13	8.47E+13	2.56E+13	4.25E+13
2500	4.72E+13	9.07E+13	2.50E+13	4.25E+13
2750	4.59E+13	9.06E+13	2.33E+13	4.01E+13
3000	4.16E+13	8.37E+13	2.03E+13	3.55E+13
3500	5.99E+13	1.23E+14	2.81E+13	4.95E+13
4000	3.98E+13	8.32E+13	1.79E+13	3.19E+13
4500	2.48E+13	5.30E+13	1.06E+13	1.91E+13
5000	1.43E+13	3.12E+13	5.81E+12	1.06E+13
5500	8.54E+12	1.90E+13	3.30E+12	6.12E+12
6000	4.20E+12	9.58E+12	1.50E+12	2.85E+12
7000	1.40E+12	3.39E+12	4.17E+11	8.18E+11
8000	2.67E+11	6.86E+11	6.54E+10	1.33E+11
8063	4.38E+09	1.13E+10	1.21E+09	2.25E+09

For an expected on orbit life of three years, the total radiation received in one MeV equivalent electrons for front and back exposure is 5.14E+15 for voltage and power and 2.82E+15 for current. This equivalent radiation exposure results in degradation percentages for 12 mil liquid phase epitaxy (LPE) GaAs solar cells listed in table V-6. The radiation degradation experienced by 6 mil cells will be lower resulting in higher EOL performance.

TABLE V-6. RADIATION DEGRADATION RESULTS

Cell Parameter	Final Parameter Percentages
V_{oc}	0.892
V_{mp}	0.86
I_{sc}	0.77
I_{mp}	0.768

b. Temperature Effects

An advantage of the GaAs cells over silicon cells is their stability at higher temperature. This stability becomes important as the array temperatures increase toward the end-of-life with decreasing array efficiencies. The temperature effects for gallium arsenide cells, referenced to 28° C, are listed in table V-7.

TABLE V-7. TEMPERATURE EFFECTS FOR GALLIUM ARSENIDE

Parameter	Temperature Coefficient
V_{oc}	-1.94 mV / deg C
I_{sc}	0.014 mA / cm^2 / deg C
Efficiency	-0.033 % abs. / deg C
V_{max}	-2.15 mv / deg C

c. Design Results

The design of the array was performed using an Excel spreadsheet on a Macintosh. The parameters used in the design were:

- Radiation effects on cell parameters
- Cell Size

- UV and Micrometeorite effects
- Cell Temperature
- Thermal Cycling
- Solar Intensity
- Cell Mismatch
- Assembly Losses
- Cell Efficiency
- Packing Factor
- Cell Absorption and emission
- Sun Incidence Angle

The design was iterated until the required EOL output power was achieved at an operating temperature consistent with the design array area. Worst case solar flux at apehelion with an array pointing error of 8.5° (0.15 radians) were assumed. Appendix E lists the Excel spreadsheet program and the resulting values. The final design results are listed in table V-8.

TABLE V-8. FINAL ARRAY DESIGN

Cells in Series	44
Cells in Parallel	80
Total Number of Cells	3520
Total Array Area with Intercell Spacing	30307.2 cm^2
Panel Dimensions (2.5 cm boundary on all sides)	0.487 m x 3.305 m x 1.74 cm
Array Mass	12.19 kg
Worst Case Operating Temperature	46.68° C
Minimum Eclipse Temperature	-117.88° C
Maximum Power Output at 30.9 Volts	504 Watts
Minimum Power at EOL	357.53 Watts

The power values for the satellite if launched at perihelion vice apehelion are a BOL power of 540 watts and an EOL power of 382 watts.

2. Battery Design

The battery for eclipse power are 12 amp hour nickel-hydrogen battery manufactured by Eagle Picher. This battery is provided in a two cell common pressure vessel (CPV) configuration. The battery voltage per CPV cell varies from 2.2 volts to 3.2 volts at full charge. For the bus configuration of a buck converter for constant current charge and a boost converter to maintain the line voltage, the number of CPV cells is limited to eight for the 28 volt bus. This gives a maximum battery voltage of 25.6 volts and a minimum of 17.6 volts.

The battery requirements are obtained from the eclipse load requirement of 140 watts. With the boost converter efficiency of 85%, the actual power supplied by the battery during the eclipse period will be 164 watts. The maximum eclipse period is 37 minutes of the 4 hour 48 minute orbit. This gives an available recharge time of 4 hours 11 minutes. In general, the eclipse period will be considerably less then 37 minutes. For the three year projected mission lifetime, the satellite will experience a maximum of 4500 eclipse periods. While nickel cadmium batteries can be used for that number of discharge cycles, the nickel-hydrogen battery is much more capable of withstanding the rigors of a large number of discharge cycles while still being able to undergo large depths of discharge. Other cells, such as silver cadmium, were investigated, but did not possess the ability to undergo the high number of discharge cycles.

The battery recharge requirements are based on the amount of power removed from the battery during the discharge period. For a LEO satellite for which the charge and discharge cycles are numerous, the amount of energy that is removed from the battery must be replaced by an additional 10%. For example, if 10 amps are drawn from the battery for one hour, the recharge cycle must provide an equivalent 11 amp hours for the charge period. This determines the required charge time for the battery. The maximum recommended charge rate is C/3, where C is the battery capacity in amp-hours. In this design, this would correspond to charging at 4 amps or requiring a maximum of approximately 120 watts for the charge time. This amount of power is excessive if one considers the total amount of power to be used by the satellite. If the battery is not to be used to supply any power during the illuminated portion of the orbit, then the optimum recharge scheme would result in completing the charge just as the next eclipse period starts. This technique is rather risky, so a median approach of completing the charge one half hour before the next eclipse period starts was taken.

The charge rate chosen for this satellite is C/7. At this rate, the charging current is 1.7 amps, and the maximum power required for charge, including charger efficiencies, is 52.5 watts. The time required for charging the battery after a discharge of 164 watts at 17.6 volts minimum for 37 minutes is determined by calculating the number of amp hours removed and adding ten percent. For this design, 5.74 amp hours have been removed and will be replaced by 6.32 amp hours. Charging at 1.7 amps yields a required charge time of 3.7 hours.

3. Power Electronics Control Unit

The power electronics control section of the power subsystem is responsible for maintaining the proper level of voltage for the satellite bus. The bus will be a fully regulated bus at 28 volts. This regulation is accomplished by employing a shunt regulator for periods when the solar array is powering the spacecraft and by using a boost regulator for periods when the battery system is supplying the power.

a. Shunt Regulator

The shunt regulator is used to dissipate the excess power supplied by the solar cells during periods when the maximum amount of power available is not being used in the satellite. This is critical during initial satellite life before radiation degradation has significantly reduced the output capabilities of the array. Each array will be connected to the shunt regulator through a series switch to allow for the disconnection of an array when power requirements are less than the amount that one array can supply. When the bus output voltage drops below 28 volts, indicating that the power drawn is higher than the capability of the single operating array, the unused array will be brought on line and will assist in powering the bus.

The array voltage at the point of the shunt regulator will be 28 volts. This voltage level results from a 1.3 volt drop from the array slip ring, and will accomodate two 0.8 volt diode drops for each array. A diode separates each array panel and a diode is present on each series string in the array. The shunt regulator consists of a set of four parallel power MOSFET transistors operating in the switching mode to shunt current through a resistor bank to dissipate the excess power. The switching action of the MOSFET's produces a square current pulse through the shunt resistor bank and to the load. A large inductor is placed after the shunt regulator to provide a constant current source to the battery charger and the system. A flyback diode is placed on the array side of the inductor to allow a current path during switching operations of the array. The output capacitor filter will provide a sink for the current pulses and maintain a constant regulated output voltage. This switching action will pull the array voltage down to the desired 30.9 volts at the array and remove any excess current that is being supplied. A standard buck converter could have been placed in the circuit to regulate the output at 28 volts, but the placement of a series switch in the main current loop requires a higher voltage at the array in addition to being a point of failure that would disable the satellite.

The switch rate of the shunt regulator will be 50 kHz to synchronize with the buck battery charge regulator. The shunt regulator is a step down regulator, and on a time average, it must drop the voltage and current down to the required levels. At the beginning of life, the output power of the array, at 30.9 volts, is approximately 505 watts if the satellite is launched at apehelion or 540 watts if launched at perihelion. Using the switching array technique, such that only the minimum excess power is dissipated in the shunt regulator, the maximum amount of power dissipated is 270 watts. In a shunt bank consisting of four parallel resistors, the maximum amount of power that each bank should have to dissipate is approximately 90 watts at 28 volts if one of the shunts were to fail open. For four parallel banks, each bank must be approximately 9 Ω.

The minimum duty cycle seen by the shunt regulator will be approximately 50%. This value is determined from having to dissipate a maximum of one half of the available power. The output capacitor required to ensure a minimum voltage ripple of 50 mV can be determined from the maximum expected current output and the desired ripple amount. For a maximum current of 12.25 amps and a maximum change in voltage of 50 mV in 10 μsec, the capacitance required is 2.2 mF.

b. Battery Charge and Discharge Regulator

The battery charge and discharge unit is an integral part of the power subsystem. It is responsible for maintaining the proper charge on the battery and for ensuring that the voltage supplied by the battery meets the bus requirements. This is accomplished by utilizing a combination charge and discharge unit that incorporates the required reactive elements for both the buck and boost circuits in one circuit design. This is accomplished by sharing the inductor used in all switchmode converters between the two stages.

The battery used is a 12 amp hour-battery with a constant current charge requirement. This charge current is calculated to be 1.7 amps to provide for a charge period of 3.7 hours on a full discharge. The converter chosen for the constant current charge was a current regulated continuous mode buck converter. This converter was selected for its frequency independence and because its operation depends only on the duty cycle of the converter. The duty cycle of the converter is defined to be the ratio of the converters' power switch on time to the total switching period. As the inductive component is common between both the boost and the buck converter, the boost cycle will also be operated in the continuous mode.

The range of battery voltages, as described in the battery subsection, is from 2.2 to 3.2 volts per CPV cell. For the eight cells, this gives a total voltage range from 17.6 to 25.6 volts. The constant current charge circuit must be able to operate in the continuous mode while dropping the input voltage from 28 volts to the required voltage to ensure the proper charge rate. The switch mode operating frequency is chosen to be 50 kHz as a compromise between the smaller inductive components at higher frequencies and the higher losses and higher noise levels at the higher frequencies.

The inductance value for the buck circuit was obtained by determining the equivalent output resistance of the battery. At the maximum battery voltage of 25.6 volts and 1.73 amps of charging current, the power required to charge the battery is 44.8 watts. This corresponds to an equivalent resistance of 14.63 ohms. At 17.6 volts, the power is 33 watts and the resistance is 10.2 ohms. The inductance value required to operate this converter is given by

$$L_b = \frac{R_{max} T(1 - D_L)^2}{2} \tag{1}$$

where D_L is the minimum duty cycle and T is the period. The minimum duty cycle period is determined by the voltage conversion ratio for the buck converter from

$$\frac{V_o}{V_i} = \frac{D}{1 - D} \tag{2}$$

The value for the minimum duty cycle was obtained when the output voltage is at a minimum. For the buck operation to 17.6 volts, the duty cycle is 0.386 and for 25.6 volts, the duty cycle is 0.478. Substituting the values into the equation to determine the inductance at an operating frequency of 50 KHz yields a required inductance of 550 µH. This inductor can be made by using the T300-26D core with approximately 90 turns of 16 gauge wire. This inductor will be capable of passing the required 10 amps of the discharging boost regulator [Ref. 15].

The output capacitance used for filtering the output was chosen to minimize the ripple associated with the pulsing operation of the switch. The output filter capacitance can be calculated from

$$\frac{\Delta V_o}{V_o} = \frac{D_H T}{R_{min} C} \tag{3}$$

For an output ripple of 50 mV at 17.6 volts, the minimum capacitance required is 336 μF.

The other components of the buck converter need to be chosen to permit proper operation of the device. An example of compatible components are the Motorola MUR 405 power rectifier diode and the Phillips BUZ 10 power MOSFET. These devices are chosen for their ability to handle the required reverse voltages and current. In the case of the MUR 405, the ability of the device to turn off very rapidly is crucial in the design of the continuous mode converter. Additionally, the BUZ 10 power MOSFET has a very low drain-to-source resistance without having excessive drain-to-source capacitance. The device used to measure the current for the battery charging will be a Hall effect device and the controller will operate on an overvoltage shut down condition. The converter efficiency has been assumed as 85%.

The boost converter will use the same inductor as the buck converter, and the design must be based on using that device. The boost regulator will operate in the continuous mode and will be a voltage regulator vice the current regulator of the buck converter. The battery will be required to supply 140 watts of power to the satellite during eclipse periods. Assuming a boost converter efficiency of 85%, the required battery power must be 164 watts at 28 volts. The maximum current that the battery must supply will occur when the battery is at the minimum charge level of 17.6 volts, and will be 9.36 amps. The duty cycle expected of the converter was determined from the voltage conversion ratio for the continuous mode boost converter

$$\frac{V_o}{V_i} = \frac{1}{1 - D} \tag{4}$$

When the battery voltage is 17.6 volts, the duty cycle is 0.39, with a 0.111 duty cycle for 25.6 volts.

4. Mechanical Integration

Masses and structure for mechanical integration were estimated based on the mass and life-span of this spacecraft relative to previous systems. The mechanical integration portion of the electric power system includes the components for array support structure, battery support structure and any other piece of mechanical hardware required to mount the electrical power system in the satellite.

The arrays will be folded for stowage on the satellite body for launch and PAM deployment. When deployed, the connection between the array and the satellite will be made with a 0.85 meter aluminum extension. The array will be folded at the base of this extension and the solar array drive motor and again at the connection between the extension and the actual array substrate. The panels will be folded in half with the top array section cells facing outward during stowage to provide power after launch and before deployment. The connections between the array and the body will be made with explosive connectors with the array under spring tension for deployment. Locking will take place after full deployment at both folds and at the drive mechanism.

Signal input to the array drive motors for array pointing will come from the attitude control computers. The control signal will contain pointing information relative to the roll axis of the spacecraft. Allowable pointing error is ±8.5° for design power levels.

5. Detailed Mass Analysis

A detailed mass breakdown is given in table V-9. Items marked with an asterisk are approximated values from other sources [Ref. 17].

TABLE V-9. DETAILED MASS BREAKDOWN

Component	Mass (kg)	Heritage
Array Structure and Cells	12.19	GaAs cells untested in space
Batteries	7.12	12 A-Hr batteries unused in space. Numerous other designs by Eagle-Picher in use.
Wire Harness*	9.15	Standard
Mechanical Integration*	4.2	Standard
Solar Array Drive Electronics*	2	Standard
Solar Array Drive Motors*	8	Intelsat V
Power Electronics*	4	Intelsat V
Shunt Resistor Bank*	1.89	Standard
Total Mass	48.55	

C. EPS PERFORMANCE

1. Lifetime Power Budget

The lifetime of the satellite is dependent on the capability of the array to provide the necessary power for operations. The design life of the satellite is three years for an apehelion launch. An analysis of the expected life was conducted and the results are detailed in Appendix E. The computed values are listed in Appendix E.4 with graphs depicting the results. The parameters iterated for each point in the satellite life are the radiation degradation, temperature and solar flux. Micrometeorite and UV damage are assumed to occur during the first three months of life and are included in all calculations after launch values.

Lifetime for an apehelion launch is expected to be slightly longer than the three year design life. This is due to the decreased radiation effects expected of the 6 mil solar cells vice the thicker 12 mil cells for which radiation data is available. The amount of time that the life can be expected to be extended is undeterminable until radiation figures for the thinner cells becomes available. Based on available information and extrapolation into future quarters of operation, it is expected that the satellite will be able to survive an additional six to nine months of operation. The current level at the end of this period will be near the limit for maximum power operations. If power levels do not require the maximum power output, the life of the satellite could be an additional 15 months after expected end of life. This is based on a minimum current level of 11.9 amps at apehelion resulting in an available power level at the bus of 333 watts. This is above the required power level, but falls into the allotted margin amount. At this point, the bus voltage level will fall below the level that is required to maintain the 28 volt regulated level. Figures V-2 and V-3 are Power vs. Time on Orbit and Voltage and Current vs. Time on Orbit for an apehelion launch.

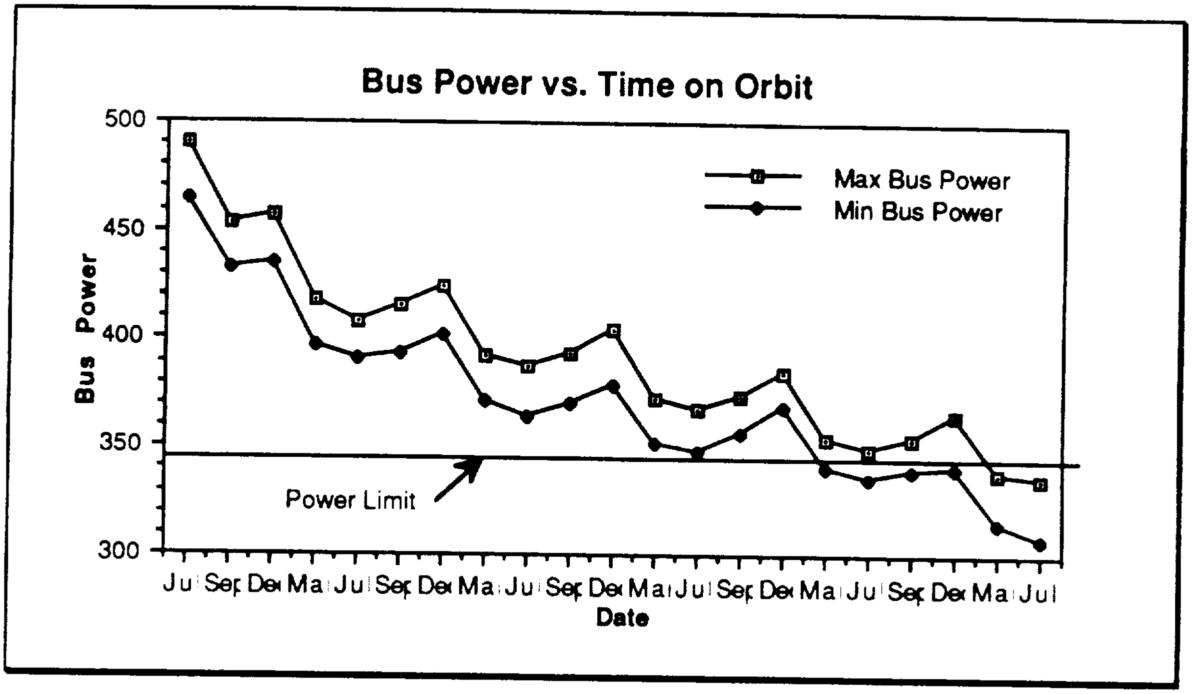

Figure V-2. Power vs. Time on Orbit

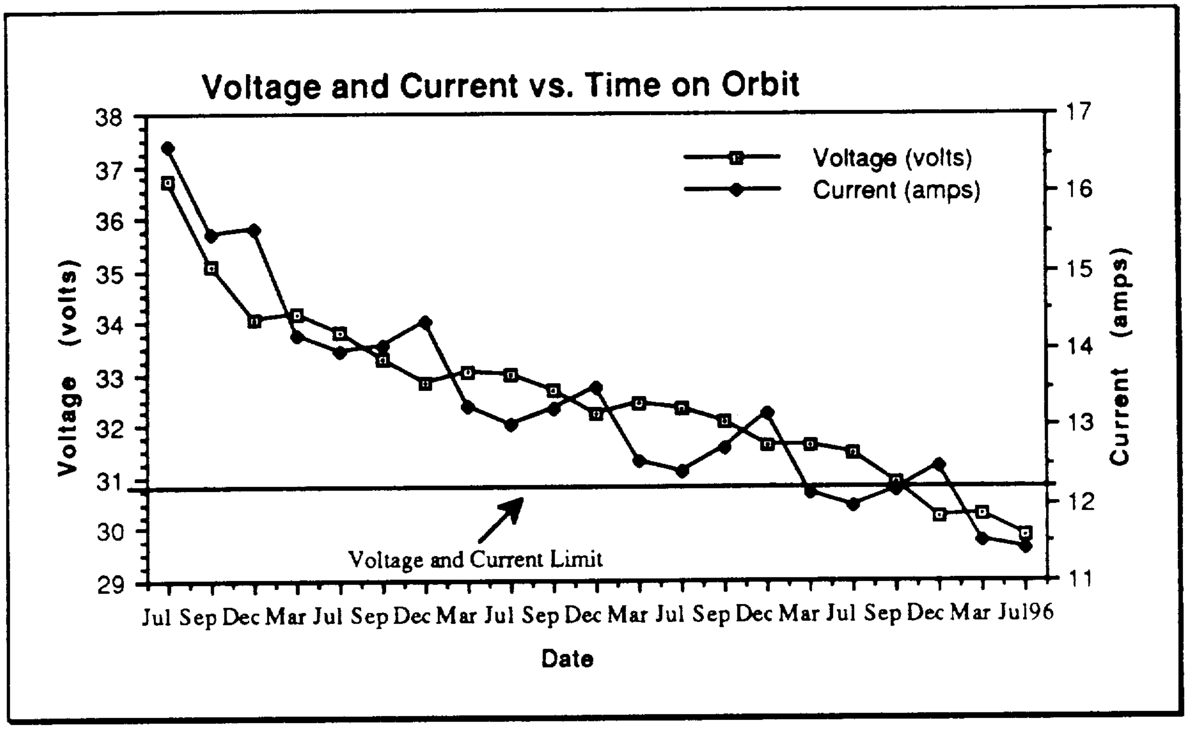

Figure V-3. Votalge and Current vs. Time on Orbit

Of interest in the voltage current relationship is the phase difference between the voltage and current throughout the life of the satellite. The current produced by the cells increases with increased temperature and the voltage decreases with increased temperature. These two effects moderate each other with respect to available power. As expected, available power levels increase at perihelion and reach a minimum at apehelion.

2. Reliability And Fault Analysis

If the system is to provide reliable power to the satellite, certain redundant configurations should be employed. A redundancy already discussed in the shunt regulator is the increased power handling capabilities of each branch of the regulator in the case of one branch failing open. Other areas of redundancy will be implemented such as

- Standby redundancy of the power converters for charge and discharge and shunt regulators.
- Multiple pole switches operating in parallel using different drive mechanisms for array switching.
- Fuses in line of the shunt regulator for short conditions in the switch.

The failure of the components can be either open or short circuit. In each case, a different result will occur. Table V-10 lists some possible conditions and their impact on the operation of the satellite. [Ref. 16:pp. 167-174]

TABLE V-10. RELIABILITY AND FAILURE MODE ANALYSIS

Subsystem	Failure Mode	Effects on Other Systems
Solar Array Section	Open	Reduces the output of the array by the amount 1/n where n = number of array segments.
	Short	Same as Above
Shunt Regulator	Open	Power capabilities of regulator can handle one open segment. If more than one segment opens, bus voltage will not be maintainable.
	Short	Fuse in segment prevent total loss of bus. Same result as above after fuse opens.
Charge and discharge regulator	Open	Redundant converter performs required operation.
	Short	Regulator must be isolated or bus will be held at battery voltage.
Battery	Open	Eclipse operation of the satellite is not possible.
	Short	Battery must be opened by means of fuse. Eclipse operation of the satellite is not possible.

VI . ATTITUDE CONTROL

A. FUNCTIONAL DESCRIPTION

The spacecraft communications antennas require accurate beam pointing for successful operations from the mission orbit. The attitude determination and control system in a spacecraft is a major factor in meeting the antenna pointing requirement by determining and maintaining the spacecraft attitude within established limits. The pointing accuracy establishes the attitude control system specifications for control of the spacecraft's orientation.

1. Requirements

The specifications under which the satellite must perform fall into two categories, customer driven and internal requirements.

The requirements put forth by the customer define the mission of the ADCS. The customer requires the satellite to be nadir pointing and 3-axis stabilized. The power needed for the satellite and the mass limitations require the spacecraft to have deployable solar arrays.

The internal requirements established for the system contribute to the ADCS by refining the missions it must perform. The communications system is fairly broad beam with ±2 degree pointing accuracy. The ADCS system configuration is designed to achieve a higher pointing accuracy of ±.5 degrees. The pointing accuracy sets the specifics for the feedback gains in the control loop. Another internal requirement is to minimize cost and mass in all systems. This requirement affects the selection of hardware and weighting of factors involved. This will be discussed later when various hardware choices are discussed. Other self imposed requirements include a monopropellant propulsion

system, which affects despin and desaturation, and sun sensing capability to maximize solar array efficiency.

2. Summary of Subsystem Operations

The HILACS is a three-axis stabilized nadir pointing system with a pointing accuracy of ±2 degrees. The block diagram of the ADCS is shown in Fig. VI-1. All the components of the ADCS are space qualified and obtainable from government contractors with no estimated excess delays or cost. The system is designed to be single fault tolerant.

The ADCS will have to perform in two different modes, transfer orbit and on-orbit. During the transfer orbit mode, the satellite will be ejected from the Delta launch vehicle with between 30 and 100 rpm. The ADCS system will begin to despin the satellite after ejection. The system will acquire the sun with sun sensors. After sun acquisition, the satellite will despin completely and acquire the earth. Once the satellite is despun, the solar cells will deploy, and the reaction wheels and gyros will power up. The ADCS will maintain 3-axis stabilization during transfer motor burn to maintain solar power. At the completion of the motor burn the spacecraft will be on its orbit .

The on-orbit mode will be similar to the end of the transfer mode. Once on orbit, the ADCS will reacquire the earth with its earth sensor, and the satellite will be oriented to become fully operational. The specifics of the ADCS will be covered in subsequent sections.

B. ACS DESIGN AND HARDWARE DESCRIPTION

1. Spacecraft Attitude Dynamics

The satellite orbit is continuously changing, forcing the HILACS to constantly apply torque to maintain its attitude. Due to the dynamic nature of the orbit and the requirement to be nadir pointing, a four reaction wheel control actuator was chosen.

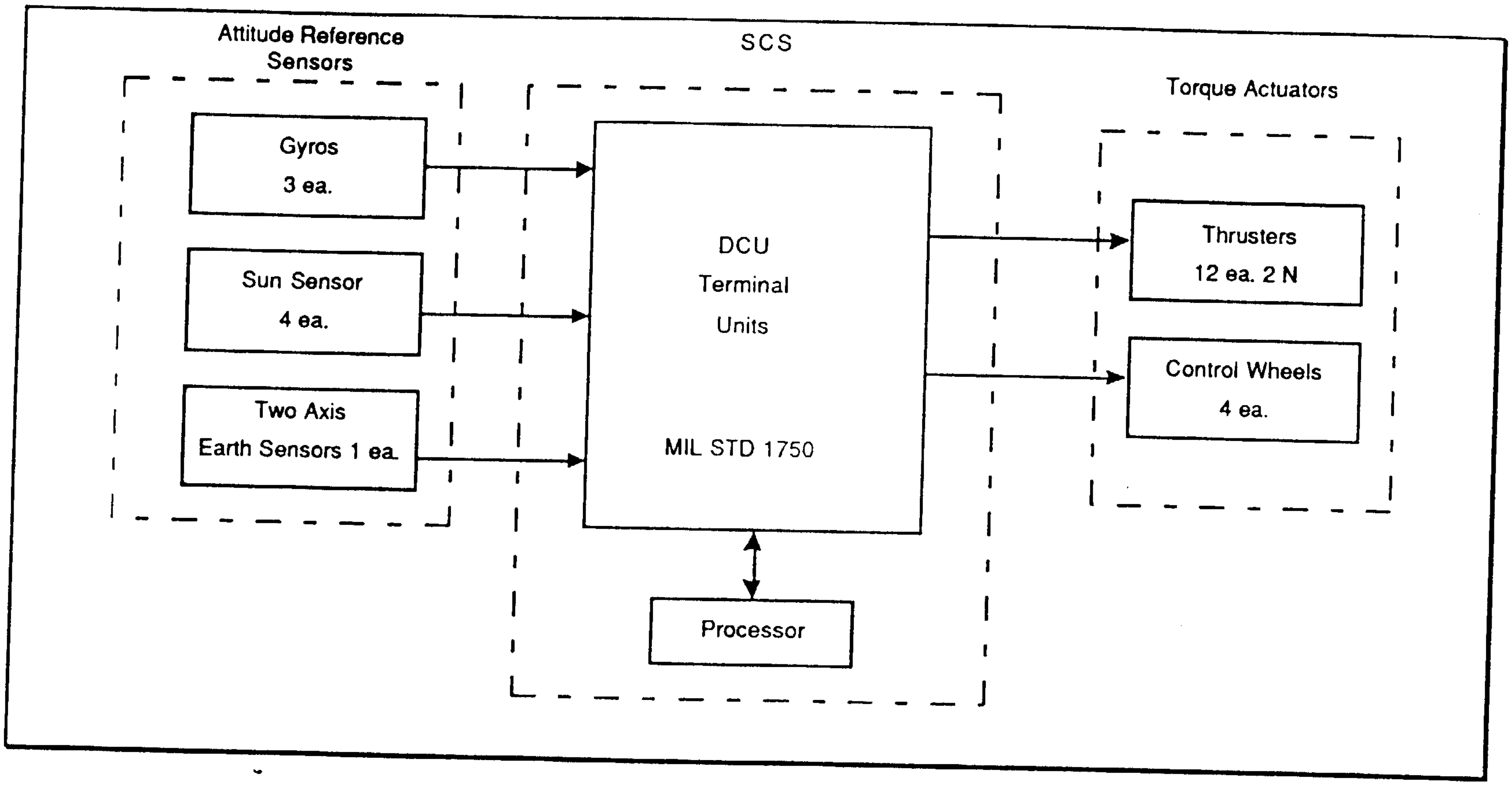

Figure VI-1. ADCS Block Diagram

The reaction wheels are configured with three wheels along the roll, pitch and yaw axis (initial spacecraft coordinates) and one wheel at a 45 degree angle to the others to provide redundancy. Reaction wheels were chosen because they could handle the yaw control that will be required as the satellite maintains proper orientation with respect to both the earth and sunline. A momentum wheel system with thrusters would require an extremely large amount of fuel to accomplish the same functions. The spacecraft will have additional redundancy for the control actuators provided by the thruster. The 2-N thrusters will be fired to desaturate the reaction wheels, despin the satellite and provide redundancy. The thrusters are discussed in detail in the propulsion system section. Disturbance torques must be accounted for when designing ADCS. The purpose of the ADCS is to sense disturbances put on the satellite and provide the necessary attitude corrections. Disturbance torques fall into three categories: internally generated, solar pressure and magnetic/gravitational torques. Internal torques are the dominant force in building up wheel speed. The internally generated torques arise from internal friction and instabilities. The satellite's computer will keep track of the disturbance torque by monitoring the wheel speeds. The computer will be able to autonomously desaturate the reaction wheels using the two 2-N thrusters assigned to each wheel for desaturation. The thrusters will be able to desaturate the wheels quickly, with minimum pointing error. The specifics of desaturation are discussed in Appendix F.

2. Attitude Determination and Sensor Configuration

The ADCS is composed of three systems: the sensors, actuators and electronics (See Fig. VI-1). This section concerns the sensors and their inputs into the electronics units. The attitude determination requirements for the systems result in the following sensor capabilities:

i.) Acquire and maintain the sun angle for solar array pointing throughout the orbit.

ii.) Acquire and maintain the nadir angle to the earth for antenna pointing.

iii.) Maintain an internal reference unit within the satellite for redundancy. These requirements drive the sensor configuration and their outputs.

The sensors for HILACS consist of an earth (horizon) sensor, sun sensors and rate gyros. The relatively large allowable pointing error gives great latitude in sensor design. For earth sensing, a two axis scanning horizon sensor will be used. This sensor will be located near the antenna on the earth face. The earth sensor is a two axis conical horizon sensor capable of accurate sensing with a worst case pitch and roll error of $\pm.07$ degrees at 1204 km altitude. The sun pointing requirement is fulfilled by four two-axis sun sensors. The sensors are mounted two each , on the earth and anti-earth faces. The sun sensors will be able to sense the sun anywhere in the satellite's orbit and give a yaw sensing with worst case error of ± 0.01 degrees. One sun sensor will be able to give an accurate sun angle independent of the other sensor. This allows for nearly 4π steradians of coverage for the satellite. The redundant element is a three gyro inertial reference unit mounted inside the spacecraft. The outputs from the sensors are fed into the control computer on board to be processed and commands sent to the actuators. Individual hardware is discussed in the hardware section as well as specification sheets in the appendix.

3. Control System Design

The ADCS system design reflects the requirements of the mission and restrictions imposed. The ADCS components are summarized in Table VI-1.

TABLE VI-1. ADS COMPONENT SUMMARY

COMPONENT	MANUFACTURER	UNITS PER S/C	UNIT WEIGHT (kg)	AVERAGE POWER (WATTS)	HERITAGE
DUAL-MODE EARTH SENSOR	BARNES *	1	3.77	4	MODIFIED GPS/DMSP
COARSE SUN SENSOR	ADCOLE	4	0.04	1	INTELSAT VII
REACTION WHEELS	HONEYWELL	4	2.3	18 ea.	DMSP, TIROS
SPRING RESTRAINT GYRO ASSEMBLY	-	1	1.2	19	INTELSAT V
MIL STD 1750 COMPUTER	BARNES *	1	2.5	6	MODIFIED GPS

*Functionally redundant system

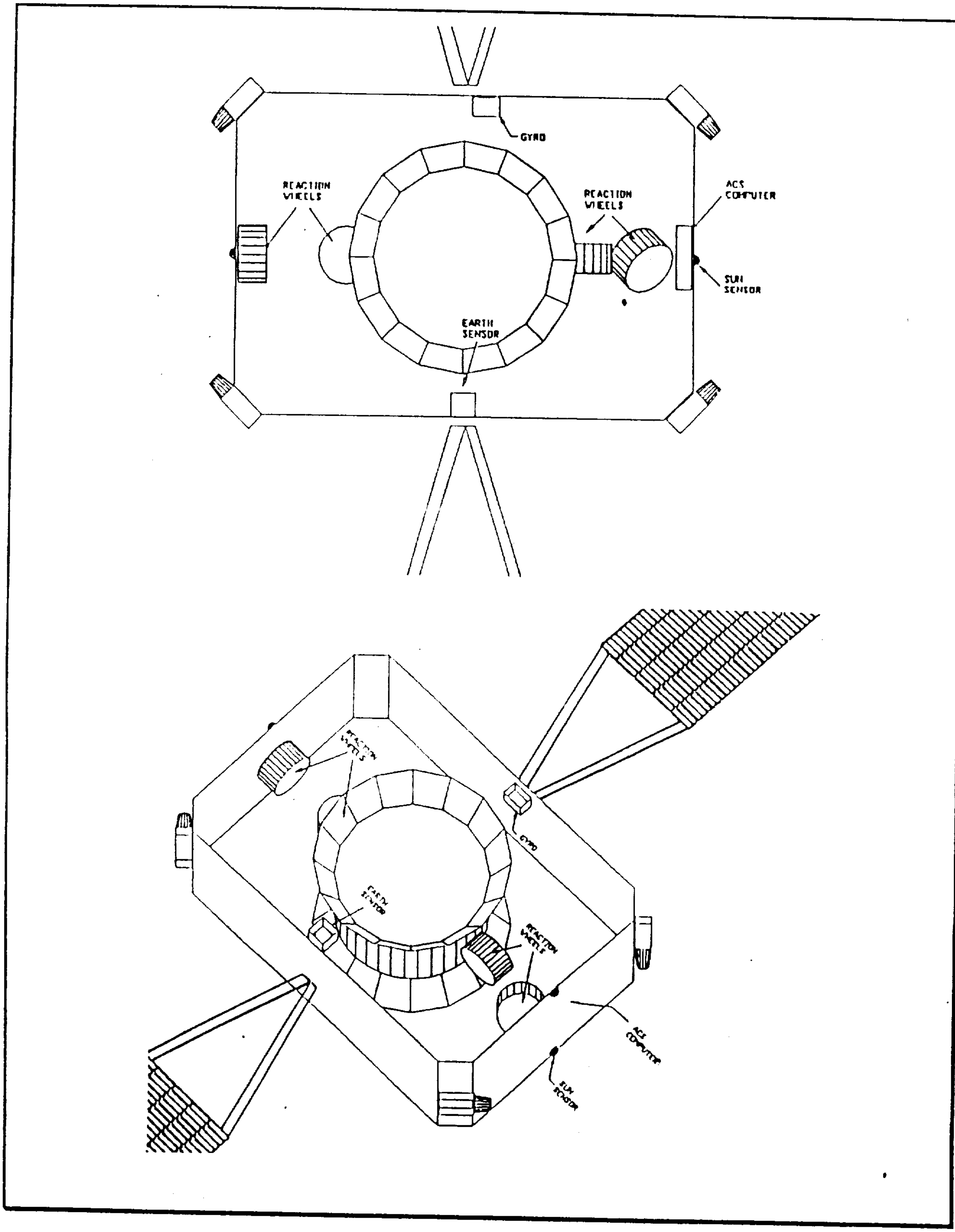

Figure VI-2. Component Placement (Top and Oblique View)

The location of the system components is shown in Fig. VI-2. The system is designed to be single fault tolerant and reliable.

For the actuator portion of the ADCS, the system parameters are computed and in Appendix.F. Reaction wheel desaturation will be done with the 2-N thrusters. Two thrusters will be used to desaturate each reaction wheel. The parameters follow in Table VI-2 :

Table VI-2. Reaction Wheel Parameters

	Pitch	Roll	Yaw
Design Torque	4.813 Nm	4.813 Nm	4.605 Nm
Pulse Time	0.3956 sec	0.3556 sec	.413 sec
Gain K	79.83 nm/rad	31.46 nm/rad	45.5 nm/rad
τ	1.948 sec	2.143 sec	3.062 sec
Moment	1.439sec	1.439 sec	1.652 sec
w	.5133	0.4667	.3226
θ_{max}	.45 °	.45 °	.25 °

The amount of propellant required to desaturate the wheels over the three years is approximately .5 Kg.

The fourth reaction wheel is a spare wheel oriented to provide redundancy for the other three wheels. It is canted at a 45 degree angle to the other three wheels. By doing this it will be able to provide torque in all three axes. This results in torque along the desired direction while the remaining two axis wheels counteract the coupled torque from the skewed wheel.

The sensor design is as stated in the sensor section. The electronics system is composed of the individual element electronics and the central processing unit where the control laws are stored. The computer is a Mil

Standard 1750 which is capable of providing autonomous control of the spacecraft.

Several different equipment configurations and hardware types were investigated. Table VI-3 contains the various sensors, reaction wheels and computers considered in the design process. Their performance was evaluated as well as radiation hardness, cost and space qualification.

It was difficult to find accurate manufacturer data on the sun sensors. The sensors chosen were the coarse sun sensors utilized on INTELSAT VII. They have superior weight and power characteristics while meeting mission requirements. The earth sensor chosen is a Barnes two axis conical horizon sensor (See appendix F for spec sheet) The weight and power characteristics are comparable to others, with smaller size and excellent performance. The sensor is also well hardened against radiation. The rate measuring assembly is a spring restrained rate gyro utilized on INTELSAT V. The gyros are packed together into one unit with good weight characteristics.

The actuator system is made up of 2-N thrusters, discussed in the propulsion section, and the reaction wheels. The reaction wheels chosen were Honeywell reaction wheels used on DSCS III. They are low power and weight with proven reliability. The amount of angular momentum they can store is small but sufficient for the size of our spacecraft.

The electronics unit is a Barnes built Mil Standard 1750 microprocessor. It is light with low power requirements and meets all requirements, including autonomous control of the spacecraft. Redundancy is provided by the ground control station.

The hardware is mounted in the spacecraft as shown in Fig. VI-2.

TABLE VI-3. ADS COMPONENT OPTIONS

COMPONENT	SOURCE	SIZE	MASS	POWER
SUN SENSOR	AFSC	5.1X3.81 cm	.2 lb(4 EA)	< 1 W
	INTELSAT VII	3X3 cm	4.0 Kg	.5 W
	NTS	5.5X4.6X2.6 in	.04 Kg	>1 W
EARTH SENSOR	AFSC	3277 cm^3	6.84 Kg	6 W
	ARABSAT	13.7X10.4X16.5 cm	1.54 Kg(2 EA)	7 W
	BARNES 103 A	16.26X10.3 cm	3.77 Kg	10 W
REACTION WHEELS	INTELSAT VII	27X16 cm	5.25 Kg(4 EA)	36 W
	ARABSAT	24X12 cm	4.9 Kg(4 EA)	61.6 W
	SPERRY	23.5X12 cm	5.2 lb(4 EA)	18 W
COMPUTER	DBS/RCA 1802	24.7X20X17.8 cm	3.8 Kg	6.2 W
	BARNES 13-103A	17.5X17.5X10.6 cm	2.5 Kg	10 W
	MIL STD 1750	11X8X8 cm	2.5 Kg	6 W
GYROS	INTELSAT V	11.4X8.2X7.5 cm	1.2 Kg	19 W
	ARABSAT	17.5X17.5X10.6 cm	2.2 Kg	28 W
	NORTHROP	11X8X8 cm	2.2 Kg	10 W

4. Mass/Power Summary

A mass and power summary for each component is contained in Table VI-1. The reaction wheels will operate at their steady state power. At any one time, no more then three of the wheels will be operating. Additionally, the gyros will only be operational when the thrusters are being fired, which reduces the power requirements considerably.

C. ACS PERFORMANCE

The system model for the orbits and the simulations for different time periods are contained in Appendix.F. As discussed in the orbital dynamics section, the satellite will have to react to the dynamics of the orbit to maintain solar pointing and nadir pointing. The way the satellite counteracts the torques and maintains its pointing accuracy will be through its sensors and reaction wheels. The yaw wheel, spacecraft z-axis, will be responsible for maintaining the solar arrays pointing at the sun. It reacts to the sun vector angle to the orbit, β (See Fig. VI-3). Due to this, the yaw reaction wheel will have a cyclic torque applied, which is within its limits to handle, and will not need desaturation. Appendix F contains a Matlab program and plots illustrating the cyclic nature of β.

The roll and pitch wheels will also be subject to cyclic torque applied as a result of the yaw rotation β. The roll/pitch wheels will be coupled in maintaining the nadir pointing for the satellite. Due to the initial pitch orientation of the satellite with the solar arrays along the roll axis and the pitch wheel pitch wheel perpendicular to the orbital plane, the pitch wheel accepts most of the torque imparted throughout the orbit. Appendix F contains a Matlab program and plot of the wheel speed for five orbits. The appropriate equations are also attached. From the simulation it can be seen that the pitch wheel will have minimum speed under a no disturbance torque situation.

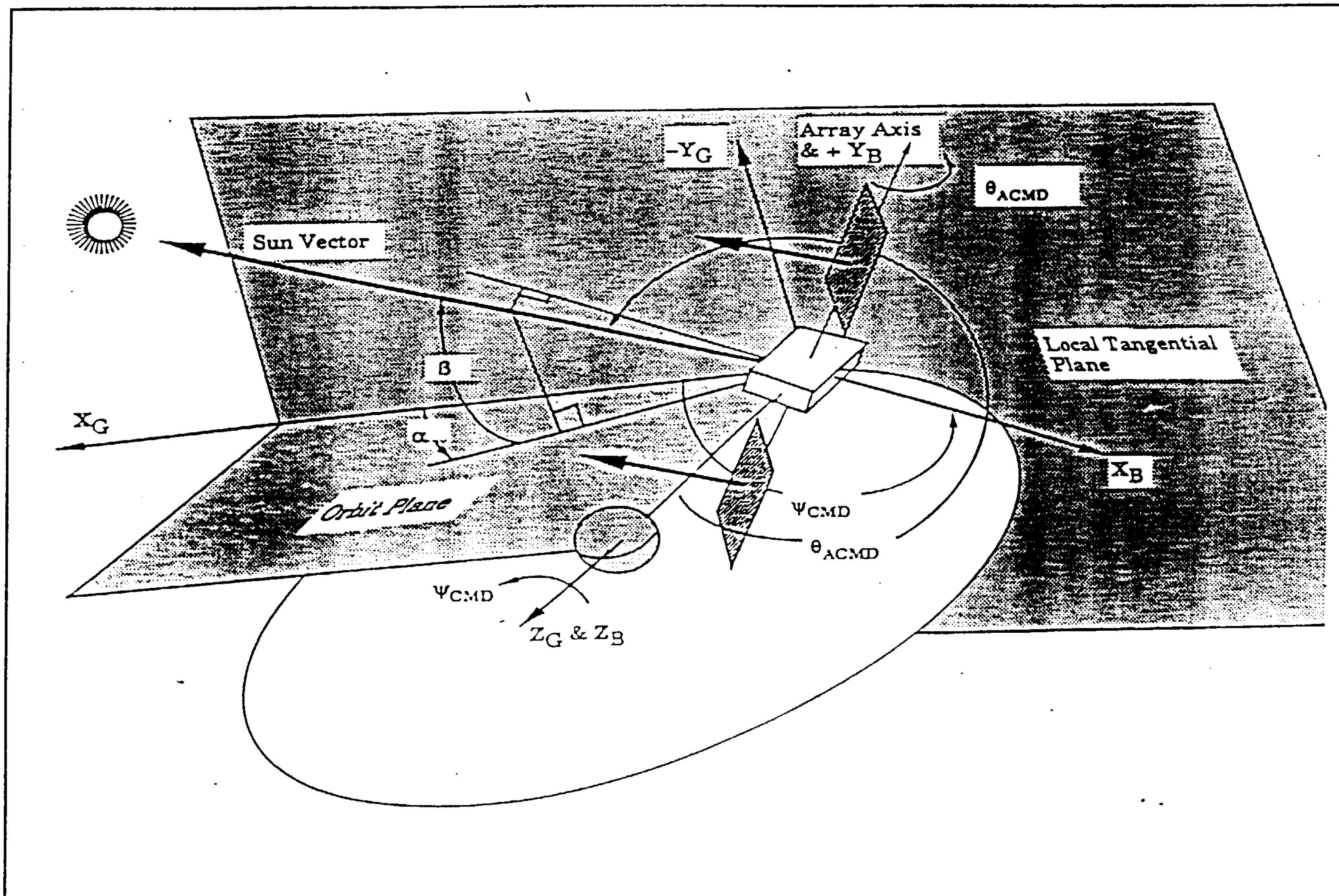

Figure VI-3. Sun/Nadir Pointing Geometry

The effect of solar torque on the satellite is small (see appendix F). The torque is cyclic with a constant secular element along each axis. The rms value of the torque over one orbit in the yaw axis is 1×10^{-6}. The secular torque acts on all the wheels adding slightly to the wheel speed over the satellites lifetime. The worst case value of the wheel speed increase is approximately 1 rpm in the yaw axis .

Magnetic torque is another secular torque affecting the satellite. Its affect is also small. Magnetic torque results from the satellites magnetic dipole being acted on by the earths magnetic field. Pertinent equations are contained in the ADCS appendix. Comparison with other satellites in similar low earth orbits show magnetic torques to have a small effect.

VII. TELEMETRY, TRACKING AND CONTROL SUBSYSTEM

A. FUNCTIONAL DESCRIPTION

1. Requirements

a. Autonomous Operations

The mission requirement for this satellite dictates a highly elliptic orbit with and inclination of 63.4°. This orbit prevents continuous control of the satellit from the mid-latitude ground station (MLG). The TT&C must, therfore, be capable of controlling the satellite operations for a significant part of its life.

b. Commanded Operations

When the satellite is in line of sight with the MLG it must be able to downlink its telemetry as well as respond to commands. These commands include initial maneuvers into operating orbit, modifications to current functions and modifications to onboard programs to adapt the satellite to changes in operating conditions.

c. Remote Monitoring

Since the satellite cannot be continuously controlled by ground for many of its orbits, it will have the ability to link to the net control station (NCS) during its operating cycle. During the time that it is linked to the NCS it will be polled as any other mobile station (MS). Once polled, it will downlink telemetry data specific to its operations such as transponder status and power system information.

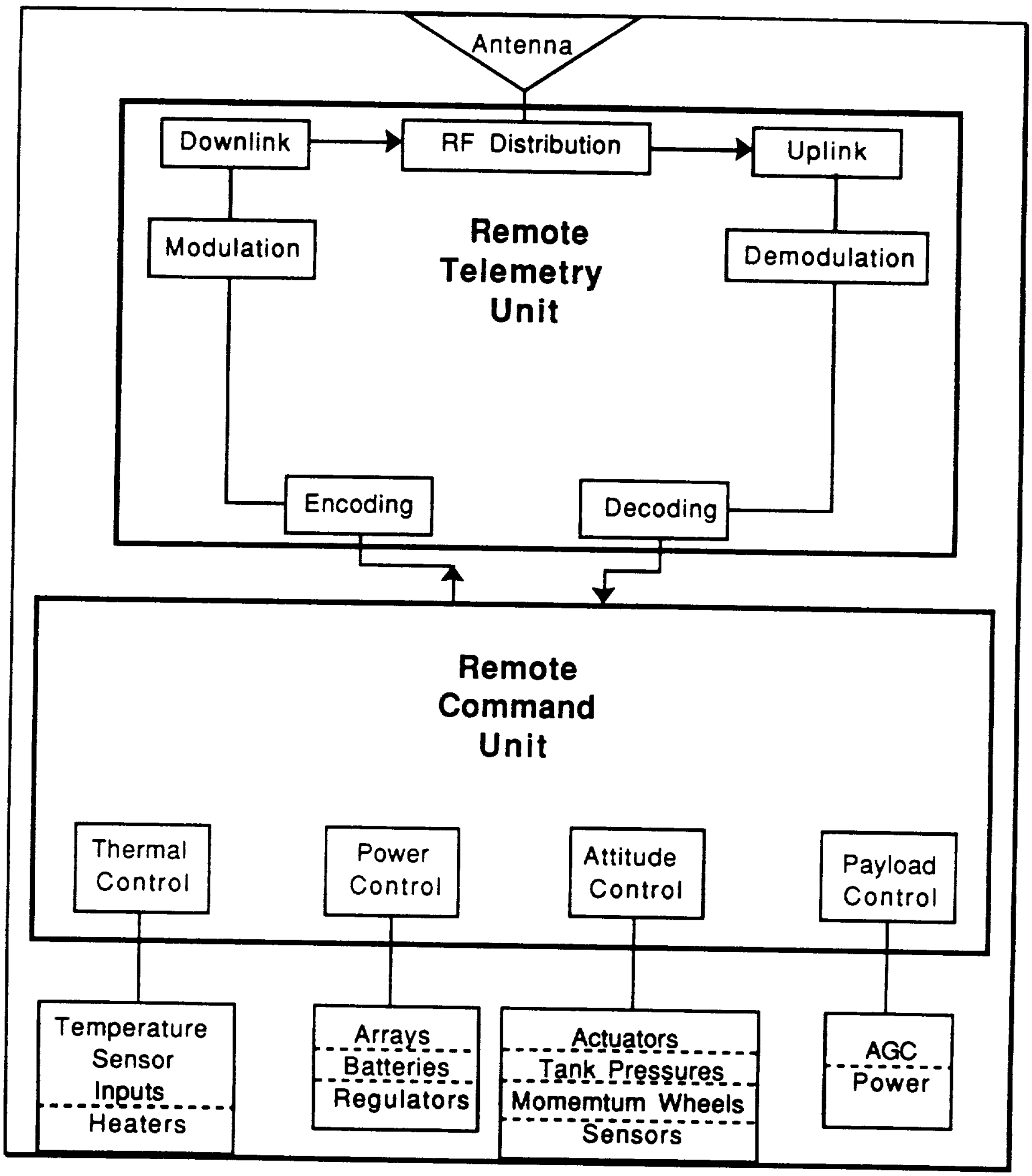

2. Component Operation

a. Remote Telemetry Unit

The RTU is essentially the interface between the telemetry antenna and the remote command unit (RCU). It performs all the function of a transceiver including RF distribution to the single antenna, modulation, demodulation and encoding/decoding of the telemetry data. The RTU uplink is at 350 MHz and its downlink is 253 MHz. The information is transmitted at a 1200 bit per second data rate, but it is encoded using a linear block code resulting in a 2400 bit per second transmission rate.

b. Remote Command Unit

The RCU performs satellite control operations through the use of coded algorithms resident in memory. Dual microprocessors perform redundant operations based on these algorithms and their commands are correlated to ensure destabilizing operations due to single event upsets (SEU) are not initiated. The RCU formats and relays telemetry to the RTU and acts on this telemetry in performing autonomous control of the satellite. The RCU also receives command signals from the RTU and performs these operations which have priority over onboard generated commands.

B. FUNCTIONAL INTERFACE

1. RTU

a. Antenna

The antenna is a crossed dipole hybrid which is resonant at 350 and 253 MHz. The RTU's RF distribution system switches the transmitter and receiver to this antenna with the default position to the receiver.

b. RCU

The RCU sends formatted commands to the RTU which are then encoded to modulation to the downlink frequency and transmitted. The RCU also receives uplinked telemetry commands from the RTU which are demodulated and decoded to the acceptable format for the RCU.

c. Transponder

When the satellite is performing transponder operations, the RTU sends limited telemetry data to the NCS. The RCU controls the operation of the transmit/receive in accordance with an algorithm similar to the MS link operations.

2. RCU

The RCU generally receives analog information from various sensors. It samples and performs pulse code modulation on the signals and then relays this data to the microprocessors for control functions in accordance with the current operation code.

a. Thermal Control

The RCU commands heater operation based on temperature sensor data received from sensors throughout the satellite. Once the heater is enabled the thermistors control local operation of the heater. There are a total of ninety-two sensors in the satellite which are provided a range of 512°C.

b. Power Control

The RCU monitors voltages and currents and controls the array drives. It controls battery charging, solar array switching and current regulation via the shunt regulator.

c. Attitude Control

The RCU monitors the attitude control system and propulsion system operation. The sensors receive data from the momentum wheels, earth/sun sensors as well as the thruster actuators and propellant tank pressure sensors. There is margin in the memory for the addition of an attitude control algorithm in case of failure of the attitude control system.

d. Payload Control

Transponder operations are monitored by the RCU. The automatic gain control for the receiver and the transmit power are input to the RCU.

TABLE VII-1. MASS AND POWER BUDGET

Subsystem	Mass(kg)	Avg Power (W)
RCU	5.81	.12
TCU	7.57	2.25

VIII. PROPULSION SUBSYSTEM

A. FUNCTIONAL DESCRIPTION

The propulsion subsystem is a catalytic monopropellant hydrazine subsystem. The subsystem consists of four propellant tanks with positive expulsion elastomeric diaphragms separating the pressurant from the propellant. The tanks are manifolded to two redundant sets of thrusters. The two sets of thrusters are interconnected and isolated by latching valves to provide redundancy for all on-orbit control functions.

1. REQUIREMENTS

After separation from the Delta II upper stage and established on the 1203x15742 km. orbit, the first of the three satellites will be slowed down to achieve the final orbit of 1203x14932 km. Four 38-N thrusters (1D, 2D, 3D, 4D) and four 2-N thrusters (1C, 2B, 3C, 4B) will be fired at perigee to slow down the first satellite. The same process will be repeated for the remaining two satellites after meeting the required period for separation. The 2-N thrusters only will be used for roll, pitch, yaw desaturation and despin. See Table VIII-1 for thruster operation and the corresponding axis effected.

2. SUMMARY OF SUBSYSTEM OPERATIONS

The propulsion subsystem consists of four 38-N and twelve 2-N thrusters, four propellant/pressurant tanks made of titanium alloy, fill/drain valves for propellant and pressurant, latching isolation valves, filters, pressure regulators, pressure transducers and lines made of titanium alloy. See Fig. VIII-1 for the schematic diagram.

a. 38-N Thrusters

Four 38-N thrusters will be used for perigee burn to slow down the satellite to achieve the desired orbit. These thrusters are located at the bottom of the spacecraft, see Table VIII-2 and Fig. VIII-2 for exact location. See Table VIII-3 for thruster characteristics. See Fig. VIII-3 for photograph and dimensions.

TABLE VIII-1. THRUSTER OPERATIONS

Operation	Thruster Number
Spinup	4C/2C
Spindown	3B/1B
Delta V correction	1D,2D,3D,4D,1C,2C,3C, 4C
Positive roll(+X)	4A
Negative roll(-X)	1A and 3A
Positive pitch(+Y)	1A and 4A
Negative pitch(-Y)	2A and 3A
Positive yaw(+Z)	4C
Negative yaw(-Z)	3B
Redundant positive roll(+X)	1C and 2B
Redundant negative roll(-X)	4B and 3C
Redundant positive pitch(+Y)	2B and 3C
Redundant negative pitch(-Y)	1C and 4B
Redundant positive yaw(+Z)	2C
Redundant negative yaw(-Z)	1B

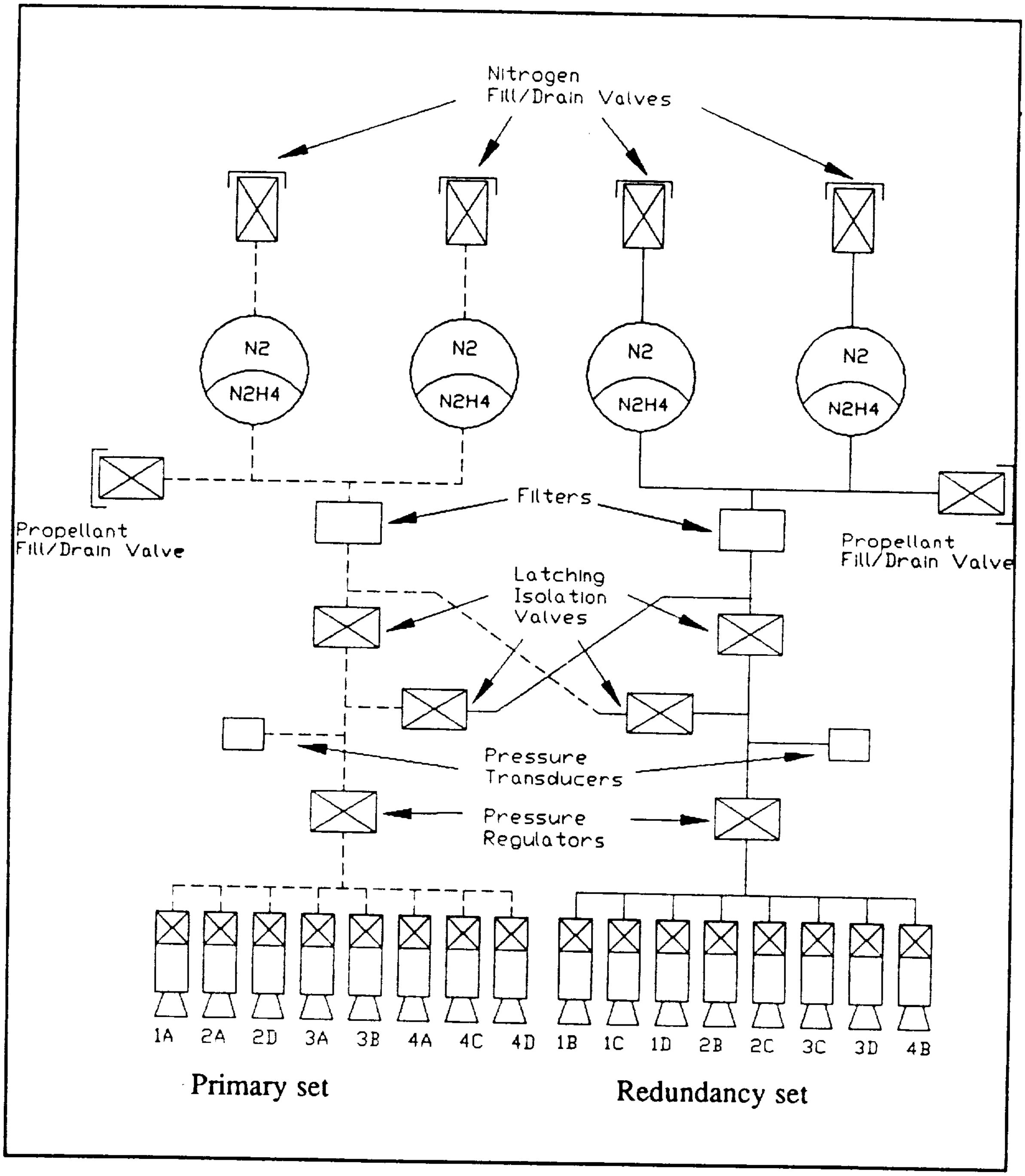

Figure. VIII-1. Schematic Diagram of Propulsion Subsystem.

b. 2-N Thrusters

Twelve 2-N thrusters provide pitch, yaw, roll and spacecraft despin control. See Table VIII-2 and Fig. VIII-2 for exact location and Table VIII-3 for thruster characteristics. Table VIII-1, shows the pairing of each thruster to give the required maneuvers. See Fig. VIII-4 for photograph and dimensions.

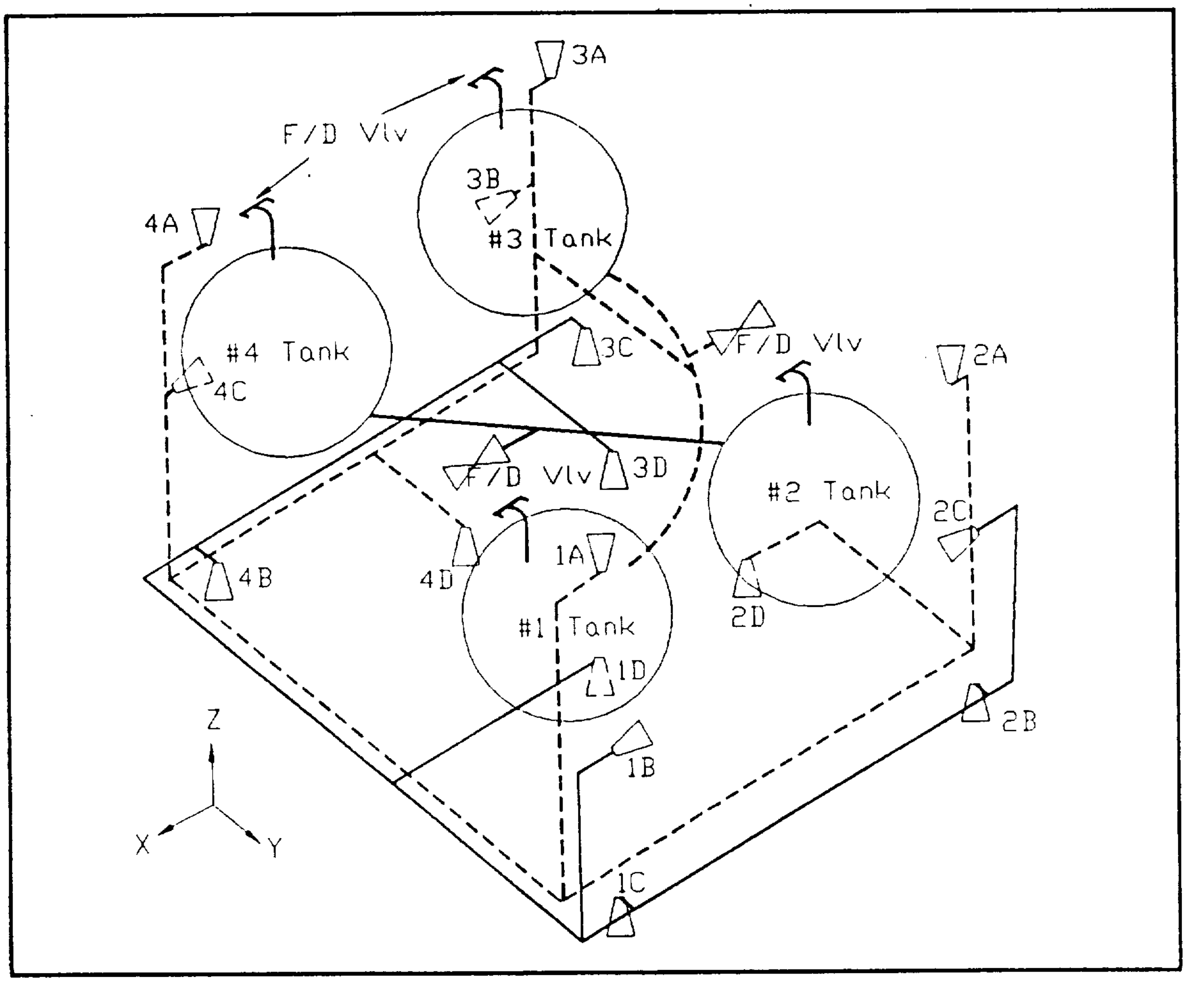

Figure. VIII-2. Physical Location of Thrusters.

c. Propellant Tanks

Four tanks, made of titanium alloy TI-6AL-4V, and manufactured by TRW Pressure Systems Inc., provide storage for hydrazine propellant. A strain gauge is bonded around the equator of each tank for pre-launch monitoring of the Nitrogen pressure. An elastomeric diaphragm inside the tank separates the pressurant from the propellant.

Table VIII-2. Thruster Location.

Thruster Designation	Spacecraft Coordinates*		
	X	Y	Z
1A	+55.000	+85.000	+69.492
2A	-55.000	+85.000	+69.492
3A	-55.000	-85.000	+69.492
4A	+55.000	-85.000	+69.492
1B	+55.000	+85.000	+00.501
2B	-59.000	+89.000	+35.000
3B	-55.000	-85.000	+00.501
4B	+59.000	-89.000	+35.000
1C	+59.000	+89.000	+35.000
2C	-55.000	+85.000	+00.501
3C	-59.000	-89.000	+35.000
4C	+55.000	-85.000	+00.501
1D	+24.192	+44.075	-01.175
2D	-24.192	+44.075	-01.175
3D	-24.192	-44.075	-01.175
4D	+24.192	-44.075	-01.175

*Centered at the initial center of gravity of the spacecraft (in cm.)

Table VIII-3. Thrusters Characteristics.

Designator	MR-50F (38-N)	MR-111(2-N)
Design Characteristics		
Catalyst	Shell 405	Shell 405
Thrust, steady state (N)	38.69 - 14.67	2 - 0.89
Feed pressure (N/sq m)	3309K - 930K	2206K-827.4K
Chamber pressure (N/sq m)	1144K- 448K	1268K-579K
Expansion ratio	40:1	200:1
Flow rate (kg/sec)	0.0173-0.0067	0.000909-0.000409
Valve	Parker-Hannifin Dual Seat	Wright Component Dual Seat Bifilar
Heater power	1.2 W per element (2 elements/thruster)	1 W per element (2 elements/thruster
Valve power	19 W @33 vdc @ 35 deg F	12 W/Coil @ 42 vdc @40 deg F
Weight (kg)	0.73	0.319
Engine	0.36	0.117
Valve	0.39	0.2.2
Demonstrated Performance	used on Viking	used on Intelsat V
Specific impulse	228-221	223-215
Total impulse (N-s)	62,272	260,208
Total pulses	20,000	420,000
Minimum impulse bit	0.09 @ 2,482,200 N & 25 ms ON	0.071 @ 1,620,000N &22 ms ON
Steady state firing (sec)	3504	8500

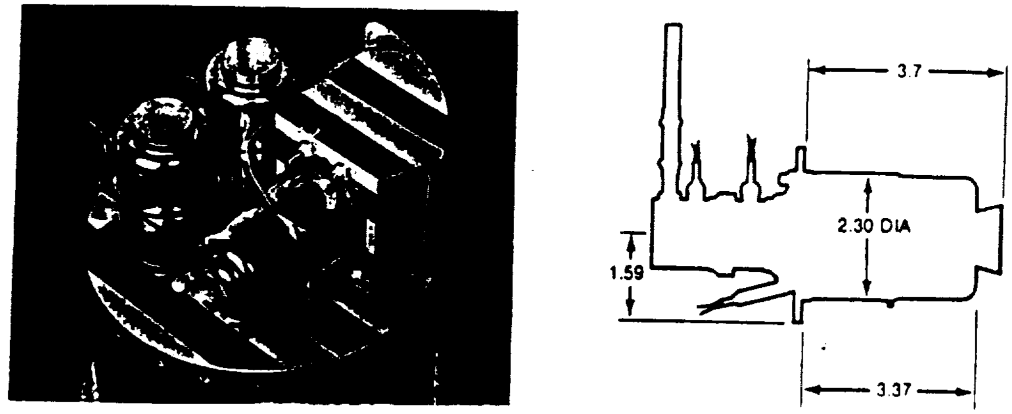

Figure. VIII-3. 38-N Thruster.

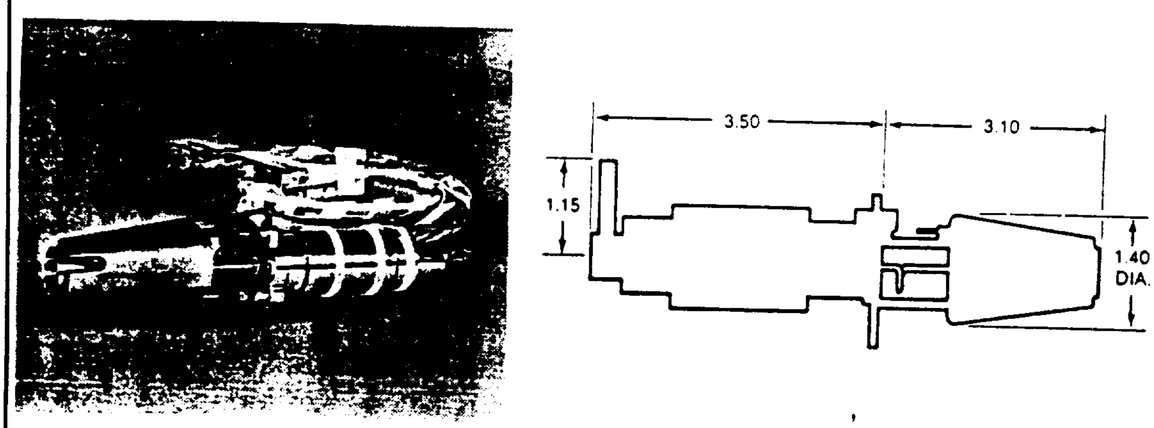

Figure. VIII-4. 2-N Thruster.

The operational characteristics of the tank are:

-nominal internal volume- 48,000 cu. cm. / tank

-operating pressure- 3,309,600 N/sq m.

-operating temperature- 70 degree F

-proof pressure- 4,137,000 N/sq m.

-burst pressure- 6,619,200 N/sq m.

d. Fill/Drain Valves

Fill and drain valves, four for pressurant and two for propellant, are used to service the propulsion subsystem during prelaunch operations. These valves are also used during subsystem functional tests, external and internal leakage tests, cleanliness verification, and pressurant and propellant loading or unloading operation. The valves are manually operated and self contained.

e. Pressure Regulator

Two pressure regulators are incorporated and operate over an inlet pressure of 3,309,000 N/sq m. to 827,400 N/sq m. The failure mode of the regulators is open, hence series redundancy is employed. The regulators are required to provide different pressure requirements to the two type thrusters.

f. Pressure Transducer

Two pressure transducers measure absolute pressure by sensing the deflection of a metal diaphragm by metal foil strain gages. The transducers contain integral hybrid electronic circuits for power conditioning, voltage regulation, signal amplification, and EMI filtering.

g. Latching Isolation Valves

Four latching isolation valves provide isolation of the redundant thruster sets in the event of a thruster failure or tank failure. The valve is a torque-motor actuated unit with latching forces supplied by permanent magnets. The flow path sealing element is an elastomeric "soft seat" plug retained in a spherically mounted shell. The amount of elastomeric plug compression, while in the closed position, is controlled by nonsliding metal-to-metal contact between the spherical shell and the outer diameter of the seat.

h. Filters

Each propellant tank is equipped with a 18 micron filter in the propellant outlet upstream of the latching valve and other subsystem components. The filter entraps any particulate matter carried by the propellant supply to protect the latch valve seats from contamination and to reduce the binder on the various filters at the thruster valve inlet. See Fig. VIII-3 for location.

i. Interconnect Tubings and Fittings

The interconnecting lines are 6.35-mm (0.25-in.) welded titanium tubing to minimize both Nitrogen and propellant leakage. The only mechanical joints in the design are the fill and drain valves and the propellant valve seats. With titanium-to-steel joints, diffusion bonded transition sections will be used.

The dual seat propellant valve for flow control into the catalytic thruster consists basically of electromagnetic and permanent magnets, a flapper and flexural tube assembly, and dual tungsten carbide seats.

j. Heaters

Separate and redundant heaters are supplied for each of the various subsystem components. The 38-N thruster uses two button-type catalyst bed heaters manufactured by Clayborn Laboratories and require 1.2 W per element or 2.4 W per thruster. The 2-N thruster uses a circular welded catalyst bed heater, provided by Tayco Engineering. Power requirements are 1 W per element or 2 W per thruster.

B. PROPULSION SUBSYSTEM DESIGN AND HARDWARE

1. LAUNCH VEHICLE SELECTION AND INTERFACE

The Delta II launcher adaptability and cost were the primary selection criteria. The launch is configured as three satellites stacked. As shown on Table VIII-4, Taurus, Atlas II and Delta II will all satisfy the mass and volume requirements for the launch.

Table VIII-4. Launch Vehicle Threshold.

Launcher	Orbit	Volume	Mass (kg)	Cost ($M)
Taurus	650x8063 nm	3.08 cu. m	516	16
Atlas II	650x8500 nm	68 cu. m	2272	53*
Delta II	650x8500 nm	40 cu. m	1500	42*

*Cost for a cluster of three satellites

The Delta II 7925 upper stage consists of the Morton Thiokol Star 48B solid rocket motor, a cylindrical payload attach fitting with clamp assembly and four separation springs, a spin table with bearing assembly and motor separation system, see Fig. VIII-5. The upper stage also contains a nutation control system.

a. Payload Attach Fitting

The Delta II 3712B attach fitting is the interface between the upper stage motor and the spacecraft. It supports the clamp assembly which attaches the spacecraft to the upper stage and allows the spacecraft to be released at separation. It mounts the four separation springs, two electrical disconnects, even sequencing system, upper stage telemetry, and the nutation control systems (NCS).

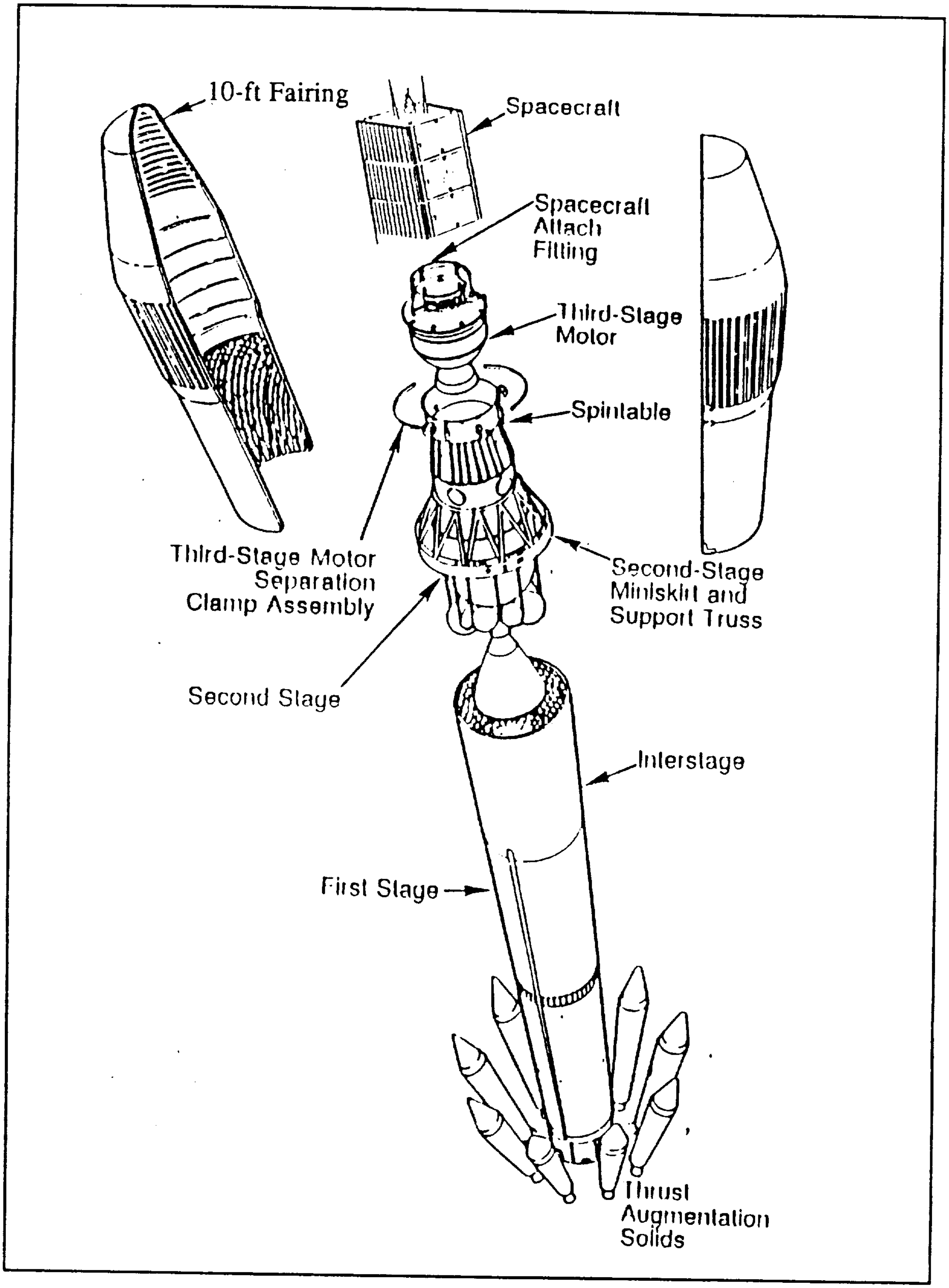

Figure. VIII- 5. Delta II 7925 Separation System.

b. Solid Motor

The Morton Thiokol Star 48B solid propellant rocket is nearly spherical with a major diameter of 1244.6 mm and an overall length of 2032 mm., including an extended nozzle . The motor has two integral flanges, the lower for attachment to the upper stage spin table and the upper for attachment to the 3712B payload attach fitting.

c. Spin Table

The spin table has four to eight spin rockets that spin up the upper stage to initial spin rate prior to third stage ignition. The motors have nominal thrust of 34 kg, 84 kg, and 95 kg respectively for 1 sec. These rockets are used in various combinations to achieve the spin rate. Spin rates of 30 rpm to 110 rpm are achievable.

d. Nutation Control System

The nutation control system (NCS) is designed to maintain a small cone angle of the combined upper stage and spacecraft. It operates during the Payload Assist Module (PAM) motor burn and the postburn coast phase, with NCS propellant flowdown occuring before upper stage spacecraft separation. The NCS design concept uses a single-axis Rate Gyro Assembly (RGA) to sense coning and a monopropellant (hydrazine) propulsion module to provide control thrust.

e. Separation/Despin

The spacecraft is fastened to the attach fitting by means of a two-piece V-block-type clamp assembly, which is secured by actuation of ordnance cutters that sever the two studs. Clamp assembly design is such that cutting either stud will permit spacecraft separation. To maintain spacecraft stability the upper stage will stay with the spacecraft as long as possible to assist in the nutation control. Springs assist in retracting the clamp assembly into retainers after release. A relative separation velocity of about 0.61 to 2.4 m/s is imparted to the spacecraft by four separation springs. A yo-weight tumble system despins and imparts a coning motion to the expended third-stage motor 2 sec after spacecraft separation to change the direction of its momentum vector and prevent spacecraft recontact with the third stage.

2. RCS DESIGN

The reaction control system consists of twelve 2-N thrusters. Four of the twelve thrusters also assist the four 38-N thrusters for the perigee burn. These four are located at the bottom along with the 38-N thrusters. Location of the thrusters was carefully chosen to avoid plume impingement on the solar arrays and other sensors, see Table VIII-2 and Fig. VIII-2. The four top and bottom 2-N thrusters are used for pitch and roll control. The four located on the side corners are used for despin/spin and yaw control. See Table VIII-2 for thruster operation. Other design characteristics are available in Table VIII-4.

3. MASS/POWER SUMMARY

As shown by Table VIII-5, 136.77 kg is alloted for stationkeeping. As of this writing, the propellant required for station keeping has not been determined. The value shown is only an estimate.

See Table VIII-3 for power requirement.

C. PROPULSION SUBSYSTEM PERFORMANCE

After the satellites are mechanically separated, the propulsion system will be used to orient the spacecraft in preparation for the perigee burn. Delta V of 42 m/s is required to achieve the final orbit. This maneuver will last less than two minutes. The 38-N thrusters have steady state firing of 8500 sec., while the 2-N thrusters have 3,504 sec. See Table VIII-2 for other performance characteristics of the two thrusters.

Table VIII-5. Propulsion Mass Breakdown.

Propellant (stationkeeping)	136.77 kg
Propellant (delta V change)*	7.21 kg
Propellant (desaturation)**	1.00 kg
Twelve 2-N Thrusters (12x0.319kg)	3.83 kg
Four 38-N Thrusters (4x0.735 kg)	2.94 kg
Tanks (4x5.897 kg)	23.59kg
Tubings, Valves and Fittings	4.31 kg
Nitrogen Pressurant	0.23 kg
Total	**179.88 kg**

* See Appendix A for computation.

** See Appendix F for computation.

IX. THERMAL CONTROL SUBSYSTEM

A. FUNCTIONAL DESCRIPTION

1. Requirements

The purpose of the thermal control subsystem is to maintain the spacecraft temperatures within the operating temperature limits of its various components. Typical temperature ranges are listed in Table IX-1.

Table IX -1. Temperature Ranges for Components

Component	Operating temperature(°C)
Electric power:	
Control unit	-25/+30
Solar array	-160/+80
Shunt	-45/+60
Battery	0/+40
Payload:	
Receiver electronics	-20/+45
Transmitter electronics	-15/+45
Antenna	-170/+90
Attitude control:	
Earth/sun sensors	-25/+60
Angular rate assembly	-10/+60
Reaction wheels:	-10/+55
Propulsion:	
Tank	-5/+60
Valves	-5/+60
Thrusters	-5/+60

2. Summary of Subsystem Operation:

Passive thermal control techniques are used throughout and are shown in Fig. IX-1. The major components of the system are:

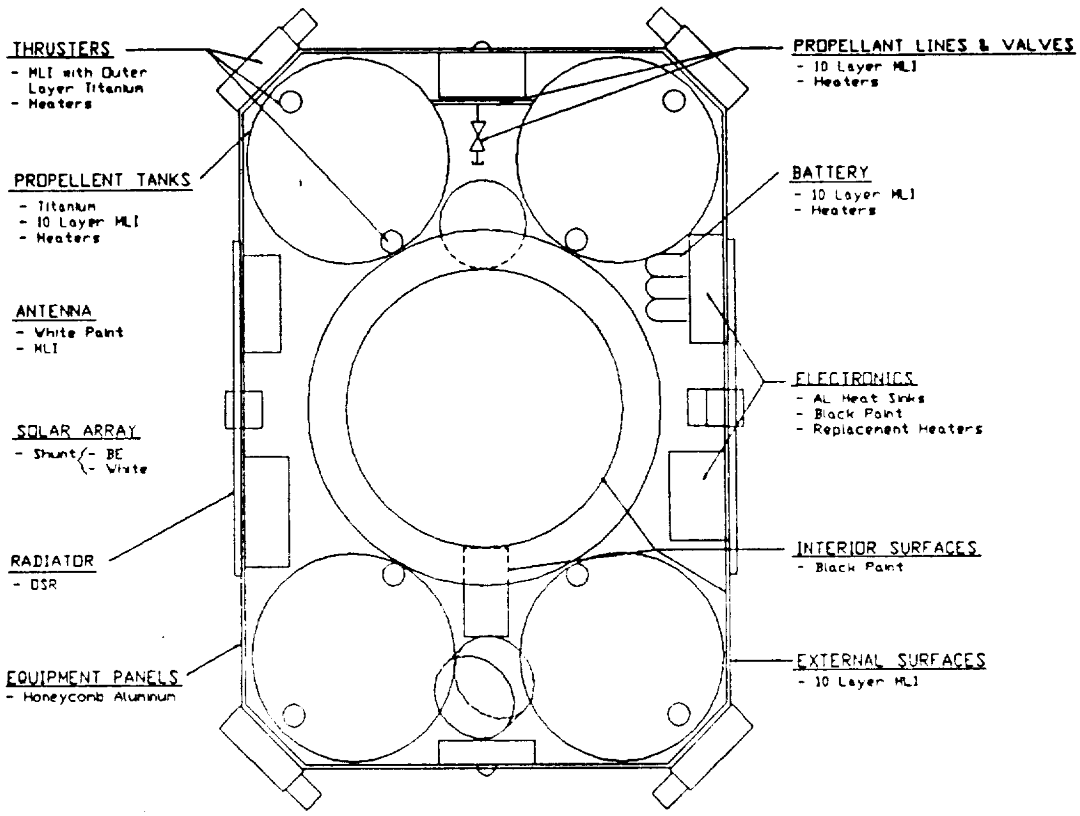
THRUSTERS
- MLI with Outer Layer Titanium
- Heaters
PROPELLENT TANKS
- Titanium
- 10 Layer MLI
- Heaters
ANTENNA
- White Paint
- MLI
SOLAR ARRAY
- Shunt (- BE (- White
RADIATOR
- OSR
EQUIPMENT PANELS
- Honeycomb Aluminum
PROPELLANT LINES & VALVES
- 10 Layer MLI
- Heaters
BATTERY
- 10 Layer MLI
- Heaters
ELECTRONICS
- AL Heat Sinks
- Black Paint
- Replacement Heaters
INTERIOR SURFACES
- Black Paint
EXTERNAL SURFACES
- 10 Layer MLI

Figure IX-1.

a. Radiator

Two radiators made of Optical Solar Reflector material, each 0.9 x 0.7 meters, are used to radiatively couple the spacecraft to the space sink. They are placed on the east and west faces of the spacecraft which are always edge-on to the sun, thus receiving albedo and earth radiated flux, but no solar flux.

b. Electronics

All electronic modules are located on the equipment panels that are mounted back-to-back with the OSR to minimize conductive paths. The equipment panel is of aluminum honeycomb construction with aluminum heatsinks as required. No detailed thermal analysis of the substrates was attempted.

Multilayer Insulation (MLI): MLI is used throughout to thermally isolate components. "Low" temperature applications use MLI with outside layers of aluminum kapton (spacecraft sides, etc). "Hot" temperature locations use MLI with outside layers of titanium kapton (thrusters). A nominal thickness of 10 layers was used throughout.

c. Surface Coatings

The following surface coatings with the listed emissivities and absorptances are used to optimize radiative coupling:

Table IX-2. Emissivity and Absorptance of Materials

Material	Emissivity BOL	Emissivity EOL	Absorptivity BOL	Absorptivity EOL
Natural aluminum	.06	.06	.95	.95
Anodized aluminum	.78	78	.35	.30
Black paint	.90	.90	.95	.95
White paint	.90	.90	.20	.45
OSR	.80	.80	.08	.21

Aluminum kapton	.35	.50	.60	.60
Titanium kapton	.60	.60	.60	.60
Solar cells	.85	.85	.70	.75
MLI	.02 (Effective emissivity)			

d. Thermal Paths

Thermal paths raise two significant issues. The first is ensuring that electronic equipment is mounted on equipment panels to minimize conductance paths to the radiators. Another consideration is to dissipate excess electric power from the solar panel at BOL to a shunt mounted on the array itself which in turn radiates the heat to surrounding space. The remaining factor is to minimize plume impingement and soakback from the thrusters. Other than these considerations, subsystems are allowed to place components to optimize their own requirements.

e. Heaters:

There are two basic types of heaters used: redundant and replacement. Redundant heaters are used as additional sources of thermal dissipation to maintain certain equipments (tanks, lines, valves, etc.) above minimum operating temperature. These consist of heat filament elements wound in layered material such as kapton. The other type of heater is the replacement heater that is turned on when certain equipments (payload transmitter) are turned off in order to minimize thermal excursions. The former require additional power requirements whereas the latter do not. Thrusters have their own heaters for their catalytic beds. Control of the heaters is by two methods:

(1) enable/disable command from the ground and

(2) once enabled, automatic control by thermistor to maintain temperatures within allowed range. The following table describes the various heaters and location:

Table IX-3. Heater Location

Component	Number	Thermal dissipation (each)
Tanks	4	4.5
Thruster: 38-N	2	5.0
Thruster: 2-N	12	1.5
Valves	5	0.5
Lines	6	7.0
Batteries	2	25.0
Reaction wheels	3	8.0
Sensors	5	25.0
Replacement heater	1	26.5

B. THERMAL CONROL SUBSYSTEM DESIGN

1. Thermal Design Process:

The thermal design process involves eight major steps:

(1) Conceptual spacecraft configuration

(2) Preliminary analysis

(3) Preliminary spacecraft configuration

(4) Final spacecraft configuration

(5) Spacecraft thermal analytical model I

(6) Thermal balance test

(7) Spacecraft thermal analytical model II

(8) Spacecraft thermal vacuum test

For this report steps (1) - (5) were accomplished. Steps (6) - (8) are beyond the scope of this project.

The spacecraft was divided into four major temperature zones:

(1) Spacecraft main body

(2) Antennas

(3) Solar arrays

(4) Equipment panels

The solar array zone includes the solar array panels, array support structure, and shunt assembly. The equipment panel will include a detailed analysis of the equipment modules, substrates, heatsinks, and equipment panels. The antenna zone consists of the antennas and their support structures. The spacecraft main body temperature zone is the entire satellite excluding the other zones. The equipment panels are included, but only as lumped components. Complete analysis was conducted only of the spacecraft main body temperature zone.

2. Thermal Environment:

There are four basic thermal environments to consider:

Pre-launch: This involves the spacecraft as stowed inside the fairing of the launch vehicle on the launchpad. This environment is controlled through launch services (providing AC, heat, etc.). Software and time limitations prevent inclusion here.

Launch: This involves controlling the temperature of the satellite during transit through the atmosphere. The major concern here is the radiative coupling of the fairing with the satellite. This analysis is deferred for similar reasons.

Transfer orbit: This involves modeling the thermal behavior of the satellite from orbital insertion through transfer to final orbit. This analysis is also deferred.

On-orbit: This case is the subject of this report. The analysis involved two cases (hot and cold) in the steady-state mode.

The on-orbit heat inputs are from two sources: internal and external. The internal heat sources consist of thermal dissipation from the electronic equipment and soakback from engine firings:

Table IX-4. Internal Heat Sources

Equipment	Thermal dissipation (Watts)
TT&C:	
Remote command unit #3	0.5
Remote telemetry #4	1.1
Payload:	
Receiver	7.1
Receiver synthesizer	5.3
Receiver power supply	2.1
Transmitter	26.5
Transmitter clock	1.2
Downlink antenna ground	0.5
ACS	35.0
Electric power:	
Battery	7.8
Control	5.0
Shunt	30.0
Solar array:	
Shunt	250.0
Heaters	50.0
Thrusters:	
38-N thrusters (4)	Thrust duration dependent
2-N thrusters (12)	Thrust duration dependent

The on-orbit external heat fluxes include are displayed in Table IX-5. The values for heat flux must be multiplied by the appropriate geomentric factor.

Table IX-5. On-orbit External Heat Fluxes

Source	Flux (Watts/square meter)
Solar (winter)	1399
Solar (summer)	1309
Solar (vernal equinox)	1362
Solar (autumnal equinox)	1345

Albedo (Average)	507
Earth radiation (Average)	217

C. THERMAL CONTROL SUBSYSTEM PERFORMANCE.

Before looking at the detailed temperature results, a brief discussion of the thermal modeling process, tools, and their limitations. A lumped parameter or finite element method of modeling was used to determine temperatures at designated points throughout the spacecraft. The basic heat equation of the total spacecraft is:

HEAT STORED = HEAT IN + HEAT DISSIPATED - HEAT OUT

Rather than looking at the spacecraft in total, it can be divided into a number of finite elements commonly called nodes. A heat equation can then be written for each node and then all the nodes can be combined into a matrix equation that can be solved for the temperatures to yield a thermal map of the spacecraft. Each node can be connected to all the other nodes through a radiative or conductive branch with an associated conductance. The computation of the conductance can be rather complicated involving spatial and material properties. In addition, each node can have heat and temperature inputs in the model. These properties are determined from the configuration and materials used, the conductances computed and then the matrix is solved. The complexity quickly grows with each additional node and branch, but the solution is well within the capacity of most computers.

In order to compute the conductances of the different paths, a Data Base Management (DBM) Program (Q&A) was used. A data file was created for each path or branch (131 total) with 33 data entries per file to provide identification and spatial and material properties. The DBM Program combined with external FORTRAN routines computed areas, cross-section areas, view factors, emissivity factors, flux inputs and ultimately the conductances. The essential outputs of this program, required as inputs for the next program, are:

(1) Branch

(2) From node

(3) To node

(4) Type of path (radiative or conductive)

(5) Conductance

A second program written by Prof. Kraus of the Naval Postgraduate School was used to solve the matrix equation. His program consists of two programs: THANSS and TASS. The data for each branch listed above is input into THANSS, which builds a model of the system. The output of this program is then input into TASS, which actually solves for nodal temperatures.

This procedure is inflexible and extremely time intensive, which complicates the ability of the thermal control designer to react to design changes or optimize the design through iteration. Although the data base can be manipulated quite easily through "mass updates", the THANSS model builder requires that any changes to any of the nodes must be entered individually and manually. This effectively precludes quick changes in thermal properties such as emmissivity and absorptance as well as spatial changes that can be used to manipulate conductances and hence control temperatures. A second limitation is that only steady-state analysis can be performed. The steady-state "hot" case is the direct output of the analyzer program. However, for the "cold" case, the steady state output temperatures are never reached because of the short eclipse period (35 minutes). A separate FORTRAN program based on the radiative cooling equations was used to compute the transient cold temperatures from these steady state values.

The model used for this project included 61 nodes and 131 thermal paths as shown in Fig. IX-2. This was considered to be the minimum number of nodes which would yield a reasonable sampling of spacecraft temperatures.

The "hot" case was found to be perigee with most equipment operating, and with maximum external flux.

Table IX-6. Hot Case Heat Input

Source	Heat Input (Watts)
Equipment	43
Solar	4634
Albedo	1003
Earth radiated	645

The "cold" case was determined to be at end of eclipse with partial equipment load and earth radiated flux only.

Table IX-7. Cold Case Heat Input

Source	Heat Input (Watts)
Equipment	140
Earth radiated	645

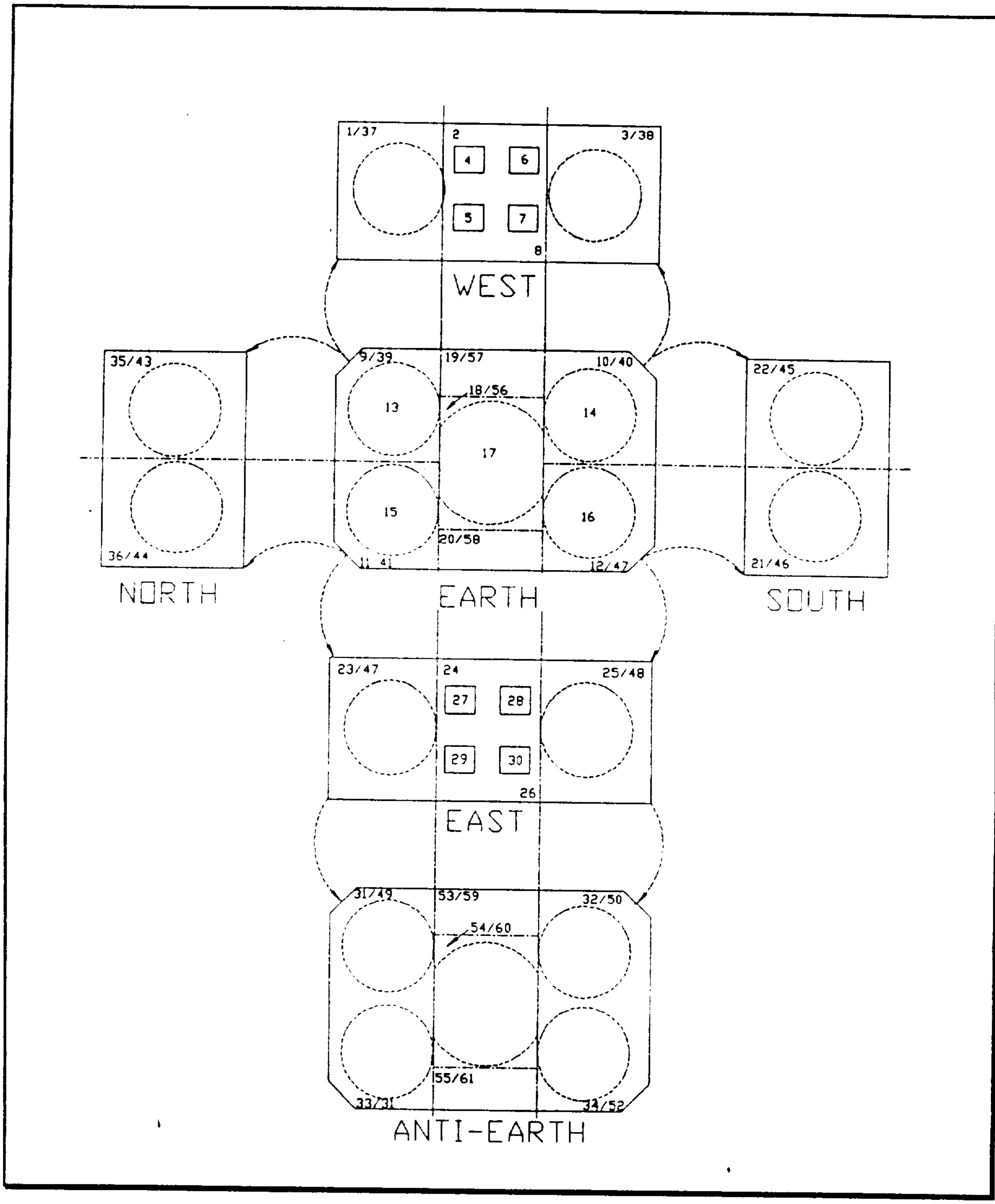
1/37
2
3/38
4
6
5
7
8
WEST
35/43
9/39
19/57
10/40
22/45
18/56
13
14
17
15
16
20/58
36/44
11/41
12/47
21/46
NORTH
EARTH
SOUTH
23/47
24
25/48
27
28
29
30
26
EAST
31/49
53/59
32/50
54/60
55/61
33/51
34/52
ANTI-EARTH

Figure IX-2.

Using the thermal control data specified in the previous section (radiator size, coatings, insulation, heaters, component location, etc.) to compute the conductances and using the above heat inputs, "hot" and"cold" computer runs were accomplished with the following results. The high temperatures are associated with external nodes with large incident fluxes. The interior of the spacecraft is insulated from these extremes by MLI insulation. Thus the remaining temperatures are within the temperature operating limits of the equipment. The cold temperatures can be elevated by turning on appropriate heaters. The range of hot and cold temperatures could be reduced by optimization of thermal properties such as emissivity, absorptivity, and conductivity. As discussed above, software limitations prevented these values from easily being changed and entered

Table IX-7. Thermal Simulation Temperatures

Node	Component	Hot	Cold
1	West face panel 1	26.8	7.5
2	West radiator	1.5	-11.9
3	West face panel 2	25.9	7.1
4	Electronics 1	1.5	-12.5
5	Electronics 2	1.5	-12.5
6	Electronics 31.5	-12.5	
7	Electronics 4	1.5	-12.5
8	West equipment panel	1.5	-12.5
9	Earth face panel 1	31.0	11.5
10	Earth face panel 2	31.3	10.7
11	Earth face panel 3	28.3	8.2
12	Earth face panel 4	33.3	12.7
13	Tank 1	40.3	17.0
14	Tank 2	39.7	17.0
15	Tank 3	38.8	16.0
16	Tank 4	44.1	21.0
17	Center tube	38.5	15.4
18	Earth face panel 5	30.2	11.5

19	Earth face panel 6	44.1	2.5
20	Earth face panel 7	8.2	-6.1
21	South face panel 1	26.8 17.1	
22	South face panel 2	35.8	13.8
23	East face panel 1	21.1	3.1
24	East radiator	-10.1	-21.5
25	East face panel 2	42.6	18.4
26	East equipment panel	-10.1 -21.7	
27	Electronics 5	-10.1	-21.7
28	Electronics 6	-10.1	-21.7
29	Electronics 7	-10.1	-21.7
30	Electronics 8	-10.1	-21.7
31	Anti-earth face panel 1	43.3	19.6
32	Anti-earth face panel 2	50.0	24.4
33	Anti-earth face panel 3	44.8	20.5
34	Anti-earth face panel 4	46.0	21.9
35	North face panel 1	38.5	15.5
36	North face panel 2	36.3	16.5
37	West face MLI 1	90.7	50.1
38	West face MLI 2	90.3	50.7
39	Earth face MLI 1	154.0	86.5
40	Earth face MLI 2	162.0	90.2
41	Earth face MLI 3	153.5	86.6
42	Earth face MLI 4	154.5	87.0
43	North face MLI 1	296.4	139.0
44	North face MLI 2	296.4	139.0
45	South face MLI 1	94.0	53.0
46	South face MLI 2	95.1	53.4
47	East face MLI 1	89.1	49.5
48	East face MLI 2	95.6	53.8
49	Anti-earth face MLI 1	298.3	140.0
50	Anti-earth face MLI 2	298.1	140.0
51	Anti-earth face MLI 3	298.3	140.0
52	Anti-earth face MLI 4	297.8	140.0

53	Anti-earth face panel 5	58.4	30.5
54	Anti-earth face panel 6	46.6	21.4
55	Anti-earth face panel 7	55.5	27.3
56	Earth face MLI 5	151.5	84.0
57	Earth face MLI 6	152.9	84.9
58	Earth face MLI 7	150.4	285.0
59	Anti-earth face MLI 5	299.7	140.0
60	Anti-earth face MLI 6	302.9	141.0
61	Anti-earth face MLI 7	299.4	140.0

REFERENCES

1. NASA Solar Cell Array Design Handbook, Vol I, equation 9.10-18

2. NASA Solar Cell Array Design Handbook, Vol I, equation 9.10-27

3. B. N. Agrawal, *Design of Geosynchronous Spacecraft,* Prentice-Hall, Inc. Englewood Cliffs, NJ. 1986.

4. TRE Corporation, "ASTECH® Design Allowables Manual, ADAM-100," TRE Corporation, Santa Ana, CA. June 1985.

5. TRE Corporation, "ASTECH® Design Manual, ADM-300," TRE Corporation, Santa Ana, CA. April 1977.

6. "Delta II User's Manual," McDonnell Douglas Astronautics Corporation.

7. Bernard Sklar, *Digital Communications*, New Jersey, Prentice Hall, 1988.

8. Tri T. Ha, *Digital Satellite Communications*, New York, Macmillan, 1986.

9. Richard C. Johnson and Henry Jasik, *Antenna Engineering Handbook*, 2d Ed, New York, 1984.

10. C.C. Kilgus, "Resonant Quadrifilar Helix Design," *Microwave J.*, vol. 13, December 1970, pp. 49-54.

11. John D. Kraus, *Antennas*, 2d Ed, USA, McGraw-Hill, 1988.

12. Bruce S. Hale, The ARRL Handbook for the Radio Amateur, Sixty-sixth Ed, CT, American Radio Relay League, 1988.

13. Tada, H.Y., et. al., *Solar Cell Radiation Handbook*, Third Edition and Addendum 1, JPL Publication 82-69. November 1, 1982.

14. JPL and NASA, *Solar Cell Array Design Handbook*, Volumes 1 and 2. JPL Publication SP 43-38. October 1976.

15. Chryssis, George C., *High-Frequency Switching Power Supplies. Theory and Design*, Second Edition, McGraw Hill Publishing Co., New York, 1989.

16. Chetty, P.R.K., *Switch-Mode Power Supply Design*, Tab Professional and Reference Books, Blue Ridge Summit, Pa. 1986.

17. Intelsat Corp., *Intelsat 5 book*

APPENDIX A

1. ALTERNATE ORBITS

a. Ten Hour Orbit

perigee = 1204 KM

apogee = 33169 KM

radius of perigee = 7582 KM (r_p)

radius of apogee = 39548 KM (r_a)

semi major axis = 23565KM (a)

$$V_{circ}\ 650 = 7.2508\ \text{km/s} = \left(\sqrt{\frac{\mu}{\text{orbit radius}}}\right)$$

$$V_{perigee} = 9.3932\ \text{km/s} = \left(\sqrt{\frac{2\mu r_a}{(r_a + r_p)r_p}}\right)$$

ΔV = 2.1424 km/s (7028.74 ft/s)

Propellant Mass:

I_{sp} = 230 s PKM dry mass = 45.5 kg

M_i = 411.917 kg efficiency = .99

$M_p = (M_i + PKM + M_p) * (1 - \exp(-\Delta V/g*I_{sp}*n)) = 737.3$ kg

b. Twelve Hour Orbit

perigee = 1204 KM

apogee = 39261 KM

radius of perigee = 7582 KM

radius of apogee = 45639 KM

period = 12.0 hour

semi major axis = 26610 KM

Vcirc 650 = 7.2508 km/s

Vperigee = 9.4956 km/s

ΔV = 2.2448 km/s (7365 ft/s)

Propellant Mass:

I_{sp} = 230 s PKM dry mass = 45.5 kg

M_i = 411.917 kg efficiency = .99 M_p = 793.4 kg

2. LAUNCH ORBIT (FIVE HOUR ORBIT)

perigee = 1204 KM

apogee = 15729 KM

radius of perigee = 7582 KM

radius of apogee = 22107 KM

period = 5.0 hour

semi major axis = 14846 KM

$$V_{perigee}\ 1204\text{x}15729 = \left(\sqrt{\frac{2\mu r_a}{(r_a + r_p)r_p}}\right) = 8.8489 \text{ km/s}$$

$V_{perigee}$ 1204x14933 = 8.8063 km/s

ΔV = -42.2 m/s

Propellant Mass for Mission Orbit Burn:

Isp = 225s Mi = 411.917 kg

efficiency = .99 Mp = 8.04 kg

3. ORBITAL PERTURBATIONS

a. PRECESSION OF THE LINE OF NODES

$$\frac{d\Omega}{dt} = \frac{3nJ_2Re^2}{2a^2(1-e^2)^2} \cos(i) \qquad \text{(rad/sec)}$$

from "Spaceflight Dynamics" by W.E. Wiesel

$J_2 = 0.001082$ $\qquad$ $Re = 6378$ km

$\mu = 398601.2$ km^3/s^2 $\qquad$ $a = 14446$ km

$i = 63.435$ deg $\qquad$ $e = 0.47517$

$\frac{d\Omega}{dt} = -0.425$ deg/day

b. INCLINATION PERTURBATIONS

1. SUN

After eliminating those short period terms which are periodic with the true anomaly of the orbit, the perturbation of the orbit inclination due to the sun is given by:

$$\frac{di}{dt} = \frac{3\mu_s a^2}{4hr_s{}^3}(\sin(\Omega)\cos(\Omega)\sin(i)\sin\text{^}2(i_s) + \sin(\Omega)\cos(i)\sin(i_s)\cos(i_s))$$

i_s = solar inclination = 23.44 deg

i = orbit inclination = 63.435 deg

Ω = orbit right ascension

h = orbit angular velocity = R x V

= (7582 km) * (8.806 km/s) = 6.67e4 km^2/s at perigee

μ_s = solar gravitational constant = 1.32686e11 km^3/s^2

a = orbit semi-major axis = 14446 km

r_s = solar radius = 1.49592e8 km

This equation is plotted for several values of the right ascension in Figure II-4, with Table II-3 listing the associated computed values.

2. MOON

A similar equation for the perturbations due to the moon is given below:

$$\frac{di}{dt} = \frac{3\mu_l a^2}{4hr_l{}^3}(\sin(\Omega)\cos(\Omega)\sin(i)\sin\text{^}2(i_l) + \sin(\Omega)\cos(i)\sin(i_l)\cos(i_l))$$

i_l = lunar inclination = 18.3 deg to 28.6 deg

μ_l = lunar gravitational constant = 4.9028e3 km^3/s^2

r_l = lunar radius = 3.844e5 km

This equation is periodic in both the orbit right ascension and the inclination of the moon. Table II-3 and Figure II-4 show the inclination change for several values of right ascension and the two limits of lunar inclination.

Since the right ascension of the ascending node is precessing at the rate of -0.425 degree/day, both of these effects will complete a full cycle each 847 days. With the worst case alignment of these two bodies, the maximum total d(i)/dt is 0.1175 degree/yr. Over the difference between the 1095 day planned life of the spacecraft and the 847 day cycle of these disturbances, the worst case accumulated perturbation in inclination will be less than 0.08 degree - an amount small enough to not require correction.

c. PRECESSION OF THE ARGUMENT OF PERIGEE

The precession of the argument of perigee is given by the following equation:

$$\frac{d\omega}{dt} = \frac{-3nJ_2\, Re^2}{2a^2(1 - e^2)^2}\left(\frac{5}{2} * \sin^2(i) - 2\right)$$

n = orbital mean motion = $\sqrt{\frac{\mu}{a^3}}$ = 3.6362e-4 (1/sec)

J_2 = 0.001082

Re = earth radius = 6378 km

a = orbit semi-major axis = 14446 km

e = orbit eccentricity = 0.47517

i = orbit inclination = 63.435 deg

This equation yields $d\omega/dt$ = 0 for an orbit at the critical inclination of 63.435 deg. However, due to higher order effects, an orbit at this inclination does still precess about its orbit normal, changing the argument of perigee. For this orbit, the higher order drift has been calculated through numerical integrtation of the orbital dynamic equations. At the critical inclination, the perigee will circulate through 360 degrees with a period of approximately 1100 years - yielding a rate of 0.327 deg/yr. This orbit is fairly sensitive to error in inclination however. For an error in inclination of 0.1 degree, the period of this circulation drops to 250 years and the associated rate climbs to 1.44 deg/yr.

APPENDIX B: MOMENT OF INERTIA CALCULATIONS

The spacecraft moments of inertia were calculated using the detailed mass and component breakdown of the spacecraft. All components were assumed to be simple solids of uniform density. Since the greatest contribution to the spacecraft moments by most components resulted from component distance from the spacecraft center of mass, this is a reasonable assumption.

Most spacecraft components were modeled using the geometric shape that best approximated the shape of the component: rectangular parallelepipeds for equipment boxes and structural panels, spherical shells for the fuel tanks, etc. Miscellaneous small components were assumed to the uniformly distributed within the spacecraft, which probably overestimates their contribution to the total moment of inertia, but the contribution is small. Including these items allows a cross-check with the spacecraft mass summary to ensure that all components have been included.

The moment of inertia calculations were performed using a spreadsheet. The inputs were the component dimensions, mass, and position within the spacecraft (measured as the distance from the center of the component to a reference point). The center of mass location, distance from the spacecraft's center of mass, and and contribution to the spacecraft's moments of inertia were calculated from the input information. The spacecraft's total mass, center of mass, and total moments were calculated from the component contributions.

The change in the spacecraft's mass, center of mass, and moments of inertia over the spacecraft's life are summarized in Table B-1. The detailed spreadsheets used to calculate these values are given in Tables B-2 to B-5. All distances were measured from the center of the anti-earth equipment panel. The positive X direction is toward the housekeeping equipment panel, and the positive Z direction is toward the earth face. The positive Y direction is defined to make a right-handed coordinate system.

A copy of the spreadsheet showing the equations is included as Table B-6.

Table B.1 Summary of Spacecraft Statistics

ITEM	MASS (kg)	CENTER OF MASS (cm)			TOTAL MOMENT OF INERTIA (kg-m^2)					
		Cx	Cy	Cz	Ixx	Iyy	Izz	Ixy	Ixz	Iyz
SEPARATION, SOLAR ARRAY FOLDED	411.917	3.397	-0.632	35.911	122.673	96.858	195.807	-0.832	1.007	0.291
SEPARATION, SOLAR ARRAY EXTENDED	411.917	3.397	-0.632	35.911	153.173	275.074	377.224	-0.832	1.007	0.291
50% PROPELLANT REMAINING	339.505	4.233	-0.786	36.133	118.950	263.125	333.257	-0.813	0.979	0.296
10% PROPELLANT REMAINING	281.265	5.250	-0.977	36.409	91.419	253.466	297.847	-0.789	0.944	0.302

ORIGIN AT CENTER OF ANTIEARTH PANEL
POSITIVE Z DIRECTION--EARTH FACE
POSITIVE X DIRECTION --HOUSEKEEPING EQUIPMENT PANEL (EAST FACE)
POSITIVE Y DIRECTION -- (SOUTH FACE)

1/18/90 9:25		MOMENTS OF INERTIA WITH THE SOLAR ARRAY FOLDED AND THE PROPELLANT TANKS FULL								
ITEM	ITEM DIMENSIONS (cm)			MASS (kg)	ITEM MOMENTS (kg-m^2)			ITEM POSITION (cm)		
	a	b	c		Ix	Iy	Iz	x	y	z
TELEMETRY, TRACKING & COMMAND										
REMOTE COMMAND UNIT 3 (RCU 3)	16.230	20.400	14.480	5.797	0.030	0.023	0.033	56.885	-34.800	12.240
REMOTE TELEMETRY UNIT 4 (RTU 4)	20.220	20.400	14.480	7.552	0.039	0.039	0.052	54.891	-34.800	57.760
DOSIMETER	6.730	9.810	3.990	0.363	0.000	0.000	0.000	81.635	-40.095	35.000
		SUBSYSTEM TOTAL		13.712						
RADIO FREQUENCY SUBSYSTEM										
PAYLOAD RECEIVER	14.610	32.080	32.080	6.713	0.115	0.070	0.070	-57.695	-23.960	48.960
PAYLOAD RECEIVER SYNTHESIZER	11.760	19.690	12.700	1.724	0.008	0.004	0.008	-59.120	-30.158	11.350
PAYLOAD RECEIVER POWER SUPPLY	8.890	22.230	16.940	1.814	0.012	0.006	0.009	-60.555	28.890	13.471
PAYLOAD TRANSMITTER	17.150	35.830	22.230	6.169	0.095	0.041	0.085	-56.425	21.585	53.885
PAYLOAD RECEIVER STABILIZED CLOCK	3.810	10.160	9.650	0.454	0.001	0.000	0.000	-63.095	34.920	34.825
PAYLOAD CTS	1.910	10.160	2.540	0.045	0.000	0.000	0.000	-64.045	19.920	31.270
ANTENNA #1 (point mass)				1.498	0.000	0.000	0.000	0.000	0.000	79.000
ANTENNA #2 (r/h)	14.800	29.600		1.680	0.021	0.018	0.018	-30.200	60.200	84.600
ANTENNA #3 (r/h)	10.700	21.400		0.450	0.003	0.003	0.003	34.300	-64.300	80.700
GROUND PLANE	43.000	43.000	0.001	0.417	0.006	0.006	0.013	0.000	0.000	70.000
CABLES (uniform distribution)	130.000	190.000	4.000	0.9072	0.273	0.128	0.401	0.000	0.000	35.000
		SUBSYSTEM TOTAL		21.871						
ATTITUDE CONTROL SYSTEM										
ATTITUDE CONTROL COMPUTER	36.200	6.350	14.900	2.500	0.005	0.032	0.028	0.000	-92.345	35.000
REACTION WHEEL +X DIRECTION (r/h)	11.750	12.000		2.375	0.016	0.011	0.011	0.000	-49.250	35.000
REACTION WHEEL +Y DIRECTION (r/h)	11.750	12.000		2.375	0.011	0.016	0.016	0.000	89.520	35.000
REACTION WHEEL +Z DIRECTION (r/h)	11.750	12.000		2.375	0.011	0.011	0.016	0.000	49.250	35.000
REACTION WHEEL -X/-Y/+Z DIRECTION	11.750	12.000		2.375	0.011	0.011	0.011	-32.500	-32.500	17.500
GYROSCOPE	7.500	11.400	8.200	1.200	0.002	0.001	0.002	61.250	-10.000	60.900
EARTH SENSOR (r/h)	5.150	16.256		3.770	0.011	0.011	0.005	62.000	0.000	75.000
SUN SENSOR #1	2.500	2.500	2.500	0.040	0.000	0.000	0.000	0.000	96.250	1.250
SUN SENSOR #2	2.500	2.500	2.500	0.040	0.000	0.000	0.000	0.000	96.250	61.250
SUN SENSOR #3	2.500	2.500	2.500	0.040	0.000	0.000	0.000	0.000	-96.250	1.250
SUN SENSOR #4	2.500	2.500	2.500	0.040	0.000	0.000	0.000	0.000	-96.250	61.250
		SUBSYSTEM TOTAL		17.130						
REACTION CONTROL SYSTEM										
PROPELLANT TANK #1 (radius)	27.500			5.897	0.297	0.297	0.297	36.500	66.500	35.000
PROPELLANT TANK #2 (radius)	27.500			5.897	0.297	0.297	0.297	-36.500	66.500	35.000
PROPELLANT TANK #3 (radius)	27.500			5.897	0.297	0.297	0.297	36.500	-66.500	35.000
PROPELLANT TANK #4 (radius)	27.500			5.897	0.297	0.297	0.297	-36.500	-66.500	35.000
PROPELLANT IN TANK #1 (radius)	27.500			36.303	1.098	1.098	1.098	36.500	66.500	35.000
PROPELLANT IN TANK #2 (radius)	27.500			36.303	1.098	1.098	1.098	-36.500	66.500	35.000
PROPELLANT IN TANK #3 (radius)	27.500			36.303	1.098	1.098	1.098	36.500	-66.500	35.000
PROPELLANT IN TANK #4 (radius)	27.500			36.303	1.098	1.098	1.098	-36.500	-66.500	35.000
THRUSTER #1A	3.500	3.500	16.764	0.319	0.001	0.001	0.000	55.000	85.000	69.492
THRUSTER #1B	3.500	3.500	16.764	0.319	0.001	0.001	0.000	55.000	85.000	0.501
THRUSTER #1C	3.500	16.764	3.500	0.319	0.001	0.000	0.001	59.000	89.000	35.000
THRUSTER #2A	3.500	3.500	16.764	0.319	0.001	0.001	0.000	-55.000	85.000	69.492
THRUSTER #2B	3.500	16.764	3.500	0.319	0.001	0.000	0.001	-59.000	89.000	35.000
THRUSTER #2C	3.500	3.500	16.764	0.319	0.001	0.001	0.000	-55.000	85.000	0.501
THRUSTER #3A	3.500	3.500	16.764	0.319	0.001	0.001	0.000	-55.000	-85.000	69.492
THRUSTER #3B	3.500	3.500	16.764	0.319	0.001	0.001	0.000	-55.000	-85.000	0.501
THRUSTER #3C	3.500	16.764	3.500	0.319	0.001	0.000	0.001	-59.000	-89.000	35.000
THRUSTER #4A	3.500	3.500	16.764	0.319	0.001	0.001	0.000	55.000	-85.000	69.492
THRUSTER #4B	3.500	16.764	3.500	0.319	0.001	0.000	0.001	59.000	-89.000	35.000
THRUSTER #4C	3.500	3.500	16.764	0.319	0.001	0.001	0.000	55.000	-85.000	0.501
ORBIT INJECTION THRUSTER #1	5.84	5.84	16.45	0.735	0.002	0.002	0.000	24.192	44.075	-1.175
ORBIT INJECTION THRUSTER #2	5.84	5.84	16.45	0.735	0.002	0.002	0.000	24.192	-44.075	-1.175
ORBIT INJECTION THRUSTER #3	5.84	5.84	16.45	0.735	0.002	0.002	0.000	-24.192	44.075	-1.175
ORBIT INJECTION THRUSTER #4	5.84	5.84	16.45	0.735	0.002	0.002	0.000	-24.192	-44.075	-1.175
TUBING AND VALVES (uniform dist)	130.000	190.000	70.000	4.310	1.473	0.783	1.904	0.000	0.000	35.000
		SUBSYSTEM TOTAL		179.878						
STRUCTURAL SUBSYSTEM										
PANEL #1 (EARTH FACE)	130.000	190.000	1.044	1.670	0.502	0.235	0.738	0.000	0.000	70.000
PANEL #2 (+X FACE)	190.000	1.044	70.000	0.918	0.037	0.314	0.276	65.000	0.000	35.000
PANEL #3 (-X FACE)	190.000	1.044	70.000	0.918	0.037	0.314	0.276	-65.000	0.000	35.000
PANEL #4 (+Y FACE)	1.044	130.000	70.000	0.624	0.113	0.025	0.088	0.000	95.000	35.000
PANEL #5 (-Y FACE)	1.044	130.000	70.000	0.624	0.113	0.025	0.088	0.000	-95.000	35.000
PANEL #6 (ANTI-EARTH FACE)	130.000	190.000	1.020	1.179	0.355	0.166	0.521	0.000	0.000	0.000
MISC (BRACKETS, STRUTS, ETC.)	130.000	190.000	70.000	18.194	6.216	3.305	8.036	0.000	0.000	35.000
UPPER CENTRAL CONE (r1/r2/h)	37.500	47.760	18.000	5.221	0.495	0.495	0.963	0.000	0.000	60.639
CENTRAL CYLINDER (r/h)	37.500	55.000		8.192	1.335	1.335	2.478	0.000	0.000	33.500
LOWER CENTRAL CONE (r1/r2/h)	37.500	47.760	15.000	9.082	0.854	0.854	1.674	0.000	0.000	7.801
		SUBSYSTEM TOTAL		46.622						
ELECTRIC POWER SUBSYSTEM										
BATTERIES	23.000	30.000	26.000	7.120	0.094	0.071	0.085	53.570	27.500	28.000
POWER CONTROL ELECTRONICS	15.000	40.000	15.000	6.000	0.091	0.023	0.091	57.500	25.000	57.500
SOLAR ARRAY DRIVE #1 (r/h)	8.000	10.000		4.000	0.006	1.390	0.121	60.000	0.000	35.000
SOLAR ARRAY DRIVE #2 (r/h)	8.000	10.000		4.000	0.013	0.010	1.390	70.000	0.000	35.000
SOLAR ARRAY PANEL #1	4.300	165.250	48.700	6.095	1.507	0.121	1.388	77.150	0.000	35.000
SOLAR ARRAY PANEL #2	4.300	165.250	48.700	6.095	1.507	0.121	1.388	-77.150	0.000	35.000
SHUNT RESISTOR BANK #1	1.000	23.100	48.700	0.945	0.023	0.019	0.004	77.150	0.000	35.000
SHUNT RESISTOR BANK #2	1.000	23.100	48.700	0.945	0.023	0.019	0.004	-77.150	0.000	35.000
ELECTRICAL INTEGRATION (uniform dist)	130.000	190.000	70.000	13.350	4.561	2.425	5.896	0.000	0.000	35.000
		SUBSYSTEM TOTAL		48.650						
THERMAL CONTROL SUBSYSTEM										
OPTICAL SOLAR REFLECTOR (OSR) #1	0.500	90.000	70.000	17.771	0.726	1.925	1.200	65.000	0.000	35.000
OPTICAL SOLAR REFLECTOR (OSR) #2	0.500	90.000	70.000	17.771	0.726	1.925	1.200	-65.000	0.000	35.000
MULTILAYER INSULATION (uniform dist)	130.000	190.000	70.000	5.092	0.925	1.740	2.249	0.000	0.000	35.000
MISC (HEATERS, ETC.) (uniform dist)	130.000	190.000	70.000	2.000	0.363	0.683	0.883	0.000	0.000	35.000
		SUBSYSTEM TOTAL		42.634						
		SUBSYSTEM TOTALS		370.397					CENTER OF MASS	
			MASS MARGIN	41.520						
		TOTAL SPACECRAFT MASS		411.917						

TABLE B-2. MOMENTS OF INERTIA AT SEPARATION WITH THE SOLAR ARRAY FOLDED

ORIGINAL PAGE IS OF POOR QUALITY

1/18/90 9:40		MOMENTS OF INERTIA WITH THE SOLAR ARRAY EXTENDED AND THE PROPELLANT TANKS FULL								
ITEM	ITEM DIMENSIONS (cm)			MASS (kg)	ITEM MOMENTS (kg-m^2)			ITEM POSITION (cm)		
	a	b	c		Ix	Iy	Iz	x	y	z
TELEMETRY, TRACKING & COMMAND										
REMOTE COMMAND UNIT 3 (RCU 3)	16.230	20.400	14.480	5.797	0.030	0.023	0.033	56.885	-34.800	12.240
REMOTE TELEMETRY UNIT 4 (RTU 4)	20.220	20.400	14.480	7.552	0.039	0.039	0.052	54.891	-34.800	57.760
DOSIMETER	6.730	9.810	3.990	0.363	0.000	0.000	0.000	61.635	-40.095	35.000
		SUBSYSTEM TOTAL		13.712						
RADIO FREQUENCY SUBSYSTEM										
PAYLOAD RECEIVER	14.610	32.080	32.080	6.713	0.115	0.070	0.070	-57.695	-23.960	48.960
PAYLOAD RECEIVER SYNTHESIZER	11.760	19.690	12.700	1.724	0.008	0.004	0.008	-59.120	-30.158	11.350
PAYLOAD RECEIVER POWER SUPPLY	8.890	22.230	16.940	1.814	0.012	0.006	0.009	-60.555	28.890	13.471
PAYLOAD TRANSMITTER	17.150	36.830	22.230	6.169	0.095	0.041	0.085	-56.425	21.586	53.885
PAYLOAD RECEIVER STABILIZED CLOCK	3.810	10.160	9.650	0.454	0.001	0.000	0.000	-63.095	34.920	34.825
PAYLOAD CTS	1.910	10.160	2.540	0.045	0.000	0.000	0.000	-64.045	19.920	31.270
ANTENNA #1 (point mass)				1.498	0.000	0.000	0.000	0.000	0.000	79.000
ANTENNA #2 (r/h)	14.800	29.600		1.680	0.021	0.018	0.018	-30.200	60.200	84.800
ANTENNA #3 (r/h)	10.700	21.400		0.450	0.003	0.003	0.003	34.300	-64.300	80.700
GROUND PLANE	43.000	43.000	0.001	0.417	0.006	0.006	0.013	0.000	0.000	70.000
CABLES (uniform distribution)	130.000	190.000	4.000	0.9072	0.273	0.128	0.401	0.000	0.000	35.000
		SUBSYSTEM TOTAL		21.871						
ATTITUDE CONTROL SYSTEM										
ATTITUDE CONTROL COMPUTER	36.200	6.350	14.900	2.500	0.005	0.032	0.028	0.000	-92.345	35.000
REACTION WHEEL +X DIRECTION (r/h)	11.750	12.000		2.376	0.016	0.011	0.011	0.000	-49.250	35.000
REACTION WHEEL +Y DIRECTION (r/h)	11.750	12.000		2.375	0.011	0.016	0.016	0.000	89.520	35.000
REACTION WHEEL +Z DIRECTION (r/h)	11.750	12.000		2.375	0.011	0.011	0.016	0.000	49.250	35.000
REACTION WHEEL -X/-Y/+Z DIRECTION	11.750	12.000		2.375	0.011	0.011	0.011	-32.500	-32.500	17.500
GYROSCOPE	7.500	11.400	8.200	1.200	0.002	0.001	0.002	61.250	-10.000	60.900
EARTH SENSOR (r/h)	5.150	16.256		3.770	0.011	0.011	0.005	62.000	0.000	75.000
SUN SENSOR #1	2.500	2.500	2.500	0.040	0.000	0.000	0.000	0.000	96.250	1.250
SUN SENSOR #2	2.500	2.500	2.500	0.040	0.000	0.000	0.000	0.000	96.250	61.250
SUN SENSOR #3	2.500	2.500	2.500	0.040	0.000	0.000	0.000	0.000	-96.250	1.250
SUN SENSOR #4	2.500	2.500	2.500	0.040	0.000	0.000	0.000	0.000	-96.250	61.250
		SUBSYSTEM TOTAL		17.130						
REACTION CONTROL SYSTEM										
PROPELLANT TANK #1 (radius)	27.500			5.897	0.297	0.297	0.297	36.500	66.500	35.000
PROPELLANT TANK #2 (radius)	27.500			5.897	0.297	0.297	0.297	-36.500	66.500	35.000
PROPELLANT TANK #3 (radius)	27.500			5.897	0.297	0.297	0.297	36.500	-66.500	35.000
PROPELLANT TANK #4 (radius)	27.500			5.897	0.297	0.297	0.297	-36.500	-66.500	35.000
PROPELLANT IN TANK #1 (radius)	27.500			36.303	1.098	1.098	1.098	36.500	66.500	35.000
PROPELLANT IN TANK #2 (radius)	27.500			36.303	1.098	1.098	1.098	-36.500	66.500	35.000
PROPELLANT IN TANK #3 (radius)	27.500			36.303	1.098	1.098	1.098	36.500	-66.500	35.000
PROPELLANT IN TANK #4 (radius)	27.500			36.303	1.098	1.098	1.098	-36.500	-66.500	35.000
THRUSTER #1A	3.500	3.500	16.764	0.319	0.001	0.001	0.000	55.000	85.000	69.492
THRUSTER #1B	3.500	3.500	16.764	0.319	0.001	0.001	0.000	55.000	85.000	0.501
THRUSTER #1C	3.500	16.764	3.500	0.319	0.001	0.000	0.001	59.000	89.000	35.000
THRUSTER #2A	3.500	3.500	16.764	0.319	0.001	0.001	0.000	-55.000	85.000	69.492
THRUSTER #2B	3.500	16.764	3.500	0.319	0.001	0.000	0.001	-59.000	89.000	35.000
THRUSTER #2C	3.500	3.500	16.764	0.319	0.001	0.001	0.000	-55.000	85.000	0.501
THRUSTER #3A	3.500	3.500	16.764	0.319	0.001	0.001	0.000	-55.000	-85.000	69.492
THRUSTER #3B	3.500	3.500	16.764	0.319	0.001	0.001	0.000	-55.000	-85.000	0.501
THRUSTER #3C	3.500	16.764	3.500	0.319	0.001	0.000	0.001	-59.000	-89.000	35.000
THRUSTER #4A	3.500	3.500	16.764	0.319	0.001	0.001	0.000	55.000	-85.000	69.492
THRUSTER #4B	3.500	16.764	3.500	0.319	0.001	0.000	0.001	59.000	-89.000	35.000
THRUSTER #4C	3.500	3.500	16.764	0.319	0.001	0.001	0.000	55.000	-85.000	0.501
ORBIT INJECTION THRUSTER #1	5.84	5.84	16.45	0.735	0.002	0.002	0.000	24.192	44.075	-1.175
ORBIT INJECTION THRUSTER #2	5.84	5.84	16.45	0.735	0.002	0.002	0.000	24.192	-44.075	-1.175
ORBIT INJECTION THRUSTER #3	5.84	5.84	16.45	0.735	0.002	0.002	0.000	-24.192	44.075	-1.175
ORBIT INJECTION THRUSTER #4	5.84	5.84	16.45	0.735	0.002	0.002	0.000	-24.192	-44.075	-1.175
TUBING AND VALVES (uniform dist)	130.000	190.000	70.000	4.310	1.473	0.783	1.904	0.000	0.000	35.000
		SUBSYSTEM TOTAL		179.878						
STRUCTURAL SUBSYSTEM										
PANEL #1 (EARTH FACE)	130.000	190.000	1.044	1.670	0.502	0.235	0.738	0.000	0.000	70.000
PANEL #2 (+X FACE)	190.000	1.044	70.000	0.918	0.037	0.314	0.276	65.000	0.000	35.000
PANEL #3 (-X FACE)	190.000	1.044	70.000	0.918	0.037	0.314	0.276	-65.000	0.000	35.000
PANEL #4 (+Y FACE)	1.044	130.000	70.000	0.624	0.113	0.025	0.088	0.000	95.000	35.000
PANEL #5 (-Y FACE)	1.044	130.000	70.000	0.624	0.113	0.025	0.088	0.000	-95.000	35.000
PANEL #6 (ANTI-EARTH FACE)	130.000	190.000	1.020	1.179	0.355	0.166	0.521	0.000	0.000	0.000
MISC (BRACKETS, STRUTS, ETC.)	130.000	190.000	70.000	18.194	6.216	3.305	8.036	0.000	0.000	35.000
UPPER CENTRAL CONE (r1/r2/h)	37.500	47.760	18.000	5.221	0.495	0.495	0.963	0.000	0.000	60.839
CENTRAL CYLINDER (r/h)	37.500	55.000		8.192	1.335	1.335	2.478	0.000	0.000	33.500
LOWER CENTRAL CONE (r1/r2/h)	37.500	47.760	15.000	9.082	0.854	0.854	1.674	0.000	0.000	7.801
		SUBSYSTEM TOTAL		46.622						
ELECTRIC POWER SUBSYSTEM										
BATTERIES	23.000	30.000	26.000	7.120	0.094	0.071	0.085	53.570	27.500	26.000
POWER CONTROL ELECTRONICS	15.000	40.000	15.000	6.000	0.091	0.023	0.091	57.500	25.000	57.500
SOLAR ARRAY DRIVE #1 (r/h)	8.000	10.000		4.000	33.288	16.764	5.548	60.000	0.000	35.000
SOLAR ARRAY DRIVE #2 (r/h)	8.000	10.000		4.000	0.013	0.010	16.764	70.000	0.000	35.000
SOLAR ARRAY PANEL #1	330.500	48.700	1.740	6.095	0.121	5.548	5.668	325.250	0.000	35.000
SOLAR ARRAY PANEL #2	330.500	48.700	1.740	6.095	0.121	5.548	5.668	-325.250	0.000	35.000
SHUNT RESISTOR BANK #1	23.100	48.700	1.000	0.945	0.019	0.004	0.023	407.875	0.000	35.000
SHUNT RESISTOR BANK #2	23.100	48.700	1.000	0.945	0.019	0.004	0.023	-407.875	0.000	35.000
ELECTRICAL INTEGRATION (uniform dist)	130.000	190.000	70.000	13.350	4.561	2.425	5.896	0.000	0.000	35.000
		SUBSYSTEM TOTAL		48.550						
THERMAL CONTROL SUBSYSTEM										
OPTICAL SOLAR REFLECTOR (OSR) #1	0.500	90.000	70.000	17.771	0.726	1.925	1.200	65.000	0.000	35.000
OPTICAL SOLAR REFLECTOR (OSR) #2	0.500	90.000	70.000	17.771	0.726	1.925	1.200	-65.000	0.000	35.000
MULTILAYER INSULATION (uniform dist)	130.000	190.000	70.000	5.092	0.925	1.740	2.249	0.000	0.000	35.000
MISC (HEATERS, ETC.) (uniform dist)	130.000	190.000	70.000	2.000	0.363	0.683	0.883	0.000	0.000	35.000
		SUBSYSTEM TOTAL		42.634						
			SUBTOTAL	370.397					CENTER OF MASS	
			MASS MARGIN	41.520						
		TOTAL SPACECRAFT MASS		411.917						

TABLE B-3. MOMENTS OF INERTIA AT SEPARATION WITH THE SOLAR ARRAY EXTENDED

1/18/90 10:20		MOMENTS OF INERTIA WITH THE SOLAR ARRAY EXTENDED AND THE PROPELLANT TANKS HALF FULL								
ITEM	ITEM DIMENSIONS (cm)			MASS (kg)	ITEM MOMENTS (kg-m^2)			ITEM POSITION (cm)		
	a	b	c		Ix	Iy	Iz	x	y	z
TELEMETRY, TRACKING & COMMAND										
REMOTE COMMAND UNIT 3 (RCU 3)	16.230	20.400	14.480	5.797	0.030	0.023	0.033	56.885	-34.800	12.240
REMOTE TELEMETRY UNIT 4 (RTU 4)	20.220	20.400	14.480	7.552	0.039	0.039	0.052	54.891	-34.800	57.760
DOSIMETER	6.730	9.810	3.990	0.363	0.000	0.000	0.000	61.635	-40.095	35.000
		SUBSYSTEM TOTAL		13.712						
RADIO FREQUENCY SUBSYSTEM										
PAYLOAD RECEIVER	14.610	32.080	32.080	6.713	0.115	0.070	0.070	-57.695	-23.960	48.960
PAYLOAD RECEIVER SYNTHESIZER	11.760	19.690	12.700	1.724	0.008	0.004	0.008	-59.120	-30.158	11.350
PAYLOAD RECEIVER POWER SUPPLY	8.890	22.230	16.940	1.814	0.012	0.006	0.009	-60.555	28.890	13.471
PAYLOAD TRANSMITTER	17.150	36.830	22.230	6.169	0.095	0.041	0.085	-56.425	21.585	53.885
PAYLOAD RECEIVER STABILIZED CLOCK	3.810	10.160	9.650	0.454	0.001	0.000	0.000	-63.095	34.920	34.825
PAYLOAD CTS	1.910	10.160	2.540	0.045	0.000	0.000	0.000	-64.045	19.920	31.270
ANTENNA #1 (point mass)				1.498	0.000	0.000	0.000	0.000	0.000	79.000
ANTENNA #2 (r/h)	14.600	29.600		1.680	0.021	0.018	0.018	-30.200	60.200	84.800
ANTENNA #3 (r/h)	10.700	21.400		0.450	0.003	0.003	0.003	34.300	-64.300	80.700
GROUND PLANE	43.000	43.000	0.001	0.417	0.006	0.006	0.013	0.000	0.000	70.000
CABLES (uniform distribution)	130.000	190.000	4.000	0.9072	0.273	0.128	0.401	0.000	0.000	35.000
		SUBSYSTEM TOTAL		21.871						
ATTITUDE CONTROL SYSTEM										
ATTITUDE CONTROL COMPUTER	36.200	6.350	14.900	2.500	0.005	0.032	0.028	0.000	-92.345	35.000
REACTION WHEEL +X DIRECTION (r/h)	11.750	12.000		2.375	0.016	0.011	0.011	0.000	-49.250	35.000
REACTION WHEEL +Y DIRECTION (r/h)	11.750	12.000		2.375	0.011	0.016	0.016	0.000	89.520	35.000
REACTION WHEEL +Z DIRECTION (r/h)	11.750	12.000		2.375	0.011	0.011	0.016	0.000	49.250	35.000
REACTION WHEEL -X/-Y/+Z DIRECTION	11.750	12.000		2.375	0.011	0.011	0.011	-32.500	-32.500	17.500
GYROSCOPE	7.500	11.400	8.200	1.200	0.002	0.001	0.002	61.250	-10.000	60.900
EARTH SENSOR (r/h)	5.150	16.256		3.770	0.011	0.011	0.005	62.000	0.000	75.000
SUN SENSOR #1	2.500	2.500	2.500	0.040	0.000	0.000	0.000	0.000	96.250	1.250
SUN SENSOR #2	2.500	2.500	2.500	0.040	0.000	0.000	0.000	0.000	96.250	61.250
SUN SENSOR #3	2.500	2.500	2.500	0.040	0.000	0.000	0.000	0.000	-96.250	1.250
SUN SENSOR #4	2.500	2.500	2.500	0.040	0.000	0.000	0.000	0.000	-96.250	61.250
		SUBSYSTEM TOTAL		17.130						
REACTION CONTROL SYSTEM										
PROPELLANT TANK #1 (radius)	27.500			5.897	0.297	0.297	0.297	36.500	66.500	35.000
PROPELLANT TANK #2 (radius)	27.500			5.897	0.297	0.297	0.297	-36.500	66.500	35.000
PROPELLANT TANK #3 (radius)	27.500			5.897	0.297	0.297	0.297	36.500	-66.500	35.000
PROPELLANT TANK #4 (radius)	27.500			5.897	0.297	0.297	0.297	-36.500	-66.500	35.000
PROPELLANT IN TANK #1 (radius)	27.500			18.200	0.551	0.551	0.551	36.500	66.500	35.000
PROPELLANT IN TANK #2 (radius)	27.500			18.200	0.551	0.551	0.551	-36.500	66.500	35.000
PROPELLANT IN TANK #3 (radius)	27.500			18.200	0.551	0.551	0.551	36.500	-66.500	35.000
PROPELLANT IN TANK #4 (radius)	27.500			18.200	0.551	0.551	0.551	-36.500	-66.500	35.000
THRUSTER #1A	3.500	3.500	16.764	0.319	0.001	0.001	0.000	55.000	85.000	69.492
THRUSTER #1B	3.500	3.500	16.764	0.319	0.001	0.001	0.000	55.000	85.000	0.501
THRUSTER #1C	3.500	16.764	3.500	0.319	0.001	0.000	0.001	59.000	89.000	35.000
THRUSTER #2A	3.500	3.500	16.764	0.319	0.001	0.001	0.000	-55.000	85.000	69.492
THRUSTER #2B	3.500	16.764	3.500	0.319	0.001	0.000	0.001	-59.000	89.000	35.000
THRUSTER #2C	3.500	3.500	16.764	0.319	0.001	0.001	0.000	-55.000	85.000	0.501
THRUSTER #3A	3.500	3.500	16.764	0.319	0.001	0.001	0.000	-55.000	-85.000	69.492
THRUSTER #3B	3.500	3.500	16.764	0.319	0.001	0.001	0.000	-55.000	-85.000	0.501
THRUSTER #3C	3.500	16.764	3.500	0.319	0.001	0.000	0.001	-59.000	-89.000	35.000
THRUSTER #4A	3.500	3.500	16.764	0.319	0.001	0.001	0.000	55.000	-85.000	69.492
THRUSTER #4B	3.500	16.764	3.500	0.319	0.001	0.000	0.001	59.000	-89.000	35.000
THRUSTER #4C	3.500	3.500	16.764	0.319	0.001	0.001	0.000	55.000	-85.000	0.501
ORBIT INJECTION THRUSTER #1	5.84	5.84	16.45	0.735	0.002	0.002	0.000	24.192	44.075	-1.175
ORBIT INJECTION THRUSTER #2	5.84	5.84	16.45	0.735	0.002	0.002	0.000	24.192	-44.075	-1.175
ORBIT INJECTION THRUSTER #3	5.84	5.84	16.45	0.735	0.002	0.002	0.000	-24.192	44.075	-1.175
ORBIT INJECTION THRUSTER #4	5.84	5.84	16.45	0.735	0.002	0.002	0.000	-24.192	-44.075	-1.175
TUBING AND VALVES (uniform dist)	130.000	190.000	70.000	4.310	1.473	0.783	1.904	0.000	0.000	35.000
		SUBSYSTEM TOTAL		107.466						
STRUCTURAL SUBSYSTEM										
PANEL #1 (EARTH FACE)	130.000	190.000	1.044	1.670	0.502	0.235	0.738	0.000	0.000	70.000
PANEL #2 (+X FACE)	190.000	1.044	70.000	0.918	0.037	0.314	0.276	65.000	0.000	35.000
PANEL #3 (-X FACE)	190.000	1.044	70.000	0.918	0.037	0.314	0.276	-65.000	0.000	35.000
PANEL #4 (+Y FACE)	1.044	130.000	70.000	0.624	0.113	0.025	0.088	0.000	95.000	35.000
PANEL #5 (-Y FACE)	1.044	130.000	70.000	0.624	0.113	0.025	0.088	0.000	-95.000	35.000
PANEL #6 (ANTI-EARTH FACE)	130.000	190.000	1.020	1.179	0.355	0.166	0.521	0.000	0.000	0.000
MISC (BRACKETS, STRUTS, ETC.)	130.000	190.000	70.000	18.194	6.216	3.305	8.036	0.000	0.000	35.000
UPPER CENTRAL CONE (r1/r2/h)	37.500	47.760	18.000	5.221	0.495	0.495	0.963	0.000	0.000	60.639
CENTRAL CYLINDER (r/h)	37.500	55.000		8.192	1.335	1.335	2.478	0.000	0.000	33.500
LOWER CENTRAL CONE (r1/r2/h)	37.500	47.760	15.000	9.082	0.854	0.854	1.674	0.000	0.000	7.801
		SUBSYSTEM TOTAL		46.622						
ELECTRIC POWER SUBSYSTEM										
BATTERIES	23.000	30.000	26.000	7.120	0.094	0.071	0.085	53.570	27.500	26.000
POWER CONTROL ELECTRONICS	15.000	40.000	15.000	6.000	0.091	0.023	0.091	57.500	25.000	57.500
SOLAR ARRAY DRIVE #1 (r/h)	8.000	10.000		4.000	33.288	16.764	5.548	60.000	0.000	35.000
SOLAR ARRAY DRIVE #2 (r/h)	8.000	10.000		4.000	0.013	0.010	16.764	70.000	0.000	35.000
SOLAR ARRAY PANEL #1	330.500	48.700	1.740	6.095	0.121	5.548	5.668	325.250	0.000	35.000
SOLAR ARRAY PANEL #2	330.500	48.700	1.740	6.095	0.121	5.548	5.668	-325.250	0.000	35.000
SHUNT RESISTOR BANK #1	23.100	48.700	1.000	0.945	0.019	0.004	0.023	407.875	0.000	35.000
SHUNT RESISTOR BANK #2	23.100	48.700	1.000	0.945	0.019	0.004	0.023	-407.875	0.000	35.000
ELECTRICAL INTEGRATION (uniform dist)	130.000	190.000	70.000	13.350	4.561	2.425	5.896	0.000	0.000	35.000
		SUBSYSTEM TOTAL		48.550						
THERMAL CONTROL SUBSYSTEM										
OPTICAL SOLAR REFLECTOR (OSR) #1	0.500	90.000	70.000	17.771	0.726	1.925	1.200	65.000	0.000	35.000
OPTICAL SOLAR REFLECTOR (OSR) #2	0.500	90.000	70.000	17.771	0.726	1.925	1.200	-65.000	0.000	35.000
MULTILAYER INSULATION (uniform dist)	130.000	190.000	70.000	5.092	0.925	1.740	2.249	0.000	0.000	35.000
MISC (HEATERS, ETC.) (uniform dist)	130.000	190.000	70.000	2.000	0.363	0.683	0.883	0.000	0.000	35.000
		SUBSYSTEM TOTAL		42.634						
			SUBTOTAL	297.985					CENTER OF MASS	
			MASS MARGIN	41.520						
		TOTAL SPACECRAFT MASS		339.505						

TABLE B-4. MOMENTS OF INERTIA WITH THE FUEL TANKS HALF FULL

1/18/90 10:30		MOMENTS OF INERTIA WITH THE SOLAR ARRAY EXTENDED AND THE PROPELLANT TANKS 10% FULL								
ITEM	ITEM DIMENSIONS (cm)			MASS (kg)	ITEM MOMENTS (kg-m^2)			ITEM POSITION (cm)		
	a	b	c		Ix	Iy	Iz	x	y	z
TELEMETRY, TRACKING & COMMAND										
REMOTE COMMAND UNIT 3 (RCU 3)	16.230	20.400	14.480	5.797	0.030	0.023	0.033	56.885	-34.800	12.240
REMOTE TELEMETRY UNIT 4 (RTU 4)	20.220	20.400	14.480	7.552	0.039	0.039	0.052	54.891	-34.800	57.760
DOSIMETER	6.730	9.810	3.990	0.363	0.000	0.000	0.000	61.635	-40.095	35.000
		SUBSYSTEM TOTAL		13.712						
RADIO FREQUENCY SUBSYSTEM										
PAYLOAD RECEIVER	14.610	32.080	32.080	6.713	0.115	0.070	0.070	-57.695	-23.960	48.960
PAYLOAD RECEIVER SYNTHESIZER	11.760	19.890	12.700	1.724	0.008	0.004	0.008	-59.120	-30.158	11.350
PAYLOAD RECEIVER POWER SUPPLY	8.890	22.230	18.940	1.814	0.012	0.006	0.009	-60.555	28.890	13.471
PAYLOAD TRANSMITTER	17.150	36.830	22.230	6.169	0.095	0.041	0.085	-58.425	21.585	53.885
PAYLOAD RECEIVER STABILIZED CLOCK	3.810	10.160	9.650	0.454	0.001	0.000	0.000	-63.095	34.920	34.825
PAYLOAD CTS	1.910	10.160	2.540	0.045	0.000	0.000	0.000	-64.045	19.920	31.270
ANTENNA #1 (point mass)				1.498	0.000	0.000	0.000	0.000	0.000	79.000
ANTENNA #2 (r/h)	14.800	29.600		1.680	0.021	0.018	0.018	-30.200	60.200	84.800
ANTENNA #3 (r/h)	10.700	21.400		0.450	0.003	0.003	0.003	34.300	-64.300	80.700
GROUND PLANE	43.000	43.000	0.001	0.417	0.006	0.006	0.013	0.000	0.000	70.000
CABLES (uniform distribution)	130.000	190.000	4.000	0.9072	0.273	0.128	0.401	0.000	0.000	35.000
		SUBSYSTEM TOTAL		21.871						
ATTITUDE CONTROL SYSTEM										
ATTITUDE CONTROL COMPUTER	36.200	6.350	14.900	2.500	0.005	0.032	0.028	0.000	-92.345	35.000
REACTION WHEEL +X DIRECTION (r/h)	11.750	12.000		2.375	0.016	0.011	0.011	0.000	-49.250	35.000
REACTION WHEEL +Y DIRECTION (r/h)	11.750	12.000		2.375	0.011	0.016	0.016	0.000	89.520	35.000
REACTION WHEEL +Z DIRECTION (r/h)	11.750	12.000		2.375	0.011	0.011	0.016	0.000	49.250	35.000
REACTION WHEEL -X/-Y/+Z DIRECTION	11.750	12.000		2.375	0.011	0.011	0.011	-32.500	-32.500	17.500
GYROSCOPE	7.500	11.400	8.200	1.200	0.002	0.001	0.002	61.250	-10.000	60.900
EARTH SENSOR (r/h)	5.150	16.256		3.770	0.011	0.011	0.005	62.000	0.000	75.000
SUN SENSOR #1	2.500	2.500	2.500	0.040	0.000	0.000	0.000	0.000	96.250	1.250
SUN SENSOR #2	2.500	2.500	2.500	0.040	0.000	0.000	0.000	0.000	96.250	61.250
SUN SENSOR #3	2.500	2.500	2.500	0.040	0.000	0.000	0.000	0.000	-96.250	1.250
SUN SENSOR #4	2.500	2.500	2.500	0.040	0.000	0.000	0.000	0.000	-96.250	61.250
		SUBSYSTEM TOTAL		17.130						
REACTION CONTROL SYSTEM										
PROPELLANT TANK #1 (radius)	27.500			5.897	0.297	0.297	0.297	36.500	66.500	35.000
PROPELLANT TANK #2 (radius)	27.500			5.897	0.297	0.297	0.297	-36.500	66.500	35.000
PROPELLANT TANK #3 (radius)	27.500			5.897	0.297	0.297	0.297	36.500	-66.500	35.000
PROPELLANT TANK #4 (radius)	27.500			5.897	0.297	0.297	0.297	-36.500	-66.500	35.000
PROPELLANT IN TANK #1 (radius)	27.500			3.640	0.110	0.110	0.110	36.500	66.500	35.000
PROPELLANT IN TANK #2 (radius)	27.500			3.640	0.110	0.110	0.110	-36.500	66.500	35.000
PROPELLANT IN TANK #3 (radius)	27.500			3.640	0.110	0.110	0.110	36.500	-66.500	35.000
PROPELLANT IN TANK #4 (radius)	27.500			3.640	0.110	0.110	0.110	-36.500	-66.500	35.000
THRUSTER #1A	3.500	3.500	16.764	0.319	0.001	0.001	0.000	55.000	85.000	69.492
THRUSTER #1B	3.500	3.500	16.764	0.319	0.001	0.001	0.000	55.000	85.000	0.501
THRUSTER #1C	3.500	16.764	3.500	0.319	0.001	0.000	0.001	59.000	89.000	35.000
THRUSTER #2A	3.500	3.500	16.764	0.319	0.001	0.001	0.000	-55.000	85.000	69.492
THRUSTER #2B	3.500	16.764	3.500	0.319	0.001	0.000	0.001	-59.000	89.000	35.000
THRUSTER #2C	3.500	3.500	16.764	0.319	0.001	0.001	0.000	-55.000	85.000	0.501
THRUSTER #3A	3.500	3.500	16.764	0.319	0.001	0.001	0.000	-55.000	-85.000	69.492
THRUSTER #3B	3.500	3.500	16.764	0.319	0.001	0.001	0.000	-55.000	-85.000	0.501
THRUSTER #3C	3.500	16.764	3.500	0.319	0.001	0.000	0.001	-59.000	-89.000	35.000
THRUSTER #4A	3.500	3.500	16.764	0.319	0.001	0.001	0.000	55.000	-85.000	69.492
THRUSTER #4B	3.500	16.764	3.500	0.319	0.001	0.000	0.001	59.000	-89.000	35.000
THRUSTER #4C	3.500	3.500	16.764	0.319	0.001	0.001	0.000	55.000	-85.000	0.501
ORBIT INJECTION THRUSTER #1	5.84	5.84	16.45	0.735	0.002	0.002	0.000	24.192	44.075	-1.175
ORBIT INJECTION THRUSTER #2	5.84	5.84	16.45	0.735	0.002	0.002	0.000	24.192	-44.075	-1.175
ORBIT INJECTION THRUSTER #3	5.84	5.84	16.45	0.735	0.002	0.002	0.000	-24.192	44.075	-1.175
ORBIT INJECTION THRUSTER #4	5.84	5.84	16.45	0.735	0.002	0.002	0.000	-24.192	-44.075	-1.175
TUBING AND VALVES (uniform dist)	130.000	190.000	70.000	4.310	1.473	0.783	1.904	0.000	0.000	35.000
		SUBSYSTEM TOTAL		49.226						
STRUCTURAL SUBSYSTEM										
PANEL #1 (EARTH FACE)	130.000	190.000	1.044	1.670	0.502	0.235	0.738	0.000	0.000	70.000
PANEL #2 (+X FACE)	190.000	1.044	70.000	0.918	0.037	0.314	0.276	65.000	0.000	35.000
PANEL #3 (-X FACE)	190.000	1.044	70.000	0.918	0.037	0.314	0.276	-65.000	0.000	35.000
PANEL #4 (+Y FACE)	1.044	130.000	70.000	0.624	0.113	0.025	0.088	0.000	95.000	35.000
PANEL #5 (-Y FACE)	1.044	130.000	70.000	0.624	0.113	0.025	0.088	0.000	-95.000	35.000
PANEL #6 (ANTI-EARTH FACE)	130.000	190.000	1.020	1.179	0.355	0.166	0.521	0.000	0.000	0.000
MISC (BRACKETS, STRUTS, ETC.)	130.000	190.000	70.000	18.194	6.216	3.305	8.036	0.000	0.000	35.000
UPPER CENTRAL CONE (r1/r2/h)	37.500	47.760	18.000	5.221	0.495	0.495	0.963	0.000	0.000	60.639
CENTRAL CYLINDER (r/h)	37.500	55.000		8.192	1.335	1.335	2.478	0.000	0.000	33.500
LOWER CENTRAL CONE (r1/r2/h)	37.500	47.760	15.000	9.082	0.854	0.854	1.674	0.000	0.000	7.801
		SUBSYSTEM TOTAL		46.622						
ELECTRIC POWER SUBSYSTEM										
BATTERIES	23.000	30.000	26.000	7.120	0.094	0.071	0.085	53.570	27.500	26.000
POWER CONTROL ELECTRONICS	15.000	40.000	15.000	6.000	0.091	0.023	0.091	57.500	25.000	57.500
SOLAR ARRAY DRIVE #1 (r/h)	8.000	10.000		4.000	33.288	16.764	5.548	60.000	0.000	35.000
SOLAR ARRAY DRIVE #2 (r/h)	8.000	10.000		4.000	0.013	0.010	16.764	70.000	0.000	35.000
SOLAR ARRAY PANEL #1	330.500	48.700	1.740	6.095	0.121	5.548	5.668	325.250	0.000	35.000
SOLAR ARRAY PANEL #2	330.500	48.700	1.740	6.095	0.121	5.548	5.668	-325.250	0.000	35.000
SHUNT RESISTOR BANK #1	23.100	48.700	1.000	0.945	0.019	0.004	0.023	407.875	0.000	35.000
SHUNT RESISTOR BANK #2	23.100	48.700	1.000	0.945	0.019	0.004	0.023	-407.875	0.000	35.000
ELECTRICAL INTEGRATION (uniform dist)	130.000	190.000	70.000	13.350	4.561	2.425	5.896	0.000	0.000	35.000
		SUBSYSTEM TOTAL		48.550						
THERMAL CONTROL SUBSYSTEM										
OPTICAL SOLAR REFLECTOR (OSR) #1	0.500	90.000	70.000	17.771	0.726	1.925	1.200	65.000	0.000	35.000
OPTICAL SOLAR REFLECTOR (OSR) #2	0.500	90.000	70.000	17.771	0.726	1.925	1.200	-65.000	0.000	35.000
MULTILAYER INSULATION (uniform dist)	130.000	190.000	70.000	5.092	0.925	1.740	2.249	0.000	0.000	35.000
MISC (HEATERS, ETC.) (uniform dist)	130.000	190.000	70.000	2.000	0.363	0.683	0.883	0.000	0.000	35.000
		SUBSYSTEM TOTAL		42.634						
			TOTAL MASS	239.745					CENTER OF MASS	
			MASS MARGIN	41.520						
		TOTAL SPACECRAFT MASS		281.265						

TABLE B-5. MOMENTS OF INERTIA WITH 10% FUEL REMAINING

	A	B	C	D	E
1	31384.409722222		MOMENTS OF INERTIA WITH T|		
2					
3	ITEM	ITEM DIMENSIONS			MASS (kg)
4		a	b	c	
5	TELEMETRY, TRACKING & COMMAND				
6	REMOTE COMMAND UNIT 3 (RCU 3)	18.23	20.4	14.48	5.797
7	REMOTE TELEMETRY UNIT 4 (RTU 4)	20.22	20.4	14.48	7.552
8	DOSIMETER	6.73	9.81	3.99	0.363
9			SUBSYSTEM TOTAL		=SUM(E6.E8)
10	RADIO FREQUENCY SUBSYSTEM				
11	PAYLOAD RECEIVER	14.61	32.08	32.08	6.713
12	PAYLOAD RECEIVER SYNTHESIZER	11.76	19.69	12.7	1.724
13	PAYLOAD RECEIVER POWER SUPPLY	8.89	22.23	16.94	1.814
14	PAYLOAD TRANSMITTER	17.15	36.83	22.23	6.169
15	PAYLOAD RECEIVER STABILIZED CLOCK	3.81	10.16	9.65	0.454
16	PAYLOAD CTS	1.91	10.16	2.54	0.045
17	ANTENNA #1 (point mass)				1.4515
18	ANTENNA #2 (r/h)	14.8	29.6		1.134
19	ANTENNA #3 (r/h)	10.7	21.4		0.7938
20	GROUND PLANE	43	43	0.001	0.4173
21	CABLES (uniform distribution)	130	190	4	0.9072
22			SUBSYSTEM TOTAL		=SUM(E11:E21)
23	ATTITUDE CONTROL SYSTEM				
24	ATTITUDE CONTROL COMPUTER	36.2	6.35	14.9	2.5
25	REACTION WHEEL +X DIRECTION (r/h)	11.75	12		2.375
26	REACTION WHEEL +Y DIRECTION (r/h)	11.75	12		2.375
27	REACTION WHEEL +Z DIRECTION (r/h)	11.75	12		2.375
28	REACTION WHEEL -X/-Y/+Z DIRECTION	11.75	12		2.375
29	GYROSCOPE	7.5	11.4	8.2	1.2
30	EARTH SENSOR (r/h)	5.15	18.256		3.77
31	SUN SENSOR #1	2.5	2.5	2.5	0.04
32	SUN SENSOR #2	2.5	2.5	2.5	0.04
33	SUN SENSOR #3	2.5	2.5	2.5	0.04
34	SUN SENSOR #4	2.5	2.5	2.5	0.04
35			SUBSYSTEM TOTAL		=SUM(E24.E34)
36	REACTION CONTROL SYSTEM				
37	PROPELLANT TANK #1 (radius)	27.5			5.897
38	PROPELLANT TANK #2 (radius)	27.5			5.897
39	PROPELLANT TANK #3 (radius)	27.5			5.897
40	PROPELLANT TANK #4 (radius)	27.5			5.897
41	PROPELLANT IN TANK #1 (radius)	27.5			36.401
42	PROPELLANT IN TANK #2 (radius)	27.5			36.401
43	PROPELLANT IN TANK #3 (radius)	27.5			36.401
44	PROPELLANT IN TANK #4 (radius)	27.5			36.401
45	THRUSTER #1A	3.5	3.5	16.764	0.3193
46	THRUSTER #1B	3.5	3.5	16.764	0.3193
47	THRUSTER #1C	3.5	16.764	3.5	0.3193
48	THRUSTER #2A	3.5	3.5	16.764	0.3193
49	THRUSTER #2B	3.5	16.764	3.5	0.3193
50	THRUSTER #2C	3.5	3.5	16.764	0.3193
51	THRUSTER #3A	3.5	3.5	16.764	0.3193
52	THRUSTER #3B	3.5	3.5	16.764	0.3193
53	THRUSTER #3C	3.5	16.764	3.5	0.3193
54	THRUSTER #4A	3.5	3.5	16.764	0.3193
55	THRUSTER #4B	3.5	16.764	3.5	0.3193
56	THRUSTER #4C	3.5	3.5	16.764	0.3193
57	ORBIT INJECTION THRUSTER #1	5.84	5.84	16.45	0.7348
58	ORBIT INJECTION THRUSTER #2	5.84	5.84	16.45	0.7348
59	ORBIT INJECTION THRUSTER #3	5.84	5.84	16.45	0.7348
60	ORBIT INJECTION THRUSTER #4	5.84	5.84	16.45	0.7348
61	TUBING AND VALVES (uniform dist)	130	190	70	2.268
62			SUBSYSTEM TOTAL		=SUM(E37.E61)
63	STRUCTURAL SUBSYSTEM				
64	PANEL #1 (EARTH FACE)	130	190	1.044	1.67
65	PANEL #2 (+X FACE)	190	1.044	70	0.918
66	PANEL #3 (-X FACE)	190	1.044	70	0.918
67	PANEL #4 (+Y FACE)	1.044	130	70	0.624
68	PANEL #5 (-Y FACE)	1.044	130	70	0.624
69	PANEL #6 (ANTI-EARTH FACE)	130	190	1.02	1.179
70	MISC (BRACKETS, STRUTS, ETC.)	130	190	70	18.194
71	UPPER CENTRAL CONE (r1/r2/h)	37.5	47.76	18	5.221
72	CENTRAL CYLINDER (r/h)	37.5	55		8.192
73	LOWER CENTRAL CONE (r1/r2/h)	37.5	47.76	15	9.082
74			SUBSYSTEM TOTAL		=SUM(E64:E73)
75	ELECTRIC POWER SUBSYSTEM				
76	BATTERIES	23	30	26	7.12
77	POWER CONTROL ELECTRONICS	15	40	15	6
78	SOLAR ARRAY DRIVE #1 (r/h)	8	10		4
79	SOLAR ARRAY DRIVE #2 (r/h)	8	10		4
80	SOLAR ARRAY PANEL #1	4.3	165.25	48.7	6.095
81	SOLAR ARRAY PANEL #2	4.3	165.25	48.7	6.095
82	SHUNT RESISTOR BANK #1	1	23.1	48.7	0.945
83	SHUNT RESISTOR BANK #2	1	23.1	48.7	0.945
84	ELECTRICAL INTEGRATION (uniform dist)	130	190	70	13.35
85			SUBSYSTEM TOTAL		=SUM(E76.E84)
86	THERMAL CONTROL SUBSYSTEM				
87	OPTICAL SOLAR REFLECTOR (OSR) #1	0.5	90	70	17.771
88	OPTICAL SOLAR REFLECTOR (OSR) #2	0.5	90	70	17.771
89	MULTILAYER INSULATION (uniform dist)	130	190	70	5.092
90	MISC (HEATERS, ETC.) (uniform dist)	130	190	70	2
91			SUBSYSTEM TOTAL		=SUM(E87.E90)
92					
93				TOTAL MASS	=SUM(E6.E91)/2

TABLE B.6 MOMENT OF INERTIA EQUATIONS

	F	G
1		
2		
3	ITEM MOMENTS (kg-m^2)	
4	Ix	Iy
5		
6	=E6*(C6^2+D6^2)/120000	=E6*(B6^2+D6^2)/120000
7	=E7*(C7^2+D7^2)/120000	=E7*(B7^2+D7^2)/120000
8	=E8*(C8^2+D8^2)/120000	=E8*(B8^2+D8^2)/120000
9		
10		
11	=E11*(C11^2+D11^2)/120000	=E11*(B11^2+D11^2)/120000
12	=E12*(C12^2+D12^2)/120000	=E12*(B12^2+D12^2)/120000
13	=E13*(C13^2+D13^2)/120000	=E13*(B13^2+D13^2)/120000
14	=E14*(C14^2+D14^2)/120000	=E14*(B14^2+D14^2)/120000
15	=E15*(C15^2+D15^2)/120000	=E15*(B15^2+D15^2)/120000
16	=E16*(C16^2+D16^2)/120000	=E16*(B16^2+D16^2)/120000
17	=E17*(C17^2+D17^2)/120000	=E17*(B17^2+D17^2)/120000
18	=E18*(B18^2/40000+C18^2/120000)	=E18*(B18^2/20000)
19	=E19*(B19^2/40000+C19^2/120000)	=E19*(B19^2/20000)
20	=E20*(C20^2+D20^2)/120000	=E20*(B20^2+D20^2)/120000
21	=E21*(C21^2+D21^2)/120000	=E21*(B21^2+D21^2)/120000
22		
23		
24	=E24*(C24^2+D24^2)/120000	=E24*(B24^2+D24^2)/120000
25	=E25*(B25^2/20000)	=E25*(B25^2/40000+C25^2/120000)
26	=E26*(B26^2/40000+C26^2/120000)	=E26*(B26^2/20000)
27	=E27*(B27^2/40000+C27^2/120000)	=F27
28	=E28*(B28^2/40000+C28^2/120000)	=E28*(B28^2/40000+C28^2/120000)
29	=E29*(C29^2+D29^2)/120000	=E29*(B29^2+D29^2)/120000
30	=E30*(B30^2/40000+C30^2/120000)	=F30
31	=E31*(C31^2+D31^2)/120000	=E31*(B31^2+D31^2)/120000
32	=E32*(C32^2+D32^2)/120000	=E32*(B32^2+D32^2)/120000
33	=E33*(C33^2+D33^2)/120000	=E33*(B33^2+D33^2)/120000
34	=E34*(C34^2+D34^2)/120000	=E34*(B34^2+D34^2)/120000
35		
36		
37	=$E37*2*$B37^2/30000	=$E37*2*$B37^2/30000
38	=$E38*2*$B38^2/30000	=$E38*2*$B38^2/30000
39	=$E39*2*$B39^2/30000	=$E39*2*$B39^2/30000
40	=$E40*2*$B40^2/30000	=$E40*2*$B40^2/30000
41	=$E41*2*$B41^2/50000	=$E41*2*$B41^2/50000
42	=$E42*2*$B42^2/50000	=$E42*2*$B42^2/50000
43	=$E43*2*$B43^2/50000	=$E43*2*$B43^2/50000
44	=$E44*2*$B44^2/50000	=$E44*2*$B44^2/50000
45	=E45*(C45^2+D45^2)/120000	=E45*(B45^2+D45^2)/120000
46	=E46*(C46^2+D46^2)/120000	=E46*(B46^2+D46^2)/120000
47	=E47*(C47^2+D47^2)/120000	=E47*(B47^2+D47^2)/120000
48	=E48*(C48^2+D48^2)/120000	=E48*(B48^2+D48^2)/120000
49	=E49*(C49^2+D49^2)/120000	=E49*(B49^2+D49^2)/120000
50	=E50*(C50^2+D50^2)/120000	=E50*(B50^2+D50^2)/120000
51	=E51*(C51^2+D51^2)/120000	=E51*(B51^2+D51^2)/120000
52	=E52*(C52^2+D52^2)/120000	=E52*(B52^2+D52^2)/120000
53	=E53*(C53^2+D53^2)/120000	=E53*(B53^2+D53^2)/120000
54	=E54*(C54^2+D54^2)/120000	=E54*(B54^2+D54^2)/120000
55	=E55*(C55^2+D55^2)/120000	=E55*(B55^2+D55^2)/120000
56	=E56*(C56^2+D56^2)/120000	=E56*(B56^2+D56^2)/120000
57	=E57*(C57^2+D57^2)/120000	=E57*(B57^2+D57^2)/120000
58	=E58*(C58^2+D58^2)/120000	=E58*(B58^2+D58^2)/120000
59	=E59*(C59^2+D59^2)/120000	=E59*(B59^2+D59^2)/120000
60	=E60*(C60^2+D60^2)/120000	=E60*(B60^2+D60^2)/120000
61	=E61*(C61^2+D61^2)/120000	=E61*(B61^2+D61^2)/120000
62		
63		
64	=E64*(C64^2+D64^2)/120000	=E64*(B64^2+D64^2)/120000
65	=E65*(C65^2+D65^2)/120000	=E65*(B65^2+D65^2)/120000
66	=E66*(C66^2+D66^2)/120000	=E66*(B66^2+D66^2)/120000
67	=E67*(C67^2+D67^2)/120000	=E67*(B67^2+D67^2)/120000
68	=E68*(C68^2+D68^2)/120000	=E68*(B68^2+D68^2)/120000
69	=E69*(C69^2+D69^2)/120000	=E69*(B69^2+D69^2)/120000
70	=E70*(C70^2+D70^2)/120000	=E70*(B70^2+D70^2)/120000
71	=E71*(C71^2+B71^2)/40000+E71*D71^2*(1+2*C71*B71/(C71+B71)^2)/180000	=F71
72	=E72*((C72^2)/2+(B72^2)/12)/10000	=F72
73	=E73*(C73^2+B73^2)/40000+E73*D73^2*(1+2*C73*B73/(C73+B73)^2)/180000	=F73
74		
75		
76	=E76*(C76^2+D76^2)/120000	=E76*(B76^2+D76^2)/120000
77	=E77*(C77^2+D77^2)/120000	=E77*(B77^2+D77^2)/120000
78	=E80*B80^2/20000	=E80*(B80^2/40000+C80^2/120000)
79	=E78*B78^2/20000	=E78*(B78^2/40000+C78^2/120000)
80	=E80*(C80^2+D80^2)/120000	=E80*(B80^2+D80^2)/120000
81	=E81*(C81^2+D81^2)/120000	=E81*(B81^2+D81^2)/120000
82	=E82*(C82^2+D82^2)/120000	=E82*(B82^2+D82^2)/120000
83	=E83*(C83^2+D83^2)/120000	=E83*(B83^2+D83^2)/120000
84	=E84*(C84^2+D84^2)/120000	=E84*(B84^2+D84^2)/120000
85		
86		
87	=E87*(B87^2+D87^2)/120000	=E87*(C87^2+D87^2)/120000
88	=E88*(B88^2+D88^2)/120000	=E88*(C88^2+D88^2)/120000
89	=E89*(B89^2+D89^2)/120000	=E89*(C89^2+D89^2)/120000
90	=E90*(B90^2+D90^2)/120000	=E90*(C90^2+D90^2)/120000
91		
92		
93		

	H	I	J	K	L
1					=A1
2					
3		ITEM POSITION (cm)			C/M CONTRIBUTION
4	Iz	x	y	z	Cx
5					
6	=E6*(C6^2+B6^2)/120000	58.885	-34.8	12.24	=E6*I6
7	=E7*(C7^2+B7^2)/120000	54.891	-34.8	57.76	=E7*I7
8	=E8*(C8^2+B8^2)/120000	61.635	-40.095	35	=E8*I8
9					
10					
11	=E11*(C11^2+B11^2)/120000	-57.895	-23.96	48.96	=E11*I11
12	=E12*(C12^2+B12^2)/120000	-59.12	-30.158	11.35	=E12*I12
13	=E13*(C13^2+B13^2)/120000	-60.555	28.89	13.471	=E13*I13
14	=E14*(C14^2+B14^2)/120000	-58.425	21.585	53.885	=E14*I14
15	=E15*(C15^2+B15^2)/120000	-63.095	34.92	34.825	=E15*I15
16	=E16*(C16^2+B16^2)/120000	-64.045	19.92	31.27	=E16*I16
17	=E17*(C17^2+B17^2)/120000	0	0	79	=E17*I17
18	=G18	-30.2	60.2	84.8	=E18*I18
19	=G19	34.3	-64.3	80.7	=E19*I19
20	=E20*(C20^2+B20^2)/120000	0	0	70	=E20*I20
21	=E21*(C21^2+B21^2)/120000	0	0	35	=E21*I21
22					
23					
24	=E24*(C24^2+B24^2)/120000	0	-92.345	35	=E24*I24
25	=G25	0	-49.25	35	=E25*I25
26	=G26	0	89.52	35	=E26*I26
27	=E27*(B27^2/20000)	0	49.25	35	=E27*I27
28	=E28*(B28^2/40000+C28^2/120000)	-32.5	-32.5	17.5	=E28*I28
29	=E29*(C29^2+B29^2)/120000	61.25	-10	60.9	=E29*I29
30	=E30*(B30^2)/20000	62	0	75	=E30*I30
31	=E31*(C31^2+B31^2)/120000	0	96.25	1.25	=E31*I31
32	=E32*(C32^2+B32^2)/120000	0	96.25	61.25	=E32*I32
33	=E33*(C33^2+B33^2)/120000	0	-96.25	1.25	=E33*I33
34	=E34*(C34^2+B34^2)/120000	0	-96.25	61.25	=E34*I34
35					
36					
37	=$E37*2*$B37^2/30000	36.5	66.5	35	=E37*I37
38	=$E38*2*$B38^2/30000	-36.5	66.5	35	=E38*I38
39	=$E39*2*$B39^2/30000	36.5	-66.5	35	=E39*I39
40	=$E40*2*$B40^2/30000	-36.5	-66.5	35	=E40*I40
41	=$E41*2*$B41^2/50000	36.5	66.5	35	=E41*I41
42	=$E42*2*$B42^2/50000	-36.5	66.5	35	=E42*I42
43	=$E43*2*$B43^2/50000	36.5	-66.5	35	=E43*I43
44	=$E44*2*$B44^2/50000	-36.5	-66.5	35	=E44*I44
45	=E45*(C45^2+B45^2)/120000	55	85	69.492	=E45*I45
46	=E46*(C46^2+B46^2)/120000	55	85	0.501	=E46*I46
47	=E47*(C47^2+B47^2)/120000	59	89	35	=E47*I47
48	=E48*(C48^2+B48^2)/120000	-55	85	69.492	=E48*I48
49	=E49*(C49^2+B49^2)/120000	-59	89	35	=E49*I49
50	=E50*(C50^2+B50^2)/120000	-55	85	0.501	=E50*I50
51	=E51*(C51^2+B51^2)/120000	-55	-85	69.492	=E51*I51
52	=E52*(C52^2+B52^2)/120000	-55	-85	0.501	=E52*I52
53	=E53*(C53^2+B53^2)/120000	-59	-89	35	=E53*I53
54	=E54*(C54^2+B54^2)/120000	55	-85	69.492	=E54*I54
55	=E55*(C55^2+B55^2)/120000	59	-89	35	=E55*I55
56	=E56*(C56^2+B56^2)/120000	55	-85	0.501	=E56*I56
57	=E57*(C57^2+B57^2)/120000	24.192	44.075	-1.175	=E57*I57
58	=E58*(C58^2+B58^2)/120000	24.192	-44.075	-1.175	=E58*I58
59	=E59*(C59^2+B59^2)/120000	-24.192	44.075	-1.175	=E59*I59
60	=E60*(C60^2+B60^2)/120000	-24.192	-44.075	-1.175	=E60*I60
61	=E61*(C61^2+B61^2)/120000	0	0	35	=E61*I61
62					
63					
64	=E64*(C64^2+B64^2)/120000	0	0	70	=E64*I64
65	=E65*(C65^2+B65^2)/120000	65	0	35	=E65*I65
66	=E66*(C66^2+B66^2)/120000	-65	0	35	=E66*I66
67	=E67*(C67^2+B67^2)/120000	0	95	35	=E67*I67
68	=E68*(C68^2+B68^2)/120000	0	-95	35	=E68*I68
69	=E69*(C69^2+B69^2)/120000	0	0	0	=E69*I69
70	=E70*(C70^2+B70^2)/120000	0	0	35	=E70*I70
71	=E71*(C71^2+B71^2)/20000	0	0	60.639	=E71*I71
72	=E72*C72^2/10000	0	0	33.5	=E72*I72
73	=E73*(C73^2+B73^2)/20000	0	0	=D73*((2*C73+B73)/(C7	=E73*I73
74					
75					
76	=E76*(C76^2+B76^2)/120000	53.5699	27.5	26	=E76*I76
77	=E77*(C77^2+B77^2)/120000	57.5	25	57.5	=E77*I77
78	=G80	60	0	35	=E78*I78
79	=G79	70	0	35	=E79*I79
80	=E80*(C80^2+B80^2)/120000	77.15	0	35	=E80*I80
81	=E81*(C81^2+B81^2)/120000	-77.15	0	35	=E81*I81
82	=E82*(C82^2+B82^2)/120000	77.15	0	35	=E82*I82
83	=E83*(C83^2+B83^2)/120000	-77.15	0	35	=E83*I83
84	=E84*(C84^2+B84^2)/120000	0	0	35	=E84*I84
85					
86					
87	=E87*(C87^2+B87^2)/120000	65	0	35	=E87*I87
88	=E88*(C88^2+B88^2)/120000	-65	0	35	=E88*I88
89	=E89*(C89^2+B89^2)/120000	0	0	35	=E89*I89
90	=E90*(C90^2+B90^2)/120000	0	0	35	=E90*I90
91					
92					
93			CENTER OF MASS		=SUM(L6:L90)/E93

	M	N	O	P	Q
1	=A1		=C1		
2					
3			DISTANCE FROM CENTER O		
4	Cy	Cz	Dx	Dy	Dz
5					
6	=E6*J6	=E6*K6	=ABS($L$93-I6)	=ABS($M$93-J6)	=ABS($N$93-K6)
7	=E7*J7	=E7*K7	=ABS($L$93-I7)	=ABS($M$93-J7)	=ABS($N$93-K7)
8	=E8*J8	=E8*K8	=ABS($L$93-I8)	=ABS($M$93-J8)	=ABS($N$93-K8)
9					
10					
11	=E11*J11	=E11*K11	=ABS($L$93-I11)	=ABS($M$93-J11)	=ABS($N$93-K11)
12	=E12*J12	=E12*K12	=ABS($L$93-I12)	=ABS($M$93-J12)	=ABS($N$93-K12)
13	=E13*J13	=E13*K13	=ABS($L$93-I13)	=ABS($M$93-J13)	=ABS($N$93-K13)
14	=E14*J14	=E14*K14	=ABS($L$93-I14)	=ABS($M$93-J14)	=ABS($N$93-K14)
15	=E15*J15	=E15*K15	=ABS($L$93-I15)	=ABS($M$93-J15)	=ABS($N$93-K15)
16	=E16*J16	=E16*K16	=ABS($L$93-I16)	=ABS($M$93-J16)	=ABS($N$93-K16)
17	=E17*J17	=E17*K17	=ABS($L$93-I17)	=ABS($M$93-J17)	=ABS($N$93-K17)
18	=E18*J18	=E18*K18	=ABS($L$93-I18)	=ABS($M$93-J18)	=ABS($N$93-K18)
19	=E19*J19	=E19*K19	=ABS($L$93-I19)	=ABS($M$93-J19)	=ABS($N$93-K19)
20	=E20*J20	=E20*K20	=ABS($L$93-I20)	=ABS($M$93-J20)	=ABS($N$93-K20)
21	=E21*J21	=E21*K21	=ABS($L$93-I21)	=ABS($M$93-J21)	=ABS($N$93-K21)
22					
23					
24	=E24*J24	=E24*K24	=ABS($L$93-I24)	=ABS($M$93-J24)	=ABS($N$93-K24)
25	=E25*J25	=E25*K25	=ABS($L$93-I25)	=ABS($M$93-J25)	=ABS($N$93-K25)
26	=E26*J26	=E26*K26	=ABS($L$93-I26)	=ABS($M$93-J26)	=ABS($N$93-K26)
27	=E27*J27	=E27*K27	=ABS($L$93-I27)	=ABS($M$93-J27)	=ABS($N$93-K27)
28	=E28*J28	=E28*K28	=ABS($L$93-I28)	=ABS($M$93-J28)	=ABS($N$93-K28)
29	=E29*J29	=E29*K29	=ABS($L$93-I29)	=ABS($M$93-J29)	=ABS($N$93-K29)
30	=E30*J30	=E30*K30	=ABS($L$93-I30)	=ABS($M$93-J30)	=ABS($N$93-K30)
31	=E31*J31	=E31*K31	=ABS($L$93-I31)	=ABS($M$93-J31)	=ABS($N$93-K31)
32	=E32*J32	=E32*K32	=ABS($L$93-I32)	=ABS($M$93-J32)	=ABS($N$93-K32)
33	=E33*J33	=E33*K33	=ABS($L$93-I33)	=ABS($M$93-J33)	=ABS($N$93-K33)
34	=E34*J34	=E34*K34	=ABS($L$93-I34)	=ABS($M$93-J34)	=ABS($N$93-K34)
35					
36					
37	=E37*J37	=E37*K37	=ABS($L$93-I37)	=ABS($M$93-J37)	=ABS($N$93-K37)
38	=E38*J38	=E38*K38	=ABS($L$93-I38)	=ABS($M$93-J38)	=ABS($N$93-K38)
39	=E39*J39	=E39*K39	=ABS($L$93-I39)	=ABS($M$93-J39)	=ABS($N$93-K39)
40	=E40*J40	=E40*K40	=ABS($L$93-I40)	=ABS($M$93-J40)	=ABS($N$93-K40)
41	=E41*J41	=E41*K41	=ABS($L$93-I41)	=ABS($M$93-J41)	=ABS($N$93-K41)
42	=E42*J42	=E42*K42	=ABS($L$93-I42)	=ABS($M$93-J42)	=ABS($N$93-K42)
43	=E43*J43	=E43*K43	=ABS($L$93-I43)	=ABS($M$93-J43)	=ABS($N$93-K43)
44	=E44*J44	=E44*K44	=ABS($L$93-I44)	=ABS($M$93-J44)	=ABS($N$93-K44)
45	=E45*J45	=E45*K45	=ABS($L$93-I45)	=ABS($M$93-J45)	=ABS($N$93-K45)
46	=E46*J46	=E46*K46	=ABS($L$93-I46)	=ABS($M$93-J46)	=ABS($N$93-K46)
47	=E47*J47	=E47*K47	=ABS($L$93-I47)	=ABS($M$93-J47)	=ABS($N$93-K47)
48	=E48*J48	=E48*K48	=ABS($L$93-I48)	=ABS($M$93-J48)	=ABS($N$93-K48)
49	=E49*J49	=E49*K49	=ABS($L$93-I49)	=ABS($M$93-J49)	=ABS($N$93-K49)
50	=E50*J50	=E50*K50	=ABS($L$93-I50)	=ABS($M$93-J50)	=ABS($N$93-K50)
51	=E51*J51	=E51*K51	=ABS($L$93-I51)	=ABS($M$93-J51)	=ABS($N$93-K51)
52	=E52*J52	=E52*K52	=ABS($L$93-I52)	=ABS($M$93-J52)	=ABS($N$93-K52)
53	=E53*J53	=E53*K53	=ABS($L$93-I53)	=ABS($M$93-J53)	=ABS($N$93-K53)
54	=E54*J54	=E54*K54	=ABS($L$93-I54)	=ABS($M$93-J54)	=ABS($N$93-K54)
55	=E55*J55	=E55*K55	=ABS($L$93-I55)	=ABS($M$93-J55)	=ABS($N$93-K55)
56	=E56*J56	=E56*K56	=ABS($L$93-I56)	=ABS($M$93-J56)	=ABS($N$93-K56)
57	=E57*J57	=E57*K57	=ABS($L$93-I57)	=ABS($M$93-J57)	=ABS($N$93-K57)
58	=E58*J58	=E58*K58	=ABS($L$93-I58)	=ABS($M$93-J58)	=ABS($N$93-K58)
59	=E59*J59	=E59*K59	=ABS($L$93-I59)	=ABS($M$93-J59)	=ABS($N$93-K59)
60	=E60*J60	=E60*K60	=ABS($L$93-I60)	=ABS($M$93-J60)	=ABS($N$93-K60)
61	=E61*J61	=E61*K61	=ABS($L$93-I61)	=ABS($M$93-J61)	=ABS($N$93-K61)
62					
63					
64	=E64*J64	=E64*K64	=ABS($L$93-I64)	=ABS($M$93-J64)	=ABS($N$93-K64)
65	=E65*J65	=E65*K65	=ABS($L$93-I65)	=ABS($M$93-J65)	=ABS($N$93-K65)
66	=E66*J66	=E66*K66	=ABS($L$93-I66)	=ABS($M$93-J66)	=ABS($N$93-K66)
67	=E67*J67	=E67*K67	=ABS($L$93-I67)	=ABS($M$93-J67)	=ABS($N$93-K67)
68	=E68*J68	=E68*K68	=ABS($L$93-I68)	=ABS($M$93-J68)	=ABS($N$93-K68)
69	=E69*J69	=E69*K69	=ABS($L$93-I69)	=ABS($M$93-J69)	=ABS($N$93-K69)
70	=E70*J70	=E70*K70	=ABS($L$93-I70)	=ABS($M$93-J70)	=ABS($N$93-K70)
71	=E71*J71	=E71*K71	=ABS($L$93-I71)	=ABS($M$93-J71)	=ABS($N$93-K71)
72	=E72*J72	=E72*K72	=ABS($L$93-I72)	=ABS($M$93-J72)	=ABS($N$93-K72)
73	=E73*J73	=E73*K73	=ABS($L$93-I73)	=ABS($M$93-J73)	=ABS($N$93-K73)
74					
75					
76	=E76*J76	=E76*K76	=ABS($L$93-I76)	=ABS($M$93-J76)	=ABS($N$93-K76)
77	=E77*J77	=E77*K77	=ABS($L$93-I77)	=ABS($M$93-J77)	=ABS($N$93-K77)
78	=E78*J78	=E78*K78	=ABS($L$93-I78)	=ABS($M$93-J78)	=ABS($N$93-K78)
79	=E79*J79	=E79*K79	=ABS($L$93-I79)	=ABS($M$93-J79)	=ABS($N$93-K79)
80	=E80*J80	=E80*K80	=ABS($L$93-I80)	=ABS($M$93-J80)	=ABS($N$93-K80)
81	=E81*J81	=E81*K81	=ABS($L$93-I81)	=ABS($M$93-J81)	=ABS($N$93-K81)
82	=E82*J82	=E82*K82	=ABS($L$93-I82)	=ABS($M$93-J82)	=ABS($N$93-K82)
83	=E83*J83	=E83*K83	=ABS($L$93-I83)	=ABS($M$93-J83)	=ABS($N$93-K83)
84	=E84*J84	=E84*K84	=ABS($L$93-I84)	=ABS($M$93-J84)	=ABS($N$93-K84)
85					
86					
87	=E87*J87	=E87*K87	=ABS($L$93-I87)	=ABS($M$93-J87)	=ABS($N$93-K87)
88	=E88*J88	=E88*K88	=ABS($L$93-I88)	=ABS($M$93-J88)	=ABS($N$93-K88)
89	=E89*J89	=E89*K89	=ABS($L$93-I89)	=ABS($M$93-J89)	=ABS($N$93-K89)
90	=E90*J90	=E90*K90	=ABS($L$93-I90)	=ABS($M$93-J90)	=ABS($N$93-K90)
91					
92					
93	=SUM(M6:M90)/E93	=SUM(N6:N90)/E93		TOTAL SPACECRAFT MOMENTS	

	R	S	T
1			
2			
3		TOTAL MOMENT OF INERTIA (kg-m^2)	
4	Ixx	Iyy	Izz
5			
6	=F6+E6*(P6^2+Q6^2)/10000	=G6+E6*(O6^2+Q6^2)/10000	=H6+E6*(O6^2+P6^2)/10000
7	=F7+E7*(P7^2+Q7^2)/10000	=G7+E7*(O7^2+Q7^2)/10000	=H7+E7*(O7^2+P7^2)/10000
8	=F8+E8*(P8^2+Q8^2)/10000	=G8+E8*(O8^2+Q8^2)/10000	=H8+E8*(O8^2+P8^2)/10000
9			
10			
11	=F11+E11*(P11^2+Q11^2)/10000	=G11+E11*(O11^2+Q11^2)/10000	=H11+E11*(O11^2+P11^2)/10000
12	=F12+E12*(P12^2+Q12^2)/10000	=G12+E12*(O12^2+Q12^2)/10000	=H12+E12*(O12^2+P12^2)/10000
13	=F13+E13*(P13^2+Q13^2)/10000	=G13+E13*(O13^2+Q13^2)/10000	=H13+E13*(O13^2+P13^2)/10000
14	=F14+E14*(P14^2+Q14^2)/10000	=G14+E14*(O14^2+Q14^2)/10000	=H14+E14*(O14^2+P14^2)/10000
15	=F15+E15*(P15^2+Q15^2)/10000	=G15+E15*(O15^2+Q15^2)/10000	=H15+E15*(O15^2+P15^2)/10000
16	=F16+E16*(P16^2+Q16^2)/10000	=G16+E16*(O16^2+Q16^2)/10000	=H16+E16*(O16^2+P16^2)/10000
17	=F17+E17*(P17^2+Q17^2)/10000	=G17+E17*(O17^2+Q17^2)/10000	=H17+E17*(O17^2+P17^2)/10000
18	=F18+E18*(P18^2+Q18^2)/10000	=G18+E18*(O18^2+Q18^2)/10000	=H18+E18*(O18^2+P18^2)/10000
19	=F19+E19*(P19^2+Q19^2)/10000	=G19+E19*(O19^2+Q19^2)/10000	=H19+E19*(O19^2+P19^2)/10000
20	=F20+E20*(P20^2+Q20^2)/10000	=G20+E20*(O20^2+Q20^2)/10000	=H20+E20*(O20^2+P20^2)/10000
21	=F21+E21*(P21^2+Q21^2)/10000	=G21+E21*(O21^2+Q21^2)/10000	=H21+E21*(O21^2+P21^2)/10000
22			
23			
24	=F24+E24*(P24^2+Q24^2)/10000	=G24+E24*(O24^2+Q24^2)/10000	=H24+E24*(O24^2+P24^2)/10000
25	=F25+E25*(P25^2+Q25^2)/10000	=G25+E25*(O25^2+Q25^2)/10000	=H25+E25*(O25^2+P25^2)/10000
26	=F26+E26*(P26^2+Q26^2)/10000	=G26+E26*(O26^2+Q26^2)/10000	=H26+E26*(O26^2+P26^2)/10000
27	=F27+E27*(P27^2+Q27^2)/10000	=G27+E27*(O27^2+Q27^2)/10000	=H27+E27*(O27^2+P27^2)/10000
28	=F28+E28*(P28^2+Q28^2)/10000	=G28+E28*(O28^2+Q28^2)/10000	=H28+E28*(O28^2+P28^2)/10000
29	=F29+E29*(P29^2+Q29^2)/10000	=G29+E29*(O29^2+Q29^2)/10000	=H29+E29*(O29^2+P29^2)/10000
30	=F30+E30*(P30^2+Q30^2)/10000	=G30+E30*(O30^2+Q30^2)/10000	=H30+E30*(O30^2+P30^2)/10000
31	=F31+E31*(P31^2+Q31^2)/10000	=G31+E31*(O31^2+Q31^2)/10000	=H31+E31*(O31^2+P31^2)/10000
32	=F32+E32*(P32^2+Q32^2)/10000	=G32+E32*(O32^2+Q32^2)/10000	=H32+E32*(O32^2+P32^2)/10000
33	=F33+E33*(P33^2+Q33^2)/10000	=G33+E33*(O33^2+Q33^2)/10000	=H33+E33*(O33^2+P33^2)/10000
34	=F34+E34*(P34^2+Q34^2)/10000	=G34+E34*(O34^2+Q34^2)/10000	=H34+E34*(O34^2+P34^2)/10000
35			
36			
37	=F37+E37*(P37^2+Q37^2)/10000	=G37+E37*(O37^2+Q37^2)/10000	=H37+E37*(O37^2+P37^2)/10000
38	=F38+E38*(P38^2+Q38^2)/10000	=G38+E38*(O38^2+Q38^2)/10000	=H38+E38*(O38^2+P38^2)/10000
39	=F39+E39*(P39^2+Q39^2)/10000	=G39+E39*(O39^2+Q39^2)/10000	=H39+E39*(O39^2+P39^2)/10000
40	=F40+E40*(P40^2+Q40^2)/10000	=G40+E40*(O40^2+Q40^2)/10000	=H40+E40*(O40^2+P40^2)/10000
41	=F41+E41*(P41^2+Q41^2)/10000	=G41+E41*(O41^2+Q41^2)/10000	=H41+E41*(O41^2+P41^2)/10000
42	=F42+E42*(P42^2+Q42^2)/10000	=G42+E42*(O42^2+Q42^2)/10000	=H42+E42*(O42^2+P42^2)/10000
43	=F43+E43*(P43^2+Q43^2)/10000	=G43+E43*(O43^2+Q43^2)/10000	=H43+E43*(O43^2+P43^2)/10000
44	=F44+E44*(P44^2+Q44^2)/10000	=G44+E44*(O44^2+Q44^2)/10000	=H44+E44*(O44^2+P44^2)/10000
45	=F45+E45*(P45^2+Q45^2)/10000	=G45+E45*(O45^2+Q45^2)/10000	=H45+E45*(O45^2+P45^2)/10000
46	=F46+E46*(P46^2+Q46^2)/10000	=G46+E46*(O46^2+Q46^2)/10000	=H46+E46*(O46^2+P46^2)/10000
47	=F47+E47*(P47^2+Q47^2)/10000	=G47+E47*(O47^2+Q47^2)/10000	=H47+E47*(O47^2+P47^2)/10000
48	=F48+E48*(P48^2+Q48^2)/10000	=G48+E48*(O48^2+Q48^2)/10000	=H48+E48*(O48^2+P48^2)/10000
49	=F49+E49*(P49^2+Q49^2)/10000	=G49+E49*(O49^2+Q49^2)/10000	=H49+E49*(O49^2+P49^2)/10000
50	=F50+E50*(P50^2+Q50^2)/10000	=G50+E50*(O50^2+Q50^2)/10000	=H50+E50*(O50^2+P50^2)/10000
51	=F51+E51*(P51^2+Q51^2)/10000	=G51+E51*(O51^2+Q51^2)/10000	=H51+E51*(O51^2+P51^2)/10000
52	=F52+E52*(P52^2+Q52^2)/10000	=G52+E52*(O52^2+Q52^2)/10000	=H52+E52*(O52^2+P52^2)/10000
53	=F53+E53*(P53^2+Q53^2)/10000	=G53+E53*(O53^2+Q53^2)/10000	=H53+E53*(O53^2+P53^2)/10000
54	=F54+E54*(P54^2+Q54^2)/10000	=G54+E54*(O54^2+Q54^2)/10000	=H54+E54*(O54^2+P54^2)/10000
55	=F55+E55*(P55^2+Q55^2)/10000	=G55+E55*(O55^2+Q55^2)/10000	=H55+E55*(O55^2+P55^2)/10000
56	=F56+E56*(P56^2+Q56^2)/10000	=G56+E56*(O56^2+Q56^2)/10000	=H56+E56*(O56^2+P56^2)/10000
57	=F57+E57*(P57^2+Q57^2)/10000	=G57+E57*(O57^2+Q57^2)/10000	=H57+E57*(O57^2+P57^2)/10000
58	=F58+E58*(P58^2+Q58^2)/10000	=G58+E58*(O58^2+Q58^2)/10000	=H58+E58*(O58^2+P58^2)/10000
59	=F59+E59*(P59^2+Q59^2)/10000	=G59+E59*(O59^2+Q59^2)/10000	=H59+E59*(O59^2+P59^2)/10000
60	=F60+E60*(P60^2+Q60^2)/10000	=G60+E60*(O60^2+Q60^2)/10000	=H60+E60*(O60^2+P60^2)/10000
61	=F61+E61*(P61^2+Q61^2)/10000	=G61+E61*(O61^2+Q61^2)/10000	=H61+E61*(O61^2+P61^2)/10000
62			
63			
64	=F64+E64*(P64^2+Q64^2)/10000	=G64+E64*(O64^2+Q64^2)/10000	=H64+E64*(O64^2+P64^2)/10000
65	=F65+E65*(P65^2+Q65^2)/10000	=G65+E65*(O65^2+Q65^2)/10000	=H65+E65*(O65^2+P65^2)/10000
66	=F66+E66*(P66^2+Q66^2)/10000	=G66+E66*(O66^2+Q66^2)/10000	=H66+E66*(O66^2+P66^2)/10000
67	=F67+E67*(P67^2+Q67^2)/10000	=G67+E67*(O67^2+Q67^2)/10000	=H67+E67*(O67^2+P67^2)/10000
68	=F68+E68*(P68^2+Q68^2)/10000	=G68+E68*(O68^2+Q68^2)/10000	=H68+E68*(O68^2+P68^2)/10000
69	=F69+E69*(P69^2+Q69^2)/10000	=G69+E69*(O69^2+Q69^2)/10000	=H69+E69*(O69^2+P69^2)/10000
70	=F70+E70*(P70^2+Q70^2)/10000	=G70+E70*(O70^2+Q70^2)/10000	=H70+E70*(O70^2+P70^2)/10000
71	=F71+E71*(P71^2+Q71^2)/10000	=G71+E71*(O71^2+Q71^2)/10000	=H71+E71*(O71^2+P71^2)/10000
72	=F72+E72*(P72^2+Q72^2)/10000	=G72+E72*(O72^2+Q72^2)/10000	=H72+E72*(O72^2+P72^2)/10000
73	=F73+E73*(P73^2+Q73^2)/10000	=G73+E73*(O73^2+Q73^2)/10000	=H73+E73*(O73^2+P73^2)/10000
74			
75			
76	=F76+E76*(P76^2+Q76^2)/10000	=G76+E76*(O76^2+Q76^2)/10000	=H76+E76*(O76^2+P76^2)/10000
77	=F77+E77*(P77^2+Q77^2)/10000	=G77+E77*(O77^2+Q77^2)/10000	=H77+E77*(O77^2+P77^2)/10000
78	=F78+E78*(P78^2+Q78^2)/10000	=G78+E78*(O78^2+Q78^2)/10000	=H78+E78*(O78^2+P78^2)/10000
79	=F79+E79*(P79^2+Q79^2)/10000	=G79+E79*(O79^2+Q79^2)/10000	=H79+E79*(O79^2+P79^2)/10000
80	=F80+E80*(P80^2+Q80^2)/10000	=G80+E80*(O80^2+Q80^2)/10000	=H80+E80*(O80^2+P80^2)/10000
81	=F81+E81*(P81^2+Q81^2)/10000	=G81+E81*(O81^2+Q81^2)/10000	=H81+E81*(O81^2+P81^2)/10000
82	=F82+E82*(P82^2+Q82^2)/10000	=G82+E82*(O82^2+Q82^2)/10000	=H82+E82*(O82^2+P82^2)/10000
83	=F83+E83*(P83^2+Q83^2)/10000	=G83+E83*(O83^2+Q83^2)/10000	=H83+E83*(O83^2+P83^2)/10000
84	=F84+E84*(P84^2+Q84^2)/10000	=G84+E84*(O84^2+Q84^2)/10000	=H84+E84*(O84^2+P84^2)/10000
85			
86			
87	=F87+E87*(P87^2+Q87^2)/10000	=G87+E87*(O87^2+Q87^2)/10000	=H87+E87*(O87^2+P87^2)/10000
88	=F88+E88*(P88^2+Q88^2)/10000	=G88+E88*(O88^2+Q88^2)/10000	=H88+E88*(O88^2+P88^2)/10000
89	=F89+E89*(P89^2+Q89^2)/10000	=G89+E89*(O89^2+Q89^2)/10000	=H89+E89*(O89^2+P89^2)/10000
90	=F90+E90*(P90^2+Q90^2)/10000	=G90+E90*(O90^2+Q90^2)/10000	=H90+E90*(O90^2+P90^2)/10000
91			
92			
93	=SUM(R6:R90)	=SUM(S6:S90)	=SUM(T6:T90)

	U	V	W
1			
2			
3			
4	Ixy	Ixz	Iyz
5			
6	=E6*(I6-L$93)*(J6-M$93)/10000	=E6*(I6-L$93)*(K6-N$93)/10000	=E6*(J6-M$93)*(K6-N$93)/10000
7	=E7*(I7-L$93)*(J7-M$93)/10000	=E7*(I7-L$93)*(K7-N$93)/10000	=E7*(J7-M$93)*(K7-N$93)/10000
8	=E8*(I8-L$93)*(J8-M$93)/10000	=E8*(I8-L$93)*(K8-N$93)/10000	=E8*(J8-M$93)*(K8-N$93)/10000
9			
10			
11	=E11*(I11-L$93)*(J11-M$93)/10000	=E11*(I11-L$93)*(K11-N$93)/10000	=E11*(J11-M$93)*(K11-N$93)/10000
12	=E12*(I12-L$93)*(J12-M$93)/10000	=E12*(I12-L$93)*(K12-N$93)/10000	=E12*(J12-M$93)*(K12-N$93)/10000
13	=E13*(I13-L$93)*(J13-M$93)/10000	=E13*(I13-L$93)*(K13-N$93)/10000	=E13*(J13-M$93)*(K13-N$93)/10000
14	=E14*(I14-L$93)*(J14-M$93)/10000	=E14*(I14-L$93)*(K14-N$93)/10000	=E14*(J14-M$93)*(K14-N$93)/10000
15	=E15*(I15-L$93)*(J15-M$93)/10000	=E15*(I15-L$93)*(K15-N$93)/10000	=E15*(J15-M$93)*(K15-N$93)/10000
16	=E16*(I16-L$93)*(J16-M$93)/10000	=E16*(I16-L$93)*(K16-N$93)/10000	=E16*(J16-M$93)*(K16-N$93)/10000
17	=E17*(I17-L$93)*(J17-M$93)/10000	=E17*(I17-L$93)*(K17-N$93)/10000	=E17*(J17-M$93)*(K17-N$93)/10000
18	=E18*(I18-L$93)*(J18-M$93)/10000	=E18*(I18-L$93)*(K18-N$93)/10000	=E18*(J18-M$93)*(K18-N$93)/10000
19	=E19*(I19-L$93)*(J19-M$93)/10000	=E19*(I19-L$93)*(K19-N$93)/10000	=E19*(J19-M$93)*(K19-N$93)/10000
20	=E20*(I20-L$93)*(J20-M$93)/10000	=E20*(I20-L$93)*(K20-N$93)/10000	=E20*(J20-M$93)*(K20-N$93)/10000
21	=E21*(I21-L$93)*(J21-M$93)/10000	=E21*(I21-L$93)*(K21-N$93)/10000	=E21*(J21-M$93)*(K21-N$93)/10000
22			
23			
24	=E24*(I24-L$93)*(J24-M$93)/10000	=E24*(I24-L$93)*(K24-N$93)/10000	=E24*(J24-M$93)*(K24-N$93)/10000
25	=E25*(I25-L$93)*(J25-M$93)/10000	=E25*(I25-L$93)*(K25-N$93)/10000	=E25*(J25-M$93)*(K25-N$93)/10000
26	=E26*(I26-L$93)*(J26-M$93)/10000	=E26*(I26-L$93)*(K26-N$93)/10000	=E26*(J26-M$93)*(K26-N$93)/10000
27	=E27*(I27-L$93)*(J27-M$93)/10000	=E27*(I27-L$93)*(K27-N$93)/10000	=E27*(J27-M$93)*(K27-N$93)/10000
28	=E28*(I28-L$93)*(J28-M$93)/10000	=E28*(I28-L$93)*(K28-N$93)/10000	=E28*(J28-M$93)*(K28-N$93)/10000
29	=E29*(I29-L$93)*(J29-M$93)/10000	=E29*(I29-L$93)*(K29-N$93)/10000	=E29*(J29-M$93)*(K29-N$93)/10000
30	=E30*(I30-L$93)*(J30-M$93)/10000	=E30*(I30-L$93)*(K30-N$93)/10000	=E30*(J30-M$93)*(K30-N$93)/10000
31	=E31*(I31-L$93)*(J31-M$93)/10000	=E31*(I31-L$93)*(K31-N$93)/10000	=E31*(J31-M$93)*(K31-N$93)/10000
32	=E32*(I32-L$93)*(J32-M$93)/10000	=E32*(I32-L$93)*(K32-N$93)/10000	=E32*(J32-M$93)*(K32-N$93)/10000
33	=E33*(I33-L$93)*(J33-M$93)/10000	=E33*(I33-L$93)*(K33-N$93)/10000	=E33*(J33-M$93)*(K33-N$93)/10000
34	=E34*(I34-L$93)*(J34-M$93)/10000	=E34*(I34-L$93)*(K34-N$93)/10000	=E34*(J34-M$93)*(K34-N$93)/10000
35			
36			
37	=E37*(I37-L$93)*(J37-M$93)/10000	=E37*(I37-L$93)*(K37-N$93)/10000	=E37*(J37-M$93)*(K37-N$93)/10000
38	=E38*(I38-L$93)*(J38-M$93)/10000	=E38*(I38-L$93)*(K38-N$93)/10000	=E38*(J38-M$93)*(K38-N$93)/10000
39	=E39*(I39-L$93)*(J39-M$93)/10000	=E39*(I39-L$93)*(K39-N$93)/10000	=E39*(J39-M$93)*(K39-N$93)/10000
40	=E40*(I40-L$93)*(J40-M$93)/10000	=E40*(I40-L$93)*(K40-N$93)/10000	=E40*(J40-M$93)*(K40-N$93)/10000
41	=E41*(I41-L$93)*(J41-M$93)/10000	=E41*(I41-L$93)*(K41-N$93)/10000	=E41*(J41-M$93)*(K41-N$93)/10000
42	=E42*(I42-L$93)*(J42-M$93)/10000	=E42*(I42-L$93)*(K42-N$93)/10000	=E42*(J42-M$93)*(K42-N$93)/10000
43	=E43*(I43-L$93)*(J43-M$93)/10000	=E43*(I43-L$93)*(K43-N$93)/10000	=E43*(J43-M$93)*(K43-N$93)/10000
44	=E44*(I44-L$93)*(J44-M$93)/10000	=E44*(I44-L$93)*(K44-N$93)/10000	=E44*(J44-M$93)*(K44-N$93)/10000
45	=E45*(I45-L$93)*(J45-M$93)/10000	=E45*(I45-L$93)*(K45-N$93)/10000	=E45*(J45-M$93)*(K45-N$93)/10000
46	=E46*(I46-L$93)*(J46-M$93)/10000	=E46*(I46-L$93)*(K46-N$93)/10000	=E46*(J46-M$93)*(K46-N$93)/10000
47	=E47*(I47-L$93)*(J47-M$93)/10000	=E47*(I47-L$93)*(K47-N$93)/10000	=E47*(J47-M$93)*(K47-N$93)/10000
48	=E48*(I48-L$93)*(J48-M$93)/10000	=E48*(I48-L$93)*(K48-N$93)/10000	=E48*(J48-M$93)*(K48-N$93)/10000
49	=E49*(I49-L$93)*(J49-M$93)/10000	=E49*(I49-L$93)*(K49-N$93)/10000	=E49*(J49-M$93)*(K49-N$93)/10000
50	=E50*(I50-L$93)*(J50-M$93)/10000	=E50*(I50-L$93)*(K50-N$93)/10000	=E50*(J50-M$93)*(K50-N$93)/10000
51	=E51*(I51-L$93)*(J51-M$93)/10000	=E51*(I51-L$93)*(K51-N$93)/10000	=E51*(J51-M$93)*(K51-N$93)/10000
52	=E52*(I52-L$93)*(J52-M$93)/10000	=E52*(I52-L$93)*(K52-N$93)/10000	=E52*(J52-M$93)*(K52-N$93)/10000
53	=E53*(I53-L$93)*(J53-M$93)/10000	=E53*(I53-L$93)*(K53-N$93)/10000	=E53*(J53-M$93)*(K53-N$93)/10000
54	=E54*(I54-L$93)*(J54-M$93)/10000	=E54*(I54-L$93)*(K54-N$93)/10000	=E54*(J54-M$93)*(K54-N$93)/10000
55	=E55*(I55-L$93)*(J55-M$93)/10000	=E55*(I55-L$93)*(K55-N$93)/10000	=E55*(J55-M$93)*(K55-N$93)/10000
56	=E56*(I56-L$93)*(J56-M$93)/10000	=E56*(I56-L$93)*(K56-N$93)/10000	=E56*(J56-M$93)*(K56-N$93)/10000
57	=E57*(I57-L$93)*(J57-M$93)/10000	=E57*(I57-L$93)*(K57-N$93)/10000	=E57*(J57-M$93)*(K57-N$93)/10000
58	=E58*(I58-L$93)*(J58-M$93)/10000	=E58*(I58-L$93)*(K58-N$93)/10000	=E58*(J58-M$93)*(K58-N$93)/10000
59	=E59*(I59-L$93)*(J59-M$93)/10000	=E59*(I59-L$93)*(K59-N$93)/10000	=E59*(J59-M$93)*(K59-N$93)/10000
60	=E60*(I60-L$93)*(J60-M$93)/10000	=E60*(I60-L$93)*(K60-N$93)/10000	=E60*(J60-M$93)*(K60-N$93)/10000
61	=E61*(I61-L$93)*(J61-M$93)/10000	=E61*(I61-L$93)*(K61-N$93)/10000	=E61*(J61-M$93)*(K61-N$93)/10000
62			
63			
64	=E64*(I64-L$93)*(J64-M$93)/10000	=E64*(I64-L$93)*(K64-N$93)/10000	=E64*(J64-M$93)*(K64-N$93)/10000
65	=E65*(I65-L$93)*(J65-M$93)/10000	=E65*(I65-L$93)*(K65-N$93)/10000	=E65*(J65-M$93)*(K65-N$93)/10000
66	=E66*(I66-L$93)*(J66-M$93)/10000	=E66*(I66-L$93)*(K66-N$93)/10000	=E66*(J66-M$93)*(K66-N$93)/10000
67	=E67*(I67-L$93)*(J67-M$93)/10000	=E67*(I67-L$93)*(K67-N$93)/10000	=E67*(J67-M$93)*(K67-N$93)/10000
68	=E68*(I68-L$93)*(J68-M$93)/10000	=E68*(I68-L$93)*(K68-N$93)/10000	=E68*(J68-M$93)*(K68-N$93)/10000
69	=E69*(I69-L$93)*(J69-M$93)/10000	=E69*(I69-L$93)*(K69-N$93)/10000	=E69*(J69-M$93)*(K69-N$93)/10000
70	=E70*(I70-L$93)*(J70-M$93)/10000	=E70*(I70-L$93)*(K70-N$93)/10000	=E70*(J70-M$93)*(K70-N$93)/10000
71	=E71*(I71-L$93)*(J71-M$93)/10000	=E71*(I71-L$93)*(K71-N$93)/10000	=E71*(J71-M$93)*(K71-N$93)/10000
72	=E72*(I72-L$93)*(J72-M$93)/10000	=E72*(I72-L$93)*(K72-N$93)/10000	=E72*(J72-M$93)*(K72-N$93)/10000
73	=E73*(I73-L$93)*(J73-M$93)/10000	=E73*(I73-L$93)*(K73-N$93)/10000	=E73*(J73-M$93)*(K73-N$93)/10000
74			
75			
76	=E76*(I76-L$93)*(J76-M$93)/10000	=E76*(I76-L$93)*(K76-N$93)/10000	=E76*(J76-M$93)*(K76-N$93)/10000
77	=E77*(I77-L$93)*(J77-M$93)/10000	=E77*(I77-L$93)*(K77-N$93)/10000	=E77*(J77-M$93)*(K77-N$93)/10000
78	=E78*(I78-L$93)*(J78-M$93)/10000	=E78*(I78-L$93)*(K78-N$93)/10000	=E78*(J78-M$93)*(K78-N$93)/10000
79	=E79*(I79-L$93)*(J79-M$93)/10000	=E79*(I79-L$93)*(K79-N$93)/10000	=E79*(J79-M$93)*(K79-N$93)/10000
80	=E80*(I80-L$93)*(J80-M$93)/10000	=E80*(I80-L$93)*(K80-N$93)/10000	=E80*(J80-M$93)*(K80-N$93)/10000
81	=E81*(I81-L$93)*(J81-M$93)/10000	=E81*(I81-L$93)*(K81-N$93)/10000	=E81*(J81-M$93)*(K81-N$93)/10000
82	=E82*(I82-L$93)*(J82-M$93)/10000	=E82*(I82-L$93)*(K82-N$93)/10000	=E82*(J82-M$93)*(K82-N$93)/10000
83	=E83*(I83-L$93)*(J83-M$93)/10000	=E83*(I83-L$93)*(K83-N$93)/10000	=E83*(J83-M$93)*(K83-N$93)/10000
84	=E84*(I84-L$93)*(J84-M$93)/10000	=E84*(I84-L$93)*(K84-N$93)/10000	=E84*(J84-M$93)*(K84-N$93)/10000
85			
86			
87	=E87*(I87-L$93)*(J87-M$93)/10000	=E87*(I87-L$93)*(K87-N$93)/10000	=E87*(J87-M$93)*(K87-N$93)/10000
88	=E88*(I88-L$93)*(J88-M$93)/10000	=E88*(I88-L$93)*(K88-N$93)/10000	=E88*(J88-M$93)*(K88-N$93)/10000
89	=E89*(I89-L$93)*(J89-M$93)/10000	=E89*(I89-L$93)*(K89-N$93)/10000	=E89*(J89-M$93)*(K89-N$93)/10000
90	=E90*(I90-L$93)*(J90-M$93)/10000	=E90*(I90-L$93)*(K90-N$93)/10000	=E90*(J90-M$93)*(K90-N$93)/10000
91			
92			
93	=SUM(U6:U90)	=SUM(V6:V90)	=SUM(W6:W90)

APPENDIX C

A. INITIAL SIZING OF STRUCTURAL ELEMENTS

The design for the cylindrical tube with axial load due to the stacked configuration mass of 1200 kg, is as follows.

$$P = 1200 \times 9.806 \times 1.5 \times 6$$
$$= 1.059 \times 10^5 \text{ N}$$

The critical load for axial compression is given by,

$$P_{cr} = 1.2y\pi Et^2$$

where, $y = 1 - 0.9(1 - e^{-\phi})$

and, $\phi = \frac{1}{16}\sqrt{r/t} = \frac{0.03827}{\sqrt{t}}$

$$R_c = P/P_{cr}$$

The load due to bending, (noting that the CM of the spacecraft is 1.23 m from the bottom) is,

$$M = 1200 \times 9.806 \times 1.5 \times 1.23 \times 3$$
$$= 6.513 \times 10^4 \text{ N}\cdot\text{m}$$

$$M_{cr} = 0.6y'\pi Ert^2$$

where, $y' = 1 - 0.731(1 - e^{-\phi})$

$$R_b = M/M_{cr}$$

For this design a 10% margin of safety will be used.

$$M.S. = \frac{1}{R_c + R_b} - 1$$
$$= 0.10$$

From iterative calculations, the minimum required thickness for the cylindrical tube is,

$$t = 1.382 \text{ mm}$$

The axial load of 1.059×10^5 N is the same for the design of the lower frustum shell. The interface shell is a monocoque aluminum right conical cylindrical structure with minor radius of 0.375 m, height 0.15 m, and major radius of 0.4776 m (see Figure C-1). The critical load for axial compression is given by,

$$P_{cr} = 0.399\pi E t^2 \cos^2\alpha$$

where, $\alpha = 34.37°$

The bending moment (with moment arm = 1.38 m) is given by

$$M = 1200 \times 1.38 \times 1.5 \times 9.806 \times 3$$
$$= 7.307 \times 10^4 \text{ N·m}$$

The critical bending moment is given by,

$$M_{cr} = 0.248\pi E r_1 t^2 \cos\alpha, \qquad \text{(and noting } r_1 = 0.375 \text{ m)}$$

With R_c, R_b , and M.S. defined the same as above, the minimum thickness required for the conical interface shell is 3.424 mm.

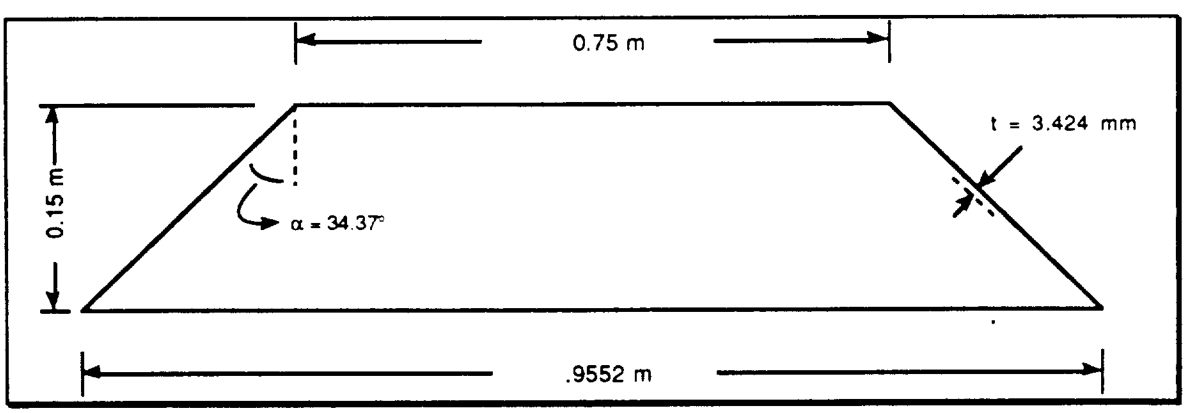

Figure C-1. Conical interface shell structure.

The design of the upper frustum shell proceeds in the same manner but with height 18 cm, and $\alpha = 29.68°$. Axial load is 7.060×10^4 N and the bending moment is 3.036×10^4 N•m. Critical load for buckling is $6.623 \times 10^{10} t^2$ N and critical bending moment for the upper frustum shell is $1.544 \times 10^{10} t^2$ N•m with moment arm of 0.86 m. Analysis results in thickness of 1.826 mm for the upper frustum shell.

The panels are made of aluminum honeycomb sandwich material. The boundary conditions are simply supported on all four sides. A uniform mass of 92.2 kg is to be supported by the panels.

The panels will have a design load of 30 g lateral. The mass per unit area is,

$$\gamma = \frac{92.2}{1.9 \times 0.70} = 69.32 \text{ kg/m}^2$$

The natural frequency for the panel from Table 4.9 [Ref. 1, p.231] is,

$$f = \frac{1}{2\pi} \beta \sqrt{\frac{D}{\gamma a^4}}$$

where, $a = 0.7$, and $b/a = 2.714$

$\beta = 11.24$

The panel stiffness, D, is given by,

$$D = \frac{Eth^2}{2(1 - \nu)}$$

$$D = \frac{7 \times 10^{10} th^2}{2(1 - .33^2)} = 3.928 \times 10^{10}\, th^2$$

Substituting, yields

$$25 = \frac{1}{2\pi} \times 11.24 \sqrt{\frac{3.928 \times 10^{10}\, th^2}{69.32 \times (0.70)^4}}$$

$$th^2 = 8.275 \times 10^{-8}$$

Assuming a panel core thickness, $h = 9.525 \times 10^{-3}$ m, (3/8 in.), the face skin thickness is,

$$t_f = 0.912 \text{ mm}$$

For the dynamic load of 30 g's, the maximum stress for the panel is given by [Ref. 1, p. 243],

$$\sigma_{max} = \beta \frac{wa^4}{6th}$$

where, w, the panel limit load per unit area is

$$w = \frac{92.2 \times 30 \times 9.806}{1.90 \times 0.70}$$
$$= 2.039 \times 10^4 \text{ N/m}^2$$

For a = 0.70, b = 1.90 m and b/a = 2.714, from Table 4.10 [Ref. 1, p. 243], $\beta = 0.6569$. Substituting into the equation for maximum stress,

$$\therefore \sigma_{max} = \frac{0.6569 \times 2.039 \times 10^4 \times (0.70)^4}{6 \times 0.912 \times 10^{-3} \times 9.525 \times 10^{-3}}$$
$$= 61.7 \text{ N/mm}^2$$

For the design of the panel with face skin thickness 0.912 mm and core thickness 0.009525 m (3/8 in.), the maximum stress is within the allowable range for the material which has as yield stress 240 N/mm^2. This results in a margin of 74.3 % over the yield stress of the material.

The dynamic analysis of the solar array panels followed in the same manner but with face thickness, t = 0.13 mm, core thickness, h = 16 mm, length and width dimensions of 1.65 m by 0.51 m, and mass of 6 kg ($\gamma = 7.13$ kg/m^2, w = 2.0975 x 10\s\up3(3) N/m\s\up3(2)). The analysis resulted in a frequency, f = 497.6 Hz, and σ_{max} = 7.857 N/mm^2. The solar arrays have a margin of 96.7 % over the yield stress of the material.

B. LATERAL VIBRATION OF STACKED CONFIGURATION

From the finite element analysis results, the seventh mode shows evidence of lateral bending. The frequency for the seventh mode is 104.0 Hz. The fundamental frequency of a cantilever beam with stiffness, EI, is given in English units as the following.

$$f = c_n\sqrt{\frac{gEI}{wl^4}}$$

where,

$c_0 = 0.56$

$g = 386 \text{ in/sec}^2$

$EI =$ Stiffness

$w =$ weight per unit length, (28.44 lbs/in.)

$l =$ length of the beam, (27.56 in.)

The effective stiffness of the spacecraft is then $EI = 1.466 \times 10^9$ lb•in^3. From the equation, the frequency of a uniform cantilever beam in lateral bending is inversely proportional to the square of the length. The mass of the finite element model is 355.5 kg (783.7 lbs). The frequency for the three satellites in the stacked configuration is as follows.

$$f = 0.56\sqrt{\frac{386 \times 1.466 \times 10^9}{28.44 \times 112.6^4}}\text{ Hz}$$

$$= 6.23 \text{ Hz}$$

Where, the length of the payload for the stacked configuration of three satellites is 2.85 m (112.6 in).

C. FINITE ELEMENT ANALYSIS MODELING

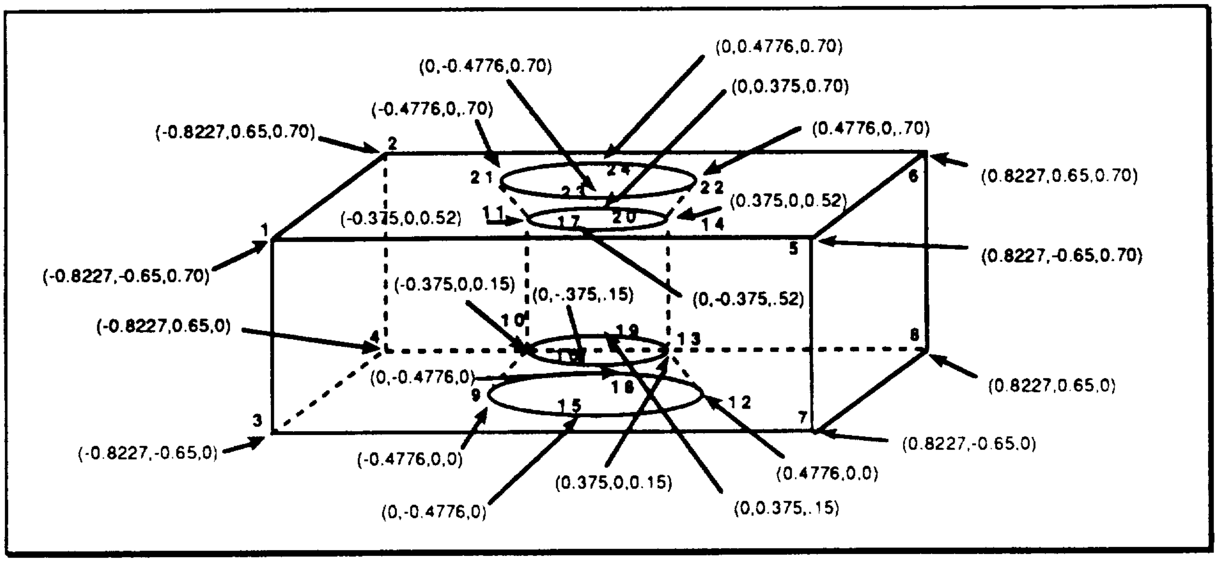

Figure C-2. Representative Nodal Input for HILACS Satellite.

Figure C-2 illustrates representative nodal inputs required in modeling the spacecraft for finite element analysis. The actual model generated for computing the modal frequencies consisted of 81 key points, 752 structural nodes, 1504 elements, and 4416 unknowns. The entire structure was modeled including the North, South, Earth-facing, and Anti-Earth facing panels; although, these would not be expected to carry heavy loads.

Masses added to the finite element model are shown in Table C-1. This table gives the values added for equipment masses such as the payload, power electronics, thermal blankets, solar array, etc. The total mass of the spacecraft calculated from the finite element analysis program was 355.5 kg. This value differs from the mass given in the structure mass summary because mass estimates of attachment fittings were not included in the finite element model. The final mass of the spacecraft after all subsystem design iterations is 367.195 kg (without mass margin); including mass margin, the spacecraft is 408.7 kg.

Table C-1. Component Mass Values

West Face (Grid Mass)	**Mass** (kg)
Payload	16.919
Shunt	2.280
Thermal (1/2)	15.70
Misc. Electronics	6.675
East Face (Grid Mass)	
TT&C	13.712
Shunt	2.280
Batteries	7.120
Power Electronics	2.610
Thermal (1/2)	15.70
Misc. Electronics	6.675
Earth-Facing Frustum Shell (Line Mass)	
Antenna	4.952
Earth Sensors	3.080
ACS Reaction Wheel	26.00
Gyros	1.2
Electronics	3.8
Point Masses	
Array Drive (2 points)	4.503 (each point)
Solar Array (8 points)	0.877 (each point)
Propellant Tanks (8 points)	25.00 (each point)
Total	**344.725 kg**

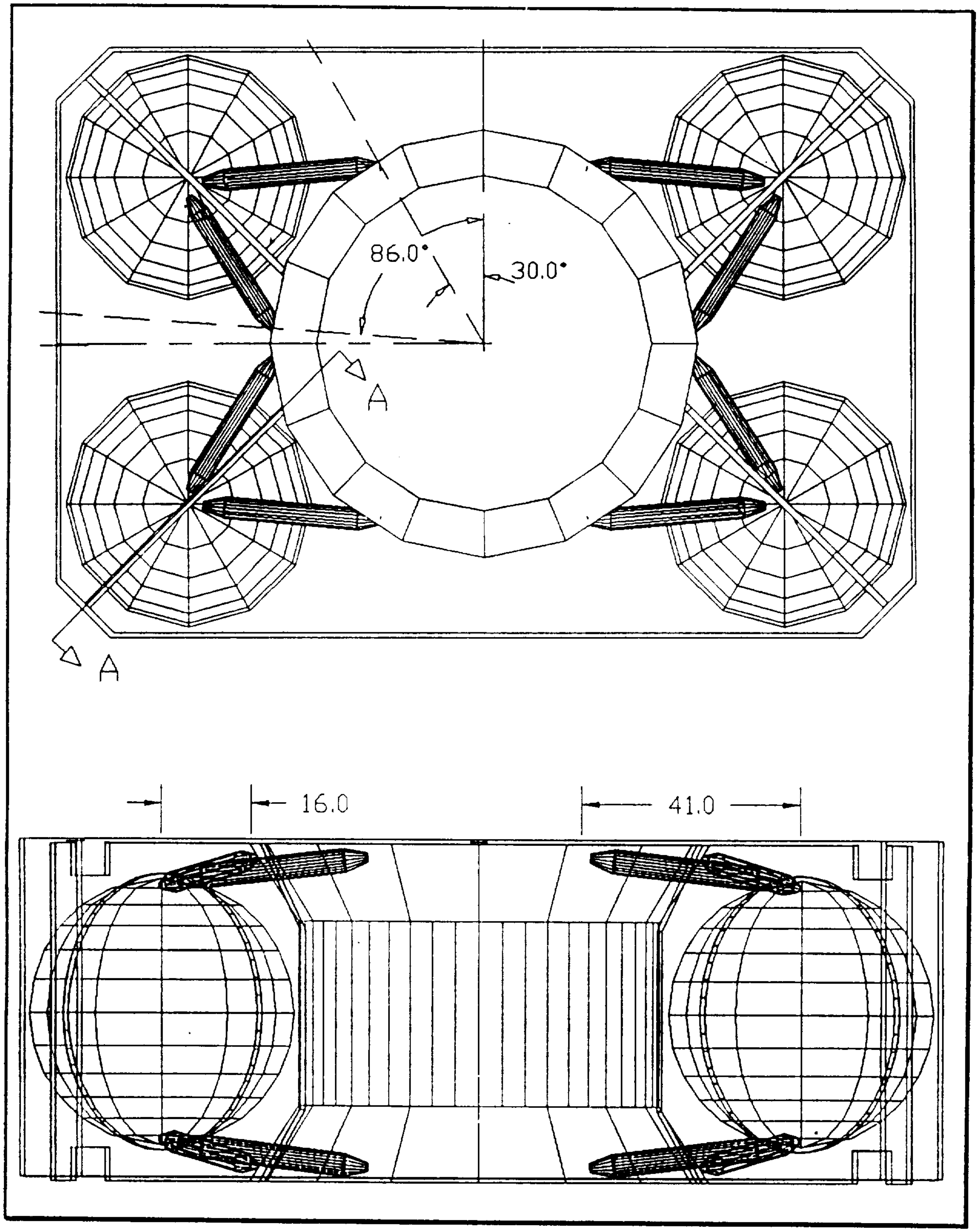

Figure C-3. Spacecraft Structural Configuration.

TABLE D-1. NCS TO MS

Parameter	Symbol	Value	Units	Uplink (dB)	Value	Downlink (dB)
Frequency (MHz)	f	350.00	MHz		253.00	
Bit Rate (bps)	Rb	9600.00	Hz	39.82		39.82
Transmitter Power (W)	Pt	100.00	W	20.00	20.00	13.01
Transmitter circuit Losses	Lc	1.00		0.00	1.00	0.00
Transmitter Ant gain	Gt			14.00		3.50
Terminal EIRP (W)				34.00		16.51
Free Space Loss (for distance)	Ls	19882.00	Km	169.29	19882.00	166.47
Atmospheric Attenuation	La	1.00		0.00	1.00	0.00
Other losses	Lo	1.00		0.00	1.00	0.00
Received Isotropic power (W)				-135.29		-149.96
Receiver Antenna Gain	G			3.50		3.00
Received signal power (W)	C			-131.79		-146.96
Receiver Antenna Temp (K)	Ta	290.00	°K	24.62	290.00	24.62
Coax Temp (K)	Tc	150.00	°K	21.76	290.00	24.62
Cable Loss	Lc	1.26		1.00	1.00	0.00
Receiver Noise Figure	F	1.59		2.00	11.50	10.61
System Temperature (K)	Ts	400.01	°K	26.02	3335.00	35.23
Boltzmann's Constant (dBW/K-Hz)	k			-228.60		-228.60
Bit duration - Bandwidth Product		2.00				
Noise Bandwidth (Hz)				42.83		42.83
Noise Spectral Density	(No=kT°)			-202.58		-193.37
System G/T (K)				-22.52		-32.23
C/N (dB)				53.97		38.80
Received Eb/No						41.81
Required Eb/No (for BPSK)						11.34
Margin (dB)						30.48

TABLE D-2. MS-NCS

Parameter	Symbol	Value	Units	Uplink (dB)	Value	Downlink (dB)
Frequency (MHz)	f	350.00	MHz		253.00	
Bit Rate (bps)	Rb	9600.00	Hz	39.82		39.82
Transmitter Power (W)	Pt	100.00	W	20.00	20.00	13.01
Transmitter circuit Losses	Lc	1.00		0.00	1.00	0.00
Transmitter Ant gain	Gt			3.00		3.50
Terminal EIRP (W)				23.00		16.51
Free Space Loss (for distance)	Ls	19882.00	Km	169.29	19882.00	166.47
Atmospheric Attenuation	La	1.00		0.00	1.00	0.00
Other losses	Lo	1.00		0.00	1.00	0.00
Received Isotropic power (W)				-146.29		-149.96
Receiver Antenna Gain	G			3.50		14.00
Received signal power (W)	C			-142.79		-135.96
Receiver Antenna Temp (K)	Ta	290.00	°K	24.62	290.00	24.62
Coax Temp (K)	Tc	150.00	°K	21.76	290.00	24.62
Cable Loss	Lc	1.26		1.00	1.00	0.00
Receiver Noise Figure	F	1.59		2.00	2.00	3.01
System Temperature (K)	Ts	400.01	°K	26.02	580.00	27.63
Boltzmann's Constant (dBW/K-Hz)	k			-228.60		-228.60
Bit duration - Bandwidth Product		2.00				
Noise Bandwidth (Hz)				42.83		42.83
Noise Spectral Density	(No=kT°)			-202.58		-200.97
System G/T (K)				-22.52		-13.63
C/N (dB)				42.97		49.80
Received Eb/No						52.81
Required Eb/No (for BPSK)						11.34
Margin (dB)						41.48

TABLE D-3. MLG TO HILACS

Parameter	Symbol	Value	Units	Uplink (dB)
Frequency (MHz)	f	350.00	MHz	
Bit Rate (bps)	Rb	9600.00	Hz	39.82
Transmitter Power (W)	Pt	1000.00	W	30.00
Transmitter circuit Losses	Lc	1.00		0.00
Transmitter Ant gain	Gt			22.00
Terminal EIRP (W)				52.00
Free Space Loss (for distance)	Ls	19882.00	Km	169.29
Atmospheric Attenuation	La	1.00		0.00
Other losses	Lo	1.00		0.00
Received Isotropic power (W)				-117.29
Receiver Antenna Gain	G			3.50
Received signal power (W)	C			-113.79
Receiver Antenna Temp (K)	Ta	290.00	°K	24.62
Coax Temp (K)	Tc	150.00	°K	21.76
Cable Loss	Lc	1.26		1.00
Receiver Noise Figure	F	1.59		2.00
System Temperature (K)	Ts	400.01	°K	26.02
Boltzmann's Constant (dBW/K-Hz)	k			-228.60
Bit duration - Bandwidth Product		2.00		
Noise Bandwidth (Hz)				42.83
Noise Spectral Density	(No=kT°)			-202.58
System G/T (K)				-22.52
C/N (dB)				71.97
Received Eb/No				74.98
Required Eb/No (for BPSK)				11.34
Margin (dB)				63.65

APPENDIX E

1. EPS OVERVIEW

The final resulting values calculated from the various spreadsheets are summarized in the following report.

Electric Power Summary Worksheet

11/20/89 16:43

Radiation Received of 1 MeV Equivalent Electrons:			
	Open Circuit Voltage and Max Power:		5.15E+15
	Open Circuit and Short Circuit Current:		2.81E+15
Radiation Degredation in % of BOL Values:			
	Open Circuit Voltage (volts):	0.86	
	Short Circuit Current (amps):	0.77	
	Maximum Power Voltage (volts):	0.892	
	Maximum Power Current (amps):	0.768	
Cell Characteristics at EOL:			
	Open Circuit Voltage (volts):	0.825	
	Short Circuit Current (amps):	0.164	
	Maximum Power Voltage (volts)	0.732	
	Maximum Power Current (amps):	0.155	

Maximum Load Power (watts):	259.32
Total Design Power (watts):	343
Eclipse Power Requirements (watts):	140

Array Dimensions (per array):		
	Length (m):	3.305
	Width (m):	0.487
	Thickness (cm):	1.7399
Total Array Area (sq m):	3.22	
Total Array Mass (kg):	12.19	

Maximum Array Temperature at EOL (°C):	46.68
Minimum Array Eclipse Temperature at EOL (°C):	-117.88
Maximum Power at BOL (watts):	504.47
Minimum Power at EOL (watts):	357.53

Battery Type:	Nickel-Hydrogen	Eagle Picher	
	Battery Rating (Amp-Hours):		12
	Number Of Cells:		16
	Required Recharge Time (hours):		3.70
	Required Charge Power (watts):		52.5
	Battery Mass (kg):		7.12
	Battery Volume (cc):		14132.20

Wiring Harness Mass From Array:	0.15
Mechanical Integration (est):	4.2
Electrical Wiring (est):	9
Power Electronic Circuitry Mass (est):	4.00
Shunt Resistor Bank Mass (est):	1.89
Solar Array Drive Motors (est):	8
Solar Array Drive Electronics (est):	2

Total Electric Power System Mass (kg):	48.55

2. CIRCUIT DESIGN

The circuit design from the array to the 28 volt bus is presented. Output filtering of the bus is not shown nor is the dc-dc converters required for the 32 and 42 volt systems.

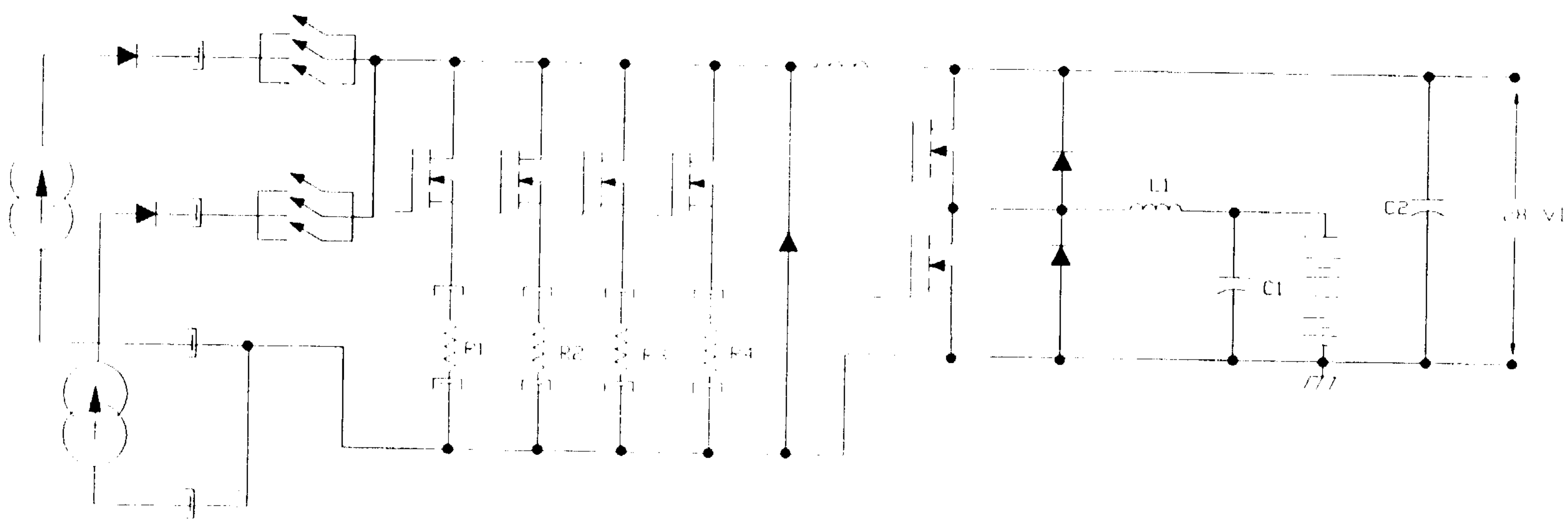

R1-R4 [illegible] ohm, 90 watt
L1 550 uH
C1 500 uF
C2 22 mF

HI-LAT SAT
POWER SUBSYSTEM
Daniel S. Hunter

Rev	Date	Comments
1	11/13/89	
2	11/22/89	Change to MOSFETs

3. SOLAR CELL DESIGN SPREADSHEET

The initial solar cells are designed using the following spreadsheet. The spreadsheet consists of several groups of areas that are interlinked to perform the size determination. The major areas in the spreadsheet are

- solar cell specific calculations,
- power requirements,
- bus and battery requirements,
- temperature calculations,
- radiation calculations for front and back,
- substrate calculations for determination of mass, thermal mass and battery mass.

The radiation calculations are obtained from orbital parameters in the spreadsheet. Once the values for total radiation are obtained, the degradation amounts are determined from a book of radiation results such as Reference 1. These degradation amounts are then placed in the solar cell area in the appropriate places. The spreadsheet is the iterated with the degradation values and the power and bus requirements to obtain the required number of cells in series and parallel to maintain a powered system. This iteration is performed by temperature analysis and iteration is complete when the temperature has stabilized with a given array panel configuration and number of cells on each panel. The equations used in the spreadsheet are listed after the value section of the appendix.

	A	B	C	D	E
1	Solar Cell Type/Coverglass Thickness		0.006 in substrate		
2	Cell size LPE GaAs	2	4.000		
3	Item		Voc (volts)	Isc (amps)	Vmp (volts)
4	Bare Cell (28 deg c)		1.014	0.232	0.876
5	Assembly process	-10	1.004		0.866
6		0.98		0.227	
7	cell mismatch	0.99		0.225	
8	Intensity	0.967479675		0.218	
9	UltraViolet Radiation	0.98		0.213	
10	Micrometeorites	0.99		0.211	
11	Charged Partical radiation				
12	Voc	0.86	0.863		
13	Vmp	0.892			0.772
14	Isc	0.77		0.163	
15	Imp	0.768			
16					
17	Maximum operating Temperature				
18	43.29				
19	Voc	-1.94	0.834		0.740
20	Isc	0.11158		0.164	
21	Imp	0.11158			
22	Thermal Cycling	0.99	0.825		0.732
23					
24	end of mission value		0.825	0.164	0.732
25					

	F
1	
2	
3	**Imp(amps)**
4	0.220
5	
6	0.215
7	0.213
8	0.206
9	0.202
10	0.200
11	
12	
13	
14	
15	0.154
16	
17	
18	
19	
20	
21	0.155
22	
23	
24	0.155
25	

	G	H	I	J
1	**Power Requirements**		**Solar Cell Calculations**	
2	Payload	101.05	**Battery Charge Requireme**	52.500
3	TT&C	11.22	**Maximum Power Level**	259.320
4	Electric power system	20	**Design Power Level**	343.002
5	ACS/RCS	70	**Bus Voltage: Sun**	30.900
6	Thermal Control	50	**Total Current Rqd**	12.250
7	Wire Losses	7.05	**Cells in Parallel**	79.815
8			**Cells in Series**	42.193
9				
10	**Total Power Required**	259.32		
11				
12	**Eclipse Loads**			
13	Electric Power System	20		
14	ACS/RCS	70		
15	Thermal Control	50		
16	**Total Eclipse Power**	140	**Total Array Cells**	3520.000
17			**Total Array Area**	30307.200
18			**Array Margin**	**Each Panel**
19				
20			**Thermal Calculations**	
21			**Packing Factor**	0.929
22			**Cell Absorptance**	0.820
23			**Cell Efficiency (eol)**	0.088
24			**Cell Solar Absorptance**	0.738
25			**Sun Incidence Angle**	0.150
26			**Emissivity of Front**	0.780
27			**Emissivity of Back**	0.900

	K	L	M	N
1		Battery Calculations		
2		Eclipse Period	37.000	
3		Eclipse Power	164.706	
4		DOD	0.600	
5		Number of Cells	15.636	16.000
6		Battery Capacity	11.756	12.000
7	80.000	Battery Charge Rate	1.714	
8	44.000	Peak Battery Voltage	24.000	
9		Min Bus Voltage	17.600	
10		Time for Charge	3.703	
11		Power For Charge	41.143	42.000
12				
13				
14				
15				
16				
17				
18	15153.600	Width(0.5 cm each side)	0.487	length(0.5 cm ea)
19		cells only	0.462	
20				
21	Solar Incidence	Operating Temperatures	Eclipse Temperatures	
22	1309.000	316.441	158.194	
23	1309.000	316.441	158.194	
24				
25		43.291	-114.956	
26		43.291	-114.956	
27				

	O	P	Q	R
1		**Beginning of Life Values**		
2		**Imp**	0.226	
3		**Voc**	0.973	
4		**Isc**	0.239	
5		**Vmp**	0.835	
6				
7		**Beginning of Life Voltage**	36.758	
8		**Beginning of Life Current**	18.105	
9		**Beginning of Life Power**	665.520	
10				
11		**Power Required to Dissipate**	231.434	
12				
13		**Shunt Resistance Needed**	0.279	
14		**Thru Current For Housekeep**	9.358	
15				
16				
17				
18	3.305	**total array area**	3.219	
19	3.280		3.031	
20		**array area each panel**	1.610	
21				
22				
23				
24				
25				
26				
27				

	A	B	C	D	E
75	**Array Mass Calculations per array**	**Structure**	**Length**	**Width**	**Area**
76		**Thermal Paint**	48.700	330.500	16095.350
77		**Al Facesheet**	48.700	330.500	16095.350
78		**Core Adhesive**	48.700	330.500	16095.350
79		**Al Core**	48.700	330.500	16095.350
80		**Core Adhesive**	48.700	330.500	16095.350
81		**Al Facesheet**	48.700	330.500	16095.350
82		**Epoxy/glass**	48.700	330.500	16095.350
83		**RTV-118**	48.700	330.500	16095.350
84		**Solar Cells**	46.200	328.000	15153.600
85		**Solder**	46.200	328.000	15153.600
86		**Glue for Slips**	46.200	328.000	15153.600
87		**Cover Slips**	46.200	328.000	15153.600
88		**Diodes**			
89		**Wiring**			
90					
91				Total Thickness (cm):	
92					
93					
94	Battery Mass Calculations		Dimensions		
95	Number of Cells	8	height (in)	8.800	
96	Mass Per Cell	0.89	width (in)	3.500	
97	Battery Mass (kg)	7.12	depth (in)	3.500	
98	(lbs)	15.69691307	Volume (cubic in	107.800	
99			Total Volume (in	862.400	
100			Cubic cm	14132.204	

	F	G	H	I	J
75	**Thickness**	**Density**	**Shield Effect (m**	**Mass**	**Thermal Coefficien**
76	0.0043	1.55	0.03	0.107275508	600
77	0.013	2.7	0.16	0.564946785	960
78	0.007	1.98	0.06	0.223081551	920
79	1.6	0.026	0.19	0.66956656	960
80	0.007	1.98	0.06	0.223081551	920
81	0.013	2.7	0.16	0.564946785	960
82	0.01	1.87	0.08	0.300983045	600
83	0.007	1.04	0.03	0.117174148	920
84	0.01524	0.086	Total Back Shiel	1.3032096	620
85	0.00254	0.011	0.77	0.1666896	960
86	0.01	1.02	in mils	0.15456672	920
87	20	0.0056	30.3149	1.6972032	600
88					600
89					600
90					920
91	1.73988			6.092725053	Total Thermal Mass
92			Total mass	12.18545011	
93			Two Arrays	26.86431896	
94			(lbs)		
95					
96					
97					
98					
99					
100					

	K
75	m*cp
76	64.365
77	542.349
78	205.235
79	642.784
80	205.235
81	542.349
82	180.590
83	107.800
84	807.990
85	160.022
86	142.201
87	1018.322
88	
89	
90	
91	4619.242
92	
93	
94	
95	
96	
97	
98	
99	
100	

	A	B	C	D	E
28					
29	**Front Shield Radiation Parameters**	**Altitude (nm)**	**Eccentric An**	**Time in min**	**Delta T**
30	**Solar Cell Radiation Calculations**				
31		150			
32		250			
33		300			
34		450			
35		600			
36		800	0.285	6.951	6.951
37		1000	0.438	10.841	3.889
38		1250	0.577	14.566	3.725
39		1500	0.691	17.790	3.224
40		1750	0.791	20.766	2.976
41		2000	0.882	23.607	2.840
42		2250	0.966	26.372	2.766
43		2500	1.046	29.103	2.730
44		2750	1.123	31.824	2.721
45		3000	1.196	34.557	2.733
46		3500	1.338	40.121	5.564
47		4000	1.474	45.905	5.785
48		4500	1.610	52.011	6.106
49		5000	1.745	58.549	6.538
50		5500	1.884	65.658	7.109
51		6000	2.030	73.536	7.877
52		7000	2.365	93.130	19.595
53		8000	2.957	131.539	38.408
54		8062.995166	3.141	143.950	12.412
55		10000			
56		11000			
57		12000			
58		13000			
59		14000			
60		15000			
61		16000			
62		17000			
63		18000			
64		19326			
65		8062.996166			
66					
67					
68	**Total Received radiation per year**				
69	**Total Time for Half period**				143.950
70	**number of years on orbit**	3			
71	**Total Radiation Received in Front**				

	F	G	H	I	J
28		electrons on	protons		
29	electrons	orbit	20 mil Voc/Pma	protons on	
30	20 mil			orbit	20 mil Isc
31	92800000000		4.95E+11		3.49E+11
32	1.44E+11		1.8E+12		1.33E+12
33	1.74E+11		3.27E+12		2.47E+12
34	2.88E+11		1.09E+13		8.33E+12
35	4.73E+11		2.91E+13		2.2E+13
36	9.68E+11	46745297053	9.93E+13	4.79526E+12	7.39E+13
37	1.96E+12	52956462338	2.63E+14	7.10589E+12	1.88E+14
38	3.74E+12	96772694176	6.54E+14	1.69223E+13	4.34E+14
39	5.16E+12	1.15571E+11	1.41E+15	3.15803E+13	8.69E+14
40	5.89E+12	1.21789E+11	2.56E+15	5.29338E+13	1.49E+15
41	6.02E+12	1.18788E+11	3.64E+15	7.18256E+13	2.03E+15
42	5.87E+12	1.12788E+11	4.41E+15	8.47349E+13	2.36E+15
43	5.79E+12	1.09811E+11	4.78E+15	9.06554E+13	2.49E+15
44	5.68E+12	1.07377E+11	4.79E+15	9.05524E+13	2.43E+15
45	5.67E+12	1.07644E+11	4.41E+15	8.37234E+13	2.19E+15
46	6.14E+12	2.37332E+11	3.18E+15	1.22918E+14	1.55E+15
47	7.05E+12	2.833E+11	2.07E+15	8.31816E+13	9.91E+14
48	8.46E+12	3.58845E+11	1.25E+15	5.30209E+13	5.85E+14
49	1.01E+13	4.58712E+11	6.86E+14	3.11561E+13	3.14E+14
50	1.24E+13	6.12369E+11	3.84E+14	1.89637E+13	1.73E+14
51	1.53E+13	8.37266E+11	1.75E+14	9.57658E+12	7.67E+13
52	2.25E+13	3.06275E+12	2.49E+13	3.38945E+12	1.03E+13
53	2.68E+13	7.15066E+12	2.57E+12	6.85716E+11	1E+12
54	3.22E+13	2.77636E+12	1.31E+11	11295115928	50800000000
55	3.51E+13		0.00183		
56	3.26E+13		0.00183		
57	2.78E+13				
58	2.42E+13				
59	1.8E+13				
60	1.17E+13				
61	8.93E+12				
62	6.49E+12				
63	4.35E+12				
64	2.13E+12				
65					
66					
67					
68		1.67678E+13		8.57732E+14	
69					
70					
71		7.54553E+13		3.8598E+15	

	K	L	M	N
28				
29				
30	**protons on orbit**			
31				**Orbit Calculations**
32				**Perigee Altitude**
33				**Apogee Altitude**
34				**Period**
35				**Eccentricity**
36	3.56868E+12			**Semi Major Axis**
37	5.0795E+12			
38	1.12298E+13			
39	1.94633E+13			
40	3.08091E+13			
41	4.00566E+13			
42	4.53457E+13			
43	4.72243E+13			
44	4.59378E+13			
45	4.15769E+13			
46	5.99127E+13			
47	3.98227E+13			
48	2.48138E+13			
49	1.42609E+13			
50	8.54354E+12			
51	4.19728E+12			
52	1.40206E+12			
53	2.66816E+11			
54	4380090757			
55				
56				
57				
58				
59				
60				
61				
62				
63				
64				
65				
66				
67				
68	4.43516E+14			
69				
70				
71	1.99582E+15			

	O	P	Q	R
28		**Back Shield Radiation Parameters**		
29		**Altitude (nm) 30 mil thick**	**Electons**	**p Voc&pmax**
30				
31	650.000	150	71700000000	3.49E+11
32	8062.996	250	1.11E+11	1.35E+12
33	4.800	300	1.33E+11	2.51E+12
34	0.475	450	2.17E+11	8.53E+12
35	7800.428	600	3.49E+11	2.27E+13
36		800	6.88E+11	7.7E+13
37		1000	1.36E+12	1.96E+14
38		1250	2.58E+12	4.48E+14
39		1500	3.53E+12	8.85E+14
40		1750	3.94E+12	1.49E+15
41		2000	3.9E+12	1.97E+15
42		2250	3.69E+12	2.21E+15
43		2500	3.59E+12	2.24E+15
44		2750	3.53E+12	2.12E+15
45		3000	3.61E+12	1.87E+15
46		3500	4.21E+12	1.28E+15
47		4000	5.04E+12	7.93E+14
48		4500	6.16E+12	4.5E+14
49		5000	7.45E+12	2.33E+14
50		5500	9.28E+12	1.24E+14
51		6000	1.16E+13	5.2E+13
52		7000	1.74E+13	6.01E+12
53		8000	2.08E+13	4.97E+11
54		9000	2.49E+13	26100000000
55		10000	2.68E+13	
56		11000	2.45E+13	
57		12000	2.07E+13	
58		13000	1.78E+13	
59		14000	1.31E+13	
60		15000	8.25E+12	
61		16000	6.19E+12	
62		17000	4.39E+12	
63		18000	2.85E+12	
64		19326	1.34E+12	
65				
66				
67				
68				
69				
70				
71				

	S	T	U	V	W	X
28						
29	protons Isc	Electrons on orbit	Voc	Isc		60 mil thick
30						
31	2.78E+11					
32	1.1E+12					
33	2.08E+12					
34	7.06E+12					
35	1.86E+13					
36	6.16E+13	33223930137	3.7184E+12	2.9747E+12		
37	1.51E+14	36745300397	5.2956E+12	4.0798E+12		
38	3.26E+14	66757633950	1.1592E+13	8.4353E+12		
39	6.03E+14	79062807758	1.9822E+13	1.3506E+13		
40	9.58E+14	81468378318	3.0809E+13	1.9809E+13		
41	1.22E+15	76956002690	3.8873E+13	2.4073E+13		
42	1.33E+15	70900657541	4.2464E+13	2.5555E+13		
43	1.32E+15	68086403572	4.2483E+13	2.5035E+13		
44	1.23E+15	66732739128	4.0077E+13	2.3252E+13		
45	1.07E+15	68535482210	3.5502E+13	2.0314E+13		
46	7.26E+14	1.62731E+11	4.9476E+13	2.8062E+13		
47	4.45E+14	2.02529E+11	3.1866E+13	1.7882E+13		
48	2.5E+14	2.61287E+11	1.9088E+13	1.0604E+13		
49	1.28E+14	3.38357E+11	1.0582E+13	5.8134E+12		
50	6.69E+13	4.58289E+11	6.1237E+12	3.3038E+12		
51	2.75E+13	6.3479E+11	2.8456E+12	1.5049E+12		
52	3.06E+12	2.36853E+12	8.181E+11	4.1653E+11		
53	2.45E+11	5.54976E+12	1.3261E+11	6.537E+10		
54	14000000000	2.14693E+12	2250400960	1207111626		
55						
56						
57						
58						
59						
60						
61						
62						
63						
64						
65						
66						
67	Total Received per year	1.27717E+13	3.9157E+14	2.3469E+14		
68	EOL Total Back	3.8315E+13	1.1747E+15	7.0406E+14		
69						
70	EOL Total Front	7.54553E+13	3.8598E+15	1.9958E+15		
71	Total Radiation Received		5.1483E+15	2.8137E+15		

	Y	Z	AA	AB	AC	AD	AE	AF
28								
29	electrons	p Voc	p Isc		Altitude	Total Elelctr	Total VOC P	Total Isc pro
30						Electron Flu	Proton Flux	Proton Flux
31	3.68E+10	2.29E+11	2E+11		800	7.9969E+10	8.5136E+12	6.5434E+12
32	5.66E+10	9.35E+11	8.25E+11		1000	8.9702E+10	1.2402E+13	9.1593E+12
33	6.74E+10	1.8E+12	1.6E+12		1250	1.6353E+11	2.8514E+13	1.9665E+13
34	1.08E+11	6.11E+12	5.41E+12		1500	1.9463E+11	5.1402E+13	3.2969E+13
35	1.69E+11	1.59E+13	1.39E+13		1750	2.0326E+11	8.3743E+13	5.0618E+13
36	3.18E+11	5.17E+13	4.46E+13		2000	1.9574E+11	1.107E+14	6.413E+13
37	6.05E+11	1.22E+14	1.02E+14		2250	1.8369E+11	1.272E+14	7.0901E+13
38	1.13E+12	2.42E+14	1.94E+14		2500	1.779E+11	1.3314E+14	7.2259E+13
39	1.54E+12	3.98E+14	3.02E+14		2750	1.7411E+11	1.3063E+14	6.919E+13
40	1.69E+12	5.58E+14	4.01E+14		3000	1.7618E+11	1.1923E+14	6.1891E+13
41	1.63E+12	6.39E+14	4.42E+14		3500	4.0006E+11	1.7239E+14	8.7975E+13
42	1.53E+12	6.36E+14	4.27E+14		4000	4.8583E+11	1.1505E+14	5.7705E+13
43	1.49E+12	5.95E+14	3.91E+14		4500	6.2013E+11	7.2108E+13	3.5418E+13
44	1.49E+12	5.23E+14	3.38E+14		5000	7.9707E+11	4.1738E+13	2.0074E+13
45	1.57E+12	4.39E+14	2.81E+14		5500	1.0707E+12	2.5087E+13	1.1847E+13
46	1.96E+12	2.78E+14	1.75E+14		6000	1.4721E+12	1.2422E+13	5.7022E+12
47	2.41E+12	1.64E+14	1.02E+14		7000	5.4313E+12	4.2075E+12	1.8186E+12
48	2.98E+12	8.79E+13	5.38E+13		8000	1.27E+13	8.1832E+11	3.3219E+11
49	3.61E+12	4.24E+13	2.56E+13		8062.99517	4.9233E+12	1.3546E+10	5587202383
50	4.55E+12	2.03E+13	1.2E+13					
51	5.86E+12	7.4E+12	4.31E+12					
52	9.03E+12	6.24E+11	3.51E+11					
53	1.07E+13	3.79E+10	2.13E+10					
54	1.26E+13	4480000000	2640000000					
55	1.31E+13							
56	1.16E+13							
57	9.45E+12							
58	7.94E+12							
59	5.62E+12							
60	3.38E+12							
61	2.4E+12							
62	1.6E+12							
63	9.57E+11							
64	4.05E+11							
65								
66								
67								
68								
69								
70								
71								

	A	B	C	D	E	F
1	Solar Cell Type/Coverglass Thickness		0.006 in substrate			
2	Cell size LPE GaAs	2	4			
3	Item		Voc (volts)	Isc (amps)	Vmp (volts)	Imp(amps)
4	Bare Cell (28 deg c)		1.014	0 232	0 876	0 2195
5	Assembly process	10	=C4-0 01		F4 0 01	
6		0 98		=D4*B6		F4*B6
7	cell mismatch	0 99		=B7*D6		=B7*F6
8	Intensity	=K23/1353		B8*D7		B8*F7
9	UltraViolet Radiation	0 98		B9*D8		B9*F8
10	Micrometeorites	0 99		B10*D9		B10*F9
11	Charged Partical radiation					
12	Voc	0 85	=B12*C5			
13	Vmp	0 849			B11*E5	
14	Isc	0 68		B14*D10		
15	Imp	0 67				B15*F10
16						
17	Maximum operating Temperature					
18	=Operating_Temperature					
19	Voc	1 94	C12+((A18 28)* 0 00194)		E13+((A18 28)*(0 00214))	
20	Isc	0 11158		D14+((0 00011158)*(A18 28))		
21	Imp	0 11158				F15+(A18 28)*(0 00011158)
22	Thermal Cycling	0 99	=C19*B22		E19*B22	
23						
24	end of mission value		=C22	D20	E22	F21
25						

	G	H	I	J	K	L
1	Power Requirements		Solar Cell Calculations			Battery Calculations
2	Payload	101.05	Battery Charge Requirements	=N11/0.8		Eclipse Period
3	TT&C	11.22	Maximum Power Level	=Power_Required		Eclipse Power
4	Electric power system	20	Design Power Level	=1.1*(J3+J2)		DOD
5	ACS/RCS	70	Bus Voltage: Sun	=28+0.8+1.3		Number of Cells
6	Thermal Control	50	Total Current Rqd	=J4/J5		Battery Capacity
7	Wire Losses	7.05	Cells in Parallel	=(J6/F24)/COS(J25)	INT(J7)+2	Battery Charge Rate
8			Cells in Series	=(J5+0.9)/E24	INT(J8)+1	Peak Battery Voltage
9						Min Bus Voltage
10	Total Power Required	=SUM(H2:H8)				Time for Charge
11						Power For Charge
12	Eclipse Loads					
13	Electric Power System	20				
14	ACS/RCS	70				
15	Thermal Control	50				
16	Total Eclipse Power	=SUM(H13:H15)	Total Array Cells	=Parallel_Cells*Series_Cells		
17			Total Array Area	=(0.1+B2)*(0.1+C2)*J16		
18			Array Margin	Each Panel	J17/2	Width(0.5 cm each side)
19						cells only
20			Thermal Calculations			
21			Packing Factor	=(C2*B2)*Parallel_Cells*Series_Cells/(J17)	Solar Incidence	Operating Temperatures
22			Cell Absorptance	0.82	1399	=($J24*K22*COS($J25)/($J26+$J27)/0.0000000566696)^0.25
23			Cell Efficiency (eol)	=J4*10000/(K22*7.97*Parallel_Cells*Series_Cells) (1.25 28)*0.00033	1309	=($J24*K23*COS($J25)/($J26+$J27)/0.0000000566696)^0.25
24			Cell Solar Absorptance	=J22 J21*J23		
25			Sun Incidence Angle	0.15		=L22 273.15
26			Emissivity of Front	0.78		=L23 273.15
27			Emissivity of Back	0.9		

	M	N	O
1			
2	37		
3	Eclipse_Power/0 85		
4	0 6		
5	(15+1 1)/(1 1+1)	16	
6	M3*M2/M4/60/N5/0 9	12	
7	=N6/7		
8	=1 5*(N5)		
9	=N5*1 1		
10	Q14*M2/60/N6*7*1 1		
11	M8*M7	=INT(M11)+1	
12			
13			
14			
15			
16			
17			
18	M19+0 05	length(0.5 cm ea)	=O19+0 05
19	Series_Cells*0 021/2		=INT(K7)*0 04)
20			
21	Eclipse Temperatures		
22	L22*(1+3*$M$18*$O$18*($J$26+$J$27)*0.00000005669*L22^3*$M$2*60/$K$91)^(1/3)		
23	L23*(1+3*$M$18*$O$18*($J$26+$J$27)*0.00000005669*L23^3*$M$2*60/$K$91)^(1/3)		
24			
25	M22 273 15		
26	M23 273 15		
27			

solar cells

	A	B	C	D	E	F	G
28							electrons on
29	Front Shield Radiation Parameters	Altitude (nm)	Eccentric An	Time in min	Delta T	electrons	orbit
30	Solar Cell Radiation Calculations					20 mil	
31		150	0			92800000000	=$E32*F32/$E$69
32		250	0			144000000000	=$E33*F33/$E$69
33		300	0			174000000000	=$E34*F34/$E$69
34		450	0			288000000000	0
35		600	0			473000000000	=$E35*F35/$E$69
36		800	=ACOS((1-(B36+3443.93)/$O$35)/$O$34)	=(C36-$O$34*SIN(C36))/(60*(62752/$O$35^3)^0.5)	=D36	968000000000	=$E36*F36/$E$69
37		1000	=ACOS((1-(B37+3443.93)/$O$35)/$O$34)	=(C37-$O$34*SIN(C37))/(60*(62752/$O$35^3)^0.5)	=D37-D36	1960000000000	=$E37*F37/$E$69
38		1250	=ACOS((1-(B38+3443.93)/$O$35)/$O$34)	=(C38-$O$34*SIN(C38))/(60*(62752/$O$35^3)^0.5)	=D38-D37	3740000000000	=$E38*F38/$E$69
39		1500	=ACOS((1-(B39+3443.93)/$O$35)/$O$34)	=(C39-$O$34*SIN(C39))/(60*(62752/$O$35^3)^0.5)	=D39-D38	5160000000000	=$E39*F39/$E$69
40		1750	=ACOS((1-(B40+3443.93)/$O$35)/$O$34)	=(C40-$O$34*SIN(C40))/(60*(62752/$O$35^3)^0.5)	=D40-D39	5890000000000	=$E40*F40/$E$69
41		2000	=ACOS((1-(B41+3443.93)/$O$35)/$O$34)	=(C41-$O$34*SIN(C41))/(60*(62752/$O$35^3)^0.5)	=D41-D40	6020000000000	=$E41*F41/$E$69
42		2250	=ACOS((1-(B42+3443.93)/$O$35)/$O$34)	=(C42-$O$34*SIN(C42))/(60*(62752/$O$35^3)^0.5)	=D42-D41	5870000000000	=$E42*F42/$E$69
43		2500	=ACOS((1-(B43+3443.93)/$O$35)/$O$34)	=(C43-$O$34*SIN(C43))/(60*(62752/$O$35^3)^0.5)	=D43-D42	5790000000000	=$E43*F43/$E$69
44		2750	=ACOS((1-(B44+3443.93)/$O$35)/$O$34)	=(C44-$O$34*SIN(C44))/(60*(62752/$O$35^3)^0.5)	=D44-D43	5680000000000	=$E44*F44/$E$69
45		3000	=ACOS((1-(B45+3443.93)/$O$35)/$O$34)	=(C45-$O$34*SIN(C45))/(60*(62752/$O$35^3)^0.5)	=D45-D44	5670000000000	=$E45*F45/$E$69
46		3500	=ACOS((1-(B46+3443.93)/$O$35)/$O$34)	=(C46-$O$34*SIN(C46))/(60*(62752/$O$35^3)^0.5)	=D46-D45	6140000000000	=$E46*F46/$E$69
47		4000	=ACOS((1-(B47+3443.93)/$O$35)/$O$34)	=(C47-$O$34*SIN(C47))/(60*(62752/$O$35^3)^0.5)	=D47-D46	7050000000000	=$E47*F47/$E$69
48		4500	=ACOS((1-(B48+3443.93)/$O$35)/$O$34)	=(C48-$O$34*SIN(C48))/(60*(62752/$O$35^3)^0.5)	=D48-D47	8460000000000	=$E48*F48/$E$69
49		5000	=ACOS((1-(B49+3443.93)/$O$35)/$O$34)	=(C49-$O$34*SIN(C49))/(60*(62752/$O$35^3)^0.5)	=D49-D48	10100000000000	=$E49*F49/$E$69
50		5500	=ACOS((1-(B50+3443.93)/$O$35)/$O$34)	=(C50-$O$34*SIN(C50))/(60*(62752/$O$35^3)^0.5)	=D50-D49	12400000000000	=$E50*F50/$E$69
51		6000	=ACOS((1-(B51+3443.93)/$O$35)/$O$34)	=(C51-$O$34*SIN(C51))/(60*(62752/$O$35^3)^0.5)	=D51-D50	15300000000000	=$E51*F51/$E$69
52		7000	=ACOS((1-(B52+3443.93)/$O$35)/$O$34)	=(C52-$O$34*SIN(C52))/(60*(62752/$O$35^3)^0.5)	=D52-D51	22500000000000	=$E52*F52/$E$69
53		8000	=ACOS((1-(B53+3443.93)/$O$35)/$O$34)	=(C53-$O$34*SIN(C53))/(60*(62752/$O$35^3)^0.5)	=D53-D52	26800000000000	=$E53*F53/$E$69
54		=B65-0.001	=ACOS((1-(B54+3443.93)/$O$35)/$O$34)	=(C54-$O$34*SIN(C54))/(60*(62752/$O$35^3)^0.5)	=D54-D53	32200000000000	=$E54*F54/$E$69
55		10000	0	=(C55-$O$34*SIN(C55))/(60*(62752/$O$35^3)^0.5)	0	35100000000000	=$E55*F55/$E$69
56		11000	0	=(C56-$O$34*SIN(C56))/(60*(62752/$O$35^3)^0.5)	=D56-D55	32600000000000	=$E56*F56/$E$69
57		12000	0	=(C57-$O$34*SIN(C57))/(60*(62752/$O$35^3)^0.5)	=D57-D56	27800000000000	=$E57*F57/$E$69
58		13000	0	=(C58-$O$34*SIN(C58))/(60*(62752/$O$35^3)^0.5)	=D58-D57	24200000000000	=$E58*F58/$E$69
59		14000	0	=(C59-$O$34*SIN(C59))/(60*(62752/$O$35^3)^0.5)	=D59-D58	18000000000000	=$E59*F59/$E$69
60		15000	0	=(C60-$O$34*SIN(C60))/(60*(62752/$O$35^3)^0.5)	=D60-D59	11700000000000	=$E60*F60/$E$69
61		16000	0	=(C61-$O$34*SIN(C61))/(60*(62752/$O$35^3)^0.5)	=D61-D60	8930000000000	=$E61*F61/$E$69
62		17000	0	=(C62-$O$34*SIN(C62))/(60*(62752/$O$35^3)^0.5)	=D62-D61	6190000000000	=$E62*F62/$E$69
63		18000	0	=(C63-$O$34*SIN(C63))/(60*(62752/$O$35^3)^0.5)	=D63-D62	4150000000000	=$E63*F63/$E$69
64		19326	0	=(C64-$O$34*SIN(C64))/(60*(62752/$O$35^3)^0.5)	=D64-D63	2130000000000	=$E64*F64/$E$69
65		=O32	0	=(C65-$O$34*SIN(C65))/(60*(62752/$O$35^3)^0.5)	=D65-D64		=$E65*F65/$E$69
66							
67							
68	Total Received radiation per year						=SUM(G30:G65)
69	Total Time for Half period				=SUM(E36:E65)		
70	number of years on orbit	3					
71	Total Radiation Received in Front						=$B$70*G68*1.5

	H	I	J	K	L
28	protons				
29	20 mil Voc/Pmax	protons on			
30		orbit	20 mil Isc	protons on orbit	
31	493000000000	=$E31*H31/$E$69	349000000000	=$E31*J31/$E$69	
32	1800000000000	=$E32*H32/$E$69	1330000000000	=$E32*J32/$E$69	
33	3270000000000	=$E33*H33/$E$69	2470000000000	=$E33*J33/$E$69	
34	10900000000000	=$E34*H34/$E$69	8330000000000	=$E34*J34/$E$69	
35	29100000000000	=$E35*H35/$E$69	22000000000000	=$E35*J35/$E$69	
36	99300000000000	=$E36*H36/$E$69	73900000000000	=$E36*J36/$E$69	
37	263000000000000	=$E37*H37/$E$69	188000000000000	=$E37*J37/$E$69	
38	654000000000000	=$E38*H38/$E$69	434000000000000	=$E38*J38/$E$69	
39	1410000000000000	=$E39*H39/$E$69	869000000000000	=$E39*J39/$E$69	
40	2560000000000000	=$E40*H40/$E$69	1490000000000000	=$E40*J40/$E$69	
41	3640000000000000	=$E41*H41/$E$69	2030000000000000	=$E41*J41/$E$69	
42	4410000000000000	=$E42*H42/$E$69	2360000000000000	=$E42*J42/$E$69	
43	4780000000000000	=$E43*H43/$E$69	2490000000000000	=$E43*J43/$E$69	
44	4790000000000000	=$E44*H44/$E$69	2430000000000000	=$E44*J44/$E$69	
45	4410000000000000	=$E45*H45/$E$69	2190000000000000	=$E45*J45/$E$69	
46	3180000000000000	=$E46*H46/$E$69	1550000000000000	=$E46*J46/$E$69	
47	2070000000000000	=$E47*H47/$E$69	991000000000000	=$E47*J47/$E$69	
48	1250000000000000	=$E48*H48/$E$69	585000000000000	=$E48*J48/$E$69	
49	686000000000000	=$E49*H49/$E$69	314000000000000	=$E49*J49/$E$69	
50	384000000000000	=$E50*H50/$E$69	173000000000000	=$E50*J50/$E$69	
51	175000000000000	=$E51*H51/$E$69	76700000000000	=$E51*J51/$E$69	
52	24900000000000	=$E52*H52/$E$69	10300000000000	=$E52*J52/$E$69	
53	2570000000000	=$E53*H53/$E$69	1000000000000	=$E53*J53/$E$69	
54	131000000000	=$E54*H54/$E$69	50800000000	=$E54*J54/$E$69	
55	0.00183	=$E55*H55/$E$69	0	=$E55*J55/$E$69	
56	0.00183	=$E56*H56/$E$69	0	=$E56*J56/$E$69	
57	0	=$E57*H57/$E$69	0	=$E57*J57/$E$69	
58	0	=$E58*H58/$E$69	0	=$E58*J58/$E$69	
59	0	=$E59*H59/$E$69	0	=$E59*J59/$E$69	
60	0	=$E60*H60/$E$69	0	=$E60*J60/$E$69	
61	0	=$E61*H61/$E$69	0	=$E61*J61/$E$69	
62	0	=$E62*H62/$E$69	0	=$E62*J62/$E$69	
63	0	=$E63*H63/$E$69	0	=$E63*J63/$E$69	
64	0	=$E64*H64/$E$69	0	=$E64*J64/$E$69	
65					
66					
67					
68		SUM(I31:I65)		SUM(K31:K65)	
69					
70					
71		$B$70*I68*1.5		$B$70*K68*1.5	

	M	N	O	P	Q	R
28				Back Shield Radiation Parameters		
29				Altitude (nm) 30 mil thick	Electons	p Vec& pons
30		Orbit Calculations		150	71700000000	349000000000
31		Perigee Altitude	650	250	111000000000	1350000000000
32		Apogee Altitude	=2*O35 2*3443 93 O31	300	133000000000	2510000000000
33		Period	4 8	450	217000000000	8530000000000
34		Eccentricity	(O32 O31)/(3443 93*2+O32+O31)	600	349000000000	22700000000000
35		Semi Major Axis	=(62752*(O33*3600)^2/(4*PI()^2))^(1/3)	800	688000000000	77000000000000
36				1000	1360000000000	196000000000000
37				1250	2580000000000	448000000000000
38				1500	3530000000000	885000000000000
39				1750	3940000000000	1490000000000000
40				2000	3900000000000	1970000000000000
41				2250	3690000000000	2210000000000000
42				2500	3590000000000	2240000000000000
43				2750	3530000000000	2120000000000000
44				3000	3610000000000	1870000000000000
45				3500	4210000000000	1280000000000000
46				4000	5040000000000	793000000000000
47				4500	6160000000000	450000000000000
48				5000	7450000000000	233000000000000
49				5500	9280000000000	124000000000000
50				6000	11600000000000	52000000000000
51				7000	17400000000000	6010000000000
52				8000	20800000000000	497000000000
53				9000	24900000000000	26100000000
54				10000	26800000000000	0
55				11000	24500000000000	0
56				12000	20700000000000	0
57				13000	17800000000000	0
58				14000	13100000000000	0
59				15000	8250000000000	0
60				16000	6190000000000	0
61				17000	4390000000000	0
62				18000	2850000000000	0
63				19326	1340000000000	0
64						
65						
66						
67						
68						
69						
70						
71						

	S	T	U	V
28				
29	protons Isc	Electrons on orbit	Voc	Isc
30				
31	27800000000000	=$E31*Q31/$E$69	=$E31*R31/$E$69	=$E31*S31/$E$69
32	11000000000000	=$E32*Q32/$E$69	=$E32*R32/$E$69	=$E32*S32/$E$69
33	20800000000000	=$E33*Q33/$E$69	=$E33*R33/$E$69	=$E33*S33/$E$69
34	70600000000000	=$E34*Q34/$E$69	=$E34*R34/$E$69	=$E34*S34/$E$69
35	186000000000000	=$E35*Q35/$E$69	=$E35*R35/$E$69	=$E35*S35/$E$69
36	616000000000000	=$E36*Q36/$E$69	=$E36*R36/$E$69	=$E36*S36/$E$69
37	1510000000000000	=$E37*Q37/$E$69	=$E37*R37/$E$69	=$E37*S37/$E$69
38	3260000000000000	=$E38*Q38/$E$69	=$E38*R38/$E$69	=$E38*S38/$E$69
39	6030000000000000	=$E39*Q39/$E$69	=$E39*R39/$E$69	=$E39*S39/$E$69
40	9580000000000000	=$E40*Q40/$E$69	=$E40*R40/$E$69	=$E40*S40/$E$69
41	12200000000000000	=$E41*Q41/$E$69	=$E41*R41/$E$69	=$E41*S41/$E$69
42	13300000000000000	=$E42*Q42/$E$69	=$E42*R42/$E$69	=$E42*S42/$E$69
43	13200000000000000	=$E43*Q43/$E$69	=$E43*R43/$E$69	=$E43*S43/$E$69
44	12300000000000000	=$E44*Q44/$E$69	=$E44*R44/$E$69	=$E44*S44/$E$69
45	10700000000000000	=$E45*Q45/$E$69	=$E45*R45/$E$69	=$E45*S45/$E$69
46	7260000000000000	=$E46*Q46/$E$69	=$E46*R46/$E$69	=$E46*S46/$E$69
47	4450000000000000	=$E47*Q47/$E$69	=$E47*R47/$E$69	=$E47*S47/$E$69
48	2500000000000000	=$E48*Q48/$E$69	=$E48*R48/$E$69	=$E48*S48/$E$69
49	1280000000000000	=$E49*Q49/$E$69	=$E49*R49/$E$69	=$E49*S49/$E$69
50	669000000000000	=$E50*Q50/$E$69	=$E50*R50/$E$69	=$E50*S50/$E$69
51	275000000000000	=$E51*Q51/$E$69	=$E51*R51/$E$69	=$E51*S51/$E$69
52	30600000000000	=$E52*Q52/$E$69	=$E52*R52/$E$69	=$E52*S52/$E$69
53	245000000000	=$E53*Q53/$E$69	=$E53*R53/$E$69	=$E53*S53/$E$69
54	14000000000	=$E54*Q54/$E$69	=$E54*R54/$E$69	=$E54*S54/$E$69
55	0	=$E55*Q55/$E$69	=$E55*R55/$E$69	=$E55*S55/$E$69
56	0	=$E56*Q56/$E$69	=$E56*R56/$E$69	=$E56*S56/$E$69
57	0	=$E57*Q57/$E$69	=$E57*R57/$E$69	=$E57*S57/$E$69
58	0	=$E58*Q58/$E$69	=$E58*R58/$E$69	=$E58*S58/$E$69
59	0	=$E59*Q59/$E$69	=$E59*R59/$E$69	=$E59*S59/$E$69
60	0	=$E60*Q60/$E$69	=$E60*R60/$E$69	=$E60*S60/$E$69
61	0	=$E61*Q61/$E$69	=$E61*R61/$E$69	=$E61*S61/$E$69
62	0	=$E62*Q62/$E$69	=$E62*R62/$E$69	=$E62*S62/$E$69
63	0	=$E63*Q63/$E$69	=$E63*R63/$E$69	=$E63*S63/$E$69
64	0	=$E64*Q64/$E$69	=$E64*R64/$E$69	=$E64*S64/$E$69
65				
66				
67	Total Received per year	=SUM(T31:T64)	=SUM(U31:U64)	=SUM(V31:V64)
68	EOL Total Back	=$B$70*T67	=$B$70*U67	=$B$70*V67
69				
70	EOL Total Front	=G71	=I71	=K71
71	Total Radiation Received		=U70+T70+U68+T68	=V70+T70+V68+T68

4. LIFE CYCLE DESIGN SPREADSHEET

This spreadsheet is similar in nature to the previous spreadsheet, but it is designed for use in determining the satellite parameters throughout the life of the satellite and determining when the end of life will occur. The inputs into the spreadsheet are the radiation degradation amounts at various periods of performance, usually done on a three month time basis, and the resulting degradation from UV and micrometeorites. A macro was written to automatically calculate the power, voltage, current, temperature, eclipse temperature and max power.

BOL values End

	I	J	K	L	M	N	O
1	**Solar Cell Calculations**						
2	**Maximum Bus Voltage**	36.40		Eclipse Period	37.00		
3	**Maximum Current Level**	13.14					
4	**Maximum Power Level**	401.02					
5	**Power at Bus Voltage**	378.50					
6	**Max Dissipated Power**	308.50					
7	**Cells in Parallel**		80.00				
8	**Cells in Series**		44.00				
9							
10							
11							
12							
13							
14							
15							
16	**Total Array Cells**	3520.00					
17	**Total Array Area**	30307.20					
18	**Array Margin**	**Each Panel**	15153.60	**Width(0.5 cm eac**	0.51	**length(0.5 cr**	3.33
19				**cells only**	0.46		3.28
20	**Thermal Calculations**						
21	**Packing Factor**	0.93	**Solar Incidence**	**Operating Tempe**	**Eclipse Temperatures**		
22	**Cell Absorptance**	0.82	1309.00	315.44	155.49		
23	**Cell Efficiency**	0.098					
24	**Cell Solar Absorptance**	0.729					
25	**Sun Incidence Angle**	0.15		42.29	-117.66		
26	**Emissivity of Front**	0.78					
27	**Emissivity of Back**	0.90					
28							

	A	B	C	D	E	F	G	H	I
35	Solar Flux	Radiation Parameters							
36	launch Jul 4	Isc	Imp	Voc	Vmp	Date	Max Voltage	Max Current	Max Power
37	1309.00	1.00	1.00	1.00	1.00	Jul-89	36.69	16.58	608.40
38	1345.00	0.93	0.93	0.94	0.97	Sep-89	35.06	15.45	541.76
39	1399.00	0.90	0.90	0.92	0.95	Dec-89	34.02	15.54	528.58
40	1311.00	0.88	0.88	0.91	0.94	Mar-89	34.13	14.18	483.93
41	1309.00	0.86	0.87	0.90	0.93	Jul-89	33.79	13.95	471.47
42	1345.00	0.85	0.85	0.89	0.92	Sep-89	33.26	14.02	466.43
43	1399.00	0.83	0.83	0.89	0.92	Dec-89	32.80	14.35	470.66
44	1311.00	0.82	0.82	0.88	0.91	Mar-89	33.02	13.26	437.79
45	1309.00	0.81	0.81	0.87	0.91	Jul-89	32.94	13.00	428.20
46	1345.00	0.80	0.80	0.87	0.91	Sep-89	32.64	13.21	431.05
47	1399.00	0.79	0.78	0.87	0.90	Dec-89	32.18	13.50	434.43
48	1311.00	0.78	0.78	0.86	0.90	Mar-89	32.40	12.54	406.41
49	1309.00	0.77	0.77	0.86	0.89	Jul-89	32.29	12.41	400.76
50									
51						Paste Zone	29.86	11.41	340.82
52	1345.00	0.76	0.77	0.86	0.89	Sep-89	32.02	12.72	407.27
53	1399.00	0.75	0.76	0.85	0.89	Dec-89	31.56	13.16	415.43
54	1311.00	0.74	0.75	0.85	0.88	Mar-89	31.60	12.15	383.84
55	1309.00	0.73	0.74	0.84	0.87	Jul-89	31.41	11.97	375.93
56	1345.00	0.72	0.73	0.83	0.86	Sep-89	30.84	12.15	374.64
57	1399.00	0.71	0.72	0.82	0.85	Dec-89	30.19	12.49	376.89
58	1311.00	0.71	0.71	0.82	0.84	Mar-89	30.24	11.51	348.04
59	1309.00	0.70	0.71	0.81	0.83	Jul-89	29.86	11.41	340.82

	J	K	L	M	N
35					
36	Op Temp	Eclipse Temp	Operating Power	INTENSITY	Min Operatin
37	312.22	155.30	490.5628068	0.97	464.280667
38	315.50	155.49	453.3932526	0.99	432.60864
39	318.63	155.68	457.0591039	1.03	435.061173
40	314.44	155.43	418.0571497	0.97	397.056718
41	314.60	155.44	408.0000406	0.97	390.676017
42	316.62	155.56	414.7706648	0.99	392.63147
43	319.58	155.73	424.4209161	1.03	401.801643
44	315.18	155.48	392.1727078	0.97	371.231547
45	315.20	155.48	386.8537581	0.97	363.960832
46	317.25	155.60	393.0441187	0.99	369.783559
47	320.17	155.76	404.3348075	1.03	378.020133
48	315.74	155.51	372.4055271	0.97	351.191624
49	315.74	155.51	368.0563735	0.97	347.526683
50					
51	316.66	155.56			
52	317.80	155.63	373.73	0.99	356.119058
53	320.75	155.80	384.25	1.03	368.594237
54	316.24	155.54	354.52	0.97	340.106614
55	316.27	155.54	349.26	0.97	335.121707
56	318.35	155.66	354.42	0.99	340.153445
57	321.30	155.83	365.16	1.03	349.589392
58	316.71	155.57	338.05	0.97	322.284412
59	316.66	155.56	335.16	0.97	319.548857

BOL values End

	A	B	C	D	E	F
1	**Solar Cell Type/Coverglass Thickness**		0.006 in substrate			
2	**Cell size LPE GaAs**	2.00	4.00			
3	**Item**		**Voc (volts)**	**Isc (amps)**	**Vmp (volts)**	**Imp(amps)**
4	**Bare Cell (28 deg c)**		1.01	0.23	0.88	0.22
5	**Assembly process**	-10.00	1.00		0.87	
6		0.98		0.23		0.22
7	**cell mismatch**	0.99		0.23		0.21
8	**Intensity**	0.97		0.22		0.21
9	**UltraViolet Radiation**	0.98		0.21		0.20
10	**Micrometeorites**	0.99		0.21		0.20
11	**Charged Partical radiation**					
12	**Voc**	0.86	0.86			
13	**Vmp**	0.89			0.77	
14	**Isc**	0.77		0.16		
15	**Imp**	0.77				0.15
16						
17	**Maximum operating Temperature**					
18	42.29					
19	**Voc**	-1.94	0.84		0.74	
20	**Isc**	0.11		0.16		
21	**Imp**	0.11				0.16
22	**Thermal Cycling**	0.99	0.83		0.73	
23						
24	**end of mission value**		0.83	0.16	0.73	0.16

5. GRAPHS OF LIFE CYCLE VARIATIONS

The following graphs of array performance are included:

- Voltage and Current vs. Time on Orbit.
- Power vs. Time on Orbit.
- Max Power vs. Time on Orbit.
- Maximum Temperatures vs. Time on Orbit.

Voltage and current limit graph is a five year plot of array voltage and maximum power current levels. The voltage and current limit line on the graph is at 12.25 amps and 30.9 volts, the levels when the maximum designed power cannot be attained and the level at which the bus voltage will not be able to stay in regulation. The minimum value of current occurring at Jul95 still provides a power level of 323 watts at bus voltage. This amount is still above the required power of the satellite. As such, the satellite is expected to be able to function until the time when the bus can no longer stay in regulation, approximately Sep95.

The power levels for time on orbit contains two curves. the top curve is the power available at bus voltage and short circuit current levels. The bottom curve is the power available at bus voltage and maximum power current levels. The actual available power will fall between the two curves, with the BOL power being closer to the top curve and the EOL power being near the bottom curve. Of note is that the power limit is not crossed until Mar96; while in the previous graph, the satellite was unable to maintain the individual voltage and current constraints earlier in life.

The maximum power curve displays the maximum power available from the satellite at maximum power voltage and maximum power current. These values are higher then the expected values throughout the life of the satellite because the actual levels are below the maximum values available.

The temperature graph illustrates the effect of the varying solar flux on the temperature of the array. The radiation degradation results in less efficient electric power production allowing more of the available solar flux to be turned into heat. The temperature effects of the cells are such that when the temperature rises, the voltage decreases and the current increases.

Voltage and Current vs. Time on Orbit

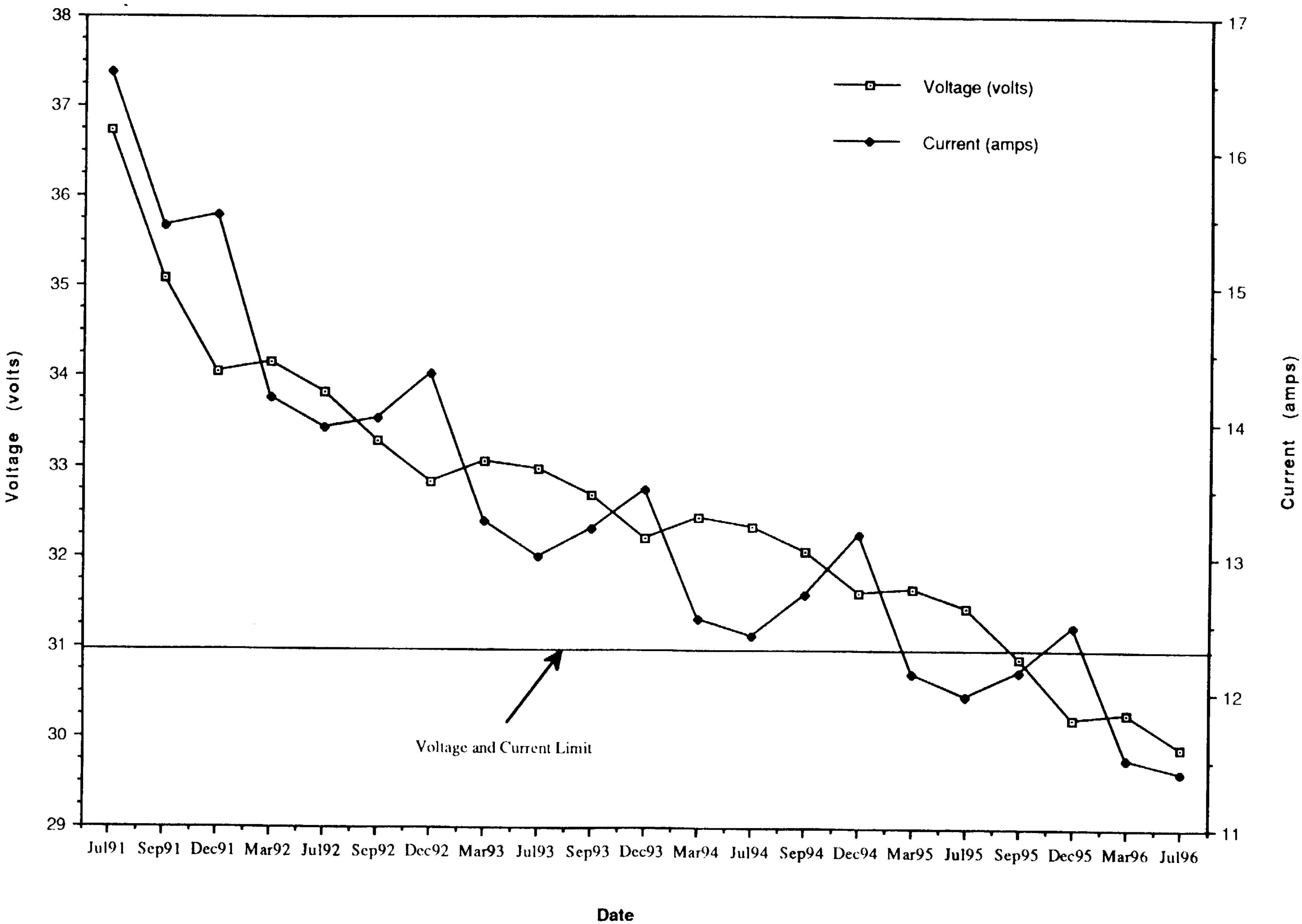

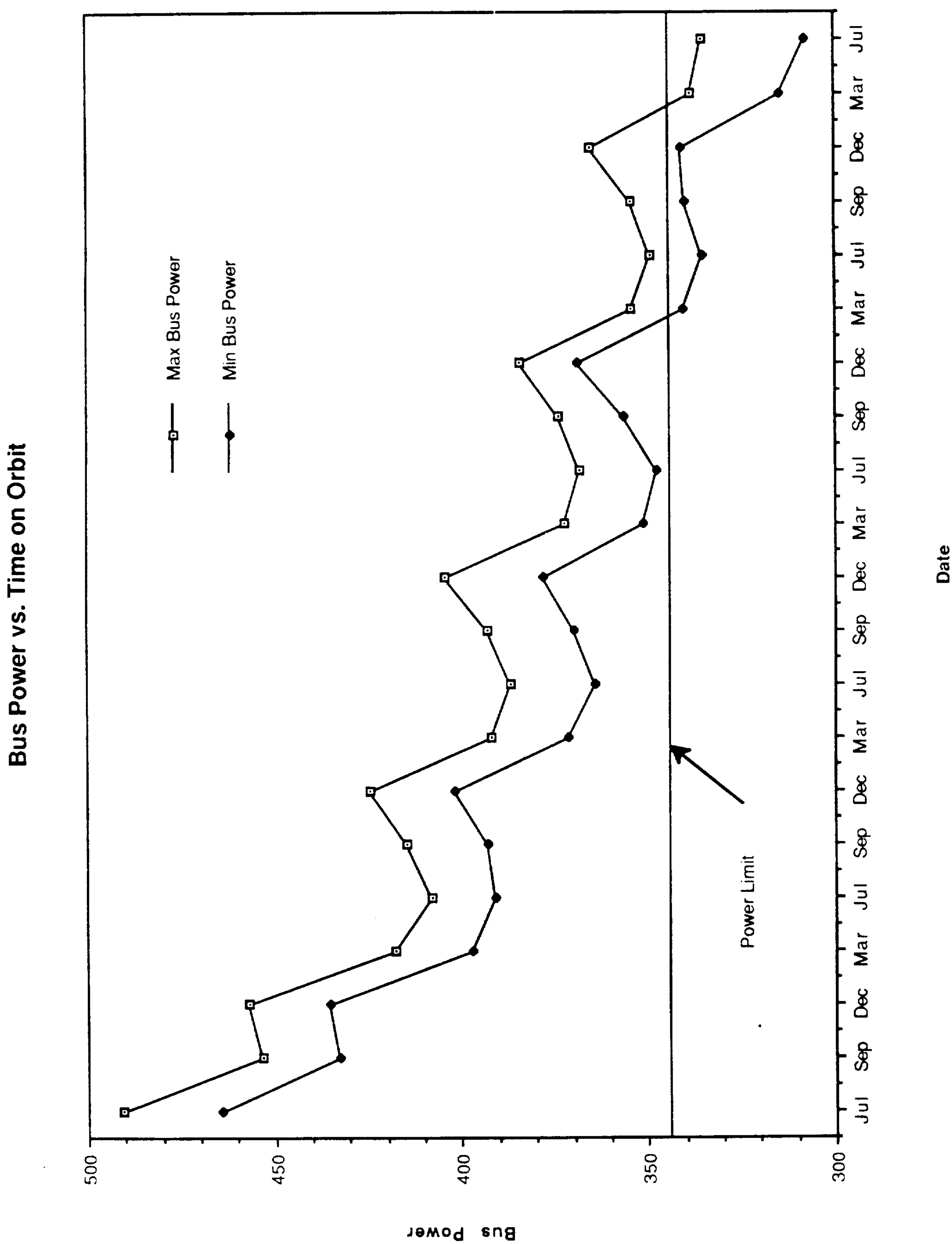
Bus Power vs. Time on Orbit
Max Bus Power
Min Bus Power
Power Limit
Bus Power
500
450
400
350
300
Jul
Sep
Dec
Mar
Jul
Sep
Dec
Mar
Jul
Sep
Dec
Mar
Jul
Sep
Dec
Mar
Jul
Sep
Dec
Mar
Jul
Date

Maximum Power vs. Time on Orbit

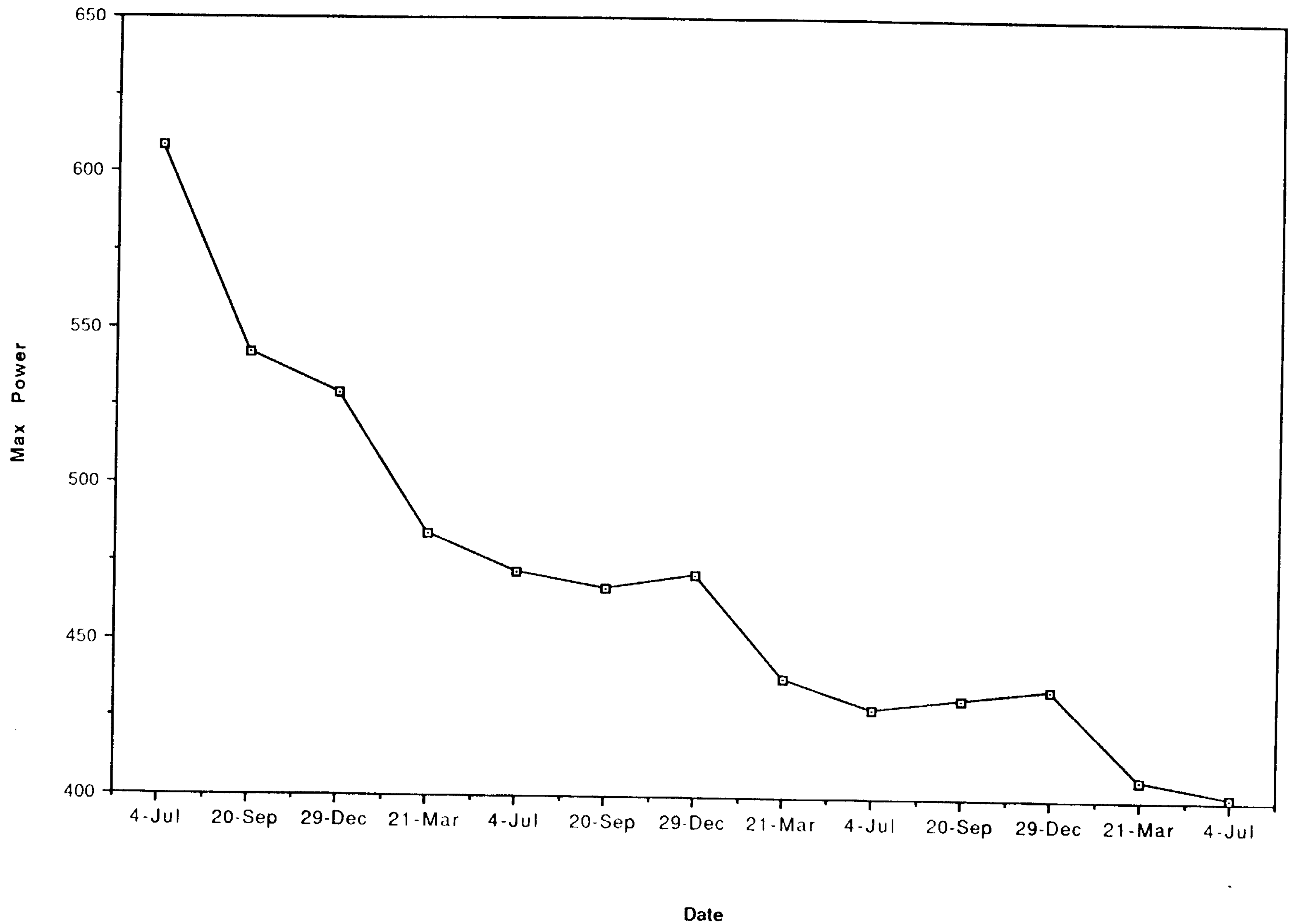

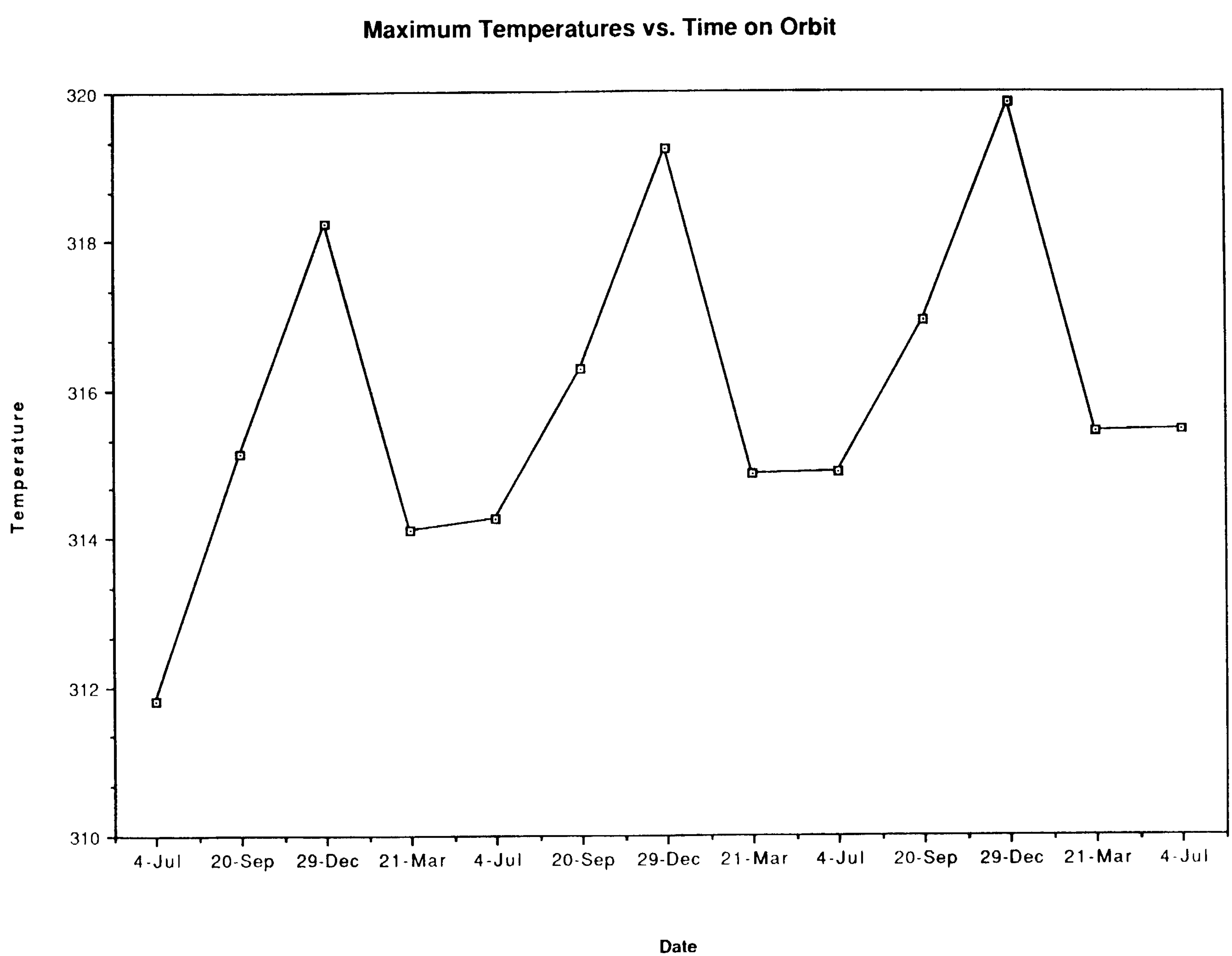
Maximum Temperatures vs. Time on Orbit
320
318
316
314
312
310
Temperature
4-Jul
20-Sep
29-Dec
21-Mar
4-Jul
20-Sep
29-Dec
21-Mar
4-Jul
20-Sep
29-Dec
21-Mar
4-Jul
Date

APPENDIX F

A. ACTUATOR CALCULATIONS

The ADCS consists of 3 fixed reaction wheels mounted orthogonal to each other with a fourth wheel skewed at 45 ° to the other three for redundancy. The fourth wheel will only be used in case of a wheel failure. Twelve thrusters are mounted for station keeping and wheel desaturation.

Analysis of the satellite is done for worst case scenario, which is the BOL with arrays extended. The moments of inertia and center of mass offset are listed in Table F-1. Figure F-1, a,b show the satellites orbit and orientation for solar array pointing. Annex F-1 contains the specification sheet for the reaction wheels.

Desaturation Thrusters- specification sheet is attached

Moment Arm

1.151 m for yaw desat thrusters

1.203 m for pitch/roll desat thrusters

Pulse Time

.025 sec

Thruster Torque

$M_z = F \bullet R$

$M_z = (4.0005\ N)(2 \bullet 1.151\ m)$

$M_z = 9.209\ Nm$

Reaction Wheels

$H_W = 1.4$ ft -lb-sec

$H_W = 1.904$ N-m-sec

TABLE F-1. LIFETIME SUMMARY

ITEM	MASS (kg)	CENTER OF MASS (cm)			TOTAL MOMENT OF INERTIA (kg-m^2)					
		Cx	Cy	Cz	Ixx	Iyy	Izz	Ixy	Ixz	Iyz
SEPARATION, SOLAR ARRAY FOLDED	411.917	3.397	-0.632	35.911	122.673	96.858	195.807	-0.832	1.007	0.291
SEPARATION, SOLAR ARRAY EXTENDED	411.917	3.397	-0.632	35.911	153.173	275.074	377.224	-0.832	1.007	0.291
50% PROPELLANT REMAINING	339.505	4.233	-0.786	36.133	118.950	263.125	333.257	-0.813	0.979	0.296
10% PROPELLANT REMAINING	281.265	5.250	-0.977	36.409	91.419	253.466	297.847	-0.789	0.944	0.302

SUMMARY OF SPACECRAFT STATISTICS

ORIGIN AT CENTER OF ANTIEARTH PANEL
POSITIVE Z DIRECTION--EARTH FACE
POSITIVE X DIRECTION --HOUSEKEEPING EQUIPMENT PANEL (EAST FACE)
POSITIVE Y DIRECTION -- (SOUTH FACE)

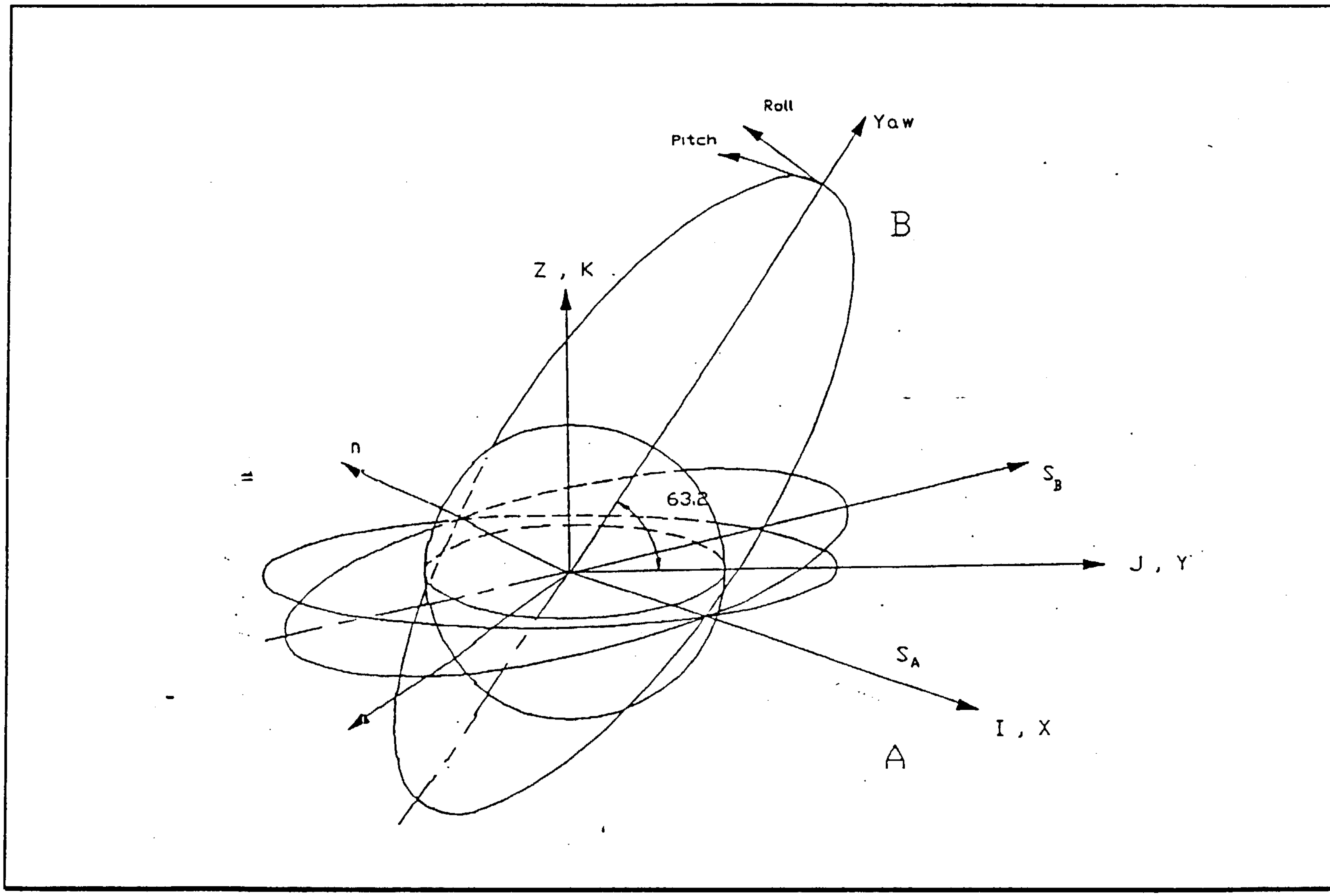

Figure F-1a. Satellite Orientation

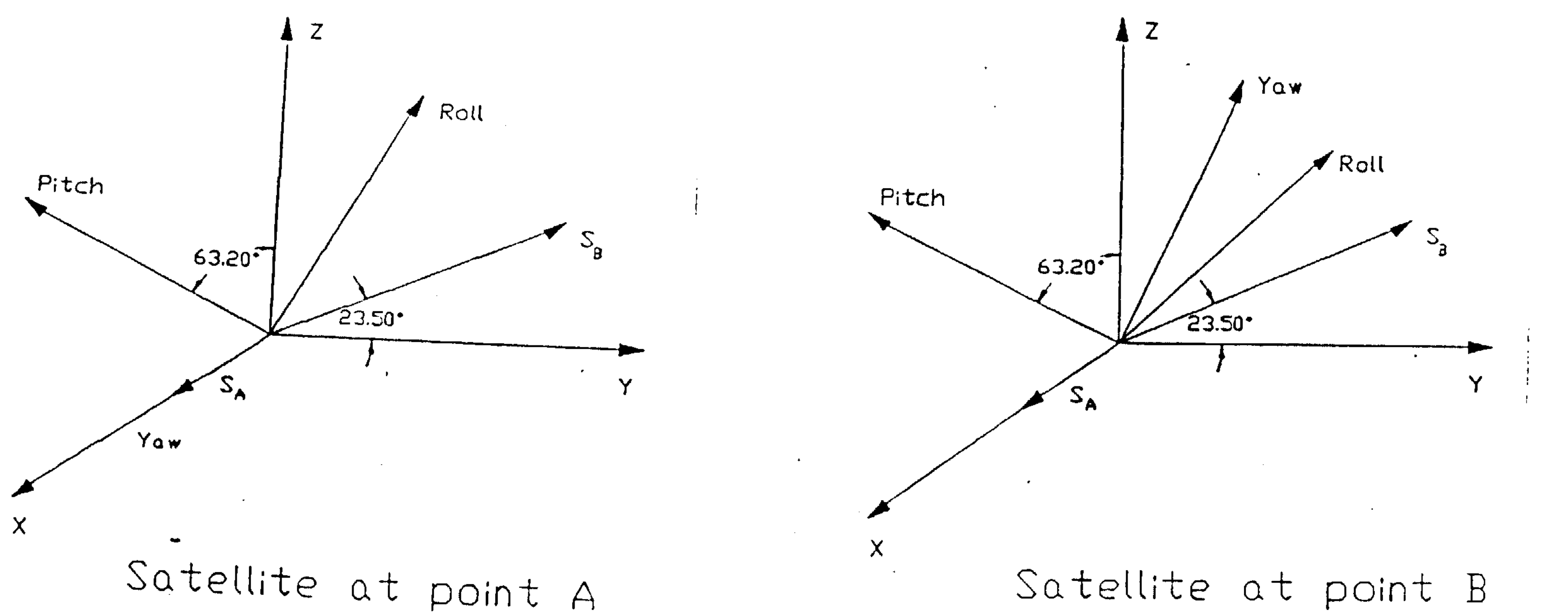

Figure F-1b. Satellite Orientation at Point A and B

Output Torque

$T_F = \pm 6.5$ oz-in

$T_F = 0.04525$ N-m

One revolution will put 4.525×10^{-2} N-m of torque on the satellite.

Desaturation Torque

Yaw

$M_z = 9.209$ N-m

Desat time $\Rightarrow \tau_d = \frac{1.904}{9.209} = 0.2068$ sec

Using pulse times of .025 sec$\Rightarrow$ #Pulses $= \frac{.2068}{.025} = 8.272 = 9$ pulses

Pitch/Roll

$M_x = M_y = 4.0005 \bullet 2 \bullet 1.203 = 9.625$ N-m

Desat time$\Rightarrow \tau_d = \frac{1.904}{9.625} = 0.1978$

#Pulses $= \frac{.1978}{.025} = 7.91 = 8$ pulses

Maximum Allowable Pointing Errors

Roll = 0.5°

Yaw = 0.3°

Pitch = 0.5°

A three axis reaction wheel system can be analyzed similar to the pitch axis of a momentum bias wheel system.

Control Parameters

$$M = H \bullet \Delta t$$

$$k = \frac{I_{zz}}{\tau^2}$$

$$\tau = \frac{\Psi max \; Izz \; e}{M_z}$$

$$\omega = \sqrt{\frac{k}{I_{zz}}}$$

$\tau_x = 2t$ lead time constant

	Yaw	Pitch	Roll
M	.230225	.2406	.2406
k	.9599	.4561	.7847
t	20.222	24.715	14.364
τ	40.444	49.430	28.728
ω	.0495	.0405	.0696

B YAW AXIS ANALYSIS -ORBIT

The yaw axis, spacecraft fixed, will rotate the solar arrays to track the sun. Rotation will be governed by the sun angle to the orbital plane ,β . Figure F-2 illustrates the cyclic nature of β over one year. Worst case analysis is for $\beta = 0$ °and $\beta = 87°$. Since the solar array tracking torque is cyclic it has no additive influence on the yaw reaction wheel. Therefore there is no desaturation requirement. Analysis is to check the wheel's ability to absorb the torque over an orbit. The satellite will rotate $\pm \beta$ degrees each orbit.

For the worst case of $\beta = 87°$, the wheel will have to store 87 ° worth of torque in 50 minutes.

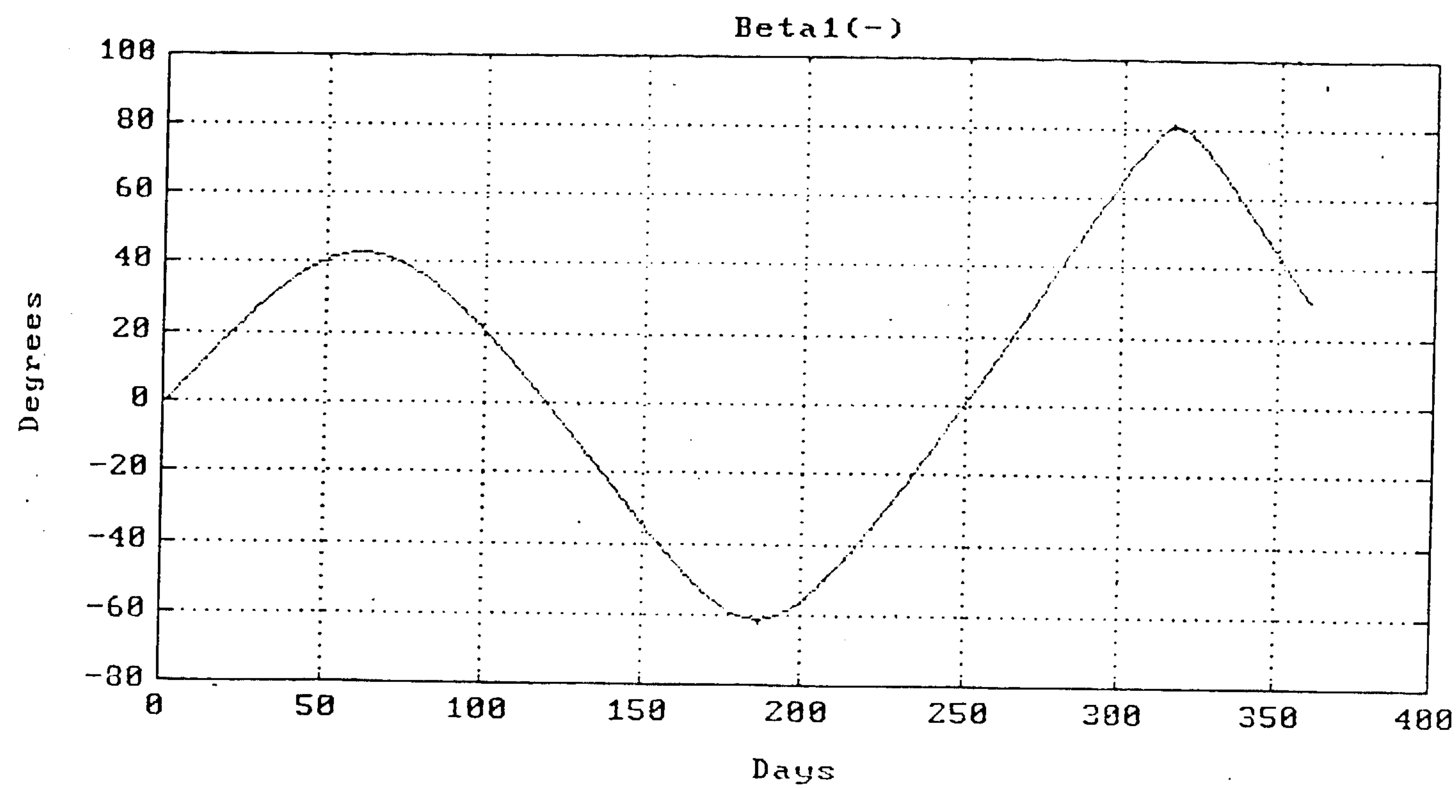

Figure F-2. Sun Line Angle Over One (1) Year

$$\omega = \frac{\pi/2}{50 \bullet 60}$$

$$h_z = I_{zz}\omega$$

$$h_z = (392.553)(\frac{\pi/2}{3000})$$

$$h_z = 0.02055 \text{ N-m-sec}$$

Since h_ω = 1.904 N-m-sec, this is within the wheel's ability to absorb. If the yaw wheel fails, the skewed wheel will control yaw rotation. For worst case:

$$h_z = \frac{h_z}{\cos 45°} = 0.291 \text{ N-m-sec}$$

A PC Matlab program that determines psi for the two extreme cases of β=0°, 87° is available upon request.

C PITCH/ROLL ORBIT ANALYSIS

The solar arrays are along the roll axis. Therefore, the pitch axis wheel will absorb the vast majority of torque. The PC Matlab program, "WheelRT.M" models the satellite's reaction wheel speed over a one year period. The program and plots for roll and pitch wheel speed is available upon request.

The program models the rotation around yaw to track the sun and solves for the torque required to keep the satellite nadir pointing. Figure F-3 shows the cyclic nature of the orbits angular velocity.

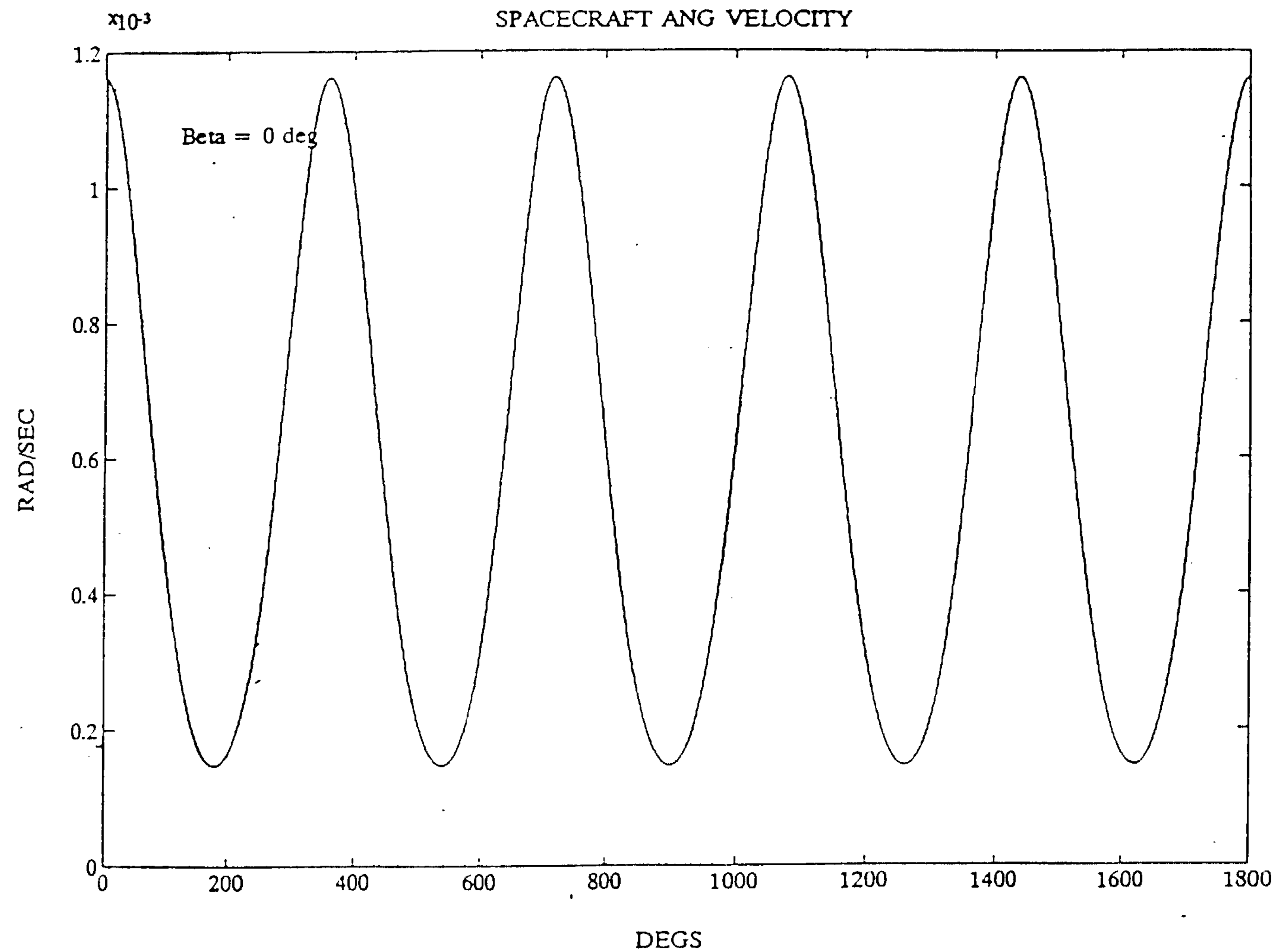

Figure F-3. Spacecraft Angular Velocity

D CONTROL LAWS

Figure F-4 illustrates a block diagram for the reaction wheels. The system will be closed loop control system with the sensors, sun for yaw and earth for roll and yaw, providing the error to the wheels to cancel out.

E. PROPELLANT ANALYSIS

The pitch and roll wheel are the only wheel requiring desaturation. From the simulation the number of desaturations is obtained. This is combined with thruster parameter, (Figure F- 5) to find mass of propellant required for desaturation.

H_ω = 1.904 Nm

Firing time for thrusters, $\tau = 0.2$ sec

Flow rate, $m = .000902$ kg/sec

Fuel mass, $M_T = \tau \bullet m = .0001814$ kg per thruster

$M_x = 2 \bullet M_T = 3.628 \times 10^{-4}$ kg per desat

Pitch Wheel Desaturations

$N = 10$

$M\rho = N \bullet M_x = 3.628 \times 10^{-3}$ kg

Roll Wheel

$M\rho = 3.628 \times 10^{-3}$ assume 10 desats

Total Propellant

$M \approx 7.5$ grams margin = 1 kg

The control law for the reaction wheels are:

$$T_y = I_{yy}\ddot{\theta} + k_y \tau_\theta \dot{\theta} + k_y \theta$$

$$T_x = I_{xx}\ddot{\phi} + k_x \tau_\phi \dot{\phi} + k_x \phi$$

$$T_z = I_{zz}\ddot{\psi} + k_z \tau_\psi \dot{\psi} + k_\psi \psi$$

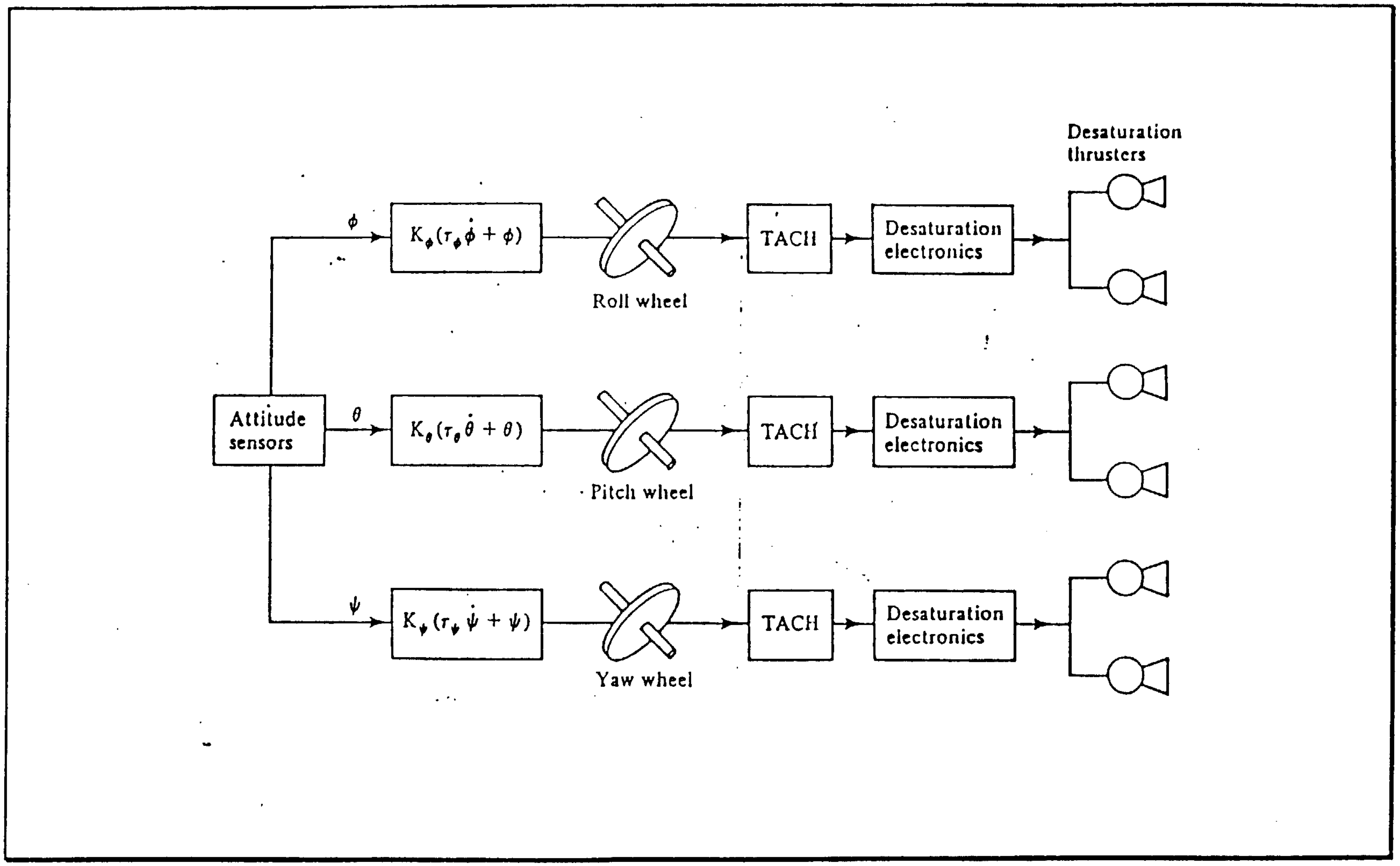

Figure F-4. Three-axis Reaction Control System

MR-111
0.45-lbf ENGINE

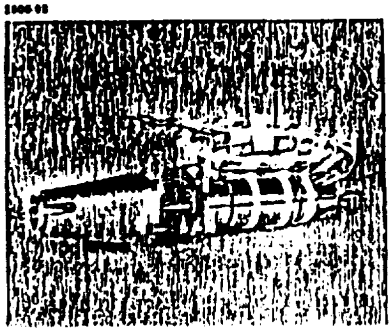

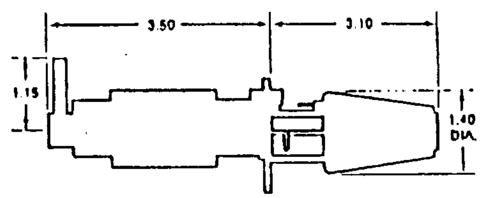

Design Characteristics

Propellant	Hydrazine
Catalyst	Shell 405
Thrust, Steady State (lbf)	0.45—0.20
Feed Pressure (psia)	320—120
Chamber Pressure (psia)	184—84
Expansion Ratio	200:1
Flow Rate (lbm/sec)	0.002—0.0009
Valve	Wright Components Dual Seat Bifilar
Valve Power	12 Watts/Coil @ 42 vdc and 40 °F
Weight (lbm)	0.704
Engine	0.259
Valve	0.445

Demonstrated Performance

Specific Impulse (lbf-sec/lbm)	223—215
Total Impulse (lbf-sec)	58,500
Total Pulses	420,000
Minimum Impulse Bit (lbf-sec)	0.016 @ 235 psia & 25 ms ON
Steady-State Firing (sec)	8,500

Flight Status

Program	Customer/User
Intelsat-V	Ford Aerospace/Intelsat

ROCKET RESEARCH COMPANY
A DIVISION OF ROCKCOR

Figure F-5. Thruster Characteristics

The satellite, in the absence of β, would use the pitch wheel exclusively for nadir pointing. The magnitude of the torque required for nadir pointing will be constant over each orbit. The reaction wheel velocity, ignoring disturbance torques, is cyclic with the orbital angular velocity. Disturbance torques result in secular torques that build up in the wheel. These secular torques are monitored by the computer which will autonomously desaturate the wheels.

F. DISTURBANCE TORQUES

The disturbance torques encountered will be solar, magnetic and internal torques. Solar radiation pressure torque was modeled using the following equations:

$$M_s = PA \begin{pmatrix} (yk_1 - zk_2 - xk_2\sin\alpha)I_o \\ (zk_1\sin\alpha - xk_1\cos\alpha)J_o \\ (-zk_2\sin\alpha + xk_2\cos\alpha)K_o \end{pmatrix}$$

Solar pressure torque was modeled and computed on a spread sheet, Annex F-4, to give the secular torque per orbit. A plot of each axis torque per degree is also attached.

The residual magnetic moment of the spacecraft interacting with the earth's magnetic field causes a torque disturbance on the spacecraft. The magnetic torque is derived from the relation

$$T_M = B \times M$$

where B is the earth's magnetic field as approximated by a simple dipole and M is the spacecraft magnetic field. From conversation with NRL, M can be approximated by

$$M = 1000i + 1000j + 1000k$$

This is an approximation for a fairly magnetic free satellite.

The earth's magnetic field can be approximated as a simple dipole. The scale potential for the simple magnetic dipole is

$$V = \frac{M_e}{r^2}\sin \theta_M$$

where : M_e = magnetic dipole strength

r = distance from earth center to the spacecraft

Θ_M = magnetic latitude of the spacecraft

The magnetic field is

$$\mathbf{B} = \text{-grad } V$$

In the spherical coordinate coordinate frame, this equation becomes:

$$\mathbf{B} = \frac{-M_e}{r^3}(2\sin\theta_M\hat{e}_r - \cos \theta_M\hat{e}_\theta)$$

In order to obtain disturbance torques in body axes, it is necessary to do several coordinate rotations. The inertial coordinate frame is the earth-centered-inertial frame (x_I, y_J,z_K,), where z_I is normal to the equator, x_I is along the vernal equinox and y_I lies in the equatorial plane. This frame is rotated by an angle, λ , measured from the vernal equinox to the prime meridian and its rate of change of the earth's rate. This is the earth-centered-geographic coordinate system. To change to the earth-centered-geomagnetic coordinates, the x_M axis is rotated an angle, Δ, in the equatorial plane and z_M is rotated an angle ε from geographic north. Finally, the vehicle centered orbital reference frame is defined such that z_o is directed toward the center of the earth, y_o is normal to the orbit plane and $x_o = y_o \times z_o$. The orbit plane is defined relative to the equatorial by an inclination, i, about the ascending node and the satellite's position is measured from the ascending node by the angle, υ. Due to lack of time and timely information, the magnetic disturbance torque was not calculated. Similarly the internal disturbance torques resulting from friction and misalignment of components were not calculated. These torques are extremely difficult to model. Most of the torque is due to the construction of the satellite. from the data base covering similar satellites it can be seen that the internal disturbance torques are small and secular.

For all the secular torques it is up to the computer to sense the wheel speed and desaturate when necessary. TT&C outputs will provide redundancy for the computer. The ground station will be able order the desaturation when necessary. The secular torque build-up will be slow, from the magnitude of the solar pressure torque and other torques.

G. SENSORS

The specification sheets for the sensors are included in this appendix. Both the sun and earth sensors are rated functionally redundant by the manufacturer. The gyros will be in standby for the entire mission except when the thrusters are fired. The use they see is well under their rated spin time.

H. TRANSFER ORBIT

The satellite will be put into transfer orbit with a maximum of 100 rpm by the Delta. Once transfer orbit is established the ADCS will begin to spin down the satellite with the thrusters. Once the satellite reaches a nominal spin rate of 5 rpm sun acquisition will commence. Upon sun acquisition the satellite will be completely spin down by the thrusters. From ephemeris data and the sun angle, the ground station will be able to command orient the satellite for earth acquisition.

With earth acquisition complete, the satellite will be in 3-axis stabilized mode. The solar arrays will then deploy . At this point the reaction wheel will take over maintaining the satellite's attitude. At the appropriate time , the gyros will spin up in preparation for insertion into its final orbit. The gyros will maintain inertial reference for the satellite during main thruster firing. The reaction wheels will then orient the satellite for thruster firing. At the completion of thruster firing the ADCS will resume normal operations.

ANNEX F-1

Optical System

o 14 to 16 micron (CO_2) spectral band

o Field-of-view: circular 2-1/2^{o} diameter.

o Rotation scan rate: 4 scan per second.

o Half scan cone angle: 20^{o}.

o Time constant from 250 milliseconds to 5 seconds.

Electronics:

o Phase and earth chord output: standard Pitch and Roll are optional.

o Employs an embedded microprocessor analog/digital signal processing, and new algorithm for precision determination of the horizon.

Mechanical Interface:

o Uncompensated angular momentum: 0.01 foot-pound-second maximum.

o Head and electronic processing module are flange mounted.

Alignment:

o Employs alignment fixture (optical cube) for autocollimation to vehicle axes.

Power:

o 10.0 watts 21.0 volts DC input voltage.

Weight:

o Head: 2.8 pounds (1.27 kg).

o Computer box: 5.5 pounds (2.5 kg).

o System Total: 8.3 pounds (3.77 kg).

CONICAL SCAN HORIZON SENSOR
MODEL 13-103

Description:

Model 13-103 is a high accuracy, high reliability conical scan system which provides a local earth vertical reference over a wide range of orbital altitudes. The system is comprised of one optical head and one electronic processing module for each axis.

Application:

Features:

- Tolerant to Single Event Upsets (S.E.U.'s).
- Graceful performance degradation.
- Self calibration.
- Sealed and pressurized optical head.

Performance

- Worst case performance in a polar orbit, at (700 km) altitude, is $\pm.07^{\circ}$ (3 sigma) pitch and $\pm 03^{\circ}$ (3 sigma) roll. (See Model 13-103A for ultra high accuracy version of this sensor.)
- Instrument accuracy is $\pm 03^{\circ}$ (3 sigma).
- Attitude Range.
- Altitude range is 120 nautical miles to synchronous.
- Auto sun/moon rejection.
- Programmable Scan Blanking

Size: (not including mounting flange).

o *Head:*
Length: 6.4 inches (16.26) long
Diameter: 4.062 inches (10.3 cm) not including mounting flange.

o *Computer Box:*
Height: 2.5 inches (6.35 cm).
Length: 10.31 inches (26.2 cm).
Width: 5.8 inches (14.9 cm) not including mounting flange.

Environment:

o Temperature range is - 25° C to 60° C.
o Hardened for radiation and EMP.

BRANCH	FROM NODE	TO NODE	METHOD	SHAPE1	LENGTH1	WIDTH1	THICKNESS1	RADIUS1	AREA1	CODE1	CS AREA1	MATERIAL1
1	1	8	1	RECTANGLE	0.7000	0.5000	0.0050		0.3500	1	0.0035	ALUMINUM
2	1	9	1	RECTANGLE	0.7000	0.5000	0.0050		0.3500	2	0.0025	ALUMINUM
3	1	13	3	RECTANGLE	0.7000	0.5000	0.0050		0.3500			ALUMINUM
4	1	33	1	RECTANGLE	0.7000	0.5000	0.0050		0.3500	2	0.0025	ALUMINUM
5	1	35	1	RECTANGLE	0.7000	0.5000	0.0050		0.3500	1	0.0035	ALUMINUM
6	1	37	3	RECTANGLE	0.7000	0.5000	0.0050		0.3500			ALUMINUM
7	2	8	1	RECTANGLE	0.9000	0.7000	0.0050		0.6300	3	0.6300	OSR
8	2	301	3	RECTANGLE	0.7000	0.5000	0.0050		0.3500			
9	2	333	10	RECTANGLE	0.9000	0.7000	0.0050		0.6300			OSR
10	3	8	1	RECTANGLE	0.7000	0.5000	0.0050		0.3500	1	0.0035	ALUMINUM
11	3	10	1	RECTANGLE	0.7000	0.5000	0.0050		0.3500	2	0.0025	ALUMINUM
12	3	14	3	RECTANGLE	0.7000	0.5000	0.0050		0.3500			ALUMINUM
13	3	22	1	RECTANGLE	0.7000	0.5000	0.0050		0.3500	1	0.0035	ALUMINUM
14	3	34	1	RECTANGLE	0.7000	0.5000	0.0050		0.3500	2	0.0025	ALUMINUM
15	3	38	3	RECTANGLE	0.7000	0.5000	0.0050		0.3500			ALUMINUM
16	4	8	1	RECTANGLE	0.1969	0.1270	0.0050		0.0250	3	0.0250	ALUMINUM
17	5	8	1	RECTANGLE	0.3208	0.3208	0.0050		0.1029	3	0.1029	ALUMINUM
18	6	8	1	RECTANGLE	0.2223	0.0889	0.0050		0.0139	3	0.0138	ALUMINUM
19	7	8	1	RECTANGLE	0.3683	0.2223	0.0050		0.0819	3	0.0819	ALUMINUM
20	8	19	1	RECTANGLE	0.9000	0.7000	0.0050		0.6300	1	0.0045	ALUMINUM
21	9	11	1	RECTANGLE	0.6500	0.5000	0.0050		0.3250	1	0.0033	ALUMINUM
22	9	13	3	RECTANGLE	0.6500	0.5000	0.0050		0.3250			ALUMINUM
23	9	18	1	RECTANGLE	0.6500	0.5000	0.0050		0.3250	4	0.0019	ALUMINUM
24	9	19	1	RECTANGLE	0.6500	0.5000	0.0050		0.3250	4	0.0014	ALUMINUM
25	9	35	1	RECTANGLE	0.6500	0.5000	0.0050		0.3250	1	0.0033	ALUMINUM
26	9	39	3	RECTANGLE	0.6500	0.5000	0.0050		0.3250			ALUMINUM
27	10	12	1	RECTANGLE	0.6500	0.5000	0.0050		0.3250	2	0.0025	ALUMINUM
28	10	14	3	RECTANGLE	0.6500	0.5000	0.0050		0.3250			ALUMINUM
29	10	18	1	RECTANGLE	0.6500	0.5000	0.0050		0.3250	4	0.0019	ALUMINUM
30	10	19	1	RECTANGLE	0.6500	0.5000	0.0050		0.3250	4	0.0014	ALUMINUM
31	10	22	1	RECTANGLE	0.6500	0.5000	0.0050		0.3250	1	0.0033	ALUMINUM
32	10	40	3	RECTANGLE	0.6500	0.5000	0.0050		0.3250			ALUMINUM
33	11	15	3	RECTANGLE	0.6500	0.5000	0.0050		0.3250			ALUMINUM
34	11	18	1	RECTANGLE	0.6500	0.5000	0.0050		0.3250	4	0.0019	ALUMINUM
35	11	20	1	RECTANGLE	0.6500	0.5000	0.0050		0.3250	4	0.0014	ALUMINUM
36	11	23	1	RECTANGLE	0.6500	0.5000	0.0050		0.3250	2	0.0025	ALUMINUM
37	11	36	1	RECTANGLE	0.6500	0.5000	0.0050		0.3250	1	0.0033	ALUMINUM
38	11	41	3	RECTANGLE	0.6500	0.5000	0.0050		0.3250			ALUMINUM
39	12	16	3	RECTANGLE	0.6500	0.5000	0.0050		0.3250			ALUMINUM
40	12	18	1	RECTANGLE	0.6500	0.5000	0.0050		0.3250	4	0.0019	ALUMINUM
41	12	20	1	RECTANGLE	0.6500	0.5000	0.0050		0.3250	4	0.0014	ALUMINUM
42	12	21	1	RECTANGLE	0.6500	0.5000	0.0050		0.3250	1	0.0033	ALUMINUM
43	12	25	1	RECTANGLE	0.6500	0.5000	0.0050		0.3250	2	0.0025	ALUMINUM
44	12	42	3	RECTANGLE	0.6500	0.5000	0.0050		0.3250			ALUMINUM
45	13	15	3	SPHERE			0.0050	0.2750	0.9503			KAPTON
46	13	17	3	SPHERE			0.0050	0.2750	0.9503			KAPTON
47	13	33	3	SPHERE			0.0050	0.2750	0.9503			KAPTON
48	13	35	3	SPHERE			0.0050	0.2750	0.9503			KAPTON
49	14	16	3	SPHERE				0.2750	0.9503			KAPTON
50	14	17	3	SPHERE			0.0050	0.2750	0.9503			KAPTON

CONDUCTIVITY1	EMISSIVITY1	ABSORBTIVITY1	FLUX1	HEAT INPUT1	TEMPERATURE INPUT1	SHAPE2	LENGHT2	WIDTH2	THICKNESS2
210.0000	0.7800	0.5000				RECTANGLE	0.9000	0.7000	0.0050
210.0000	0.7800	0.5000		0.0000		RECTANGLE	0.6500	0.5000	0.0050
210.0000	0.7800	0.5000		0.0000		SPHERE			0.0050
210.0000	0.7800	0.5000				RECTANGLE	0.6500	0.5000	0.0050
210.0000	0.7800	0.5000		0.0000		RECTANGLE	0.7000	0.6500	0.0050
210.0000	0.7800	0.5000		0.0000		RECTANGLE	0.7000	0.5000	0.0050
418.6900	0.8000	0.2100		0.0000		RECTANGLE	0.9000	0.7000	0.0050
				0.0000					
0.0000	0.8000	0.2100	122.5324	15.2130					
210.0000	0.7800	0.5000		0.0000		RECTANGLE	0.9000	0.7000	0.0050
210.0000	0.7800	0.5000		0.0000		RECTANGLE	0.6500	0.5000	0.0050
210.0000	0.7800	0.5000		0.0000		SPHERE			0.0050
210.0000	0.7800	0.5000		0.0000		RECTANGLE	0.7000	0.6500	0.0050
210.0000	0.7800	0.5000		0.0000		RECTANGLE	0.6500	0.5000	0.0050
210.0000	0.7800	0.5000		0.0000		RECTANGLE	0.7000	0.5000	0.0050
210.0000	0.7800	0.5000		0.0000		RECTANGLE	0.9000	0.7000	0.0050
210.0000	0.7800	0.5000		0.0000		RECTANGLE	0.9000	0.7000	0.0050
210.0000	0.7800	0.5000		0.0000		RECTANGLE	0.9000	0.7000	0.0050
210.0000	0.7800	0.5000		0.0000		RECTANGLE	0.9000	0.7000	0.0050
210.0000	0.7800	0.5000		0.0000		RECTANGLE	0.9000	0.2750	0.0050
210.0000	0.7800	0.5000		0.0000		RECTANGLE	0.6500	0.5000	0.0050
210.0000	0.7800	0.5000		0.0000		SPHERE			0.0050
210.0000	0.7800	0.5000		0.0000		RECTANGLE	0.9500	0.3750	0.0050
210.0000	0.7800	0.5000		0.0000		RECTANGLE	0.9000	0.2750	0.0050
210.0000	0.7800	0.5000		0.0000		RECTANGLE	0.7000	0.6500	0.0050
210.0000	0.7800	0.5000		0.0000		RECTANGLE	0.6500	0.5000	0.0050
210.0000	0.7800	0.5000		0.0000		RECTANGLE	0.6500	0.5000	0.0050
210.0000	0.7800	0.5000		0.0000		SPHERE			0.0050
210.0000	0.7800	0.5000		0.0000		RECTANGLE	0.9000	0.3750	0.0050
210.0000	0.7800	0.5000		0.0000		RECTANGLE	0.9000	0.2750	0.0050
210.0000	0.7800	0.5000		0.0000		RECTANGLE	0.7000	0.6500	0.0050
210.0000	0.7800	0.5000		0.0000		RECTANGLE	0.6500	0.5000	0.0050
210.0000	0.7800	0.5000		0.0000		SPHERE			0.0050
210.0000	0.7800	0.5000		0.0000		RECTANGLE	0.9000	0.3750	0.0050
210.0000	0.7800	0.5000		0.0000		RECTANGLE	0.9000	0.2750	0.0050
210.0000	0.7800	0.5000		0.0000		RECTANGLE	0.7000	0.5000	0.0050
210.0000	0.7800	0.5000		0.0000		RECTANGLE	0.7000	0.6500	0.0050
210.0000	0.7800	0.5000		0.0000		RECTANGLE	0.6500	0.5000	0.0050
210.0000	0.7800	0.5000		0.0000		SPHERE			0.0050
210.0000	0.7800	0.5000		0.0000		RECTANGLE	0.9000	0.3750	0.0050
210.0000	0.7800	0.5000		0.0000		RECTANGLE	0.9000	0.2750	0.0050
210.0000	0.7800	0.5000		0.0000		RECTANGLE	0.7000	0.6500	0.0050
210.0000	0.7800	0.5000		0.0000		RECTANGLE	0.7000	0.5000	0.0050
210.0000	0.7800	0.5000		0.0000		RECTANGLE	0.6500	0.5000	0.0050
0.0000	0.0100	0.1200		0.0000		SPHERE			0.0050
0.0000	0.0100	0.1200		0.0000		CYLINDER	0.7000		0.0050
0.0000	0.0100	0.1200		0.0000		RECTANGLE	0.6500	0.5000	0.0050
0.0000	0.0100	0.1200		0.0000		RECTANGLE	0.7000	0.6500	0.0050
0.0000	0.0100	0.1200		0.0000		SPHERE			0.0050
0.0000	0.0100	0.1200		0.0000		CYLINDER	0.7000		0.0050

RADIUS2	AREA2	CODE2	CS AREA2	MATERIAL2	CONDUCTIVITY2	EMISSIVITY2	ABSORBTIVITY2	FLUX2	HEAT INPUT2	TEMPERATURE INPUT
	0.6300	2	0.0025	ALUMINUM	210.0000	0.7800	0.5000			
	0.3250	2	0.0025	ALUMINUM	210.0000	0.7800	0.5000		0.0000	
0.2750	0.3503			KAPTON	0.0000	0.0100	0.1200		0.0000	
	0.3250	2	0.0025	ALUMINUM	210.0000	0.7800	0.5000			
	0.4550	1	0.0035	ALUMINUM	210.0000	0.7800	0.5000		0.0000	
	0.3500			KAPTON	0.0000	0.0100	0.1200		0.0000	
	0.6300			ALUMINUM	210.0000	0.7800	0.5000		0.0000	
									0.0000	-275.000
									0.0000	
	0.6300	2	0.0035	ALUMINUM	210.0000	0.7800	0.5000		0.0000	
	0.3250	2	0.0025	ALUMINUM	210.0000	0.7800	0.5000		0.0000	
0.2750	0.3503			KAPTON	0.0000	0.0100	0.1200		0.0000	
	0.4550	1	0.0035	ALUMINUM	210.0000	0.7800	0.5000		0.0000	
	0.3250	2	0.0025	ALUMINUM	210.0000	0.7800	0.5000		0.0000	
	0.3500			KAPTON	0.0000	0.0100	0.1200		0.0000	
	0.6300	3	0.6300	ALUMINUM	210.0000	0.7800	0.5000		0.0000	
	0.6300	3	0.6300	ALUMINUM	210.0000	0.7800	0.5000		0.0000	
	0.6300	3	0.6300	ALUMINUM	210.0000	0.7800	0.5000		0.0000	
	0.6300	3	0.6300	ALUMINUM	210.0000	0.7800	0.5000		0.0000	
	0.2475	1	0.0045	ALUMINUM	210.0000	0.7800	0.5000		0.0000	
	0.3250	1	0.0033	ALUMINUM	210.0000	0.7800	0.5000		0.0000	
0.2750	0.3503			KAPTON	0.0000	0.0100	0.1200		0.0000	
	0.3563	4	0.0013	ALUMINUM	210.0000	0.7800	0.5000		0.0000	
	0.2475	2	0.0014	ALUMINUM	210.0000	0.7800	0.5000		0.0000	
	0.4550	2	0.0033	ALUMINUM	210.0000	0.7800	0.5000		0.0000	
	0.3250			KAPTON	0.0000	0.0100	0.1200		0.0000	
	0.3250	2	0.0025	ALUMINUM	210.0000	0.7800	0.5000		0.0000	
0.2750	0.3503			KAPTON	0.0000	0.0100	0.1200		0.0000	
	0.3375	2	0.0013	ALUMINUM	210.0000	0.7800	0.5000		0.0000	
0.4750	0.2475	2	0.0014	ALUMINUM	210.0000	0.7800	0.5000		0.0000	
	0.4550	2	0.0033	ALUMINUM	210.0000	0.7800	0.5000		0.0000	
	0.3250			KAPTON	0.0000	0.0100	0.1200		0.0000	
0.2750	0.3503			KAPTON	0.0000	0.0100	0.1200		0.0000	
	0.3375	2	0.0013	ALUMINUM	210.0000	0.7800	0.5000		0.0000	
	0.2475	2	0.0014	ALUMINUM	210.0000	0.7800	0.5000		0.0000	
	0.3500	2	0.0025	ALUMINUM	210.0000	0.7800	0.5000		0.0000	
	0.4550	2	0.0033	ALUMINUM	210.0000	0.7800	0.5000		0.0000	
	0.3250			KAPTON	0.0000	0.0100	0.1200		0.0000	
0.2750	0.3503			KAPTON	0.0000	0.0100	0.1200		0.0000	
	0.3375	2	0.0013	ALUMINUM	210.0000	0.7800	0.5000		0.0000	
	0.2475	2	0.0014	ALUMINUM	210.0000	0.7800	0.5000		0.0000	
	0.4550	2	0.0033	ALUMINUM	210.0000	0.7800	0.5000		0.0000	
	0.3500	2	0.0025	ALUMINUM	210.0000	0.7800	0.5000		0.0000	
	0.3250			KAPTON	0.0000	0.0100	0.1200		0.0000	
0.2750	0.3503			KAPTON	0.0000	0.0100	0.1200		0.0000	
0.3750	1.6493			ALUMINUM	210.0000	0.7800	0.5000		0.0000	
	0.3250			ALUMINUM	210.0000	0.7800	0.5000		0.0000	
	0.4550			ALUMINUM	210.0000	0.7800	0.5000		0.0000	
0.2750	0.3503			KAPTON	0.0000	0.0100	0.1200		0.0000	
0.3750	1.6493			ALUMINUM	210.0000	0.7800	0.5000		0.0000	

VIEW FACTOR	EMISSIVITY FACTOR	DISTANCE	CONDUCTANCE
	ERR	0.5000	1.4700
	ERR	0.7000	0.7500
0.5016	0.0514	0.2850	0.0512
	ERR	0.7000	0.7500
	ERR	0.5000	1.4700
0.4301	0.0202	0.0050	0.0135
	ERR	0.0050	52753.6800
	ERR		ERR
	ERR		
	ERR	0.5000	1.4700
	ERR	0.7000	0.7500
0.5016	0.0514	0.2850	0.0512
	ERR	0.5000	1.4700
	ERR	0.7000	0.7500
0.4532	0.0211	0.0050	0.0195
	ERR	0.0050	1050.0000
	ERR	0.0050	4321.8000
	ERR	0.0050	831.6000
	ERR	0.0050	3439.8000
	ERR	0.7000	1.3500
	ERR	0.5000	1.3860
0.3817	0.0713	0.3500	0.0502
	ERR	0.5000	0.7380
	ERR	0.5000	0.5880
	ERR	0.5000	1.3850
0.4664	0.0212	0.0050	0.0182
	ERR	0.6500	0.8077
0.3817	0.0713	0.3500	0.0502
	ERR	0.5000	0.7380
	ERR	0.5000	0.5880
	ERR	0.5000	1.3850
0.4664	0.0212	0.0050	0.0182
0.3817	0.0713	0.3500	0.0502
	ERR	0.5000	0.7380
	ERR	0.5000	0.5880
	ERR	0.6500	0.8077
	ERR	0.5000	1.3850
0.4664	0.0212	0.0050	0.0182
0.3817	0.0713	0.3500	0.0502
	ERR	0.5000	0.7380
	ERR	0.5000	0.5880
	ERR	0.5000	1.3850
	ERR	0.6500	0.8077
0.4645	0.0213	0.0050	0.0182
0.0612	0.0768	0.7300	0.0253
0.1583	0.0600	0.7586	0.0512
0.1305	0.0713	0.3500	0.0501
0.1847	0.0514	0.2850	0.0512
0.0612	0.0768	0.7300	0.0253
0.1583	0.0600	0.7586	0.0512

BRANCH	FROM NODE	TO NODE	METHOD	SHAPE1	LENGTH1	WIDTH1	THICKNESS1	RADIUS1	AREA1	CODE1	CS AREA1	MATERIAL1
51	14	22	3	SPHERE				0.2750	0.3503			KAPTON
52	14	34	3	SPHERE			0.0050	0.2750	0.3503			KAPTON
53	15	17	3	SPHERE				0.2750	0.3503			KAPTON
54	15	23	3	SPHERE			0.0050	0.2750	0.3503			KAPTON
55	15	31	3	SPHERE			0.0050	0.2750	0.3503			KAPTON
56	15	35	3	SPHERE			0.0050	0.2750	0.3503			KAPTON
57	16	17	3	SPHERE			0.0050	0.2750	0.3503			KAPTON
58	16	21	3	SPHERE			0.0050	0.2750	0.3503			KAPTON
59	16	25	3	SPHERE			0.0050	0.2750	0.3503			KAPTON
60	16	32	3	SPHERE			0.0050	0.2750	0.3503			KAPTON
61	17	18	1	CYLINDER	0.7000		0.0050	0.3750	70.6858	2	0.0118	ALUMINUM
62	17	54	1	CYLINDER	0.7000		0.0050	0.3750	70.6858	2	0.0118	ALUMINUM
63	18	19	1	RECTANGLE	0.9000	0.7500	0.0050		0.6750	1	0.0045	ALUMINUM
64	18	20	1	RECTANGLE	0.9000	0.7500	0.0050		0.6750	1	0.0045	ALUMINUM
65	18	56	3	RECTANGLE	0.9000	0.7500	0.0050		0.6750	3	0.6750	ALUMINUM
66	19	57	3	RECTANGLE	0.9000	0.2750	0.0050		0.2475	3	0.2475	ALUMINUM
67	20	26	1	RECTANGLE	0.9000	0.2750	0.0050		0.2475	1	0.0045	ALUMINUM
68	20	58	3	RECTANGLE	0.9000	0.2750	0.0050		0.2475	3	0.2475	ALUMINUM
69	21	22	1	RECTANGLE	0.7000	0.6500	0.0050		0.4550	1	0.0035	ALUMINUM
70	21	25	1	RECTANGLE	0.7000	0.6500	0.0050		0.4550	1	0.0035	ALUMINUM
71	21	32	1	RECTANGLE	0.7000	0.6500	0.0050		0.4550	2	0.0033	ALUMINUM
72	21	46	3	RECTANGLE	0.7000	0.6500	0.0050		0.4550			ALUMINUM
73	22	24	1	RECTANGLE	0.7000	0.6500	0.0050		0.4550	2	0.0033	ALUMINUM
74	22	45	3	RECTANGLE	0.7000	0.6500	0.0050		0.4550			ALUMINUM
75	23	26	1	RECTANGLE	0.7000	0.5000	0.0050		0.3500	1	0.0035	ALUMINUM
76	23	31	1	RECTANGLE	0.7000	0.5000	0.0050		0.3500	2	0.0025	ALUMINUM
77	23	35	1	RECTANGLE	0.7000	0.5000	0.0050		0.3500	1	0.0035	ALUMINUM
78	23	47	3	RECTANGLE	0.7000	0.5000	0.0050		0.3500			ALUMINUM
79	24	301	3	RECTANGLE	0.9000	0.7000	0.0050		0.6300			
80	24	26	1	RECTANGLE	0.9000	0.7000	0.0050		0.6300	2	0.0035	OSR
81	24	999	10	RECTANGLE	0.9000	0.7000	0.0050		0.6300			OSR
82	25	33	1	RECTANGLE	0.7000	0.5000	0.0050		0.3500	2	0.0025	ALUMINUM
83	25	48	3	RECTANGLE	0.7000	0.5000	0.0050		0.3500			ALUMINUM
84	26	27	1	RECTANGLE	0.9000	0.7000	0.0050		0.6300	4	0.0235	ALUMINUM
85	26	28	1	RECTANGLE	0.9000	0.7000	0.0050		0.6300	4	0.0800	ALUMINUM
86	26	29	1	RECTANGLE	0.9000	0.7000	0.0050		0.6300	4	0.0293	ALUMINUM
87	26	30	1	RECTANGLE	0.9000	0.7000	0.0050		0.6300	4	0.0868	ALUMINUM
88	31	33	1	RECTANGLE	0.6500	0.5000	0.0050		0.3250	2	0.0025	ALUMINUM
89	31	36	1	RECTANGLE	0.6500	0.5000	0.0050		0.3250	1	0.0033	ALUMINUM
90	31	49	3	RECTANGLE	0.6500	0.5000	0.0050		0.3250			ALUMINUM
91	31	53	1	RECTANGLE	0.6500	0.5000	0.0050		0.3250	4	0.0014	ALUMINUM
92	31	54	1	RECTANGLE	0.6500	0.5000	0.0050		0.3250	4	0.0019	ALUMINUM
93	32	34	1	RECTANGLE	0.6500	0.5000	0.0050		0.3250	2	0.0025	ALUMINUM
94	32	50	3	RECTANGLE	0.6500	0.5000	0.0050		0.3250			ALUMINUM
95	32	53	1	RECTANGLE	0.6500	0.5000	0.0050		0.3250	4	0.0014	ALUMINUM
96	32	54	1	RECTANGLE	0.6500	0.5000	0.0050		0.3250	4	0.0019	ALUMINUM
97	33	35	1	RECTANGLE	0.6500	0.5000	0.0050		0.3250	1	0.0033	ALUMINUM
98	33	51	3	RECTANGLE	0.6500	0.5000	0.0050		0.3250			ALUMINUM
99	33	54	1	RECTANGLE	0.6500	0.5000	0.0050		0.3250	4	0.0019	ALUMINUM
100	33	55	1	RECTANGLE	0.6500	0.5000	0.0050		0.3250	4	0.0014	ALUMINUM

CONDUCTIVITY1	EMISSIVITY1	ABSORBTIVITY1	FLUX1	HEAT INPUT1	TEMPERATURE INPUT1	SHAPE2	LENGTH2	WIDTH2	THICKNESS2
0.0000	0.0100	0.1200		0.0000		RECTANGLE	0.7000	0.6500	0.0050
0.0000	0.0100	0.1200		0.0000		RECTANGLE	0.6500	0.5000	0.0050
0.0000	0.0100	0.1200		0.0000		CYLINDER	0.7000		0.0050
0.0000	0.0100	0.1200		0.0000		RECTANGLE	0.7000	0.5000	0.0050
0.5000	0.0100	0.1200		0.0000		RECTANGLE	0.6500	0.5000	0.0050
0.0000	0.0100	0.1200		0.0000		RECTANGLE	0.7000	0.6500	0.0050
0.0000	0.0100	0.1200		0.0000		CYLINDER	0.7000		0.0050
0.0000	0.0100	0.1200		0.0000		RECTANGLE	0.7000	0.6500	0.0050
0.0000	0.0100	0.1200		0.0000		RECTANGLE	0.7000	0.5000	0.0050
0.0000	0.0100	0.1200		0.0000		RECTANGLE	0.6500	0.5000	0.0050
210.0000	0.7800	0.5000		0.0000		RECTANGLE	0.3000	0.7500	0.0050
210.0000	0.7800	0.5000		0.0000		RECTANGLE	0.3000	0.7500	0.0050
210.0000	0.7800	0.5000		0.0000		RECTANGLE	0.3000	0.2750	0.0050
210.0000	0.7800	0.5000		0.0000		RECTANGLE	0.3000	0.2750	0.0050
210.0000	0.7800	0.5000		0.0000		RECTANGLE	0.3000	0.7500	0.0050
210.0000	0.7800	0.5000		0.0000		RECTANGLE	0.3000	0.2750	0.0050
210.0000	0.7800	0.5000		0.0000		RECTANGLE	0.3000	0.7000	0.0050
210.0000	0.7800	0.5000		0.0000		RECTANGLE	0.3000	0.2750	0.0050
210.0000	0.7800	0.5000		0.0000		RECTANGLE	0.7000	0.6500	0.0050
210.0000	0.7800	0.5000		0.0000		RECTANGLE	0.7000	0.5000	0.0050
210.0000	0.7800	0.5000		0.0000		RECTANGLE	0.6500	0.5000	0.0050
210.0000	0.7800	0.5000		0.0000		RECTANGLE	0.7000	0.6500	0.0050
210.0000	0.7800	0.5000		0.0000		RECTANGLE	0.6500	0.5000	0.0050
210.0000	0.7800	0.5000		0.0000		RECTANGLE	0.7000	0.6500	0.0050
210.0000	0.7800	0.5000		0.0000		RECTANGLE	0.3000	0.7000	0.0050
210.0000	0.7800	0.5000		0.0000		RECTANGLE	0.6500	0.5000	0.0050
210.0000	0.7800	0.5000		0.0000		RECTANGLE	0.7000	0.6500	0.0050
210.0000	0.7800	0.5000		0.0000		RECTANGLE	0.7000	0.5000	0.0050
				0.0000					
418.6800	0.9000	0.2100		0.0000		RECTANGLE	0.3000	0.7000	0.0050
0.0000	0.8000	0.2100	122.5324	16.2190					
210.0000	0.7800	0.5000		0.0000		RECTANGLE	0.6500	0.5000	0.0050
210.0000	0.7800	0.5000		0.0000		RECTANGLE	0.7000	0.5000	0.0050
210.0000	0.7800	0.5000		0.0000		RECTANGLE	0.1623	0.1449	0.0050
210.0000	0.7800	0.5000		0.0000		RECTANGLE	0.4000	0.2000	0.0050
210.0000	0.7800	0.5000		0.0000		RECTANGLE	0.2022	0.1449	0.0050
210.0000	0.7800	0.5000		0.0000		RECTANGLE	0.3100	0.2900	0.0050
210.0000	0.7800	0.5000		0.0000		RECTANGLE	0.6500	0.5000	0.0050
210.0000	0.7800	0.5000		0.0000		RECTANGLE	0.7000	0.6500	0.0050
210.0000	0.7800	0.5000		0.0000		RECTANGLE	0.6500	0.5000	0.0050
210.0000	0.7800	0.5000		0.0000		RECTANGLE	0.3000	0.2750	0.0050
210.0000	0.7800	0.5000		0.0000		RECTANGLE	0.3000	0.3750	0.0050
210.0000	0.7800	0.5000		0.0000		RECTANGLE	0.6500	0.5000	0.0050
210.0000	0.7800	0.5000		0.0000		RECTANGLE	0.6500	0.5000	0.0050
210.0000	0.7800	0.5000		0.0000		RECTANGLE	0.3000	0.2750	0.0050
210.0000	0.7800	0.5000		0.0000		RECTANGLE	0.3000	0.3750	0.0050
210.0000	0.7800	0.5000		0.0000		RECTANGLE	0.7000	0.6500	0.0050
210.0000	0.7800	0.5000		0.0000		RECTANGLE	0.6500	0.5000	0.0050
210.0000	0.7800	0.5000		0.0000		RECTANGLE	0.3000	0.3750	0.0050
210.0000	0.7800	0.5000		0.0000		RECTANGLE	0.3000	0.2750	0.0050

RADIUS2	AREA2	CODE2	CS AREA2	MATERIAL2	CONDUCTIVITY2	EMISSIVITY2	ABSORPTIVITY2	FLUX2	HEAT INPUT2	TEMPERATURE INPUT2
	0.4550			ALUMINUM	210.0000	0.7800	0.5000		0.0000	
	0.3250			ALUMINUM	210.0000	0.7800	0.5000		0.0000	
0.3750	1.6433			ALUMINUM	210.0000	0.7800	0.5000		0.0000	
	0.3500			ALUMINUM	210.0000	0.7800	0.5000		0.0000	
	0.3250			ALUMINUM	0.7800	0.7800	0.5000		0.0000	
	0.4550			ALUMINUM	210.0000	0.7800	0.5000		0.0000	
0.3750	1.6433			ALUMINUM	210.0000	0.7800	0.5000		0.0000	
	0.4550			ALUMINUM	210.0000	0.7800	0.5000		0.0000	
	0.3500			ALUMINUM	210.0000	0.7800	0.5000		0.0000	
	0.3250			ALUMINUM	210.0000	0.7800	0.5000		0.0000	
	0.6750	4	0.0118	ALUMINUM	210.0000	0.7800	0.5000		0.0000	
	0.6750	4	0.0118	ALUMINUM	210.0000	0.7800	0.5000		0.0000	
	0.2475	1	0.0045	ALUMINUM	210.0000	0.7800	0.5000		0.0000	
	0.2475	1	0.0045	ALUMINUM	210.0000	0.7800	0.5000		0.0000	
	0.6750	3	0.6750	KAPTON	0.0000	0.0100	0.1200		0.0000	
	0.2475	3	0.2475	KAPTON	0.0000	0.0100	0.1200		0.0000	
	0.6200	1	0.0045	ALUMINUM	210.0000	0.7800	0.5000		0.0000	
	0.2475	3	0.2475	KAPTON	0.0000	0.0100	0.1200		0.0000	
	0.4550	1	0.0035	ALUMINUM	210.0000	0.7800	0.5000		0.0000	
	0.3500	1	0.0035	ALUMINUM	210.0000	0.7800	0.5000		0.0000	
	0.3250	1	0.0033	ALUMINUM	210.0000	0.7800	0.5000		0.0000	
	0.4550			KAPTON	0.0000	0.0100	0.1200		0.0000	
	0.3250	1	0.0033	ALUMINUM	210.0000	0.7800	0.5000		0.0000	
	0.4550			KAPTON	0.0000	0.0100	0.1200		0.0000	
	0.5300	2	0.0035	ALUMINUM	210.0000	0.7800	0.5000		0.0000	
	0.3250	2	0.0025	ALUMINUM	210.0000	0.7800	0.5000		0.0000	
	0.4550	1	0.0035	ALUMINUM	210.0000	0.7800	0.5000		0.0000	
	0.3500			KAPTON	0.0000	0.0100	0.1200		0.0000	
									0.0000	-275.0000
	0.6300	2	0.0035	ALUMINUM	210.0000	0.7800	0.5000		0.0000	
									0.0000	
	0.3250	2	0.0025	ALUMINUM	210.0000	0.7800	0.5000		0.0000	
	0.3500			KAPTON	0.0000	0.0100	0.1200		0.0000	
	0.0235	3	0.0235	ALUMINUM	210.0000	0.7800	0.5000		0.0000	
	0.0800	3	0.0800	ALUMINUM	210.0000	0.7800	0.5000		0.0000	
	0.0293	3	0.0293	ALUMINUM	210.0000	0.7800	0.5000		0.0000	
	0.0868	3	0.0868						0.0000	
	0.3250	2	0.0025	ALUMINUM	210.0000	0.7800	0.5000		0.0000	
	0.4550	2	0.0033	ALUMINUM	210.0000	0.7800	0.5000		0.0000	
	0.3250			KAPTON	0.0000	0.0100	0.1200		0.0000	
	0.2475	2	0.0014	ALUMINUM	210.0000	0.7800	0.5000		0.0000	
	0.3375	2	0.0019	ALUMINUM	210.0000	0.7800	0.5000		0.0000	
	0.3250	2	0.0025	ALUMINUM	210.0000	0.7800	0.5000		0.0000	
	0.3250			KAPTON	0.0000	0.0100	0.1200		0.0000	
	0.2475	2	0.0014	ALUMINUM	210.0000	0.7800	0.5000		0.0000	
	0.3375	2	0.0019	ALUMINUM	210.0000	0.7800	0.5000		0.0000	
	0.4550	2	0.0033	ALUMINUM	210.0000	0.7800	0.5000		0.0000	
	0.3250			KAPTON	0.0000	0.0100	0.1200		0.0000	
	0.3375	2	0.0019	ALUMINUM	210.0000	0.7800	0.5000		0.0000	
	0.2475	2	0.0014	ALUMINUM	210.0000	0.7800	0.5000		0.0000	

VIEW FACTOR	EMISSIVITY FACTOR	DISTANCE	CONDUCTANCE
0.1847	0.0514	0.2850	0.0512
0.1305	0.0713	0.3500	0.0501
0.1593	0.0500	0.7595	0.0512
0.1847	0.0514	0.2850	0.0512
0.1305	0.0713	0.3500	0.0501
0.1847	0.0514	0.2850	0.0512
0.1593	0.0500	0.7586	0.0512
0.1847	0.0514	0.2850	0.0512
0.1847	0.0514	0.2850	0.0512
0.1305	0.0713	0.3500	0.0501
	ERR	0.7000	3.5400
	ERR	0.7000	3.5400
	ERR	0.7500	1.2600
	ERR	0.7500	1.2500
0.4495	0.0221	0.0050	0.0379
0.7155	0.0138	0.0050	0.0139
	ERR	0.2750	3.4354
0.7155	0.0138	0.0050	0.0139
	ERR	0.6500	1.1309
	ERR	0.6500	1.1309
	ERR	0.7000	0.3300
0.4117	0.0238	0.0050	0.0253
	ERR	0.7000	0.3300
0.4117	0.0238	0.0050	0.0253
	ERR	0.5000	1.4700
	ERR	0.7000	0.7500
	ERR	0.5000	1.4700
0.4201	0.0202	0.0050	0.0135
	ERR		ERR
	ERR	0.3000	1.6282
	ERR		
	ERR	0.7000	0.7500
0.4201	0.0202	0.0050	0.0135
	ERR	0.0050	297.0000
	ERR	0.0050	3350.0000
	ERR	0.0050	1230.6000
	ERR	0.0050	3645.6000
	ERR	0.6500	0.8077
	ERR	0.5000	1.3860
0.4545	0.0213	0.0050	0.0182
	ERR	0.6500	0.4523
	ERR	0.5000	0.7390
	ERR	0.6500	0.8077
0.4545	0.0213	0.0050	0.0182
	ERR	0.5000	0.5890
	ERR	0.5000	0.7390
	ERR	0.5000	1.3050
0.4545	0.0213	0.0050	0.0182
	ERR	0.5000	0.7390
	ERR	0.5000	0.5890

BRANCH	FROM NODE	TO NODE	METHOD	SHAPE1	LENGTH1	WIDTH1	THICKNESS1	RADIUS1	AREA1	CODE1	CS AREA1	MATERIAL1
101	34	53	3	RECTANGLE	0.6500	0.5000	0.0050		0.3250			ALUMINUM
102	34	54	1	RECTANGLE	0.6500	0.5000	0.0050		0.3250	4	0.0013	ALUMINUM
103	34	55	1	RECTANGLE	0.6500	0.5000	0.0050		0.3250	4	0.0014	ALUMINUM
104	35	35	1	RECTANGLE	0.7000	0.6500	0.0050		0.4550	1	0.0035	ALUMINUM
105	35	43	3	RECTANGLE	0.7000	0.6500	0.0050		0.4550			ALUMINUM
106	36	44	3	RECTANGLE	0.7000	0.6500	0.0050		0.4550			ALUMINUM
107	37	333	10	RECTANGLE	0.7000	0.5000	0.0050		0.3500			KAPTON
108	38	333	10	RECTANGLE	0.7000	0.5000	0.0050		0.3500			KAPTON
109	39	333	10	RECTANGLE	0.6500	0.5000	0.0050		0.3250			KAPTON
110	40	333	10	RECTANGLE	0.6500	0.5000	0.0050		0.3250			KAPTON
111	41	333	10	RECTANGLE	0.6500	0.5000	0.0050		0.3250			KAPTON
112	42	333	10	RECTANGLE	0.6500	0.5000	0.0050		0.3250			KAPTON
113	43	333	10	RECTANGLE	0.7000	0.6500	0.0050		0.4550			KAPTON
114	44	333	10	RECTANGLE	0.7000	0.6500	0.0050		0.4550			KAPTON
115	45	333	10	RECTANGLE	0.7000	0.6500	0.0050		0.4550			KAPTON
116	46	333	10	RECTANGLE	0.7000	0.6500	0.0050		0.4550			KAPTON
117	47	333	10	RECTANGLE	0.7000	0.5000	0.0050		0.3500			KAPTON
118	48	333	10	RECTANGLE	0.7000	0.5000	0.0050		0.3500			KAPTON
119	49	333	10	RECTANGLE	0.6500	0.5000	0.0050		0.3250			KAPTON
120	50	333	10	RECTANGLE	0.6500	0.5000	0.0050		0.3250			KAPTON
121	51	333	10	RECTANGLE	0.6500	0.5000	0.0050		0.3250			KAPTON
122	52	333	10	RECTANGLE	0.6500	0.5000	0.0050		0.3250			KAPTON
123	53	59	3	RECTANGLE	0.9000	0.2750	0.0050		0.2475	3	0.2475	ALUMINUM
124	54	60	3	RECTANGLE	0.9000	0.7000	0.0050		0.6300	3	0.6300	ALUMINUM
125	55	61	3	RECTANGLE	0.9000	0.2750	0.0050		0.2475	3	0.2475	ALUMINUM
126	56	333	10	RECTANGLE	0.9000	0.7500	0.0050		0.6750			KAPTON
127	57	333	10	RECTANGLE	0.9000	0.2750	0.0050		0.2475			KAPTON
128	58	333	10	RECTANGLE	0.9000	0.2750	0.0050		0.2475			KAPTON
129	59	333	10	RECTANGLE	0.9000	0.2750	0.0050		0.2475			KAPTON
130	60	333	10	RECTANGLE	0.9000	0.7500	0.0050		0.6750			KAPTON
131	61	333	10	RECTANGLE	0.9000	0.2750	0.0050		0.2475			KAPTON

CONDUCTIVITY1	EMISSIVITY1	ABSORPTIVITY1	FLUX1	HEAT INPUT1	TEMPERATURE INPUT1	SHAPE2	LENGHT2	WIDTH2	THICKNESS2
210.0000	0.7800	0.5000		0.0000		RECTANGLE	0.6500	0.5000	0.0050
210.0000	0.7800	0.2100		0.0000		RECTANGLE	0.3000	0.3750	0.0050
210.0000	0.7800	0.5000		0.0000		RECTANGLE	0.3000	0.2750	0.0050
210.0000	0.7800	0.5000		0.0000		RECTANGLE	0.7000	0.6500	0.0050
210.0000	0.7800	0.5000		0.0000		RECTANGLE	0.7000	0.6500	0.0050
210.0000	0.7800	0.5000		0.0000		RECTANGLE	0.7000	0.6500	0.0050
0.0000	0.0100	0.1200	122.5924	5.1483					
0.0000	0.0100	0.1200	122.5924	5.1483					
0.0000	0.0100	0.1200	268.1417	10.4575					
0.0000	0.0100	0.1200	286.1417	11.1595					
0.0000	0.0100	0.1200	268.1417	10.4575					
0.0000	0.0100	0.1200	268.1417	10.4575					
0.0000	0.0100	0.1200	302.3211	43.2335					
0.0000	0.0100	0.1200	302.3211	43.2335					
0.0000	0.0100	0.1200	132.2188	7.2131					
0.0000	0.0100	0.1200	132.2188	7.2131					
0.0000	0.0100	0.1200	122.5924	5.1483					
0.0000	0.0100	0.1200	122.5924	5.1483					
0.0000	0.0100	0.1200	318.4873	35.8210					
0.0000	0.0100	0.1200	318.4873	35.8210					
0.0000	0.0100	0.1200	318.4873	35.8210					
0.0000	0.0100	0.1200	318.4873	35.8210					
210.0000	0.7800	0.5000		0.0000		RECTANGLE	0.3000	0.2750	0.0050
210.0000	0.7800	0.5000		0.0000		RECTANGLE	0.3000	0.7000	0.0050
210.0000	0.7800	0.5000		0.0000		RECTANGLE	0.3000	0.2750	0.0050
0.0000	0.0100	0.1200	268.1476	21.7200					
0.0000	0.0100	0.1200	268.1417	7.3539					
0.0000	0.0100	0.1200	268.1417	7.3539					
0.0000	0.0100	0.1200	318.4873	27.2791					
0.0000	0.0100	0.1200	318.4873	74.3375					
0.0000	0.0100	0.1200	318.4873	27.2791					

RADIUS2	AREA2	CODE2	CS AREA2	MATERIAL2	CONDUCTIVITY2	EMISSIVITY2	ABSORBTIVITY2	FLUX2	HEAT INPUT2	TEMPERATURE INPUT2
	0.3250			KAPTON	0.0000	0.0100	0.1200		0.0000	
	0.3375	2	0.0019	ALUMINUM	210.0000	0.7800	0.5000		0.0000	
	0.2475	2	0.0014	ALUMINUM	210.0000	0.7800	0.5000		0.0000	
	0.4550	1	0.0035	ALUMINUM	210.0000	0.7800	0.5000		0.0000	
	0.4550			KAPTON	0.0000	0.0100	0.1200		0.0000	
	0.4550			KAPTON	0.0000	0.0100	0.1200		0.0000	
									0.0000	
									0.0000	
									0.0000	
									0.0000	
									0.0000	
									0.0000	
									0.0000	
									0.0000	
									0.0000	
									0.0000	
									0.0000	
									0.0000	
									0.0000	
									0.0000	
									0.0000	
									0.0000	
	0.2475	3	0.2475	KAPTON	0.0000	0.0100	0.1200		0.0000	
	0.6300	3	0.6300	KAPTON	0.0000	0.0100	0.1200		0.0000	
	0.2475	3	0.2475	KAPTON	0.0000	0.0100	0.1200		0.0000	
									0.0000	
									0.0000	
									0.0000	
									0.0000	
									0.0000	
									0.0000	

VIEW FACTOR	EMISSIVITY FACTOR	DISTANCE	CONDUCTANCE
0.4541	0.0213	0.0050	0.0192
	ERR	0.5000	0.7200
	ERR	0.5000	0.5880
	ERR	0.6500	1.1309
0.4117	0.0239	0.0050	0.0253
0.4117	0.0239		0.0253
	ERR		
	ERR		
	ERR		
	ERR		
	ERR		
	ERR		
	ERR		
	ERR		
	ERR		
	ERR		
	ERR		
	ERR		
	ERR		
	ERR		
	ERR		
	ERR		
0.7155	0.0139	0.0050	0.0139
0.4485	0.0221	0.0050	0.0354
0.7155	0.0139	0.0050	0.0139
	ERR		
	ERR		
	ERR		
	ERR		
	ERR		
	ERR		